

**Elaia, the maritime harbour city
of ancient Pergamon (Turkey) –
Coastal evolution and human impact
over the past eight millennia**

**Inaugural-Dissertation
zur
Erlangung des Doktorgrades
der Mathematisch-Naturwissenschaftlichen Fakultät
der Universität zu Köln**

**Vorgelegt von
Martin Seeliger
aus Heide in Holstein**

Köln 2016

**Berichterstatter/Gutachter: Prof. Dr. Helmut Brückner
Prof. Dr. Olaf Bubenzer**

Tag der mündlichen Prüfung: 29. Juni 2016

Abstract

During Hellenistic and Roman times, Elaia, the harbour city of ancient Pergamon, was an important place of trade and traffic at the western coast of Asia Minor. Intense military and mercantile activities are documented by literary sources and archaeological evidences.

This dissertation focuses on (I) the reconstruction of shoreline displacements; (II) the detection of sea-level fluctuations; (III) the usability and history of the three harbour sites; and (IV) the investigation of human impact on the environment since mid-Holocene times in the environs of Pergamon's so-called "maritime satellite" Elaia. The geo-bio-archives of the area were studied using terrestrial and semi-aquatic vibracorings and geophysical exploration. Investigated sites were measured by Differential GPS. The sediments were examined using sedimentological, micropalaeontological and geochemical methods. Palynological and archaeobotanical analyses provided evidence for the former vegetation. Robust chronostratigraphies were established using radiocarbon (^{14}C) and optically stimulated luminescence (OSL) dating as well as archaeological dating of artefacts.

The postglacial marine transgression drowned the later settled shores of the Bay of Elaia 5500 BC, reaching its maximum ca. 1 km inland around 1500 BC. Since 850 BC, increasing settlement activities in the area led to accelerated hinterland erosion, sedimentation and a seaward shift in the shoreline. The time of the Pergamenian occupation (250 BC–AD 180) is documented by intense building activities and an increased population, which is also visible in the palynological record.

During its prime, Elaia operated three harbours: the closed harbour, the open harbour and a beach harbour. The construction of the closed harbour basin was determined by a series of interdisciplinary methods to 246–215 BC. Estimations of the water depths in the closed harbour basin (~2.5 m in Hellenistic times) and the open harbour area (~1 m in Hellenistic times) led to the conclusion that the closed harbour basin could be exploited by common ship classes until AD 150. Shortly afterwards, increased siltation led to its abandonment. The closed harbour basin, which shows no signs of dredging activities, acted as a favourable sink for human waste, as evidenced by eggs of parasites, enhanced heavy-metal concentration and debris of craftsmanship. The first detection of the Black Sea dinocyst species *Peridinium ponticum* in the Mediterranean Sea documents traffic relations with the Black-Sea region. This is supported by archaeological finds of coins, seals and ceramics originating from abroad. Water depth in the open harbour area in front of the ship sheds was insufficient to anchor larger vessels. Thus, the ships were slipped to the ship sheds. The beach harbour in the eastern district of the city of Elaia acted as an area where foreign soldiers and merchants beached their ships and put up their camps.

For the first time, a reliable regional sea-level (RSL) curve for a continental site on the Turkish Aegean coast was established using a new type of reliable sea-level index point. The curve correlates well with actual RSL curves of the nearby Aegean region; it is also in good agreement with sea-level curves derived from glacio-hydro-isostatic models.

Five stages of human impact are evident over the past eight millennia. The natural vegetation (deciduous oak forests) existed before ca. 850 BC. It is followed by a degradation period caused by increased settlement activities and lumbering until around 250 BC. During Elaia's most flourishing time, ca. 250 BC–AD 180, the human impact is on its maximum, documented by a significant vegetation change, the occurrence of human parasites, debris of craftsmanship, higher heavy-metal concentrations, economic relations and intense construction activity.

The siltation of the harbours in addition to the declining political importance of the city from late Roman times onwards led to its abandonment. Thus, the human impact on the environment decreased up to around AD 800. Since those days, the absence of human impact led to a new natural vegetation: pines. The climax vegetation of the period before 850 BC never re-established.

To sum up, this PhD thesis is a valuable example of an interdisciplinary cooperation, focused on solving the questions dealing with shoreline displacements, sea-level studies, coastal evolution, hazards and ancient harbour research in an archaeological context.

Kurzzusammenfassung

In hellenistischer und römischer Zeit war Elaia, die Hafenstadt des antiken Pergamon, ein wichtiger Handelsknotenpunkt an der Westküste Kleinasiens. Die umfangreichen Handels- und Militärfunktionen der Stadt werden durch historische Überlieferungen und archäologische Befunden belegt.

Diese Dissertation behandelt schwerpunktmäßig vier Themenfelder im Umfeld der antiken Hafenstadt Elaia, dem „maritimen Satelliten“ Pergamons: (I) die raumzeitlichen Küstenverlagerungen, (II) die Beschreibung der holozänen Meeresspiegelschwankungen, (III) die Entwicklungsgeschichte und Nutzungsmöglichkeiten der drei Häfen der Stadt und (IV) die Mensch-Umwelt-Beziehungen seit dem Mittelholozän. Hierfür wurden die Geo-Bio-Archive des Untersuchungsgebietes mittels Rammkernsondierung und geophysikalischer Prospektionsmethoden erschlossen und durch DGPS verortet. Die Sedimente wurden geochemisch, sedimentologisch und mikrofaunistisch untersucht. Des Weiteren lassen palynologische und archäobotanische Studien Rückschlüsse auf die frühere Vegetation zu. Robuste Altersmodelle basieren auf ¹⁴C- und OSL-Datierung, ergänzt durch diagnostische archäologischer Funde.

Der postglaziale Meeresspiegelanstieg erreicht die Bucht von Elaia ca. 5500 v. Chr.; sein Maximalstand um 1500 v. Chr. lag etwa 1 km landeinwärts. Ab ca. 850 v. Chr. führt ein erhöhter Siedlungsdruck und dadurch bedingte erhöhte Erosion zu einer seewärtigen Verschiebung der Küstenlinie.

Der Machtübernahme durch Pergamon um 250 v. Chr. folgt ein deutlicher Bevölkerungszuwachs und ein Höchstmaß an Bautätigkeit. Während seiner Blüte (ca. 250 v. Chr.–180 n. Chr.) verfügt Elaia über drei Häfen: den Geschlossenen Hafen, den Offenen Hafen und einen Strandhafen. Mit Hilfe interdisziplinärer Methoden konnte der Bau des Geschlossenen Hafens auf 246–241 v. Chr. datiert werden. Die Bestimmung der Wassertiefen im geschlossenen Hafenbecken (ca. 2.5 m in hellenistischer Zeit) zeigten, dass es bis etwa 150 n. Chr. von den gängigen Schiffstypen jener Zeit nutzbar war. Kurze Zeit später zwang zunehmende Verlandung zur Aufgabe des Hafens. Da im geschlossenen Hafenbecken keine Anzeichen für Dredschen vorliegen, eignet es sich als hervorragendes Archiv, das anthropogene Einflüsse klar erkennen lässt (Konservierung von menschlichen Parasiten und Abfall aus der Kunsthandwerksproduktion, Anreicherung von Schwermetallen, gute Pollenerhaltung). Darüber hinaus belegt das erstmalige Auffinden der im Schwarzen Meer und im Marmarameer endemischen Dinozyste *Peridinium ponticum* im Mittelmeer die Handelsbeziehungen zwischen Elaia und dem Schwarzmeerraum. Dies ergänzt den Nachweis durch Münz-, Siegel- und Keramikfunde. Die Wassertiefe im Offenen Hafen (ca. 1 m in

hellenistischer Zeit) war zum Ankern größerer Schiffe nicht geeignet. Statt dessen wurden die Schiffe hier über Rampen in die unmittelbar an Land liegenden Schiffshäuser gezogen. Der Strandhafen im Osten des Stadtgebietes zeigt keinerlei Hafeninfrastrukturen; seine Wassertiefe unterschied sich kaum vom Offenen Hafen. Die Schiffe wurden dort an Land gezogen und das Gebiet diente fremden Händlern und Soldaten als Lager- und Handelsplatz.

Durch die Entwicklung eines neuen Meeresspiegelindikators konnte erstmals eine belastbare Meeresspiegelkurve für eine Lokalität an der türkischen Ägäisküste erstellt werden. Sie korreliert gut mit Kurven aus dem angrenzenden Ägäisraum und mit den aus glazio-hydro-isostatischen Modellen abgeleiteten Kurven.

Als Ergebnis der Studien zur Mensch-Umweltbeziehung lassen sich fünf Phasen anthropogener Einflussnahme auf die Umgebung von Elaia in den vergangenen rund 8000 Jahren rekonstruieren. Bis etwa 850 v. Chr. ist die Region aufgrund der weitgehenden Abwesenheit des Menschen von der Klimaxvegetation aus sommergrünen Eichenwäldern geprägt. Bis etwa 250 v. Chr. kommt es durch erhöhten Siedlungsdruck und Rodung zu einer Degradation der Vegetation hin zur Macchie. Während der Blütezeit Elaias (ca. 250 v. Chr.–180 n. Chr.) erreicht der anthropogene Einfluss sein Maximum, veranschaulicht durch einen signifikanten Vegetationswandel, das verstärkte Aufkommen von menschlichen Parasiten, Abfallprodukten des Kunsthandwerks, Bautätigkeit und vermehrten Handelsbeziehungen. Die Verlandung des Hafens und der abnehmende politische Einfluss der Stadt ab der späten Römerzeit führen zur Aufgabe der Stadt und einem Verschwinden des menschlichen Einflusses bis 800 n. Chr. Seit jener Zeit führt die Abwesenheit des Menschen zu einer Erholung der Vegetation mit der Etablierung von Kiefernwäldern. Die seinerzeitige Klimaxvegetation von vor 850 v. Chr. stellt sich allerdings nicht wieder ein.

Zusammenfassend sind die in dieser Doktorarbeit vorgestellten Ergebnisse aus Elaia ein anschauliches Beispiel für den Mehrwert einer interdisziplinär angelegten Forschung zur Beantwortung von Fragen bezüglich Meeresspiegelschwankungen, Küstenentwicklung, Naturgefahren und antiker Hafenentwicklung in einem archäologischen Kontext.

Acknowledgements

This dissertation presents the results of my scientific research on Elaia, the harbour city of ancient Pergamon. I am grateful for the opportunity to undertake my studies in the group of Prof. Dr. Helmut Brückner at the Universities of Marburg and Cologne. With his support, I undertook fieldwork in the region of Elaia and hold the expertise gained during those journeys to Turkey in high regard. Not only did he facilitate the project in Elaia and helped to carry out fieldwork several times, he also continuously supported my work, encouraged me in many ways, and left space for me to develop my own ideas. Furthermore, he gave me the opportunity to work on the Kane- and Ainos projects.

I will always look back fondly on my time as a PhD student and extend my thanks to all those people who accompanied me during my years in Marburg and Cologne, and who contributed on a professional or personal level to the success of my work.

Prof. Dr. Olaf Bubbenzer is thanked for his willingness to co-supervise this thesis. The commission for the defence of this dissertation was completed by Prof. Dr. Frank Schäbitz and Dr. Andreas Bolten, and I would like to thank them for their time and expertise.

All of this would have not been possible without the permanent and generous support of the excavation director in Pergamon, Prof. Dr. Felix Pirson (German Archaeological Institute, Istanbul, Turkey). Yrd. Doç. Dr. Güler Ateş (Celal Bayar Üniversitesi, Manisa, Turkey), Dr. Stefan Feuser (Heinrich Schliemann-Institute of Ancient Studies, Rostock, Germany) and Prof. Dr. Wolf-Rüdiger Teegen (Ludwig Maximilian University, Munich, Germany) are thanked for their assistance with fieldwork in Elaia, and with interpreting and discussing the archaeological and historical contexts of this work. I wish to thank Bernhard Ludwig (M.Sc.), Alexandra Wirsching (M.A.), and the long-standing caretaker of the excavation house in Pergamon Idris Uysal for providing a cosy place to stay during those months in Turkey. The Ministry of Culture and Tourism of the Republic of Turkey kindly granted the research permits.

I thank Prof. Dr. Saït Başaran (excavation director of Ainos; İstanbul Üniversitesi, Turkey) for his generous support during our fieldwork in Ainos (modern: Enez) and the inspirational discussions on the history and archaeology of the Aegean region. His open and sincere nature whilst leading the excavation in Ainos provided valuable insights into the Turkish way of life.

Special thanks are dedicated to the entire working group of Prof. Dr. Wolfgang Rabbel (Applied Geophysics; University of Kiel, Germany) for their cooperation not only in Elaia but also in Ainos and Kane. A very special thanks is due to Dr. Dennis Wilken and Dipl. Geophys. Ercan Erkul for their assistance in interpreting geophysical images of Elaia.

PD. Dr. Peter Frenzel (University of Jena, Germany) and Dr. Anna Pint (University of Cologne, Germany) are thanked for the identification and interpretation of foraminifera and ostracoda in the sediment samples, and Dr. Lyudmila Shumilovskikh (University of Göttingen, Germany) for her expertise in investigating the pollen of core Ela 70.

Prof. Dr. Christophe Morhange (Aix-Marseille Université, Marseille, France) was an inspiring discussion partner during his stay in Pergamon/Elaia in summer 2014; his interest in my research was very motivating.

Dr. Steffen Schneider (Lower Saxony Institute for Historical Coastal Research, Wilhelmshaven, Germany) offered valuable insights related to fieldwork and discussion of topics relating to the region of Elaia, following his own doctoral research in the nearby Bergama Graben.

To Marita Budde, Christine Günther, Dr. Walter-Wilhelm Jungmann, Dr. Kristof Dorau, Dr. Corinna Földi, Dipl. Geogr. Karin Greef and Dr. Stefan Opitz my dearest thanks are given for their continuous and patient guidance during sediment analyses in the laboratories of Marburg and Cologne.

Franz-Rudolf Kniel (car-fleet manager of the German Research Foundation) is thanked for providing us with well-maintained vehicles for our trips to Turkey.

On a personal level, I would like to take this opportunity to express my endless gratitude to Dr. Dominik Brill and Dr. Max Engel, my office colleagues during my time in Cologne. They created a friendly office atmosphere which I thoroughly enjoyed – not to forget Dr. Daniel Kelterbaum for being my closest companion and friend at work. Special thanks are also dedicated to Marina Herbrecht for her help during fieldwork and in the laboratory.

Further supporting the fieldwork I would like to thank: Anja Anklamm (M.Sc.), Angela Balk (M.Sc.), Melanie Bartz (M.Sc.), Dr. Nicole Klasen, Laura Linck (B.Sc.), PD Dr. Nick Marriner, Verena Medinger (M.Sc.), Dipl. Geogr. Florian Steininger, Dr. Levent Uncu and Karl Wutzer (B.Sc.). Dipl. Geogr. Florian Steininger maintained the coring and fieldwork equipment and gave helpful hints for its proper use.

PD Dr. Nick Marriner (Université de Franche-Comté, Besançon, France), Dr. Christine Seeliger (Garvan Institute of Medical Research, Sydney, Australia), Dr. Georgina King (University of Cologne), and Svenja Riedesel (B.A.; University of Cologne, Germany) spent time reading this manuscript and provided valuable feedback on structure, figures, and last but not least language editing.

The studies in Elaia were funded by the German Research Foundation (DFG; ref. nos. PI 740/1-3 and BR 877/32-1). The “Graduate School of Geosciences (GSGS)” of the University of Cologne, the

“German Work Group on Geomorphology (AK Geomorphologie)” and the “Charles McBurney Laboratory for Geoarchaeology” of the University of Cambridge provided travel grants for me to present the research results at international conferences. The “Dr. Wolff’sche Stiftung” Marburg financed the dating of four radiocarbon ages.

I would like to take this opportunity to express my warmest thanks to my parents Elke and Friedrich-Wilhelm Seeliger, my sister Christine and my brother Ulrich. This thesis would not have been possible without their continuous support, especially during the time of this dissertation.

Finally, I wish to thank Svenja Riedesel for being such a lovely partner and for all her help, support and patience during the last months.

Table of Contents

Abstract.....	I
Kurzzusammenfassung	III
Acknowledgements	V
Table of Contents	VIII
List of Figures and Tables.....	X
1 Introduction	1
1.1 Eastern Mediterranean coastal areas in the focus of geoarchaeological research.....	1
1.2 Aims of the study	2
1.3 General approach	4
1.4 Study area.....	7
1.5 History of Elaia.....	10
2 Taken from the sea, reclaimed by the sea: The fate of the closed harbour of Elaia, the maritime satellite city of Pergamum (Turkey).....	12
3 The environs of Elaia’s ancient open harbour – A reconstruction based on microfaunal evidence	27
4 Elaia, Pergamon’s maritime satellite – Rise and fall of an ancient harbour city due to shoreline migration.....	44
5 The purpose and age of underwater walls in the Bay of Elaia of Western Turkey: A multidisciplinary approach	76
6 The harbour of Elaia: A palynological archive for human/environmental interactions during the last 7500 years.....	95
7 Discussion	117
7.1 Coastal evolution, shoreline displacements and sea-level fluctuations in the Bay of Elaia.	117
7.1.1 Goal 1: Determining the spatial and temporal dimensions of coastline changes.....	117
7.1.1.1 Shoreline displacements in the Bay of Elaia	117
7.1.1.2 Progradation of the Bakırçay delta	119
7.1.1.3 Summary	119

7.1.2 Goal 2: Establishing a regional sea-level curve based on RSL indicators for the Bay of Elaia and discussing it within a wider Aegean context.	120
7.1.2.1 Changing sea level: a general overview	120
7.1.2.2 Sea-level indicators: a general overview.....	122
7.1.2.3 Sea-level indicators used in Elaia	122
7.1.2.4 A RSL-curve for the Bay of Elaia	126
7.1.2.5 RSL-curve Elaia vs. Aegean-wide curves	127
7.1.2.6 Summary	129
7.2 Elaia's different harbour sites during the period of prosperity.....	130
7.2.1 Goal 1: Describing the lifecycle of the closed harbour basin of Elaia.....	130
7.2.1.1 The closed harbour basin of Elaia – a brief overview	130
7.2.1.2 Construction age of the closed harbour basin	130
7.2.1.3 Silting up of the closed harbour basin	136
7.2.1.4 Tsunami impact in the Bay of Elaia?	136
7.2.1.5 Summary	137
7.2.2 Goal 2: Determining the water depths of Elaia's harbours and their accessibility by different ship classes during Hellenistic and Roman times.	138
7.2.2.1 The draughts of common war and merchant ships during Hellenistic and Roman times	138
7.2.2.2 Reconstructed water depths of the closed and open harbours of Elaia.....	141
7.2.2.3 Summary	142
7.3 Human impact in the Bay of Elaia over the past millennia.....	144
7.3.1 Main goal: To identify and quantify human impact on the Bay of Elaia over the past millennia.....	144
7.3.1.1 Human impact and human-induced landscape changes over time.....	144
7.3.1.2 Summary	147
8 Conclusions	149
References.....	151
Supplementary Material.....	163
Paper Contribution	164
Erklärung	165

List of Figures and Tables

Fig. 1 Study design	4
Fig. 2 The area of research at the Aegean coast of Turkey.....	7
Fig. 3 Structural map of the research area and the surrounding mountain ranges.....	8
Fig. 4 Locations of selected vibracores carried out in the Bay of Elaia.....	9
Fig. 5 Timeline of the historic periods, linked with Elaia’s most flourishing period.....	10
Fig. 6 Microfossil content in context of the transgressive contact.....	123
Fig. 7 Breakwater construction in Hellenistic times.....	124
Fig. 8 Modelled RSL-curve for the Bay of Elaia.....	126
Fig. 9 Modelled RSL-curve for the Bay of Elaia compared to other curves for the Aegean region.....	128
Fig. 10 The closed harbour basin of Elaia.....	131
Fig. 11 Results of the geoseismic profile 7.....	134
Fig. 12 Synoptic chronology of different approaches to detect the shift from shallow-marine conditions to lagoonal ones in the closed harbour basin as a result of the construction of its breakwaters.....	135
Fig. 13 Modelled water depths in the closed harbour basin of Elaia for the past 8000 years.....	139
Fig. 14 Modelled water depths in the open harbour area of Elaia for the past 8000 years.....	140
Fig. 15 Detailed view on the water depths	142
Fig. 16 Geographic distribution of <i>Peridinium ponticum</i>	146
Fig. 17 Selection of carved bones out of coring Ela 58.....	146
Tab. 1 Radiocarbon data sheet.....	163

Chapter 1

1 Introduction

1.1 Eastern Mediterranean coastal areas in the focus of geoarchaeological research

Around 6000 BC at the “dawn of civilisations” (Lambeck & Purcell, 2007), the major part of the Holocene marine transgression had nearly ended and a more or less stable sea level enabled societies to settle the Mediterranean coasts (Murray-Wallace & Woodroffe, 2014, Khan et al., 2015). During the following millennia, a seaside location was an important factor in establishing a flourishing settlement for many civilisations and harbour sites acted as important hubs for trade, travel and traffic. Nevertheless, the sea always showed an ambivalent character to humans and their coastal settlements. In contrast to cities located in the hinterland, harbour settlements were exposed to risks from the sea, such as sea-level fluctuations and extreme wave events (storms, tsunamis). Additionally, harbours were also prone to siltation by fluvial or colluvial sediment inputs. In the worst cases, this led to the abandonment of a city (Knoblauch, 1981; Marriner & Morhange, 2007; Morhange & Marriner, 2010).

Various examples from the eastern Mediterranean region are known where shifting shorelines and changing sea level influenced the rise and decline of ancient settlements and their harbours. Beginning with the Neolithic settlements of the Çukuriçi Höyük near ancient Ephesus (Horejs, 2012; Horejs et al., 2015; Stock et al., 2015), Hoca Çeşme in Thrace (Başaran, 2010; Özbek 2010) and Hamaylıtarla on the Gallipoli peninsula (Özbek, 2010) to the prominent ancient cities like Caesarea (Reinhardt & Raban, 1999), Tyre (Marriner & Morhange, 2006a), Corinth (Morhange et al., 2012; Hadler, 2014), Miletus (Müllenhoff, 2005; Brückner et al., 2006, 2013), Ephesus (Kraft et al., 1977, 2007; Brückner et al., 2013; Delile et al., 2015; Stock, 2015), Ainos (Başaran, 2010; Brückner et al., 2015), Yenikapı/Istanbul (Bony et al., 2012) and Troia (Kraft et al., 1980, 2003), just to name a few. Additionally, a vivid overview of recent ancient harbour research is published by Ladstätter et al. (2015).

No previous geoarchaeological studies have been conducted in the Bay of Elaia. This research is therefore timely and pioneering. It is important in helping to understand, why and when ancient settlements rose, flourished and decayed in the Mediterranean region.

1.2 Aims of the study

The DAI (German Archaeological Institute) has been excavating the ancient city of Pergamon for more than 100 years. The scientific scope was widened to include the city of Pergamon and its environs, within the framework of the DFG priority program (SPP) 1209 "*The Hellenistic Polis as a Living Space – Urban Structures and Civic Identity between Tradition and Innovation*", which started in 2006. Thus, Elaia, the harbour city of Pergamon, and Atarneus, an important pre-Hellenistic predecessor settlement of the region, came into focus (Schneider et al., 2013, 2014, 2015; Pirson, 2014; Pirson & Zimmermann, 2015; Pirson et al., 2015; Zimmermann et al., 2015). Except for small, sporadic archaeological field observations in the 20th century, travel reports in the early 19th century (cf. Prokesch von Osten, 1837) and ancient sources, not much was known about the Elaia region before the interdisciplinary fieldwork started. Several questions arose during the studies of Pergamon's "maritime satellite" (Pirson, 2004), mostly focusing on human-environment interactions, shoreline displacements and the usability and history of the three different harbour sites of the city. Geoarchaeological methods were applied to solve these questions. Three working hypotheses, including five research goals, form the basis for a final presentation of human-environment interaction in the Elaia region during the last millennia.

Working hypothesis 1: Coastal evolution, shoreline displacements and sea-level fluctuations in the Bay of Elaia.

- *In the Bay of Elaia, the peak of the postglacial marine transgression reached much further inland than today. Thereafter, alluvial and colluvial sedimentation caused a major seaward shift in the shoreline.*

Goal 1: Determining the spatial and temporal dimensions of coastline changes during the past millennia.

No investigation dealing with this topic had been conducted in the Bay of Elaia. Results from other studies at the Aegean coast demonstrated that, in the course of the postglacial transgression, marine embayments extended far inland, later filled by alluvial sediments. Studies in Miletus (Kraft et al., 1977; Müllenhoff, 2005; Brückner et al., 2006), Ephesus (Kraft et al., 1977, 2007; Brückner, 2005; Stock 2015), Troia (Kraft et al., 1980), and Ainos (Alpar, 2001; Brückner et al., 2015) act as valuable examples. The shoreline displacements in the Bay of Elaia and the adjacent Bergama Graben are discussed.

Goal 2: Establishing a regional sea-level curve based on RSL indicators for the Bay of Elaia and discussing it within a wider Aegean context.

Like the shoreline displacements, sea-level fluctuations in the Bay of Elaia were still unknown. A robust regional sea-level curve (RSL-curve) is established by choosing reliable sea-level indicators and comparing them to other studies of the Aegean Sea and the modelled curve by Lambeck (1996) and Lambeck & Purcell (2005).

Working hypothesis 2: Elaia's different harbour sites during the period of prosperity

- *During its period of prosperity, the city of Elaia successfully operated several harbours, which can be elucidated using geoarchaeological evidence*

Goal 1: Describing the lifecycle of the closed harbour basin of Elaia.

The closed harbour basin is of special research interest being the only visible ancient remain in Elaia, and incorporated into the Hellenistic city walls. Here, the lifecycle of the closed harbour basin, from its foundation up to its abandonment, is described. A special focus is the construction date of the harbour's breakwaters, which is detectable by several architectural, literary and geoscientific methods.

Goal 2: Determining the water depths of Elaia's harbours and their accessibility by different ship classes during Hellenistic and Roman times.

This chapter solves the question concerning when and which ship classes were able to reach the closed harbour basin and the open harbour area of Elaia. Estimation of the water depths in the two areas are compared to the draughts of common ships of those periods.

Working hypothesis 3: Human impacts in the Bay of Elaia over the past millennia

- *The temporal changes and the intensity of human impact on the environment can be elucidated by geoarchaeological research.*

Main goal: To identify and quantify human impacts on the Bay of Elaia over the millennia.

As economic centres and points for naval navigation, ancient harbour cities are of particular geoarchaeological interest. The combination of all information gained by interdisciplinary research helps to reconstruct multi-temporal landscape scenarios (Morhange et al., 2014). In this chapter, the human impact on the landscape caused by the Elaïtans is presented chronologically.

1.3 General approach

In closing the gap between physical geography, natural sciences, and archaeology by integrating methods of all three disciplines, geoarchaeology acts as an interesting toolbox to reconstruct changes in the palaeo-landscape and to detect human impact on it (Rapp & Hill, 2006). A modified version of the geoarchaeological approach of Brückner & Gerlach (2011) is used in this dissertation, which is mainly based on the investigation of geo-bio-archives (Fig. 1).

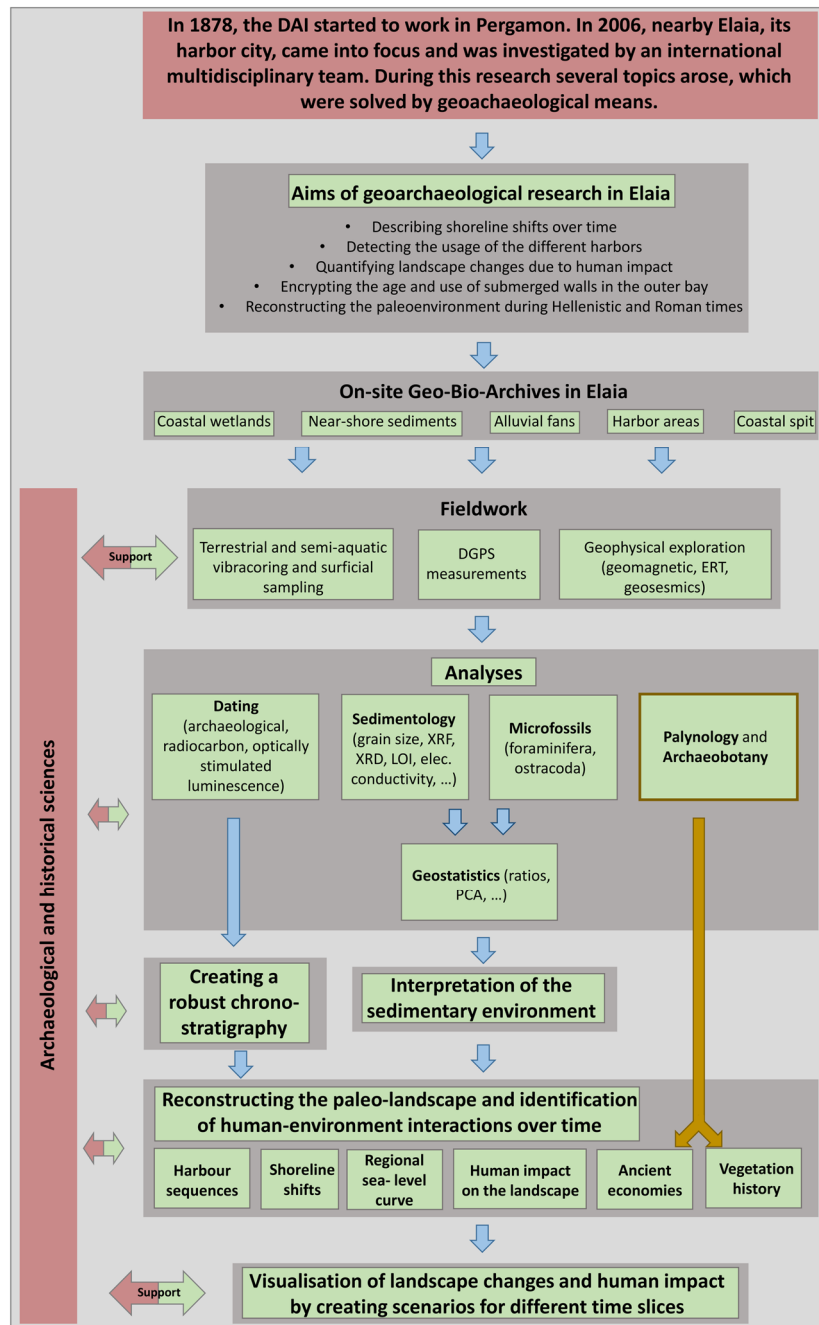


Fig. 1 Study design following Brückner & Gerlach (2011), modified.

The Bay of Elaia presents several geo-bio-achieves such as coastal wetlands, near-shore sediments, a coastal spit, alluvial fans, and harbour sediments. Between 2008 and 2012 these archives were studied using terrestrial and semi aquatic vibracoring (Atlas Copco Cobra TT) and geophysical exploration (gEOelectric (ERT), geomagnetic and geoseismic). All coring and geophysics sites were levelled using DGPS (Leica DGPS System 530).

The sediments were investigated using sedimentological, geochemical, and microfaunal tools. Statistically evaluated, this allows the interpretation of different sedimentary environments (shallow marine, littoral, limnic, lagoonal, colluvial etc.). In addition, palynological and archaeobotanical analyses enable the determination of the palaeovegetation. Robust chronostratigraphies of the sediment sequences were established by radiocarbon (^{14}C) and optically stimulated luminescence (OSL) dating as well as archaeological dating of artefacts. The combination of this information, coupled with information from the archaeological record, allows to resolve the questions outlined above, to reconstruct landscape changes, and to decipher human-environment interactions over the last millennia.

This dissertation includes five publications (Chapters 2–6) concerning different aspects of the geoarchaeological research in Elaia with a special focus on coastal changes, the identification and investigation of Elaia's harbour sites, and human-environment interactions. The following describes the main focus of each paper.

Chapter 2 deals with the closed harbour basin of Elaia. Nowadays, it is completely silted up and it is hard to imagine that ships once anchored here. Drilling cores inside and outside the harbour basin were investigated by means of geochemistry and sedimentology to decipher the history of the basin and its surroundings. The lifecycle of the harbour is described. In addition, an ERT profile and a coring were performed directly at the closed harbour's western breakwater to decipher its construction style and age.

Chapter 3 focuses on the open harbour area of Elaia. Archaeological research in Elaia suggested the need for ship sheds to store and maintain the valuable warships when not in action. From an archaeological point of view, the area between the closed harbour basin to the west and the so-called *diateichisma* – an internal city wall – to the east seemed to be the most appropriate location for such installations. This is supported by geomagnetic interpretations (Pirson, 2010). Therefore, 3D-gEOelectric measurements in this area were conducted to estimate the extension and shape of the supposed buildings. In addition, 2D-gEOelectric profiles in front of the assumed ship sheds heading towards the sea were carried out. One sediment core was recovered directly

in front of the assumed ships sheds and analysed in detail with regards to its geochemical, sedimentological, and microfaunal characteristics. Altogether, five radiocarbon ages were used to establish a robust chronology for the profile. In addition to the coring, surficial sampling of different contemporary environments of the study area was performed to establish a present-day referential for the microfauna. This allows for estimating water depths of the area for the prosperous periods of Elaia and solves the question of whether the assumed ship sheds could be accessed by ship.

Chapter 4 links and widens the topic of shoreline displacements and possible harbour sites by integrating the results of Chapters 2 and 3 into a broader framework of five intensively-studied core transects covering the entire study area. This allows for determining the spatial and temporal extension of the marine trans- and regression as well as the verification of the beach harbour area as a third harbour site of Elaia.

In contrast to Chapters 2-4, Chapter 5 focuses on the age and function of submerged wall structures in the western part of the embayment. Today, their upper surface is 0.5–1.0 m below present sea level. The subsoil of the walls and the construction style were investigated by semi-aquatic coring and water-borne geoelectrics, while further corings inside and outside the wall structures yielded material for radiocarbon dating. Additionally, sediments directly below the brickworks were dated by OSL to estimate the burial age and indirectly date the construction of the walls.

Chapter 6 deals with the reconstruction of the vegetation and environmental history of the wider Bay of Elaia since 7500 BP. Therefore, coring Ela 70 out of the closed harbour basin of Elaia was investigated by means of palynology and archaeobotany. A total of 11 radiocarbon ages provided a detailed age-depth model.

Finally, Chapter 7 discusses the results of the conducted research with a focus on the working hypotheses of Chapter 1.2, followed by a conclusion (Chapter 8).

1.4 Study area

Elaia is situated on the northern Aegean coast of modern Turkey (Fig. 2). In sum, two large-scale landscape-forming processes have affected the contemporary appearance of the area.

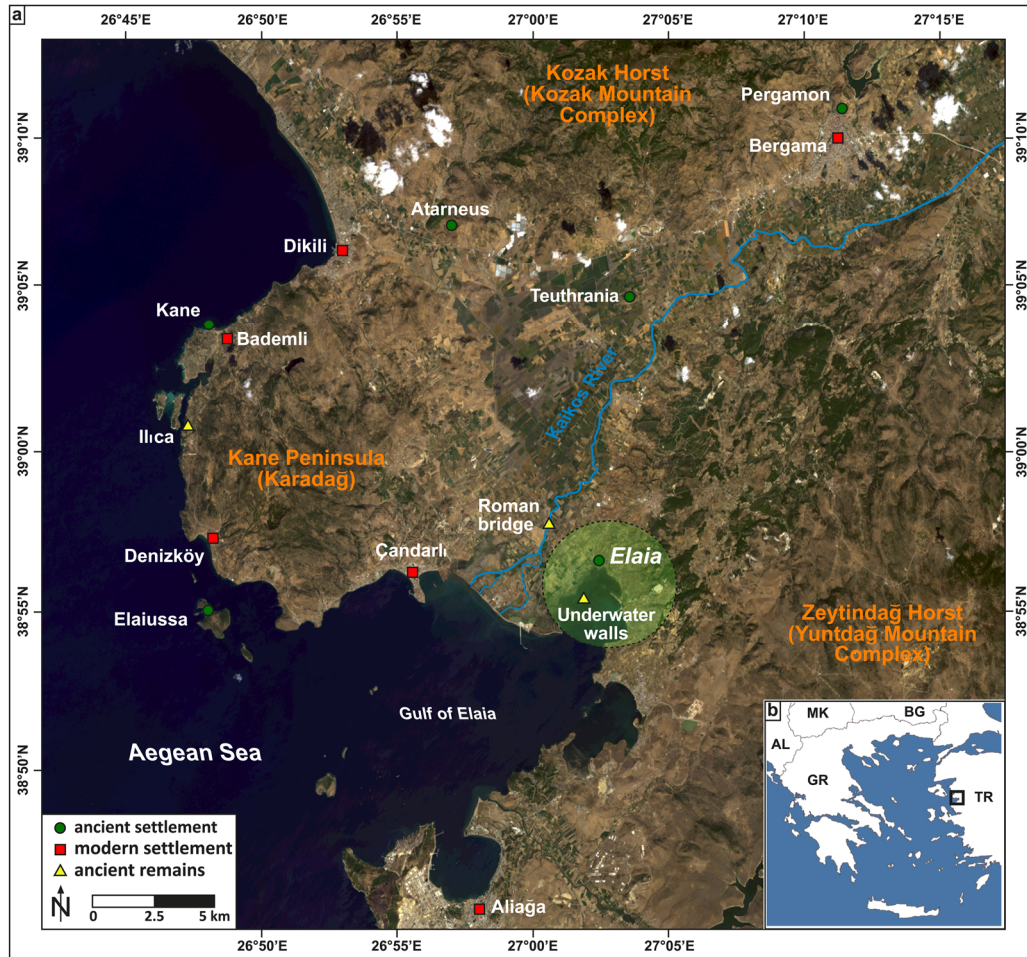


Fig. 2 The area of research at the Aegean coast of Turkey. (a) Landsat 8 satellite image (acquired 23 September 2013; RGB composite based on bands 4, 3, 1), with locations mentioned in the text. Insert: (b) General map the Aegean Sea with position of the research area.

The study area is part of the westwards moving Aegean-Anatolian microplate (Brückner et al., 2010; Vacchi et al., 2014). With its westward drift, several rift structures formed during Miocene to Pliocene times, such as the Bergama Graben and its tributary Zeytindağ Graben (Fig. 3, Demirci et al., 2015). Some of them act as outlet channels for rivers today, such as the Büyük and Küçük Menderes and the Bakırçay (Vita-Finzi, 1969; Aksu et al., 1987; Özürlan et al., 2006). The Bergama Graben is still tectonically active. This is evident from submerged archaeological remains: (i) a Roman thermal bath complex (Bademli Ilica) on Kane Peninsula; and (ii) underwater wall structures in the southwestern Bay of Elaia (Chapter 5). Additionally, Schneider (2014) provides a clear overview of more or less destructive historic earthquakes affecting the area from Roman Imperial times onwards (Garbrecht, 2003; Emre et al., 2005; Schneider, 2014).

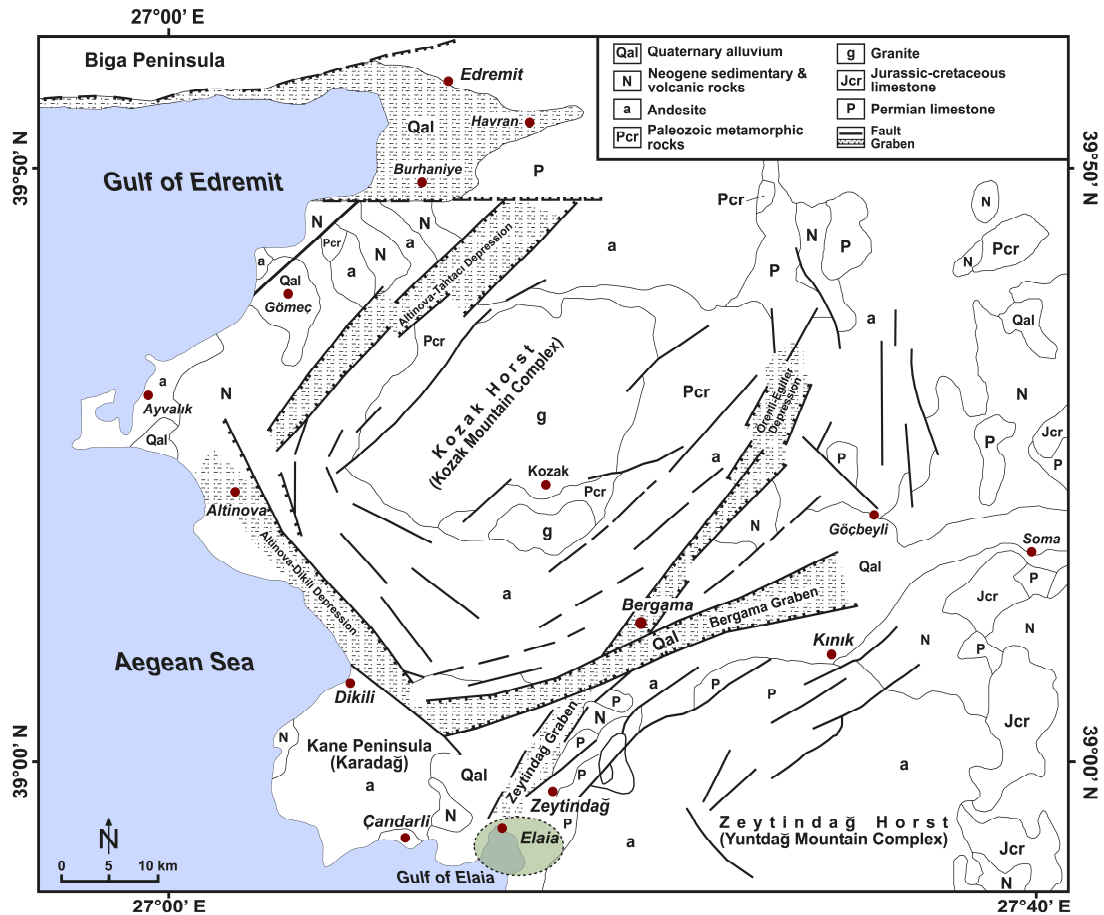


Fig. 3 Structural map of the research area and the surrounding mountain ranges. Source: Altunkaynak & Yılmaz (1998), modified.

Because of the tectonic stress, the second landscape-building agent – volcanism – started to affect the area. This is obvious in the occurrence of massive andesite layers, which covered the older Palaeozoic-Mesozoic granites of the Yuntdağ and Kozak Mountains. In addition, the landscape is littered with volcanic domes of which the Karadağ (755 m a.s.l., above sea level) and Teuthrania¹ (115 m a.s.l.) are the most prominent ones (Altunkaynak & Yılmaz, 1998; Radt, 2011).

Taking a closer look at the research area, the Kane Peninsula (Karadağ) to the west and the Yuntdağ Mountains to the east surround the Gulf of Elaia and the inner part of the Bay of Elaia. The wide alluvial plain and the cusped delta of the Bakırçay (ancient name: *Kaikos*) are located to the west of the Bay of Elaia, separated by the relatively flat ridge of Bozyertepe (40 m a.s.l.). Wetlands consisting of pioneering *Salicornia* plants are observed south of Bozyertepe.

The research area, with its three harbour sites, is situated in the inner part of the Bay of Elaia adjacent to the castle hill and the ancient city area (Fig. 4).

¹ The mythical place where Telephos, the legendary founder of Pergamon, is said to have once lived.

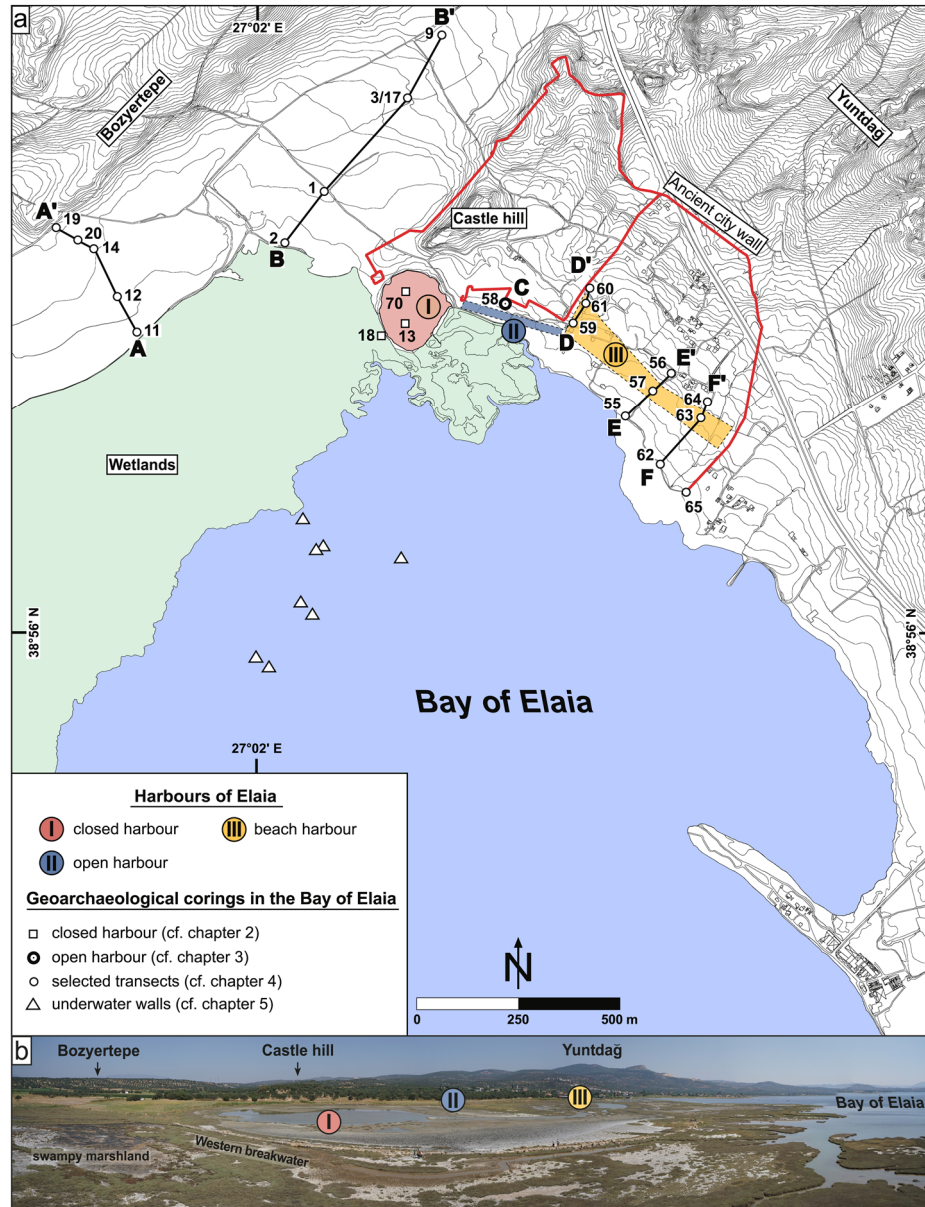


Fig. 4 Locations of selected vibracores carried out in the Bay of Elaia. (a) Locations of coring transects A–A', B–B', D–D', E–E' and F–F', and C (coring Ela 58). (b) Panoramic overview of the area of research (UAV image; taken on 01 September 2015 by Andreas Bolten).

The three harbour sites are: Firstly, the closed harbour basin which is incorporated within the fortification walls of the city. It was protected against the sea and enemies by two presently drowned breakwaters, one to the southeast and one to the west. Because the breakwaters are the most prominent ancient remains in the area, this closed harbour basin is of special interest (Chapters 2 & 6). Secondly, the ca. 250 m-long open harbour, stretched from the southern breakwater of the closed harbour south-eastwards to the point where the *diateichisma* reached the waterfront (Chapter 3). This wall divided the city area into a northern, densely populated part and a southern one (Pirson, 2011). Thirdly, an open beach harbour extended from the south

of the *diateichisma* to the south-eastern end of the city wall (Chapter 4, Pirson 2011). Submerged wall structures are situated southwest of the closed harbour in the shallow water of the embayment (Chapter 5).

1.5 History of Elaia

The historical evolution of Pergamon and Elaia is closely interwoven. Therefore, this chapter briefly focuses on the history of Elaia and its relationship to Pergamon (Fig. 5). It relies largely on the work of McShane (1964), Hansen (1971), Pirson (2004), Radt (2011), Zimmermann (2011), Pirson (2014), Pirson et al. (2015), Gehrke (2015) and Pirson & Zimmerman (2015).

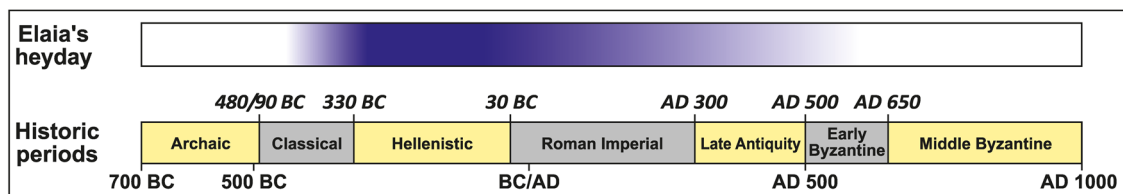


Fig. 5 Timeline of the historic periods, linked with Elaia's most flourishing period.

The settlement of Elaia is most probably of pre-Greek origin. Mythical sources date its foundation back to the times of the Trojan War and the legendary Telephos of Pergamon (Pausanias², *Graeciae descriptio* 9, 5, 14). Nevertheless, some finds dating to the early Bronze Age, as well as late Helladic and Mycenaean ceramics at the castle hill of Elaia also suggest initial settlement activities during these early periods (Pirson et al., 2015).

Historically, Elaia is first mentioned in early Classical times in the tributary lists of the Attic-Delian League (5th century BC), but paid the modest contribution of only 1/6 talent during 454–425 BC. In addition, Herodot³ (*Historíai* 1, 149) did not include Elaia in his summary of altogether 12 Aeolian settlements. This suggests a relatively small settlement during this period (Pirson & Zimmermann, 2015; Pirson et al., 2015).

The entire Kaikos region came under Macedonian rule through the military campaign by Alexander the Great, until the so-called “Wars of the Diadochi” started soon after his death in Babylon in 323 BC (Cartledge, 2004). The house of the Attalids came to power in the Kaikos region at an advanced stage of this turmoil and established – in alliance with Rome – a powerful kingdom in Asia Minor. During its most flourishing period under King Eumenes II (197–159 BC), it ruled the western half of present-day Turkey. Pergamon itself was located on top of a 330 m-

² Pausanias; Greek travel writer and geographer; ca. AD 115–180.

³ Herodot; Greek geographer, historian and ethnologist; ca. 490/480–424 BC.

high castle hill, controlling the adjacent Kaikos plain (Fig. 2a). This was an excellent strategic position, but complicated trade and transport. For economic and military reasons the city needed a maritime harbour, which was obtained by integrating the nearby city of Elaia, located on the Aegean Sea approx. 26 km southwest of Pergamon, into their realm. It is assumed that Elaia came under Pergamenian rule between 246 and 241 BC during the reign of King Eumenes I. Hereafter, the relationship between Pergamon and Elaia can be described as an interaction of taxation and subvention of the Pergamenian kings with a simultaneous autonomy of the Elaïtans (Pirson et al., 2015).

Elaia was fortified and used as the harbour city of Pergamon, which became evident in Strabo's⁴ "*Geographika*", where he mentioned Elaia as the naval base (*naustathmon*) of the Attalids and the harbour city (*epineion*) of the Pergamenians (13, 3, 5). Direct evidence for the importance of the harbour is given, e.g., in Livius's⁵ "*Ab urbe condita*" when a Pergamenian fleet of 35 *Quinquereme* (*Pentere*) ships, largely based in Elaia, jointly took part with Rome in the First Macedonian War (215-205 BC). In addition, Polybios⁶ (*Historiai* 21, 10) and Livius (*Ab urbe condita* 28, 5, 1) mentioned large Roman, Rhodesian and Pergamenian naval units stationed in Elaia during the Roman-Syrian War (192–188 BC).

Furthermore, the city did not only serve as the main harbour of Pergamon. A narrow passage was left between the slopes of the Yuntdağ Mountains and the eastern city district, easily controlled by the military garrison of Elaia (Figs. 2 & 4). Therefore, Elaia was also a defensive stronghold, which secured the southern entrance to the inner realm of the Kaikos area and the nearby coastal road heading southwards to Smyrna (Pirson, 2008, 2014; Seeliger et al., 2013; Pirson & Zimmermann, 2015). This topographic setting is quite similar to the one at Thermopylae in central Greece where, in 480 BC, the legendary 300 Spartans were able to withstand a far larger Persian army during a long battle (Kraft et al., 1987). In combination with the importance of Elaia in the economic network of Pergamon, it certainly seems to be legitimate to refer to Elaia as the "maritime satellite" of Pergamon (Pirson, 2004; Pirson & Zimmermann, 2015).

A gradual loss in the importance of the city of Elaia became obvious with its incorporation into the Roman world from 133 BC onwards (Pirson, 2004). This was most probably caused by the ongoing siltation of the harbour area of Elaia. The literary and archaeological evidence for the post-Attalid period is as poor as for the pre-Attalid one. Since the 6th/7th century AD the city was abandoned.

⁴ Strabo; Greek geographer; ca. 63 BC–AD 23.

⁵ Livius; Roman historian; ca. 59 BC–AD 17.

⁶ Polybios; Greek historian; ca. 200–120 BC.

Chapter 2

2 Taken from the sea, reclaimed by the sea: The fate of the closed harbour of Elaia, the maritime satellite city of Pergamum (Turkey)

Journal Article (2013):

Seeliger, M., Bartz, M., Erkul, E., Feuser, E., Kelterbaum, K., Klein, C., Pirson, F., Vött, A., Brückner, H., 2013. Taken from the sea, reclaimed by the sea: The fate of the closed harbour of Elaia, the maritime satellite city of Pergamum (Turkey). *Quaternary International* 312, 70–83.



Taken from the sea, reclaimed by the sea: The fate of the closed harbour of Elaia, the maritime satellite city of Pergamum (Turkey)



Martin Seeliger^{a,*}, Melanie Bartz^a, Ercan Erkul^b, Stefan Feuser^c, Daniel Kelterbaum^a, Christina Klein^b, Felix Pirson^d, Andreas Vött^e, Helmut Brückner^{a,*}

^aInstitute for Geography, University of Cologne, Albertus-Magnus-Platz, 50923 Köln (Cologne), Germany

^bInstitute of Geosciences, University of Kiel, Otto-Hahn-Platz 1, 24118 Kiel, Germany

^cHeinrich Schliemann-Institute for Ancient Studies, University Rostock, 18051 Rostock, Germany

^dGerman Archaeological Institute (DAI), İnönü Caddesi 10, 34437 İstanbul, Turkey

^eInstitute for Geography, Johannes Gutenberg-Universität Mainz, Johann-Joachim-Becher-Weg 21, 55099 Mainz, Germany

ARTICLE INFO

Article history:

Available online 14 March 2013

ABSTRACT

During Hellenistic times, when the Pergamian kingdom was prospering, Pergamum was operating an important harbour, used by merchants and military at the city of Elaia. This paper focuses on the development, utilisation and decay of the closed harbour of Elaia, which is discussed in the context of the landscape evolution of the environs of the ancient settlement. Based on geoarchaeological, archaeological and literary evidence, the construction of two harbour moles in order to provide shelter against wave action and enemies can be attributed to the early Hellenistic period. Geoelectric measurements revealed the construction profile of the moles. Coring evidence indicated that together with mole construction, a greater area of the formerly shallow marine and sublittoral terrain was consolidated, most probably to create space for harbour installations. The closed harbour basin was used intensely during Hellenistic and Roman times. Later, continued siltation hindered further usage. In combination with the decline of the city of Elaia in Late Antiquity, this was the reason why the harbour was abandoned. Scenarios for the time of the maximum transgression of the sea around 2500 BC, the early Hellenistic times around 300 BC, and Late Antiquity AD 500, are presented.

© 2013 Elsevier Ltd and INQUA. All rights reserved.

1. Introduction

Many multidisciplinary studies have focused on ancient harbours along the Mediterranean coasts throughout the last decade: the Great Harbour of Ephesus (Kraft et al., 2000, 2007), the harbour of Tyre (Marriner and Morhange, 2006b; Marriner et al., 2007; Morhange et al., 2012), the seaport of Oiniadai (Vött et al., 2007), the harbour of Luni (Bini et al., 2009), the western harbour of Corinth (Morhange et al., 2012), Herod the Great's harbour at Caesarea (Reinhardt and Raban, 1999), and the harbour of Carthage (Gifford et al., 1992), just to mention a few. The importance of the topic is underlined by the fact that in August 2012 the German Research Foundation launched a priority programme to further investigate ancient harbours from Roman Imperial to Medieval times (DFG-SPP 1630).

This paper presents the results of the first geomorphological, geoarchaeological, geophysical, and geochronological research on

the closed harbour of the ancient city of Elaia, which was also Pergamum's principal marine harbour. Its basin is situated at the foot of the city hill in the central northern part of the Gulf of Elaia (Figs. 1 and 2). The harbour was built during Hellenistic times according to historical sources and archaeological evidence. It is the only still visible ruin of Elaia, although it has almost completely been silted up with marine, alluvial and colluvial deposits (Fig. 3). The main objectives of this study are: (i) to investigate the siltation process of the closed harbour of Elaia in space and time; (ii) to compare this process within and around the harbour basin; and (iii) to provide a chronological framework for the construction of the moles from a geoarchaeological point of view.

2. Study area

2.1. Physical setting

The Bay of Elaia is the innermost part of the Gulf of Elaia (modern name: Gulf of Çandarlı). It is located between the Yuntdağ mountain complex to the east and the Karadağ mountain complex

* Corresponding authors.

E-mail addresses: martin.seeliger@uni-koeln.de (M. Seeliger), h.brueckner@uni-koeln.de (H. Brückner).

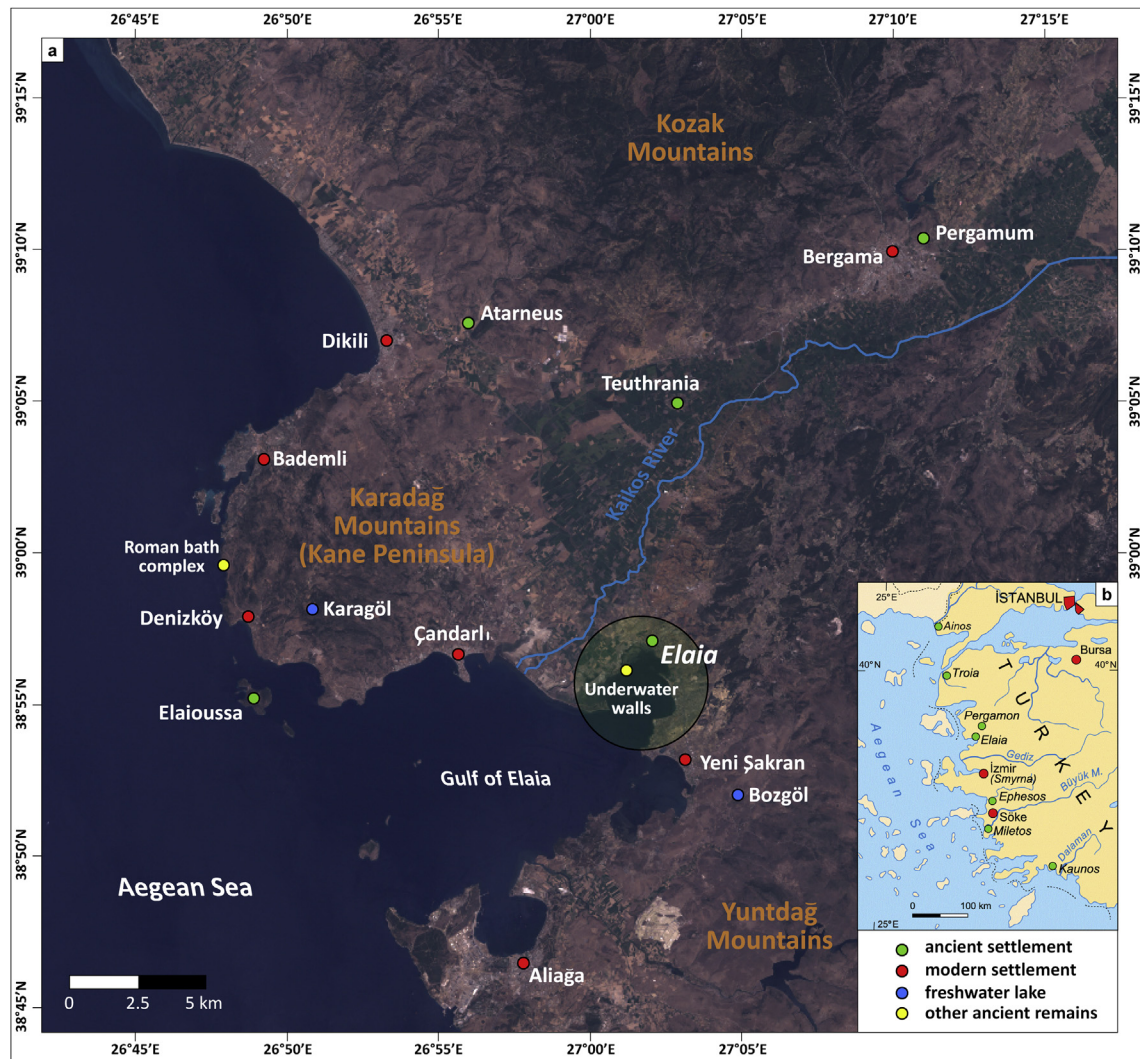


Fig. 1. Research area at the Aegean coast of Turkey. (a) Overview based on Landsat ETM+ 2005 with locations mentioned in the text; (b) General map of western Turkey with a selection of ancient and modern settlements.

on Kane Peninsula to the west (Figs. 1a and 2). The Kaikos River (modern Bakır Çay) debouches into the Aegean Sea between the Kane Peninsula and the Bay of Elaia by forming a cusped delta. The slopes of the Yuntdağ Mountains border the swampy coastal plain to the east and to the north. The latter and the Bay of Elaia are very flat with a seafloor gradient approximating 0.5% (Aksu et al., 1987). A mean tidal range of ~20 cm was inferred for the Bay of Elaia by DGPS. This value is in good agreement with studies from similar embayments in the Eastern Mediterranean (Flemming, 1978; Anzidei et al., 2011). The innermost part of the gulf is protected from stronger wave action, even during winter storms, due to its sheltered position.

The Yuntdağ and Kozak mountain ranges consist of Palaeozoic–Mesozoic granites. The Bay of Elaia is part of the Aegean–Anatolian microplate. With the westward drift of the Anatolian Plate, several E–W oriented rift structures were formed in the late Miocene, such as the Bergama graben, and its tributary, the Zeytindağ graben (Fig. 2). This tectonic ensemble represents a fractured zone which was favourable for the evolution of the Kaikos valley (Vita-Finzi, 1969; Brinkmann, 1976; Aksu et al., 1987; McHugh et al., 2006). The ongoing subsidence is evident from drowned archaeological remains: (i) a Roman thermal bath complex on Kane Peninsula

(Fig. 1a); and (ii) underwater wall structures in the south-western Bay of Elaia, probably dating to Late Roman times (Fig. 4a) (Seeliger et al., 2012).

2.2. Historical and archaeological background

The Pergamian kingdom was highly influential in Asia Minor during Antiquity. Pergamum, its capital city, is often mentioned in contemporary sources together with other important cities including Troy (Troia) and Miletus (Fig. 1b). To date, the city is known for its unique archaeological finds, among others the Pergamum Altar, and for Aelius Galenus, one of the most famous physicians of ancient times (Radt, 1999; Cimik, 2009).

Following the Wars of the Diadochi after Alexander the Great's death in 323 BC, the House of the Attalids came to power in the Kaikos region until 133 BC. Under the reign of Eumenes II (197–159 BC), the Attalids governed the whole western part of modern Turkey (Hansen, 1971; Radt, 1999; Cartledge, 2004; Pirson, 2008; Cimik, 2009).

The 330 m high city hill of Pergamum dominating the surrounding Kaikos plain provided a strategic location for the foundation of a new city. Access to the Mediterranean Sea for traffic and

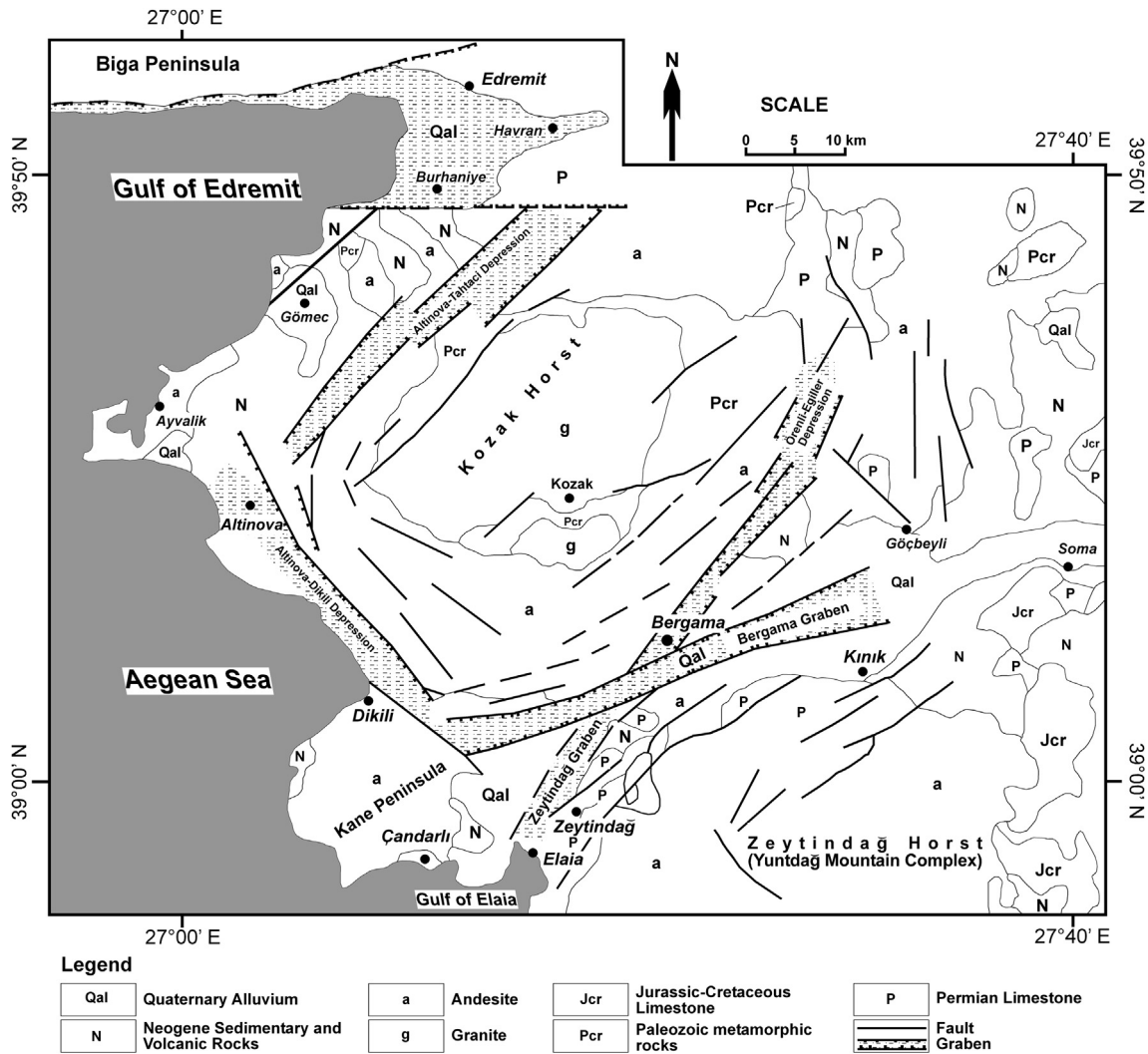


Fig. 2. Structural map of the research area and the surrounding mountain ranges. Source: Altunkaynak and Yılmaz (1998), slightly modified.

trade was provided through the acquisition of nearby Elaia, situated at the Aegean coast 26 km southwest of Pergamum, under Eumenes I (reign: 263–241 BC) (Radt, 1999; Pirson, 2004; Cimac, 2009). Strabo identified Elaia as the commercial harbour of the Pergamenians and as the military base of the Attalids (Strabo (2005), Geographica XIII, 1, 67 and XIII, 3, 5). Further literary evidence as well as archaeological findings confirm the relations between Elaia and Pergamum (Pirson, 2004, 2009).

Thus, Elaia was Pergamum's key portal to the Aegean Sea with regards to traffic, trading, and military actions, although also other naval bases existed, e.g. on the Island of Aegina. By the end of the 3rd century BC, Pergamum's navy encompassed at least 35 warships in the category of the so-called "fives" (*quinqueremes*) (Pirson, 2004). This is quite a small fleet as compared to coexisting naval bases of other poleis, e.g. on the Island of Rhodes or in Piraeus; it explains Pergamum's need for other bases (Pirson, 2004).

In the Archaic and Classical period, Elaia was of only minor importance: Herodotus does not mention the city in his list of the twelve Aeolian cities (Herodotus (2001), Historia I, 149). In the tributary lists of the Attic Delian League between 454 and 425 BC, it is quoted with a very low toll of 1/6 talent. Pergamum, and as a consequence Elaia as well, gradually lost their significance when Ephesus was nominated the capital of the Roman province of Asia in the 1st century BC (Pirson, 2004, 2008). Thus, Elaia's most

prosperous time was clearly confined to the Hellenistic era when the city was under the rule of Pergamum (Pirson, 2008; Cimac, 2009).

A major outcome of the ongoing large-scale ceramic survey was that during Archaic and Classical times the settlement of Elaia was restricted to the central city hill, which is located northeast of the closed harbour (Figs. 3 and 4), and had continuously been settled since the Bronze Age (Pirson, 2010). The situation changed during Hellenistic and Roman times, when many areas surrounding the city hill were settled as well. The fortification wall and an internal wall (*diatichisma*) were erected in the Hellenistic period. The *diatichisma* divided the city into a densely populated area in the northwest around the central city hill and the closed harbour, and a sparsely inhabited area in the southeast. During Late Antiquity, the population of Elaia shrank and was contained within the boundaries of the city hill. Finally, the city was abandoned between the 6th and the 7th century AD (Pirson, 2010).

In addition to its maritime and economic relevance, Elaia played an important strategic role in securing the southern entrance to the Kaikos plain which was the main land of the Pergamenian kingdom. As the foothills of the Yuntdağ mountains reach the sea by creating a steep slope, there is only a narrow passage north of Yeni Şakran (Fig. 1a) that could easily be controlled by the Pergamenian forces based in Elaia (Pirson, 2004). The topographic

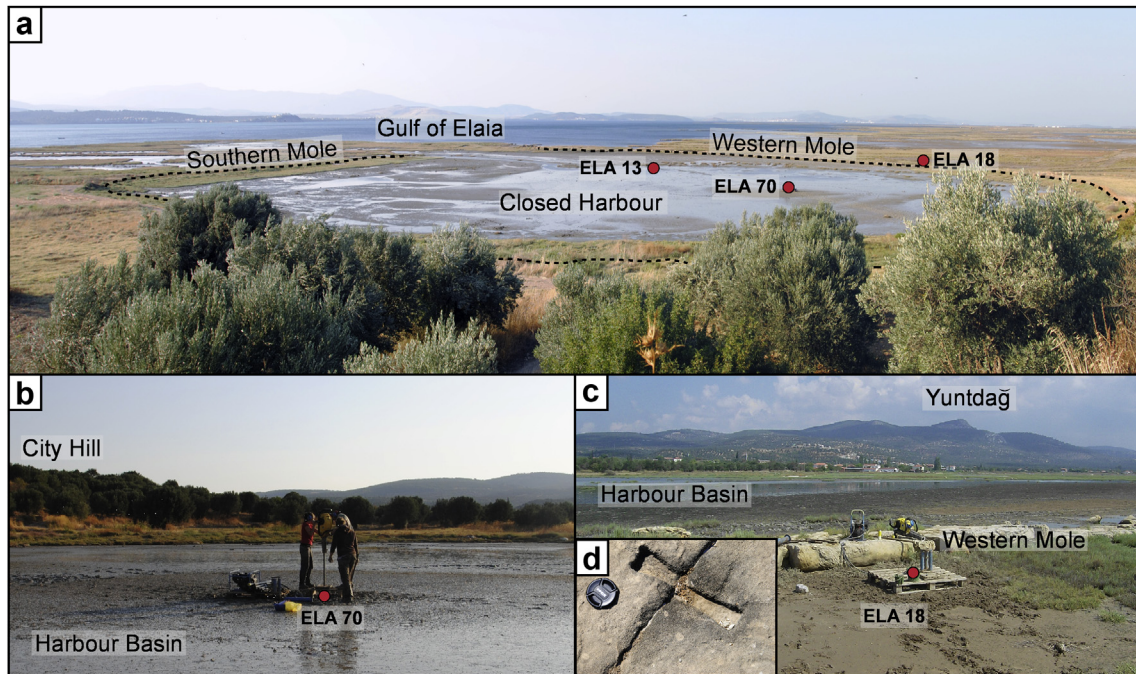


Fig. 3. The closed harbour of Elaia. (a) Overview from the top of the city hill; (b) Location of coring site ELA 70 inside the harbour basin; (c) Western mole with location of coring site ELA 18 outside the harbour basin; (d) Recess for the former wooden dovetail cramp on top of the mole. Photographs: Bartz and Seeliger (2010, 2011).

situation is slightly comparable to that at Thermopylae in Greece (Kraft et al., 1987): a narrow passage flanked by high mountains on the one side and the sea on the other.

Located 18 m higher than the coastal plain, the city hill of Elaia played an important role, at least from the archaeological point of view, as it hosted the major settlement centre from the Bronze Age up to the abandonment of the city in the 6th/7th century AD. The closed harbour basin is located to the southwest of this hill (Figs. 3b and 4a). This harbour was protected against wave action by two moles, a southern one and a western one. The upper section of the western mole can still be seen above the ground. It is constructed from ashlar masonry made of yellowish calcareous sandstone blocks up to 1.70 m × 0.80 m × 0.40 m each. Only the cap of the mole which was always above sea level is visible. Its basement most likely consists of an embankment of dumped rubble and rocks. As soon as this artificial structure had reached the sea surface, the ashlar wall was built on top of it, up to an original height of at least 2 m above the palaeo-sea level. The second mole in the southeast of the harbour basin was detected in the geophysical survey, and its construction style must have been of the same kind (Pirson, 2004, 2010).

The closed harbour was most likely incorporated into the fortification wall of Elaia. The basin had a length of about 200 m from east to west and about 250 m from north to the south; it encompassed an area of approximately 4.8 ha. The seaward entrance was some 45 m wide, and located in the south of the harbour basin, protected from the prevailing western winds (Pirson, 2004, 2008).

The building techniques of the western mole with ashlar joint together by wooden dovetail cramps (Fig. 3d) as well as lack of *opus caementitium* (Roman concrete) as building material date the mole to pre-Roman times. *Opus caementitium* was introduced to Asia Minor not before the middle of the 1st century BC (Ganzert et al., 1984; Waelkens, 1987). As written sources state, Elaia was only of minor importance in the Archaic and Classical periods, as confirmed by the archaeological survey (Pirson, 2010). Therefore, Elaia could not have implemented such a building programme

during those centuries. This leads to the conclusion that the harbour basin with its two moles was most probably constructed in Hellenistic times.

3. Methods

The detailed study of lateral and vertical changes of sedimentary facies from nearshore sediments is a well-established approach to reconstruct palaeoenvironmental variations during the Holocene. To date, 78 terrestrial and semi-aquatic cores have been taken in the area since 2008 to decipher the palaeogeographic evolution and, in particular, to detect coastline changes. This article focuses on three vibracores drilled inside and adjacent to the closed harbour basin of Elaia.

Drilling was done with an Atlas Copco Cobra mk1 vibracorer (Fig. 3b). Closed steel auger heads with 1 m PVC inliner tubes (external diameter: 50 mm) were used for coring ELA 70, while cores ELA 13 and ELA 18 were performed with open steel auger heads (diameters of 60 and 50 mm, respectively). Preliminary sedimentological studies were carried out directly in the field, including grain size, colour (Munsell Soil Color Charts), texture, roundness, and carbonate content (10% HCl) (AG Boden, 2005). Bulk samples for laboratory analyses, as well as macrofossils and ceramic fragments for a later determination were taken from open sediment cores. All coring sites were levelled with DGPS (Leica GPS System 530; lateral and vertical resolution of ≤ 2 cm). The altitude above sea level is based on the local reference system PergSys05, established by the German excavation team of Pergamum in 2005; the values have to be height-corrected by -0.875 m due to an inaccuracy of the reference system (Seeliger et al., 2012).

In the laboratory the sediment samples were air-dried, ground, and sieved to separate the matrix material < 2 mm for further analyses. The granulometry was measured with a laser particle sizer (Beckman Coulter LS13320) after the removal of the organic content with H_2O_2 . For the calculation of grain-size parameters after Folk and Ward (1957), the GRADISTAT software (Blott and

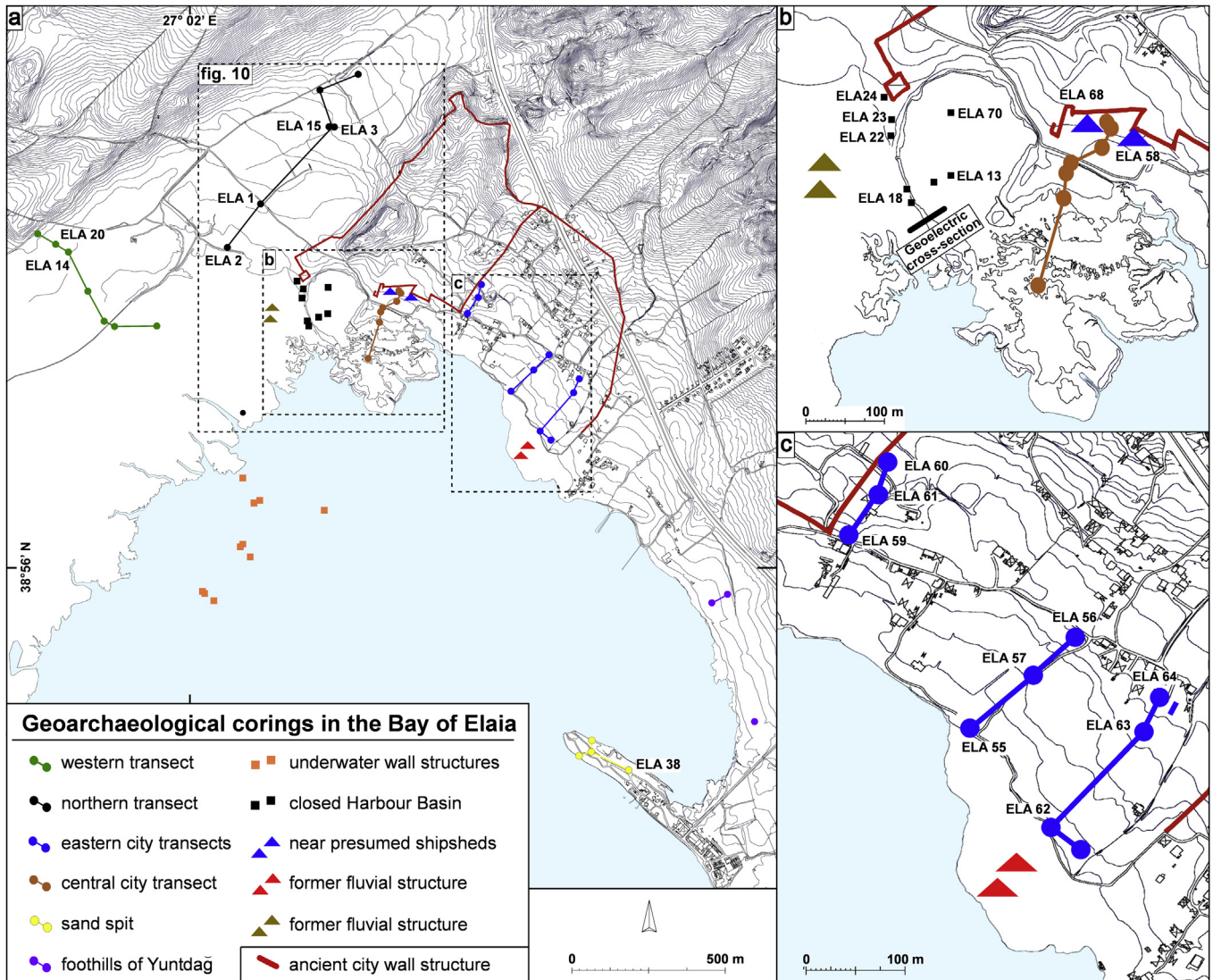


Fig. 4. Location of vibracores carried out in the Bay of Elaia 2008–2011. The maps are based on DGPS data levelled by the Pergamum excavation. (a) Synoptic view with the area of the city of Elaia; (b) Cores in the area of the so-called closed harbour; (c) Cores in the eastern part of Elaia.

Pye, 2001) was applied. Carbonate content was measured by a Scheibler device. The loss on ignition (LOI) was determined by oven-drying the samples at 105 °C for 12 h, and ignition in an annealing furnace at 550 °C for 4 h (Beck et al., 1995). The accuracy of the LOI parameter is widely discussed because two chemical processes may cause errors (Mook and Hosin, 1982; Heiri et al., 2001; Barillé-Boyer et al., 2003): the possible loss of CO₂ from carbonates consisting of inorganic material (Salehi et al., 2011), and the loss of structural water from clay minerals (Dankers and Laane, 1983). Both result in weight reduction not caused by loss of organic matter. A subsequent correction of the LOI values was not done in this study.

Measurements of the electrical conductivity were performed in an aqueous solution consisting of 15 g of sediment and 75 ml distilled water with a glass electrode (Mettler Toledo InLab[®]731-2m) (Beck et al., 1995).

A portable XRF spectrometer (Niton XI3t 900 GOLDD) was used to determine total amounts of 25 elements with a vertical resolution of several decimetres (in cases of ELA 13 and 18) and 5 cm (ELA 70), respectively. Sodium (Na), an indicator for marine environments, is not detected with this XRF technique; it was measured by

using atomic absorption spectrometry (AAS; A-Analyst 300 by Perkin Elmer).

These multi-proxy geochemical and granulometric analyses were primarily carried out in order to support the facies determination (cf. Ernst, 1970; Vött et al., 2002, 2004; Brückner et al., 2005, 2006, 2010a; Engel et al., 2009; Niwa et al., 2011).

Earth's electrical resistivity was determined with the RESECS multi-electrode system in order to detect the thickness and shape of the central harbour pier of Elaia. On profiles with a length of 47 m and an electrode spacing of 1 m, measurements with several electrode configurations such as Dipole–Dipole, Wenner and Schlumberger were done. The apparent electrical resistivity was determined as a function of the electrode geometry by the measuring instrument. Using the inversion software RESINV2D (Loke and Barker, 1995), the resistivity–depth distribution for each profile was inverted from the field data.

¹⁴C-AMS age estimates based on wood, charcoal, seagrass, and marine gastropods were performed in the Center for Applied Isotope Studies (CAIS) of the University of Georgia at Athens (USA). For calibration, the Calib 6.1.1 software was applied with a marine reservoir effect of 390 ± 85 years and a ΔR of 35 ± 70 years (Siani

et al., 2000). These ages are stated in calibrated years BC, AD, or BP, with a 2σ -standard deviation (Table 1). As the spatio-temporal variation of the marine reservoir effect for the Aegean Sea is still not known, the ^{14}C -ages of marine carbonates are estimates only. Diagnostic ceramics helped to improve the local chronology.

entrance ($38^{\circ}56'32.18''$ N, $27^{\circ}02'17.76''$ E; total depth: 10 m; elevation: 0.18 m b.s.l.; Figs. 3a, 4b and 6). In contrast to ELA 70, the lower units 1 (bedrock) and 2 (open marine environment) were not reached at this site. The lower 5 m of ELA 13 (very homogeneous clayey silts) are not shown in Fig. 6. Between 10 m and 3.10 m b.s.,

Table 1

Radiocarbon data set. AMS- ^{14}C measurements were carried out at the Center for Applied Isotope Studies (CAIS) of the University of Georgia at Athens (USA).

Sample ID	Lab no. (UGAMS)	Material	$\delta^{13}\text{C}$ (‰)	Libby-age	Cal BC/AD (2σ)	Cal BP (2σ)
ELA 13/10HK	6038	Charcoal	-26.4	1640 ± 25	340–532 AD	1418–1610 cal BP
ELA 13/13HK	6037	Charcoal	-27.5	1750 ± 25	283–381 AD	1569–1719 cal BP
ELA 13/22H	6036	Wood	-27.4	2250 ± 25	391–209 BC	2158–2340 cal BP
ELA 18/7HK	6031	Charcoal	-24.5	1740 ± 25	240–381 AD	1569–1710 cal BP
ELA 18/9HK	6030	Charcoal	-25.0	1730 ± 25	245–384 AD	1566–1705 cal BP
ELA 70/66HK	11,130	Charcoal	-27.0	1960 ± 30	39 BC–121 AD	1829–1988 cal BP
ELA 70/80H	11,131	Seagrass	-18.2	2680 ± 30	647–178 BC	2127–2596 cal BP
ELA 70/122H	11,132	Seagrass	-17.7	5920 ± 30	4530–4204 BC	6153–6479 cal BP
ELA 70/144F	11,133	Marine gastropod	-0.7	7040 ± 30	5692–5422 BC	7371–7641 cal BP

4. Results

The coring in and around the closed harbour of Elaia was carried out in order to contribute its history with geoarchaeological evidence. In this context, the timing of the construction of the moles and the later siltation process were of particular interest. Here, cores ELA 70 and ELA 13, both from inside the harbour basin, and ELA 18 directly outside the western mole are described (Figs. 3 and 4).

4.1. Sediment core ELA 70 from inside the harbour basin

ELA 70 was cored inside the harbour basin, in the direct vicinity of the ancient city ($38^{\circ}56'35.34''$ N; $27^{\circ}02'19.04''$ E; total depth: 9 m; elevation: 0.12 m b.s.l. [below present mean sea level]; for location see Figs. 3a,b and 4; for profile see Fig. 5). Neogene bedrock, compact yellowish calcareous sandstone, was reached at 8.03 m b.s. (below surface) (unit 1).

Between 8.03 m and 4.38 m b.s., unit 2 occurs, a dark to olive grey silty sand with graded bedding of pebbles at the base. The electrical conductivity shows strong variations between 4 and 27 mS; the values increase upwards to 5.08 m b.s. The Ca/Fe ratio shows remarkable fluctuations as well, with a decreasing upwards trend. The whole section is interspersed with seagrass (*Posidonia oceanica*) as well as broken shells, e.g. *Dosinia lupinus*, and gastropods. Three radiocarbon ages provide a chronological frame for this part of the core: a marine gastropod at 7.82 m b.s. yielded an age of 5692–5422 cal BC (7371–7641 cal BP; sample ELA 70/144F), *P. oceanica* at 6.72 m b.s. an age of 4530–4204 cal BC (6153–6479 cal BP; ELA 70/122H), and *P. oceanica* at 4.57 m b.s. was dated to 647–178 cal BC (2127–2596 cal BP; ELA 70/80H). The wide dating range of the latter sample is due to two facts: (i) The 2 sigma standard deviation is given which renders a confidence interval of 95.4%; and (ii) unfortunately, in this age range the ^{14}C -calibration curve has a plateau.

Between 4.38 m b.s. and the surface light grey clayey silts form unit 3. The mean grain size decreases to 30 μm . The Ca/Fe ratio drops to very low values as well, showing less variation than below. The electrical conductivity starts at high levels (30 mS), but decreases to 5 mS. A piece of charcoal at 3.77 m b.s. was ^{14}C -dated to 39 cal BC–121 cal AD (1829–1988 cal BP; ELA 70/66HK).

4.2. Sediment core ELA 13 from inside the harbour basin

Coring ELA 13 was carried out inside the harbour basin, 37 m to the east of the western mole and not far from the 45 m wide harbour

entrance. Numerous plant remains occur, with a clustering of seagrass (*P. oceanica*) at 6.75 m and 5.65 m b.s. This is reflected in the high LOI (12–13%). A piece of wood at 6.75 m b.s. dates to 391–209 cal BC (2158–2340 cal BP; ELA 13/22H). The appearance of habitat-specific bivalve and gastropod species (e.g., *Cerastoderma glaucum*) indicates a lagoonal environment.

Unit 3b (3.10 m and 1.80 m b.s.) consists of silty fine sand. The decreasing Na/Fe ratio correlates with decreasing LOI. Two pieces of charcoal at 2.55 m b.s. (283–381 cal AD, 1569–1719 BP; ELA 13/13HK) and at 1.92 m b.s. (340–532 cal AD, 1418–1610 cal BP; ELA 13/10HK) give a chronological framework.

The top of the section (unit 3c) is grey to greenish grey clayey silt and silty clay. In contrast to unit 3b, LOI increases (10–18%). The Na/Fe ratio shows remarkable alterations (0.6–1.2). The sedimentation pattern corresponds to the modern nearshore conditions in the basin of the closed harbour.

4.3. Sediment core ELA 18 from outside the harbour basin

ELA 18 was drilled outside the closed harbour basin, 2 m next to the western mole ($38^{\circ}56'31.45''$ N; $27^{\circ}02'16.66''$ E; total depth: 3 m; elevation: 0.18 m a.s.l.; Figs. 3a, c, 4b, 7). It was performed to render particular information about the characteristics of the mole's construction and foundation.

Unit 4 (3.00–1.85 m b.s.) is remarkably inhomogeneous: angular and rounded stones of up to 5 cm, rounded and weathered ceramic fragments, with almost no fine-grained matrix material. The macroflora is composed of *P. oceanica*, the macrofauna of shell debris of different marine mollusc species.

From 1.85 to 1.36 m b.s. is a dark grey, slightly silty sand (unit 5). The amount of plant remains, shell debris and other organic matter decreases towards the top. Pieces of charcoal at 1.75 m b.s. date to 245–384 cal AD (1566–1705 cal BP; ELA 18/9HK), and at 1.38 m b.s. to 240–381 cal AD (1569–1710 cal BP; ELA 18/7HK).

Above 1.36 m b.s., the mean grain size drops to 6–9 μm . This sequence of clayey silt is in parts intercalated with lenses of slightly clayey sand. Low Na/Fe ratios and relatively high values of LOI (6–7%) characterise unit 6.

5. Geoelectric cross-section of the western harbour mole

Geoelectric cross-sections were measured to detect the thickness and the shape of the mole's basement. One is presented in Fig. 8 (length: 47 m, max. depth of penetration: approx.

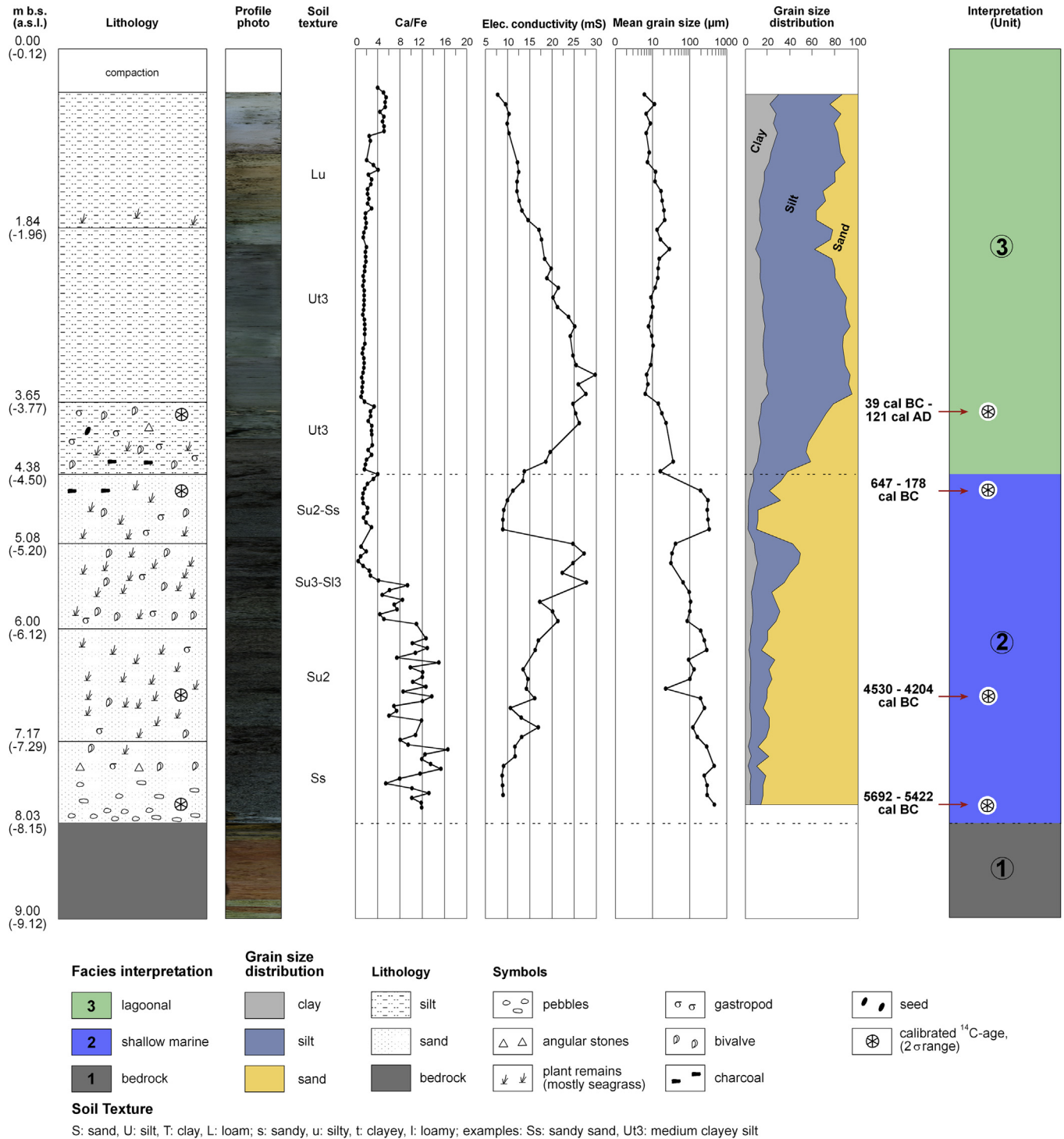


Fig. 5. Stratigraphical record and facies distribution of ELA 70, a vibracore inside the basin of the closed harbour (27°02'19.04" E, 38°56'35.34" N; ground level: 0.12 m below sea level). Facies: 1 = bedrock; 2 = shallow marine; 3 = lagoonal. For location see Figs. 3a,b and 4b.

9 m b.s.). The blocks of the mole are located in the central position of the profile. The calculated electrical resistivity has a bandwidth of less than 0.1–2 Ωm. Low resistivity (<0.256 Ωm) occurs at the outer parts of the cross-section near the surface. The highest resistivity (>1.58 Ωm) is found in the centre creating a zone of nearly 8 m lateral and 2 m vertical extension between approx. 2 m and 4 m b.s.. The measured resistivity values are very low compared with land measurements because the electrical resistivity is strongly influenced by the salty pore water.

6. Discussion

6.1. Coring ELA 70 from the centre of the harbour basin

Neogene bedrock encountered in ELA 70 at 8.03 m b.s. (unit 1; Fig. 5) forms the base of numerous cores in the study area, e.g. ELA 20, 58 and 63 (Fig. 4). It is calcareous sandstone which was used for the construction of the harbour moles (Figs. 3c and 8a). The overlying unit 2 represents a shallow marine facies with wave

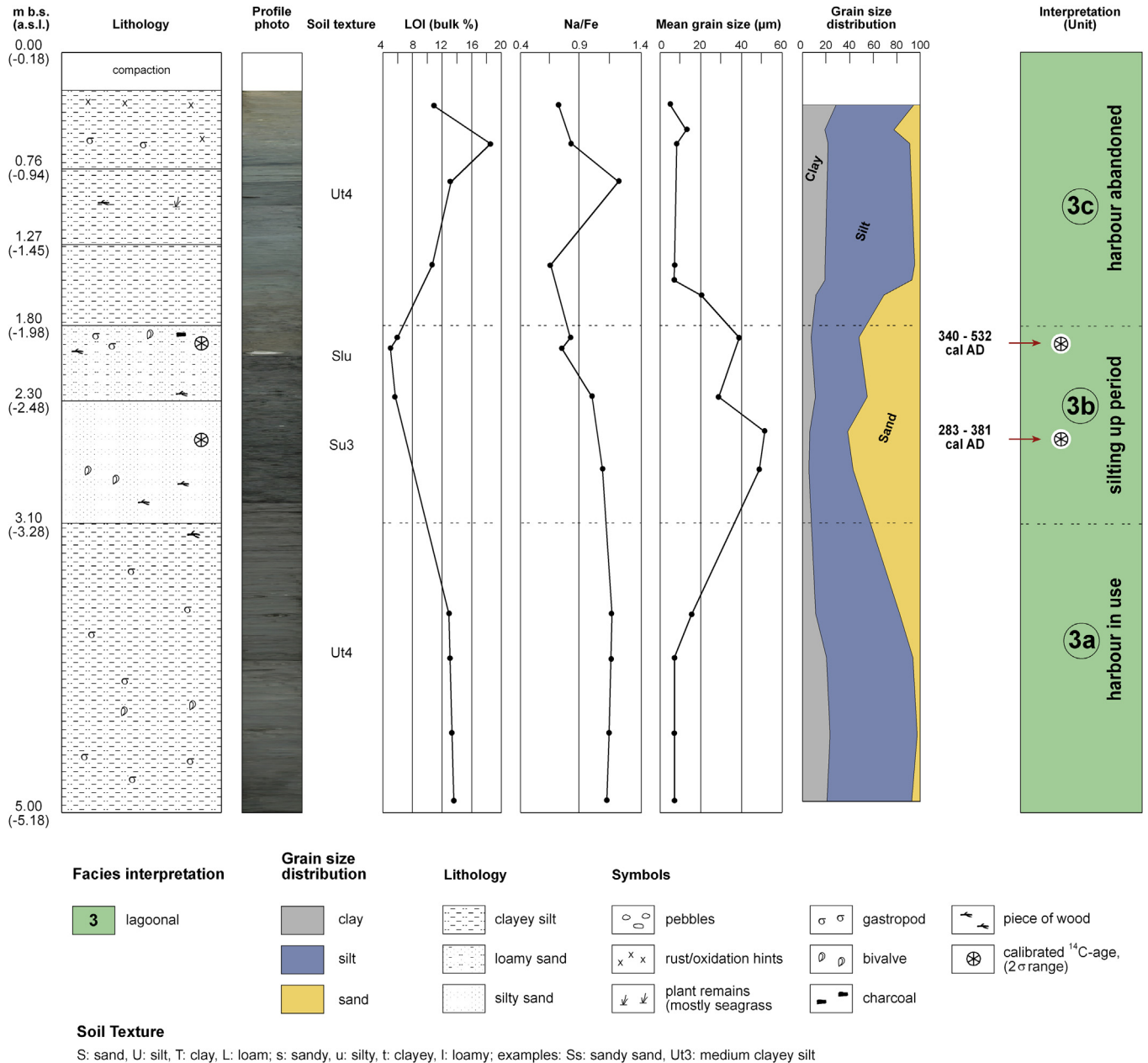


Fig. 6. Stratigraphical record and facies distribution of ELA 13, a vibrocore inside the basin of the closed harbour, near the entrance (27°02'17.76" E, 38°56'32.19" N, 0.18 m b.s.l.). Facies: 3a = lagoonal (harbour in use); 3b = lagoonal (silting up period); 3c lagoonal (silted-up, present situation). ELA 13 was cored down to 10 m b.s.; here only the upper 5 m are shown. For location see Figs. 3a and 4b.

action, based on the comparatively coarse grain size and the abundant occurrence of seagrass (*P. oceanica*) which is also reflected in LOI peaks (organic contents of >20%; cf. Short and Wyllie-Echeverria, 1996; Montefalcone, 2009). As in this context, Ca is more indicative of marine and Fe of terrestrial environments (Vött et al., 2002), high Ca/Fe values support the marine origin of this sedimentary unit. Fluctuating values of the electrical conductivity reflect minor grain size variations and point to local changes of the sublittoral environment. The post-glacial sea-level rise, represented by the base of unit 2, dates to 5692–5422 cal BC (7371–7641 cal BP). This age gives an index point for the palaeo-sea level: around the middle of the 6th millennium BC it was at ~8 m b.s.l., which is roughly in agreement with other sea-level curves of the eastern Mediterranean (Brückner et al., 2006, 2010b).

With continued transgression and increasing water depth, the littoral environment turned into a shallow marine one. This milieu of deposition prevailed at least until the 7th century BC, most likely even longer.

A definite facies change occurs at the contact between units 2 and 3, 4.38 m b.s. (4.50 m b.s.l.): the remarkable decrease in the mean grain size indicates the abrupt change to a low-energy wave climate. In addition, decreased Ca/Fe ratios document the increased terrestrial influence. For grain sizes of <30 µm, the total amount of the particle surface area is enlarged, which results in high values of electrical conductivity (Niwa et al., 2011).

The abrupt transition from unit 2 to unit 3 reflects the change from open marine to harbour-associated lagoonal conditions. It dates to 647–178 cal BC (2127–2596 cal BP). The wide dating range is due to a plateau of the radiocarbon calibration curve. However, the given

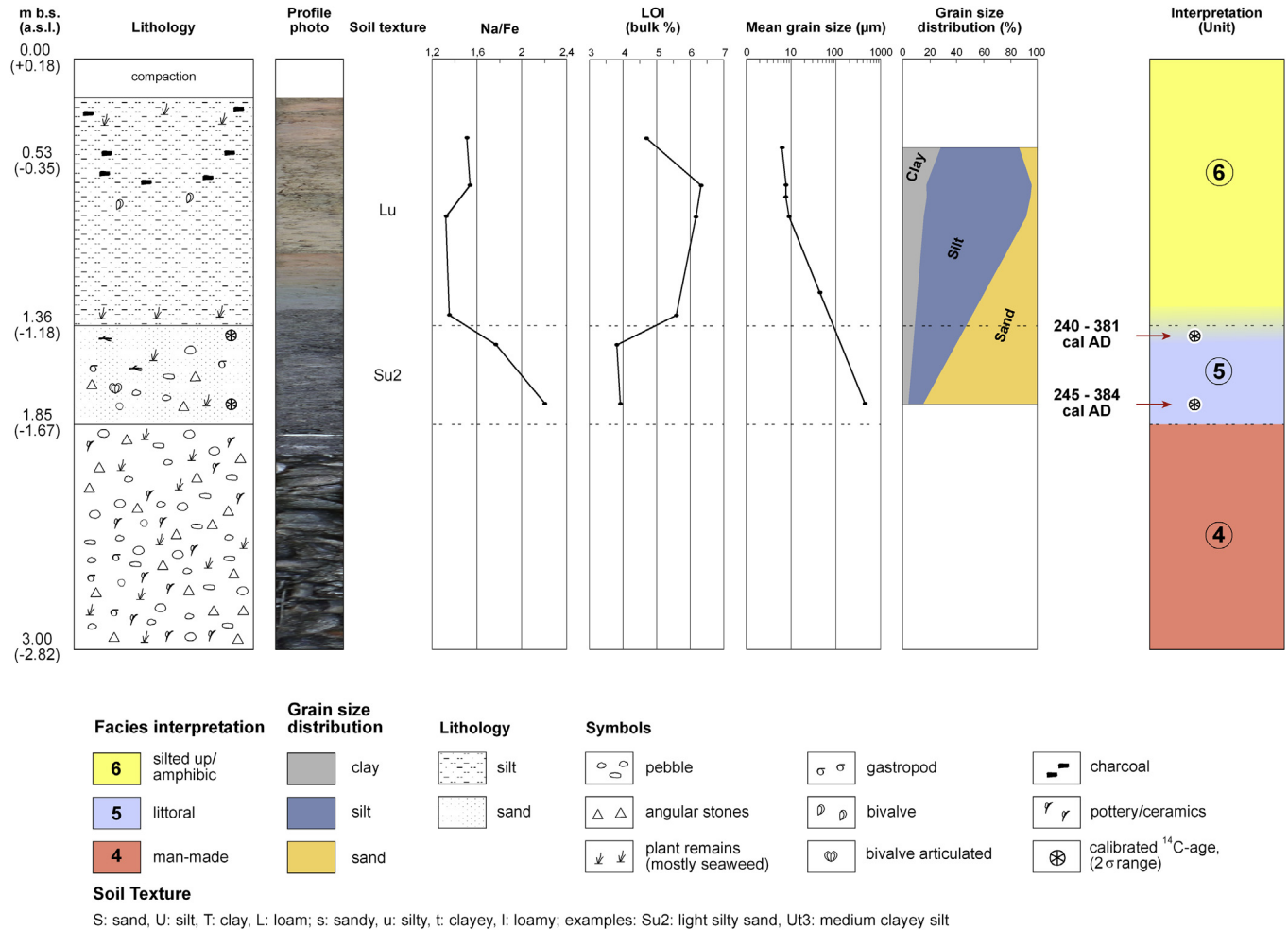


Fig. 7. Stratigraphical record and facies distribution of ELA 18, a vibracore outside the basin of the closed harbour, directly at the western mole (27°02'16.66" E, 38°56'31.45" N, 0.18 m a.s.l.). Facies: 4 = human-made basement of the mole; 5 = littoral; 6 = nearshore. For location see Figs. 3a,c and 4b.

interval does include the early Hellenistic period, which (for archaeological reasons) was the time of the construction of the mole.

The sedimentary facies sequence of ELA 70 fits well to the Ancient Harbour Parasequence (AHP) postulated by Marriner and Morhange (2006a) derived from a summary of different harbour locations, most of them situated in the southern Mediterranean, especially in Tyre's northern harbour (Marriner and Morhange, 2006b). In contrast to Marriner and Morhange (2006a, 2006b) the onset of the postulated "transgressive contact" is 1500 years earlier in Elaia; this might be explained by the contrast between the southern Mediterranean sites and the more northern ones such as ancient Elaia.

6.2. Coring ELA 13 from inside the harbour basin

In contrast to ELA 70, the entire facies of profile ELA 13 can be classified as lagoonal (Fig. 6). Internal changes of the geochemistry and granulometry allow for the differentiation of three subunits.

The grain size and the homogeneity of unit 3a are hints of a quiescent sedimentary environment. The interpretation of a lagoonal environment is supported by the presence of indicative fauna, such as *C. glaucum*, a euryhaline cockle colonizing muddy to sandy grounds in brackish lagoons and estuaries up to water depths of 10 m (Dance, 1977; Poppe and Goto, 2000; Nikula and Väinöla, 2003). The generally low Na/Fe ratio can be interpreted as terrestrial influence from the drainage area of the harbour basin.

According to the ¹⁴C age at 6.75 m b.s., the middle part of this unit was deposited in late Classical to early Hellenistic times (391–209 cal BC, 2158–2340 cal BP).

In unit 3b, still a lagoonal facies, siltation was accelerated as compared to unit 3a. Low Na/Fe ratio values, in particular towards the top, point to an increased terrestrial influence. The coarser average grain size is evidence of (a) stronger wave action due to the shallower water depth, and/or (b) the input of coarser sediment.

The uppermost silty to clayey layer (unit 3c) represents a semi-terrestrial environment; the sedimentation pattern corresponds to the modern nearshore conditions. Nowadays, the basin is periodically flooded during high tides and storms; it may, however, nearly run dry during low tides and phases of high insolation. Due to its extreme flatness, the silted-up harbour of Elaia is one of the rare locations along the shores of the Mediterranean where the effects of the tides, although only 20–30 cm, can be observed daily. Occasionally, it receives terrestrial/alluvial input, especially during the rainy season in winter.

6.3. Western harbour mole – ELA 18 and the geoelectric cross-section

Due to its characteristics, unit 4 (Fig. 7) is assumed to be an anthropogenic infill related to the western harbour mole. It was built in order to protect ships against wave action and attacks by enemies, and to facilitate an easier handling of trade goods.

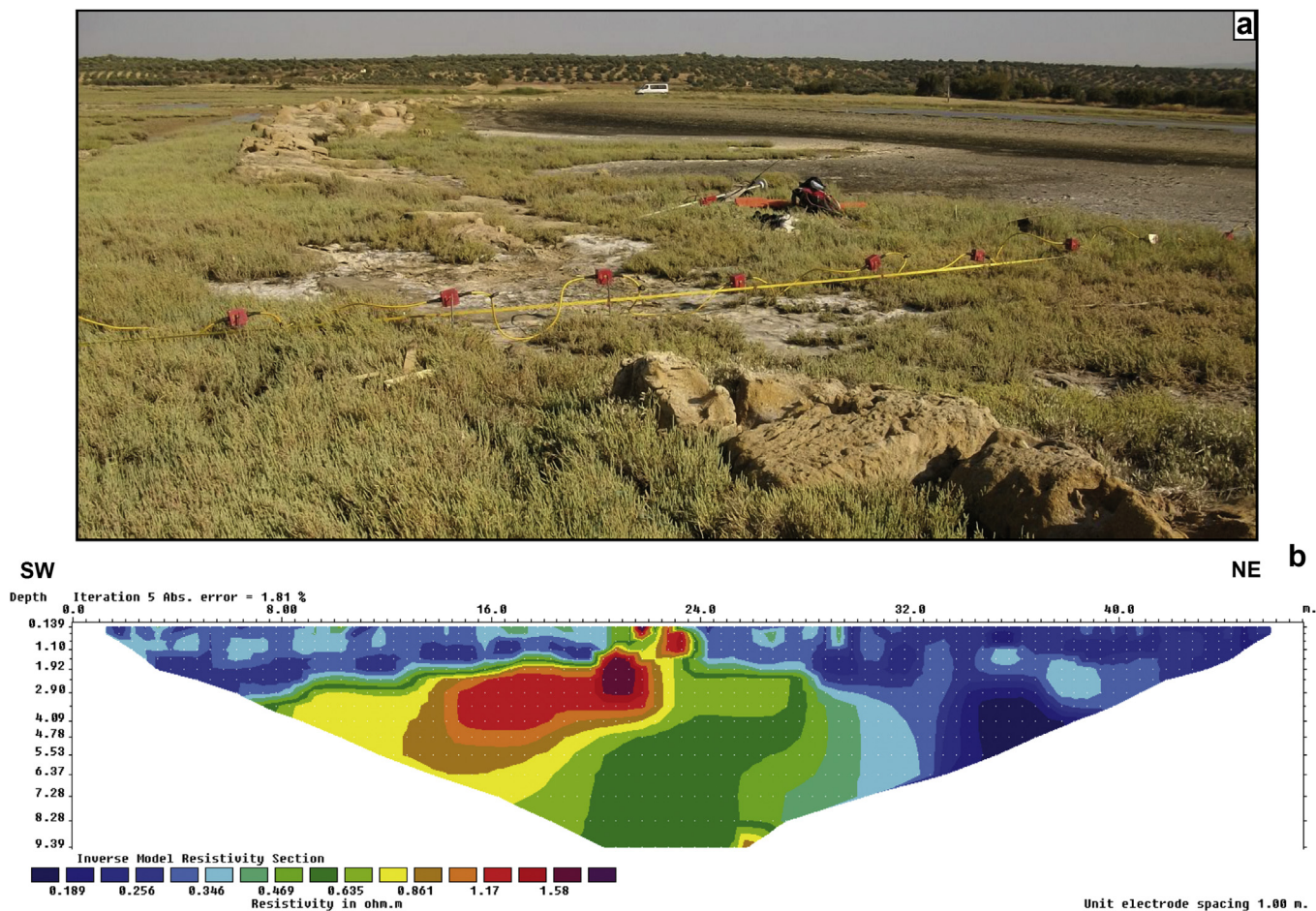


Fig. 8. Earth resistivity transect crossing the western harbour mole. Wenner–Schlumberger electrode arrangement, electrode spacing 1.0 m. (a) Transect with electrodes perpendicular to the western mole. The harbour basin is visible to the right of the mole. For location of transect see Fig. 4b. Photograph: Erkul (2010). (b) Simplified inverse model section of earth resistivity measurements. Source: Klein and Erkul (2010).

Posidonia oceanica and shell debris indicate an environment similar to the present one found on breakwaters and piers. Due to abrasion, the artefacts are well rounded. Several fragments of pottery and ceramics date to the Hellenistic – Roman era.

In the geoelectrical model, the parts with a relatively high resistivity (red colours in Fig. 8b) can be interpreted as the basement of the mole. Its width exceeds 8 m. The western, i.e. seaward, side is most likely a massive construction from a little less than 2 m down to about 4 m b.s. It is sloping gently to the west. In sharp contrast, the other side of the mole drops down like a plunging cliff. This is the inner side of the mole where ships could be moored. The geoelectric image also suggests that the top of the mole was dislocated. In the profile, the uppermost boulders are now lying in the mud of the silted-up harbour basin (Fig. 8a).

Unit 5 (Fig. 7) is a littoral facies with a high amount of sand and rounded components. The uppermost unit 6 is of nearshore origin: the lamination points to at least two different processes typical of a salt marsh. In particular during winter storms, the salt marsh area is flooded by the sea, resulting in the deposition of coarser material, mostly clayey sand. In contrast, long lasting dryness during the summer months causes the deposition of fine clayey silt layers. The present vegetation is made up of halophytes, such as *Salicornia* sp. In summary, units 5 and 6 are evidence of siltation after the harbour had been abandoned. The top of the mole's basement has since been covered by ~1.80 m of sediment. The setting is evidence that during the construction of the mole in the Hellenistic period, sea level was about 1.80 m lower than today.

6.4. Harbour area – human-made coasts

A synoptic view of all of the cores in the area under consideration shows that during Early Hellenistic times the marine embayment reached several hundred metres further to the north than it does today (cf. Brückner and Seeliger, 2009; Brückner et al., 2010a). Therefore, together with the moles part of the adjacent harbour area had to be built on shallow marine terrain (Figs. 9 and 10). Thus, there was a definite need for solid constructions. Moreover, they had to be thick enough so that the harbour could host ships.

The two moles are not the only anthropogenic structures of the closed harbour. The northern area adjacent to the harbour basin is also partly made of intentionally dumped material. It was done in order to consolidate the shallow marine and muddy terrain and create a solid ground for the erection of harbour-related facilities including warehouses and magazines. This interpretation is based on several cores, three of which are presented in Fig. 9 (locations in Fig. 4b). The anthropogenic infill is so massively consolidated that it could not be penetrated: nowhere was the marine strata below reached. It is definitely more than 2.5 m thick, most probably much thicker (Fig. 9). Further geophysical prospecting is needed in order to understand the 3D distribution of the infill.

7. Synthesis of the history of the closed harbour

Historical and archaeological evidence points to a construction of the moles in Early Hellenistic times. This is confirmed by

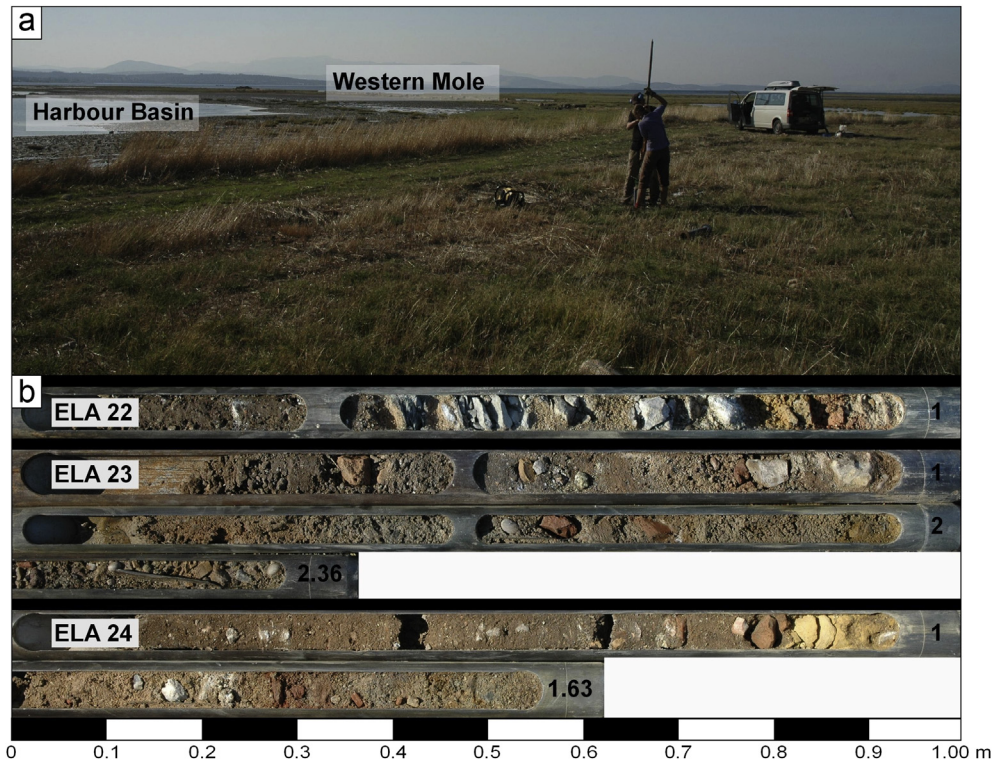


Fig. 9. Overview of the consolidated harbour area. (a) The infilled area, the harbour basin and the western mole; (b) Photographic documentation of the sediment cores ELA 22–24 (for location of cores see Fig. 4b). Due to the occurrence of angular and sharp stones as well as bricks, a strong consolidation of this area is evident. In each case, coring progress was stopped by large boulders. Photographs: Brückner and Seeliger (2009, 2010).

diagnostic ceramics in the basement of the moles. In combination with the results of the geoelectric profile, a detailed image can be given (Fig. 8). The basement has a width of nearly 8 m and a thickness of more than 2 m (1.80 m to >4 m below surface). Its asymmetric shape helped to buffer the wave energy on the seaward side, and the plunging cliff-like profile on the harbour side created opportunities for ships to be moored.

A set of cores directly north of the harbour basin revealed that this area was intentionally filled-in as one measure for the construction of the harbour. Very large boulders were deposited in order to consolidate the terrain, most probably in order to create space for loading and unloading of ships, and erect facilities for storing the goods (Figs. 9 and 10).

ELA 70 (Fig. 5) shows the definite change from a shallow marine (unit 2) to a lagoonal (unit 3) facies as a consequence of the construction of the moles. From that time, the harbour basin was connected to the open Mediterranean Sea by the 45 m wide port entrance only, resulting in a quiescent depositional environment.

Elaia's harbour was in use during Hellenistic and Roman times; it was gradually given up during late Antiquity. The siltation process is illustrated by the stratigraphical succession of ELA 13. Moderate sedimentation rates in the lower part (unit 3a) are followed by an increased sedimentation (6.9 mm/a) from 3.10 m b.s. upwards, some time before 283–391 cal AD (1569–1719 BP); sedimentary conditions similar to the present ones have existed since 340–532 cal AD (1418–1610 cal BP) with approximately 1.2 mm/a. The ^{14}C -age of ELA 13/22H (391–209 cal BC, 2158–2340 cal BP), which does not fit to this interpretation, can be explained as follows: (i) re-deposition of older material; or (ii) post-depositional contamination, e.g. by humic and fulvic acids (Törnqvist et al., 1992; Housley et al., 2012).

If the top of the mole's basement was more or less at sea level during construction in Hellenistic times, the difference to the

present sea surface is approx. -1.80 m. As a consequence a maximum mean water depth of approximately 2.60 m in the northern part of the harbour basin can be estimated for that time. This calculation takes into account that (i) at the ELA 70 site the abrupt transition between shallow marine and lagoonal facies is at 4.38 m below surface (4.50 m below present mean sea level); and (ii) sea level was ~ 1.80 m deeper than today. The tidal range is about 20–30 cm.

The original height of the mole may have been reduced by erosion/weathering, destruction of the coping blocks or by subsidence. As normally the draught of Hellenistic and Roman ships did not exceed 1.60 m, the postulated water depth was sufficient for them to make use of the harbour (Coates, 1987; Beltrame and Gaddi, 2007; Marriner and Morhange, 2007; Auriemma and Solinas, 2009).

The transition between the man-made mole basement (unit 4) and the littoral facies on top (unit 5) is dated to ca. 245–384 cal AD (1566–1705 cal BP). This is the time in late Antiquity when the harbour was given up. By then, despite the higher sea level as compared to the construction time, the littoral sediments could cover a possible walkway behind the mole top. A considerable amount of sediment was deposited in a short time, since the statistically identical ^{14}C -ages from unit 5 are 0.37 m apart from each other. The fine-grained unit 6 is an expression of the continued siltation process outside the closed harbour basin.

According to the radiocarbon ages of unit 5 in profile ELA 18, the siltation outside the harbour started sometime between the second half of the 3rd century and the end of the 4th century AD. As the beginning of strong siltation inside the basin was dated to 283–391 cal AD (1569–1719 BP; ELA 13/13HK), more or less simultaneous siltation is evident. The accelerated accumulation of sediments inside the harbour was due to the fact that the catchment area of the harbour basin is quite large, i.e., a relatively great

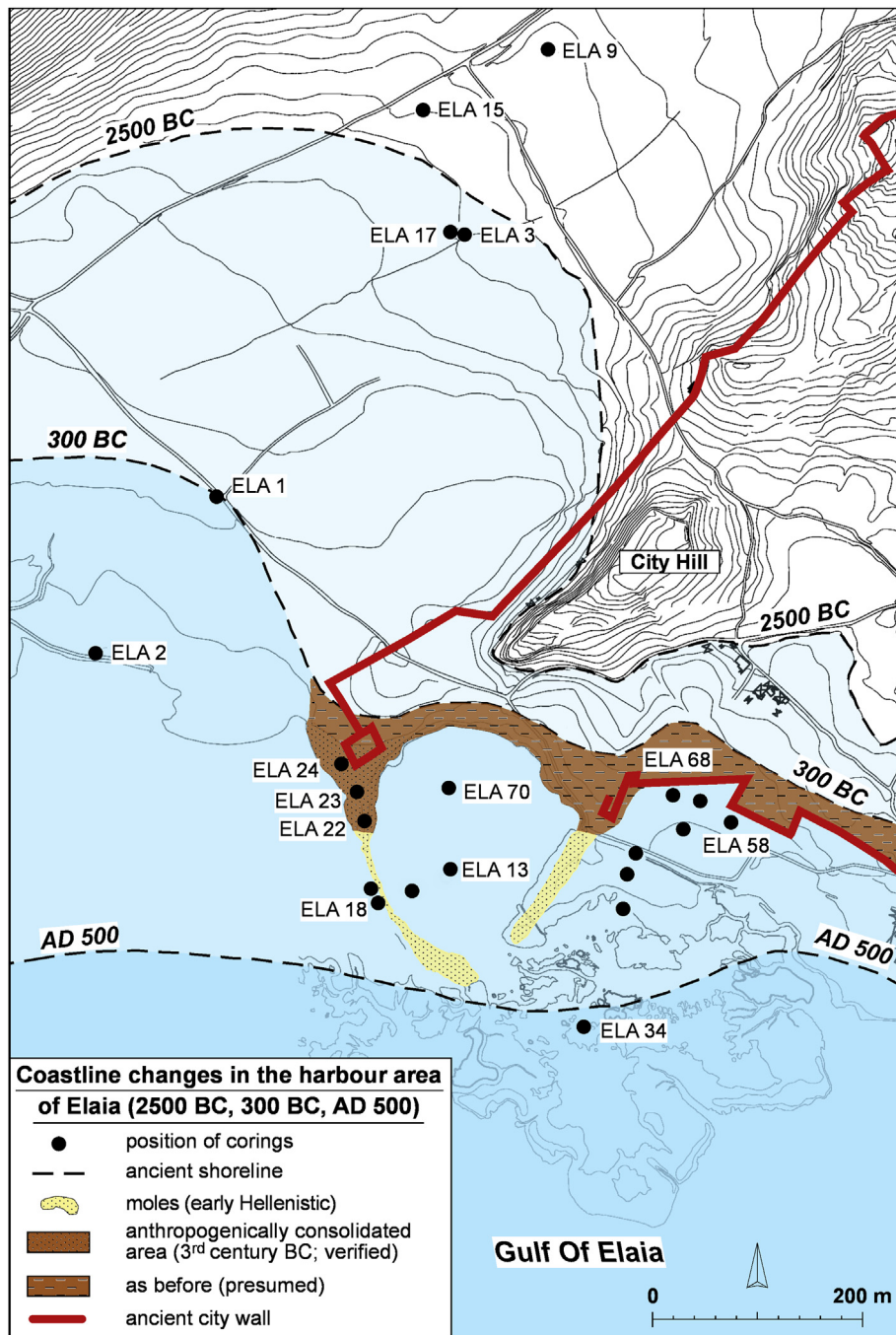


Fig. 10. Estimated coastline changes in the area of the closed harbour of Elaia 2500 BC, 300 BC and 500 AD. The palaeogeographies are based on the results of this paper, as well as on Brückner and Seeliger (2009) and Brückner et al. (2010a). For location of cores see Fig. 4.

area drains into it, whereas the siltation of the outside area was dependent on occasional strong flooding episodes with terrestrial input from the adjacent slopes and from sedimentation by marine currents.

From studies of nearby ancient settlements, it is well known that human impact is closely linked to increasing rates of erosion and sedimentation. The Great Harbour of Ephesus, for example, was endangered by siltation at the latest in Roman Imperial times when a canal was built as a reaction to the progressive siltation of the prograding Caystros delta (modern Küçük Menderes) (Kraft et al., 2000, 2007). From coring evidence, Brückner et al. (2006) concluded that the Theatre Harbour of Miletus was dredged

during the 1st/2nd century AD, when the theatre was renovated. As for Elaia's harbour, however, no evidence of dredging has been detected as yet: there is no erosional disconformity in the sediment columns of the cores or mixing of archaeological layers (Marriner and Morhange, 2006b). Other than for Ephesus (Kraft et al., 2007), no literary evidence of dredging is known for Elaia. The ^{14}C dating results do not show age inversions.

8. Tectonic movement vs. sea level rise?

Little is known about the subsidence rate of the Bergama and Zeytinadağ graben. Based on air-gun seismic reflection data gained

on Pleistocene deltaic sediments in the Bay of Çandarlı, Aksu et al. (1987) stated a subsidence tendency of the submarine basin and in further consequence of the graben complex in total of approx. 1 m per 1000 years. Two reliable sea level indicators are presented in this paper, but both are opposed to the subsidence tendency calculated by Aksu et al. (1987). The transgressive contact occurs in Elaia's closed harbour basin at a depth of ca. 8 m b.s.l., dating to 7371–7641 cal BP. Assuming a subsidence of 1 m/ky, corresponding to 7.5 m since the time of the transgressive contact, sea level would have been more or less constant over the past seven millennia and a basin used for shipping would not be conceivable. This same logic applies to the second reliable sea-level marker: the harbour moles. During their construction in Hellenistic times, sea level was about 1.80 m deeper than today. Stating a subsidence of 1 m per 1000 years, i.e. more than 2 m since Hellenistic times, sea level would have remained constant over this period of time. The assumption of a constant sea level over the past millennia is definitely false and in contrast to published studies for adjacent regions of the Eastern Mediterranean (Kayan, 1997; Sivan et al., 2004; Lambeck and Purcell, 2005; Brückner et al., 2006, 2010b; Vött, 2007).

Thus, the subsidence rate must have been significantly lower. Aksu et al. (1987) did their research far out in the Çandarlı Bay where water depth reaches 100 m and more. The superimposed sediment load in this part is much higher, resulting in higher rates of subsidence as compared to the inner part of the Bay of Elaia. Leaving aside the question of subsidence, the presented palaeo-sea level in the harbour region of Elaia is in accordance to other studies of the Eastern Mediterranean.

9. Conclusions

Until the 7th century BC, the area of the later harbour basin was part of a marine embayment which reached several hundred metres further inland to the north and to the east than today (Fig. 10; see also Brückner and Seeliger, 2009; Brückner et al., 2010a). Most probably in the Early Hellenistic period the harbour basin was constructed: two harbour moles were erected with massive sub-structures and large capping sandstone ashlar. In addition, the area directly to the north of the present basin was filled with large stones in order to consolidate the terrain and to create space for loading, unloading and storing of cargo from the ships. As a consequence, the harbour area turned into a quasi-lagoonal environment, being connected with the open sea only by a 45 m wide port entrance.

The harbour was in use during Hellenistic and early Roman times. Based on the ¹⁴C age estimates from the cores, the onset of substantial siltation occurred between the second half of the 3rd century and the end of the 4th century AD. These results confirm the archaeological evidence of a flourishing city of Elaia during the Hellenistic and early Roman periods, and its decreasing importance during Late Roman times.

Acknowledgements

This research was part of the Elaia Survey headed by Felix Pirson, Director of the DAI İstanbul, and carried out under the umbrella of the DFG priority program 1209 "The Hellenistic Polis as a Living Space – Urban Structures and Civic Identity between Tradition and Innovation" (2008–2012). Financial support by the German Research Foundation is gratefully acknowledged (DFG ref. no. PI 740/1–3). The investigation would not have been possible without the permanent and generous support of the Pergamon Excavation of the German Archaeological Institute (DAI), directed by F. Pirson. Pottery and small finds were studied by Güler Ateş (Universität Heidelberg). Harald Stümpel (Universität zu Kiel) helped with the

interpretation of the geophysical data. The Ministry of Culture and Tourism of the Republic of Turkey kindly granted the research permits.

References

- AG Boden (Ed.), 2005. *Bodenkundliche Kartieranleitung*. Schweizerbart, Stuttgart.
- Aksu, A.E., Piper, D.J.W., Konuk, T., 1987. Late Quaternary tectonic and sedimentary history of outer İzmir and Çandarlı Bays, Western Turkey. *Marine Geology* 76, 89–104.
- Altunkaynak, S., Yilmaz, Y., 1998. The Mount Kozak magmatic complex. *Western Anatolia Journal of Volcanology and Geothermal Research* 85, 211–231.
- Anzidei, M., Antonioli, F., Benini, A., Lambeck, K., Sivan, D., Serpelloni, E., Stocchi, P., 2011. Sea level change and vertical land movements since the last two millennia along the coasts of southwestern Turkey and Israel. *Quaternary International* 232, 13–20.
- Auriemma, R., Solinas, E., 2009. Archaeological remains as sea level change markers: a review. *Quaternary International* 206, 134–146.
- Barillé-Boyer, A.L., Barillé, L., Massé, H., Razet, D., Héral, M., 2003. Correction for particulate organic matter as estimated by loss on ignition in estuarine ecosystems. *Estuarine, Coastal and Shelf Science* 58, 147–153.
- Beck, R., Burger, D., Pfeffer, K.-H., 1995. *Laborskript. Kleinere Arbeiten aus dem Geographischen Institut der Universität Tübingen*. vol. 11.
- Beltrame, C., Gaddi, D., 2007. Preliminary analysis of the hull of the Roman ship from Grado Gorizia, Italy. *International Journal of Nautical Archaeology* 36, 138–147.
- Bini, M., Chelli, A., Durante, A.M., Gervasini, L., Pappalardo, M., 2009. Geoarchaeological sea-level proxies from a silted up harbour: a case study of the Roman colony of Luni (northern Tyrrhenian Sea, Italy). *Quaternary International* 206, 147–157.
- Blott, S.J., Pye, K., 2001. GRADISTAT: a grain size distribution and statistics package for the analysis of unconsolidated sediments. *Earth Surface Processes and Landforms* 26, 1237–1248.
- Brückner, R., 1976. *Geology of Turkey*. Elsevier, Stuttgart.
- Brückner, H., Vött, A., Schriever, A., Handl, M., 2005. Holocene delta progradation in the eastern Mediterranean – case studies in their historical context. *Mediterranean* 104, 95–106.
- Brückner, H., Müllenhoff, M., Gehrels, R., Herda, A., Knipping, M., Vött, A., 2006. From archipelago to floodplain – geographical and ecological changes in Miletus and its environs during the past six millennia (Western Anatolia, Turkey). *Zeitschrift für Geomorphologie N.F.* 142 (Suppl.), 63–83.
- Brückner, H., Seeliger, M., 2009. Geoarchaeologische Untersuchungen. In: Pirson, F. (Ed.), *Pergamon. Bericht über die Arbeiten der Kampagne 2008*. *Archäologischer Anzeiger* 2009 (vol. 2), 194–199.
- Brückner, H., Knipping, M., Seeliger, M., 2010a. Geoarchaeologische Untersuchungen in der Bucht von Elaia. In: Pirson, F. (Ed.), *Pergamon. Bericht über die Arbeiten der Kampagne 2009*. *Archäologischer Anzeiger* 2010 (vol. 2), 208–219.
- Brückner, H., Kelterbaum, D., Marunčak, O., Porotov, A., Vött, A., 2010b. The Holocene sea level story since 7500 BP – Lessons from the Eastern Mediterranean, the Black and the Azov Seas. *Quaternary International* 225, 160–179.
- Cartledge, P., 2004. *Alexander the Great. The Hunt for a New Past*. Overlook Press, New York.
- Cimak, F., 2009. *Pergamum*. Turizm Yagınlan Ltd., İstanbul.
- Coates, J.F., 1987. Reconstructing the ancient Greek trireme warship. *Endeavour* 11 (2), 94–99.
- Dankers, N., Laane, R., 1983. A comparison of wet oxidation and loss on ignition of organic material in suspended matter. *Environmental Technology Letters* 4, 283–290.
- Dance, S.P., 1977. *Das große Buch der Meeresmuscheln – Schnecken und Muscheln der Weltmeere*. Ulmer, Stuttgart.
- Engel, M., Knipping, M., Brückner, H., Kiderlen, M., Kraft, J.C., 2009. Reconstructing middle to late Holocene palaeogeographies of the lower Messenian plain (southwestern Peloponnese, Greece): coastline migration, vegetation history and sea level change. *Palaeogeography, Palaeoclimatology, Palaeoecology* 284 (3–4), 257–270.
- Ernst, W., 1970. *Geochemical Facies Analysis*. Elsevier, Amsterdam, London New York.
- Fleming, N.C., 1978. Holocene eustatic changes and coastal tectonics in the Northeast Mediterranean: Implications for models of crustal consumption. *Philosophical Transactions of the Royal Society of London. Mathematical and Physical Sciences* 289, 405–458.
- Folk, R.L., Ward, W.C., 1957. Brazos River bar: a study in the significance of grain size parameters. *Journal of Sedimentary Petrology* 27, 3–26.
- Ganzert, J., Grünewald, M., Herz, P., 1984. *Das Kenotaph für Gaius Caesar in Limyra: Architektur und Bauornamentik*. Tübingen: E. Wasmuth.
- Gifford, J., Rapp, G., Vitali, V., 1992. Palaeogeography of Carthage (Tunisia): coastal change during the first millennium BC. *Journal of Archaeological Science* 19, 575–596.
- Hansen, E., 1971. *The Attalids of Pergamon*. Cornell University Press, Ithaca.
- Heiri, O., Lotter, A.F., Lemcke, G., 2001. Loss on ignition as a method for estimating organic and carbonate content in sediments: reproductibility and comparability of results. *Journal of Paleolimnology* 25, 101–110.
- Herodotus, 2001. *Historia*. Books I–IX. Released and translated by Josef Feix, 2001 ed. Artemis and Winkler, Düsseldorf. (Greek to German).

- Housley, R.A., Lane, C.S., Cullen, V.L., Weber, M.-J., Riede, F., Gamble, C.S., Brock, F., 2012. Icelandic volcanic ash from the Late-glacial open-air archaeological site of Ahrenshöft LA 58 D, North Germany. *Journal of Archaeological Science* 39, 708–716.
- Kayan, I., 1997. Bronze Age regression and change of sedimentation on the Aegean Coastal plains of Anatolia (Turkey). In: Dalfes, H.N., Kukla, G., Weiss, H. (Eds.), *Third Millennium BC Climate Change and Old World Collapse*. NATO ASI Series. NATO, Berlin, Heidelberg, pp. 431–450.
- Kraft, J.C., Rapp, G., Szemler, G.J., Tziavos, C., Kase, E.W., 1987. The pass at Thermopylae, Greece. *Journal of Field Archaeology* 14, 181–198.
- Kraft, J.C., Kayan, I., Brückner, H., Rapp, G., 2000. A geological analysis of ancient landscapes and the harbours of Ephesus and the Artemision in Anatolia. *Jahreshefte des Österreichischen Archäologischen Institutes in Wien* 69, 175–233.
- Kraft, J.C., Brückner, H., Kayan, I., Engelmann, H., 2007. The geographies of ancient Ephesus and the Artemision in Anatolia. *Geoarchaeology* 22, 121–149.
- Lambeck, K., Purcell, A., 2005. Sea-level change in the Mediterranean Sea since the LGM: model predictions for tectonically stable areas. *Quaternary Science Reviews* 24, 1969–1988.
- Loke, M.H., Barker, R.D., 1995. Least-squares deconvolution of apparent resistivity pseudosections. *Geophysics* 60, 1682–1690.
- Marriner, N., Morhange, C., 2006a. The 'Ancient Harbour Parasequence': anthropogenic forcing of the stratigraphic highstand record. *Sedimentary Geology* 186, 13–17.
- Marriner, N., Morhange, C., 2006b. Geoarchaeological evidence for dredging in Tyre's ancient harbour, Levant. *Quaternary Research* 65, 164–171.
- Marriner, N., Morhange, C., 2007. Geoscience of ancient Mediterranean harbours. *Earth-science Reviews* 80, 137–194.
- McHugh, C.M., Seeber, L., Cormier, M., Dutton, J., Cagatay, N., Polonia, A., Ryan, W.B., Gorur, N., 2006. Submarine earthquake geology along the North Anatolia Fault in the Marmara Sea, Turkey: a model for transform basin sedimentation. *Earth and Planetary Science Letters* 248, 661–684.
- Mook, D.H., Hoskin, C.M., 1982. Organic determinations by ignition, caution advised. *Estuarine, Coastal and Shelf Science* 15, 697–699.
- Montefalcone, M., 2009. Ecosystem health assessment using the Mediterranean seagrass *Posidonia oceanica*: a review. *Ecological Indicators* 9 (4), 595–604.
- Morhange, C., Pirazzoli, P., Evelpidou, N., Marriner, N., 2012. Tectonic uplift and silting up of Lechaion, western harbour of ancient Corinth (Greece). *Geoarchaeology* 27, 278–283.
- Nikula, R., Väinölä, R., 2003. Phylogeography of *Cerastoderma glaucum* (Bivalvia: Cardiidae) across Europe: a major break in the eastern Mediterranean. *Marine Biology* 143, 339–350.
- Niwa, Y., Sugai, T., Saegusa, Y., Ogami, T., Sasao, E., 2011. Use of electrical conductivity to analyze depositional environments: example of a Holocene delta sequence on the Nobi Plain, central Japan. *Quaternary International* 230, 78–86.
- Pirson, F., 2004. Elaia, der maritime Satellit Pergamons. *Istanbuler Mitteilungen* 54, 197–213.
- Pirson, F., 2008. Das Territorium der hellenistischen Residenzstadt Pergamon – Herrschaftlicher Anspruch als raumbezogene Strategie. In: Jöchner, C. (Ed.), *Räume der Stadt – Von der Antike bis heute*. Reimer, Berlin, pp. 27–50.
- Pirson, F., 2009. Elaia. In: Pirson, F. (Ed.), *Pergamon. Bericht über die Arbeiten der Kampagne 2008*. *Archäologischer Anzeiger* 2009 (vol. 2), 182–200.
- Pirson, F., 2010. Survey. In: Pirson, F. (Ed.), *Pergamon. Bericht über die Arbeiten der Kampagne 2009*. *Archäologischer Anzeiger* 2010 (vol. 2), 195–201.
- Poppe, G.T., Goto, Y., 2000. *European Seashells*. Verlag Christa Hemmen, Wiesbaden.
- Radt, W., 1999. Pergamon – Geschichte und Bauten einer antiken Metropole. *Wissenschaftliche Buchgesellschaft, Darmstadt*.
- Reinhardt, E.G., Raban, A., 1999. Destruction of Herod the Great's harbor at Caesarea Maritima, Israel – geoarchaeological evidence. *Geology* 27, 811–814.
- Salehi, M.H., Hashemi, B.O., Bigi, H.H., Esfandiarpour, B.I., Motaghian, H.R., 2011. Refining soil organic matter determination by loss-on-ignition. *Pedosphere* 21 (4), 473–482.
- Seeliger, M., Bartz, M., Brückner, H., 2012. Mauern im Meer – Geoarchäologische Untersuchungen in der Bucht von Elaia. In: Pirson, F. (Ed.), *Pergamon. Bericht über die Arbeiten der Kampagne 2010*. *Archäologischer Anzeiger* 2011 (2), 175–185.
- Short, F.T., Wyllie-Echeverria, S., 1996. Natural and human-induced disturbance of seagrasses. *Environmental Conservation* 23, 17–27.
- Siani, G., Paterne, M., Arnold, M., Bard, E., Metivier, B., Tisnerat, N., Bassinot, F., 2000. Radiocarbon reservoir ages in the Mediterranean Sea and Black Sea. *Radiocarbon* 42, 271–280.
- Sivan, D., Lambeck, K., Toueg, R., Raban, A., Porath, Y., Shirman, B., 2004. Ancient coastal wells of Caesarea Maritima, Israel, an indicator for relative sea level changes during the last 2000 years. *Earth and Planetary Science Letters* 222, 315–330.
- Strabo, 2005. *Geographica*. Translation and comments by Albert Forbiger, 2005 ed. Marix Verlag, Wiesbaden. (Greek to German).
- Törnqvist, T.E., De Jong, A.F.M., Oosterbaan, W.A., van der Borg, K., 1992. Accurate dating of organic deposits by AMS ¹⁴C measurement of macrofossils. *Radiocarbon* 34, 566–577.
- Vita-Finzi, C., 1969. Late Quaternary continental deposits of central and western Turkey. *Man, New Series* 4, 605–619.
- Vött, A., Handl, M., Brückner, H., 2002. Rekonstruktion holozäner Umweltbedingungen in Akarnanien (Nordwestgriechenland) mittels Diskriminanzanalyse von geochemischen Daten. *Geologica et Palaeontologica* 36, 123–147.
- Vött, A., Brückner, H., Schriever, A., Handl, M., Besonen, M., van der Borg, K., 2004. Holocene coastal evolution around the ancient seaport of Oiniadai, Acheloos alluvial plain, NW Greece. *Coastline Reports* 1, 43–53.
- Vött, A., Schriever, A., Handl, M., Brückner, H., 2007. Holocene palaeogeographies of the central Acheloos River delta (NW Greece) in the vicinity of the ancient seaport Oiniadai. *Geodinamica Acta* 20 (4), 241–256.
- Vött, A., 2007. Relative sea level changes and regional tectonic evolution of seven coastal areas in NW Greece since the mid-Holocene. *Quaternary Science Reviews* 26, 894–919.
- Waelkens, M., 1987. The adoption of Roman building techniques in the architecture of Asia Minor. In: Macready, S., Thompson, F.H. (Eds.), *Roman Architecture in the Greek World*. London, 94–105.

Chapter 3

3 The environs of Elaia's ancient open harbour – A reconstruction based on microfaunal evidence

Journal Article (2015):

Pint, A., **Seeliger, M.**, Frenzel, P., Feuser, S., Erkul, E., Berndt, C., Klein, C., Pirson, F., Brückner, H., 2015. The environs of Elaia's ancient open harbour – A reconstruction based on microfaunal evidence. *Journal of Archaeological Science* 54, 340–355.



The environs of Elaia's ancient open harbour – a reconstruction based on microfaunal evidence



Anna Pint^{a, *}, Martin Seeliger^a, Peter Frenzel^b, Stefan Feuser^c, Ercan Erkul^d, Christopher Berndt^b, Christina Klein^d, Felix Pirson^e, Helmut Brückner^a

^a Institute of Geography, Universität zu Köln, Albertus-Magnus-Platz, D-50923 Köln, Cologne, Germany

^b Institute of Earth Sciences, Friedrich-Schiller-Universität Jena, Burgweg 11, D-07749 Jena, Germany

^c Heinrich Schliemann-Institute for Ancient Studies, University of Rostock, D-18051 Rostock, Germany

^d Institute of Geosciences, Christian-Albrechts-Universität zu Kiel, Otto-Hahn-Platz 1, D-24118 Kiel, Germany

^e German Archaeological Institute (DAI) Istanbul, İnönü Caddesi 10, TK-34437 İstanbul, Turkey

ARTICLE INFO

Article history:

Available online 27 June 2014

Keywords:

Ostracoda
Foraminifera
Ship sheds
Pergamum
Turkey

ABSTRACT

During Hellenistic and Roman times, Elaia, the harbour city of ancient Pergamum, was an important place of trading and traffic. Intense mercantile and military activities are documented by literary sources and archaeological evidences. Geomagnetic and geoelectric investigations detected building structures close to the ancient coastline, which are interpreted as ship sheds. The aim of this study was to reconstruct the coastal evolution, particularly with regard to harbour-related facilities. For that purpose, a 10 m long sediment core was drilled in the area of the ancient open harbour immediately in front of the supposed ship sheds. It was studied with the tools of micropalaeontology, geophysics, sedimentology and geochemistry. To improve the reconstruction of the palaeoenvironmental conditions, reference samples of modern environments of the area were analysed. As indicated by marine ostracod and foraminifer taxa, the sediment core shows (from bottom to top) that the initially fully marine conditions changed to a more restricted fauna indicative for a more sheltered bay with brackish waters. This layer dates to Hellenistic times. It can, however, be shown that the siltation process had produced a lagoon system already several hundred years BC. The Elaia embayment was first used as a natural harbour. It was equipped with breakwaters in the Hellenistic period. The progressive siltation caused the abandonment of the harbour in Late Roman Times.

© 2014 Elsevier Ltd. All rights reserved.

1. Introduction

For more than a decade, many multidisciplinary studies have focused on the utilisation of ancient harbours and harbour related facilities along the Mediterranean coasts. Some investigations deal with the function and history of ancient harbour settlements in general: the harbours of Tyre, Lebanon (Marriner and Morhange, 2007; Marriner et al., 2008, 2010; Morhange et al., 2012), Carthage, Tunisia (Gifford et al., 1992), Pergamum (Elaia), Turkey (Brückner et al., 2013; Seeliger et al., 2013), Ephesus, Turkey (Brückner, 1997, 2005; Stock et al., 2013), Corinth (Lechaion), Greece (Hadler et al., 2013), Marseille (Morhange et al., 2003), Rome, Italy (Goiran et al., 2010), Ostia, Italy (Goiran et al., 2014) – to

mention a few. Others describe special harbour or economy facilities like fish tanks and ship sheds in relation to the palaeo-sea level in detail. Antonioli et al. (2007) and Auriemma and Solinas (2009) provide a general overview how archaeological remains may be correlated and interpreted in relation to palaeo-sea level on the basis of different sites along the Mediterranean coast (see also Seeliger et al., 2013, 2014).

Due to the exact dating by archaeological criteria and their well-documented position in respect to former sea level, ancient fish tanks may act as a good indicator for sea-level fluctuations. Morhange et al. (2013) use Roman fish tanks in combination with biological markers to state a relative rise in sea level of 40 ± 10 cm since those days for the region of Fréjus, southeastern France. Similar work is published, e.g., by Evelpidou et al. (2012) for the Tyrrhenian Coast of Italy, by Mourtzas (2012) for the Greek island of Crete, and by Florido et al. (2011) for the Istrian and Dalmatian coast, Italy and Croatia. Ship sheds in contrast to fish tanks cannot

* Corresponding author. Tel.: +49 221 470 8249.

E-mail addresses: pinta@uni-koeln.de, annapint@web.de (A. Pint).

bear direct witness of former sea level because they have been built above the marine sphere but in close vicinity to it. Vött and Brückner (2006) as well as Vött (2007) summarise the research concerning the use and abandonment of ship sheds in ancient Oiniadai (NW Greece) used in Hellenistic and Roman times.

Following this tradition, our paper presents sedimentological and microfaunistic results of sediment core ELA 58 immediately seawards of the supposed Hellenistic ship sheds in the outer harbour region of Pergamum's harbour city Elaia (Figs. 1 and 2). Archaeological, geophysical and geoarchaeological fieldwork at Elaia started in 2006 (Pirson, 2007, 2008a, 2009, 2010, 2011; Brückner et al., 2013; Seeliger et al., 2012, 2013, 2014; Pint et al., 2013). While most of the archaeological structures and facilities of Elaia's harbour such as the closed harbour basin and a submerged Late Roman saline have already been described and dated (Pirson, 2007, 2008a; Seeliger et al., 2012, 2013, 2014; Pint et al., 2013), the hypothesis about the Hellenistic ship sheds of Elaia has not been proved so far. These structures, visible only in the geomagnetic and geoelectric measurements, are located immediately to the east of the closed harbour basin. The analysis of core ELA 58 is essential for the further interpretation of the

structures as ship sheds as a sufficient water depth in Hellenistic times is required – only then oared warships could have been pulled in for shelter.

Microfossil analyses are an important tool to reconstruct palaeoenvironmental conditions. This has been successfully demonstrated in geoarchaeological contexts at, e.g., Ras Ibn Hani, Ephesus, Miletos, Tyre, Rome and the Nile delta, just to mention some of it (Handl et al., 1999; Brückner, 2005; Marriner et al., 2008; Goiran et al., 2010; Mazzini et al., 2011; Marriner et al., 2012; Flaux et al., 2013; Stock et al., 2013). General issues like the evolution of coasts, lagoons and lakes as well as special aspects like the usage of harbours and the navigability of waterways can be solved by the aid of microfossil analyses. Inferring environmental information like salinity, temperature and water depth, it is possible to reconstruct habitat changes in space and time. Therefore it is necessary to identify species and their ecological preferences and tolerances using an actualistic approach.

Our study aims at (i) reconstructing the palaeoenvironments of the ship sheds using micropalaeontological and sedimentological proxies, and (ii) establishing a chronology of the environmental changes over the millennia.

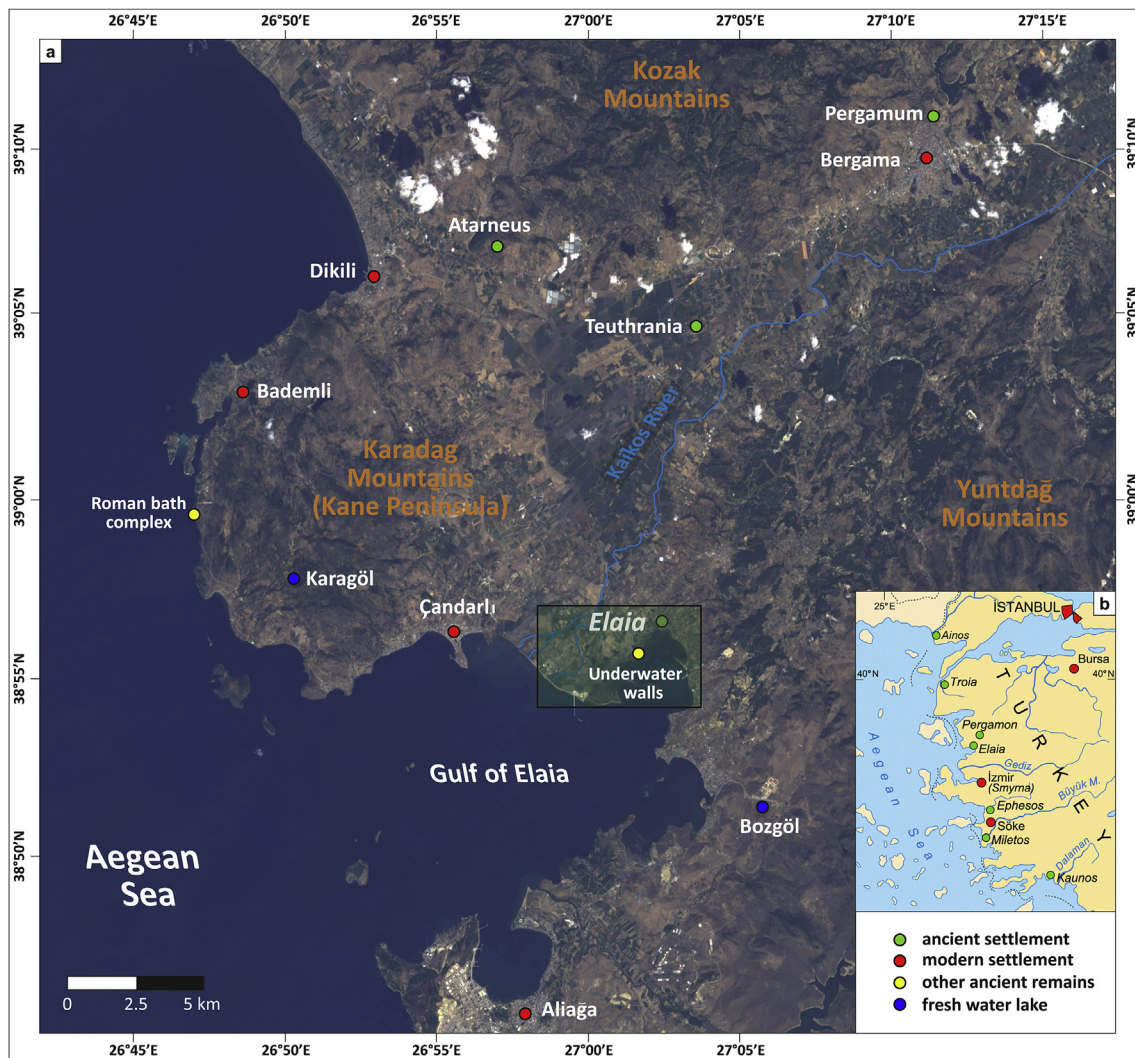


Fig. 1. Area of research at the Aegean coast of Turkey. (a) Overview based on Landsat 8 (acquired September 23, 2013; composition based on bands 4, 3, 1) with locations mentioned in the text. (b) General map of western Turkey with a selection of ancient and modern settlements.



Fig. 2. Satellite image of the Bay of Elaia with microfauna sampling sites and coring site ELA 58. (a) The bay and its environs with parts of the Bakırçay (Kaikos) delta. (b) The closed and open harbours of Elaia in the innermost embayment and coring site ELA 58. (c) Detailed view of the eastern city area of Elaia. (d) Southernmost mouth of the Bakırçay River. (e) Sand spit protruding into the bay. R1–R11: sites of the Recent samples to study the modern microfauna (Ostracoda, Foraminifera). Source of the satellite image: Quickbird 2 (acquired: April 02, 2006; composition based on bands 3, 2, 1).

2. Physical setting of the study area

The Gulf of Elaia is situated between the Karadağ Mountains (Kane Peninsula) to the west and the Yuntdağ mountain complex to the east (Fig. 1). Due to its distance from the open Aegean Sea it represents an area of low energy wave climate, even during extreme weather events. The Bay of Elaia as well as the topography of the coastal area are relatively flat; the 20 m isobaths lies c. 4 km offshore (Aksu et al., 1987). Own DGPS (Differential Global Positioning System) surveys (Leica GPS System 530) in 2010 and 2011 revealed a mean tidal range of about 20 cm. Although wind surges may increase sea level during the winter season this measurement is in good accordance with other sites in the eastern Aegean Sea (Flemming, 1978; Anzidei et al., 2011; Brückner et al., 2013; Seeliger et al., 2012, 2013, 2014).

The Bay of Elaia is located on the westwards drifting Aegean-Anatolian microplate. An ensemble of several E–W-oriented late Miocene rift structures (e.g. Bergama and Zeytindağ grabens) serves as a drainage channel for the Bakır Çay (translated: Copper River; ancient: Kaikos), which filled the Bergama Graben with sediments (Vita-Finzi, 1969; Brinkmann, 1976; Aksu et al., 1987; McHugh et al., 2006; Schneider et al., 2011). The modern Bakır

Çay forms a cusped delta between the Kane Peninsula and the Bay of Elaia before entering the Aegean Sea. Several archaeological sites testify still ongoing subsidence of the graben system, namely (i) a partly drowned Roman thermal bath complex situated on the Kane Peninsula, and (ii) the sunken harbour breakwaters and drowned underwater wall structures in the Bay of Elaia (Figs. 1a and 2; Seeliger et al., 2012, 2013, 2014). Own investigations concerning the transgressive contact in the closed harbour of Elaia and the study of archaeological sea level markers resulted in an estimated subsidence rate of the graben ensemble of far less than 1 m per 1000 years (Seeliger et al., 2013; in contrast to Aksu et al., 1987).

3. Elaia, the ancient harbour of Pergamum

With Troy (Troia, Ilium), Miletus, and Ephesus Pergamum is one of the most prominent ancient settlements in Asia Minor (Fig. 1b). Today, when dealing with Pergamum, the impressive Pergamum Altar and Aelius Galenus, a famous physician in the 2nd century AD (Radt, 2011) come to mind. After the death of Alexander the Great in 323 BC in Babylon, the so-called Wars of the Diadochi started influencing the whole realm. As a consequence of the fighting, the House of the Attalids came to power in the Kaikos region and

established their Hellenistic kingdom which on its heyday – under king Eumenes II (197–159 BC) – covered the whole western part of modern Turkey. In 133 BC the Pergamian kingdom came under Roman rule (Hansen, 1971; Cartledge, 2004; Radt, 2011; Zimmermann, 2011).

Pergamum occupies a prominent strategic location at the 330 m high city hill dominating the surrounding Kaikos plain (Fig. 1a) which was perfect for defence but restricted traffic and trade. Access to the Mediterranean Sea was provided through the acquisition of nearby Elaia, situated at the Aegean Sea some 26 km southwest of Pergamum, under Eumenes I (reign: 263–241 BC; Pirson, 2004; Radt, 2011). Then, Elaia and its harbour gained major importance for the kings of Pergamum. During the reign of Eumenes I, the fleet of Pergamum, which must have had its harbour in Elaia, is mentioned for the first time. As the city was located on the important road from Pergamum along the coast to Smyrna (modern İzmir) to the south, the city played a major role not only as the base for the royal fleet but also in the supply and protection of Pergamum (Pirson, 2004, 2008b). It is not surprising that Elaia was essential in the lengthy war fought against Antiochos III by the kings of Pergamum together with the Romans between 192 and 188 BC. Livy, a Roman historian (59 BC–AD 17), stated that during this war the harbour was used as supply base for the Roman and Pergamian fleets, as military outpost in the territory of Pergamum and as a place for diplomatic negotiation (Livy, *Ab urbe condita*, 37.37.4). Livy also records that the allied fleets of Pergamum, Rhodes and Rome met in Elaia during their campaigns (Livy, *Ab urbe condita*, 37.18.9–10). In addition to Livy, Strabo, writing around the birth of Christ, mentioned Elaia as the commercial harbour of the Pergamenians and as the military base of the Attalids (Strabon, *Geographica XIII.1.67 and XIII.3.5*).

Since the beginning of the Roman rule in Pergamum, very little is known about the history of Elaia. In Roman Imperial and Late Roman times the city is mentioned only a few times in the literary sources (Pirson, 2004). Recent archaeological research revealed that Elaia was abandoned in the 6th or the beginning of the 7th

century AD on behalf of a more secure settlement further inland (Pirson, 2010). This area called Püsküllü Tepeler is locked off from the sea by the foothills of Bozyertepe, a mountain ridge which separates the Bay of Elaia from the Kaikos delta.

The harbour zone of Elaia is to be divided into two areas (Fig. 2b): First, the closed harbour that must have been incorporated within the fortification walls. This harbour was erected in early Hellenistic times and was protected against the sea, the winds and enemies by two breakwaters, one to the west and one to the south (Pirson, 2007, 2008a; Brückner et al., 2013; Seeliger et al., 2013). The entrance to the harbour was approx. 50 m wide and located towards south–southeast (Figs. 3 and 4).

Geoarchaeological research revealed that substantial siltation occurred between the 3rd and the end of the 4th century AD; thus, from the 5th century AD onwards the closed harbour was not navigable anymore (Seeliger et al., 2013). A second c. 250 m long harbour zone stretched from the southern breakwater of the closed harbour eastwards to the point where an internal wall (*diatichisma*) reached the waterfront. It divided the city area into a northern, densely populated part and a southern one (Pirson, 2011).

4. Material and methods

4.1. Geoarchaeological field work

In 2011, coring site ELA 58 was performed just in front of the supposed ship sheds down to 10 m b.s. (below surface; Fig. 3). Drilling was done with an Atlas Copco Cobra mk1 vibrocorer using open steel auger heads (diameter: 60 and 50 mm). Preliminary sedimentological studies were carried out directly in the field, including grain size estimation, colour (Munsell Soil Color Charts), and carbonate content (10 % hydrochloric acid; AG Boden, 2005). Bulk samples for laboratory analyses, as well as macrofossils and ceramic fragments for a later determination and for radiocarbon dating were taken from the open sediment cores. All coring sites were measured using DGPS (Leica GPS System 530; accuracy of

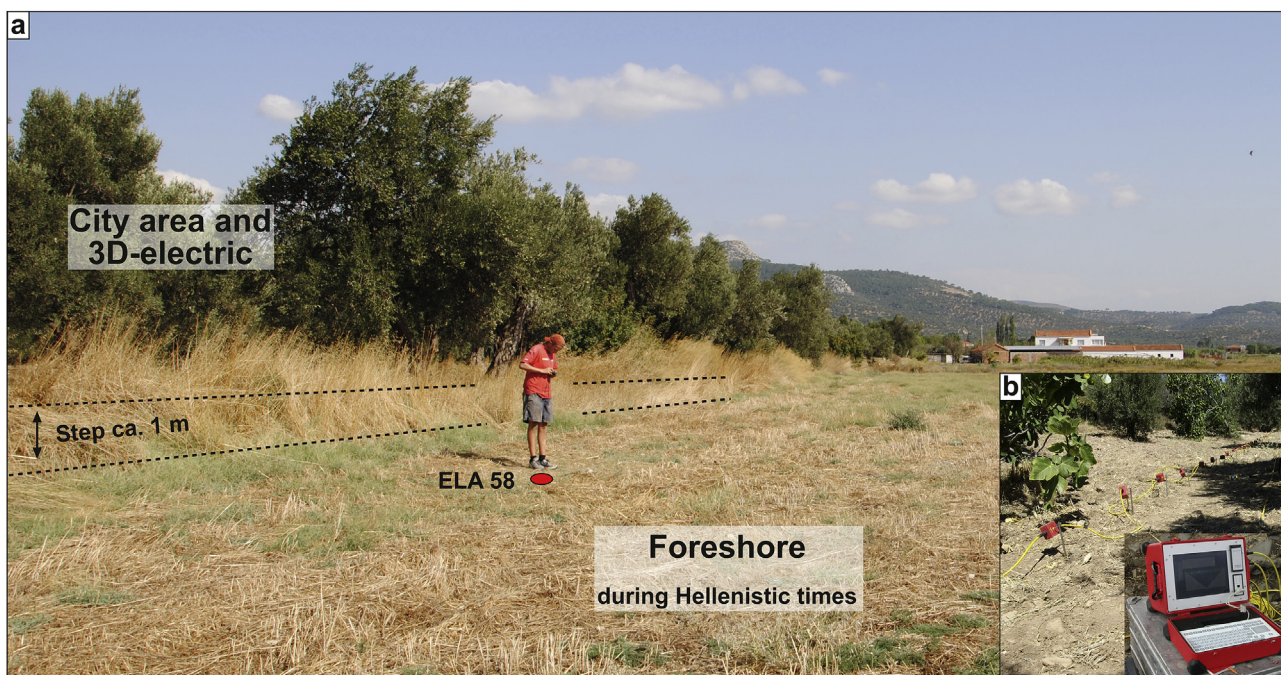


Fig. 3. Coring site ELA 58. (a) The areas of the ancient city of Elaia and the former foreshore are separated by an approx. 1 m high step (Photo: Melanie Bartz, 2011). (b) RESECS – GEOSERVE equipment to perform the geoelectric measurements featured in Figs. 5b, c and 6 (Photo: Ercan Erkul, 2009).

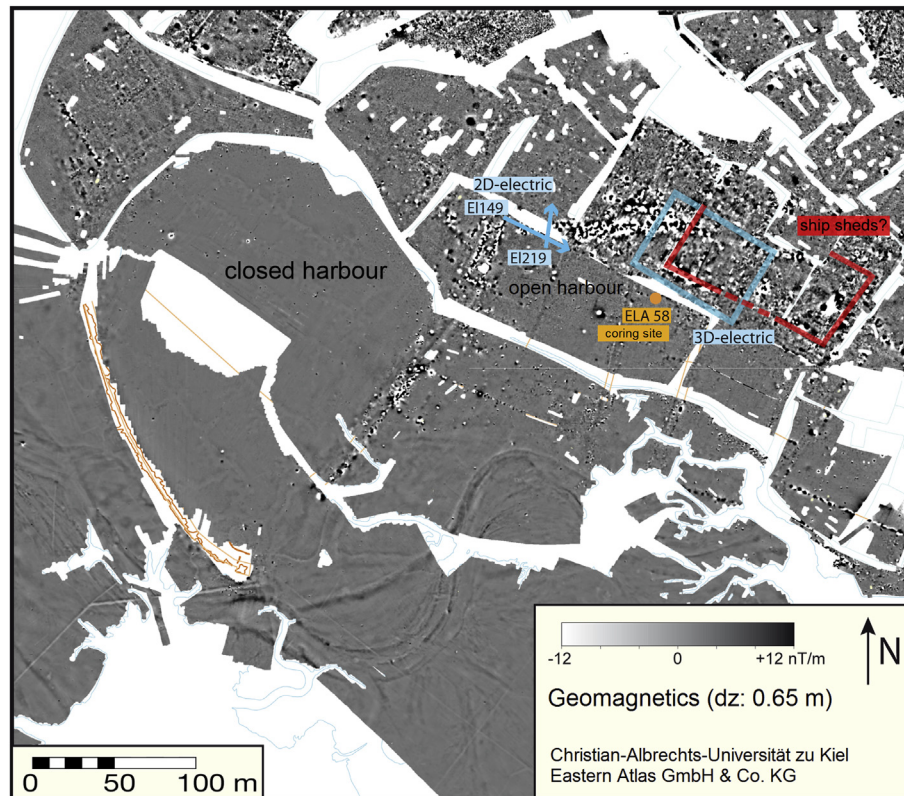


Fig. 4. Geomagnetic map of the area of the closed and open harbours and their environs, including the locations of coring site ELA 58, and the 2D and 3D geoelectrical measurements (marked blue) (cf. Figs. 5 and 6). The position of the assumed ship sheds is marked in red. (For interpretation of the references to colour in this figure legend, the reader is referred to the web version of this article.)

≤ 2 cm in all three dimensions). The altitude above sea level is based on the local reference system PergSys05 which is related to the gauge of Izmir and was established by the German excavation team of Pergamum in 2005. As a result of own DGPS measurements of the mean sea level for several weeks in 2011, the PergSys05 values have to be height-corrected by -0.875 m (Seeliger et al., 2012, 2013, 2014).

4.2. Geophysical investigations

The harbour and the inner town of Elaia were measured from 2006 to 2012 with geomagnetics, geoelectrics and georadar (Fig. 4). The aim of the measurements was to understand the structure of the subsurface layers and to detect archaeological remains in the underground.

Based on the results of the geomagnetic survey, an area of 50×70 m² was selected to carry out 3-D geoelectrical resistivity imaging (see Fig. 4, blue rectangle). The geoelectrical resistivity sections were measured with the multi-electrode system RESECS of the company GeoServe (Fig. 3b). Several electrode arrangements such as Dipole–Dipole, Wenner and Schlumberger were applied. The apparent electrical resistivity was determined as a function of the electrode geometry by the measuring instrument. Using the inversion software RES2DINV and RES3DINV (Loke and Barker, 1995), a resistivity to depth distribution was inverted from the field data.

Linear geomagnetic patterns with strong amplitudes have been observed. A total of 75 profiles have been measured with a distance of 1 m each. The electrode spacing was also 1 m, and the sections were 47 m long. Using these field data, resistivity to depth distribution down to a depth of approx. 4 m was inverted in 3D.

4.3. Sedimentology and geochemistry

To augment on-site facies interpretation, multi-proxy laboratory analyses were conducted (cf. Ernst, 1970; Vött et al., 2002, 2004; Brückner et al., 2006; Engel et al., 2009; Niwa et al., 2011; Kelterbaum et al., 2012). Samples were air-dried, ground and sieved to separate the ≤ 2 mm grain size fraction for further analyses. The granulometry was determined using a laser particle sizer (Beckman Coulter LS13320) after removal of the organic content with hydrogen peroxide. For the calculation of grain-size parameters after Folk and Ward (1957), the GRADISTAT software (Blott and Pye, 2001) was applied.

Geochemical analyses included the weight loss on ignition (LOI). Oven-dried (105 °C for 12 h) samples were combusted in a furnace at 550 °C for 4 h. The accuracy of the LOI is widely discussed because two chemical processes may cause errors (Mook and Hoskin, 1982; Heiri et al., 2001; Barillé-Boyer et al., 2003): the possible loss of structural water from clay minerals (Dankers and Laane, 1983), and the potential loss of carbon dioxide from carbonates consisting of inorganic material (Salehi et al., 2011). The combination of the two processes results in a weight reduction not caused by loss of organic substance. A subsequent correction of the LOI values was not conducted in this study. The concentrations of 30 elements were measured with a portable XRF spectrometer (Niton XI3t 900 GOLDD; Vött et al., 2011).

4.4. Micropalaeontology

Selected 1 cm³ sediment samples were wet-sieved with a 100 μ m mesh for microfaunal analysis of the core samples. A total of at least 300 foraminifer tests and ostracod valves, respectively, if

present, were picked from the residues of every sample under a low-power stereoscopic microscope. Species were mainly identified according to Bonaduce et al. (1975) and Joachim and Langer (2008) for Ostracoda as well as Meriç et al. (2004) and Cimerman and Langer (1991) for Foraminifera.

In order to obtain Recent samples for actualistic comparisons, selected aquatic habitats were sampled around the Bay of Elaia in summer 2012 (Fig. 2). The Recent samples were taken with a hand net by scraping the uppermost centimetre of sediment. Ethanol and the stain Rose Bengal were added to the sediment samples for later identification of living individuals. Sample preparation and picking followed the same procedure as listed for core samples.

Multivariate statistical analysis like Hierarchical cluster analysis (WARD method) of microfossil associations are mainly used to detect similarities between samples based on comparable environments. Ecologically controlling factors are reflected by a Principal Component Analysis (PCA).

4.5. Chronology

¹⁴C-Accelerator Mass-Spectrometric (AMS) age determinations of sea grass, charcoal and seeds were performed at the Centre for Applied Isotope Studies (CAIS) of the University of Georgia at Athens (USA). All ages were calibrated using IntCal13 or MARINE13 calibration curves of Calib 7.0 software (Reimer et al., 2013) with a marine reservoir effect of 390 ± 85 years and a ΔR of 35 ± 70 years (Siani et al., 2000); they are presented in calendar years BC/AD with a 2σ error (i.e. 95.4 % probability; Table 1). Since the spatio-temporal variation of the marine reservoir effect for the Aegean Sea is still not known in detail, ¹⁴C-ages of marine material have to be interpreted with caution. An age vs. depth model by means of P_Sequence was calculated using the OxCal 4.2.3 calibration software (Ramsey, 2008) to estimate the sedimentation rate of ELA 58.

5. Results

5.1. Mapping and geophysics

The large-scale geomagnetic measurements and archaeological mapping suggest settlement patterns on the north-eastern shore zone of the Bay of Elaia. The most prominent feature of this open zone is a structure with a size of c. $105 \times 55 \text{ m}^2$, protruding from the sea wall towards the waterfront (Figs. 4 and 5). While its south-western sea-side end emerges clearly in the geomagnetic image, the north-eastern end cannot be determined with this clearness: it disappears in the density of anomalies in this area. Inside the

structure, several linear anomalies are arranged parallel to each other, running from southwest to northeast. In areas where distances can be measured, the anomalies are separated by approximately 10 m.

Results of the geoelectric measurements are presented in Figs. 5 and 6. The calculated electric resistivities have a range between less than $0.1 \Omega\text{m}$ to several hundred Ωm . Low resistivity of less than $2 \Omega\text{m}$ occurs at approximately 3 m depth of the section. Significantly higher resistivities of more than $50 \Omega\text{m}$ are present up to a depth of 2–3 m. In areas below 3 m depth, the resistivities significantly decrease down to values lower than $2 \Omega\text{m}$ due to the influence of saline pore water.

Fig. 5 shows the magnetic map with the location of the 2D geoelectric sections below. Section EI219 is orientated north and runs approximately perpendicular to the topographic step in the field (Fig. 5) and the linear geomagnetic anomaly. Section EI149 is orientated northwest-southeast and runs parallel to the shoreline and to the south of the topographic step.

Both 2D geoelectric sections (Fig. 5b, c) display electrical resistivities of a range less than $1 \Omega\text{m}$ to several hundred Ωm . Low resistivity of less than $2 \Omega\text{m}$ is observed at approximately 2 m depth of the sections, due to the influence of saline pore water. Significantly higher resistivities of more than $100 \Omega\text{m}$ (yellow to red colours) are observed above 2 m depth.

The geoelectric measurements carried out over the western section of the structure clearly show the south-western corner and the southern and western walls down to a depth of up to 2.30 m. Within the structure, several parallel linear anomalies oriented from southwest to northeast can be traced down to a depth of 1.70 m.

5.2. Chronology and sedimentology

The sediments of ELA 58 cover the last eight millennia (Table 1, Fig. 7). Based on facies interpretation the core was divided into six units (Table 2). They start with clayey and silty sands and pebbles with some angular stones in the upper part of unit 1. The relatively well sorted sediment shows a high but decreasing Ca/Ti ratio. It was deposited in the course of the Late Pleistocene. The Holocene transgression during the Atlantic phase is reflected by unit 2 dated to 7826–7681 cal BP at its base. The sands contain marine shells and plant detritus. The same facies was also found in the closed harbour at the base of the Holocene sediments (Seeliger et al., 2012, 2013). The more than 2 m thick silty sands of unit 3 contain marine shells, partly with articulated valves and some bivalves, and many plant fragments. Ca/Ti ratio and LOI are relatively high. Unit 4 is very similar to unit 3 but is discriminated by

Table 1

Radiocarbon data set. AMS-¹⁴C measurements were carried out at the Centre for Applied Isotope Studies (CAIS) of the University of Georgia at Athens, USA (lab code: UGAMS). All ages were calibrated with IntCal13 or MARINE13 calibration curves using the Calib 7.0 software (Reimer et al., 2013). A marine reservoir effect of 390 ± 85 years and a ΔR of 35 ± 70 years (Siani et al., 2000) was applied. The ages are presented in calendar years BC/AD with a 2σ error (i.e. 95.4 % probability). Please refer that the uppermost five samples are taken out of core ELA 58 while the the last one comes from core ELA 70.

Sample codes	Lab code (UGAMS)	Material	Depth b.s.	$\delta^{13}\text{C}$ (‰)	Libby-age	Calibrated ¹⁴ C ages cal BC/cal AD (2σ)	Calibrated ¹⁴ C ages cal BC/cal AD (2σ) with relative probability	Calibrated ¹⁴ C ages cal BP (2σ)	Calibrated ¹⁴ C ages cal BP (2σ) with relative probability
ELA 58/14HK	11442	Charcoal	2.73 m	-26.7	2080 ± 25	175–41 BC	175–41 BC (100 %)	2124–1990 BP	2124–1990 BP
ELA 58/17H	11443	Seed	3.30 m	-25.0	2020 ± 25	91 BC–AD 52	91–69 BC (5.3 %) 60 BC–AD 52 (94.7 %)	2040–1898 BP	2040–2018 BP (5.3 %) 2009–1898 BP (94.7 %)
ELA 58/24Po	11444	Sea grass	4.40 m	-10.8	2740 ± 25	731–299 BC	731–299 BC (100 %)	2680–2248 BP	2680–2248 BP (100 %)
ELA 58/32	11445	Sea grass	7.75 m	-16.2	6170 ± 30	4796–4439 BC	4796–4439 BC (100 %)	6745–6388 BP	6745–6388 BP (100 %)
ELA 58/38F	11446	Charcoal	8.35 m	-26.1	6920 ± 30	5876–5731 BC	5876–5856 BC (5.4 %) 5852–5731 BC (94.6 %)	7825–7680 BP	7825–7805 (5.4 %) 7801–7680 (94.6 %)
ELA 70/80H	11131	Sea grass	4.57 m	-18.2	2680 ± 30	650–181 BC	650–181 BC (100 %)	2599–2130 BP	2599–2130 BP (100 %)

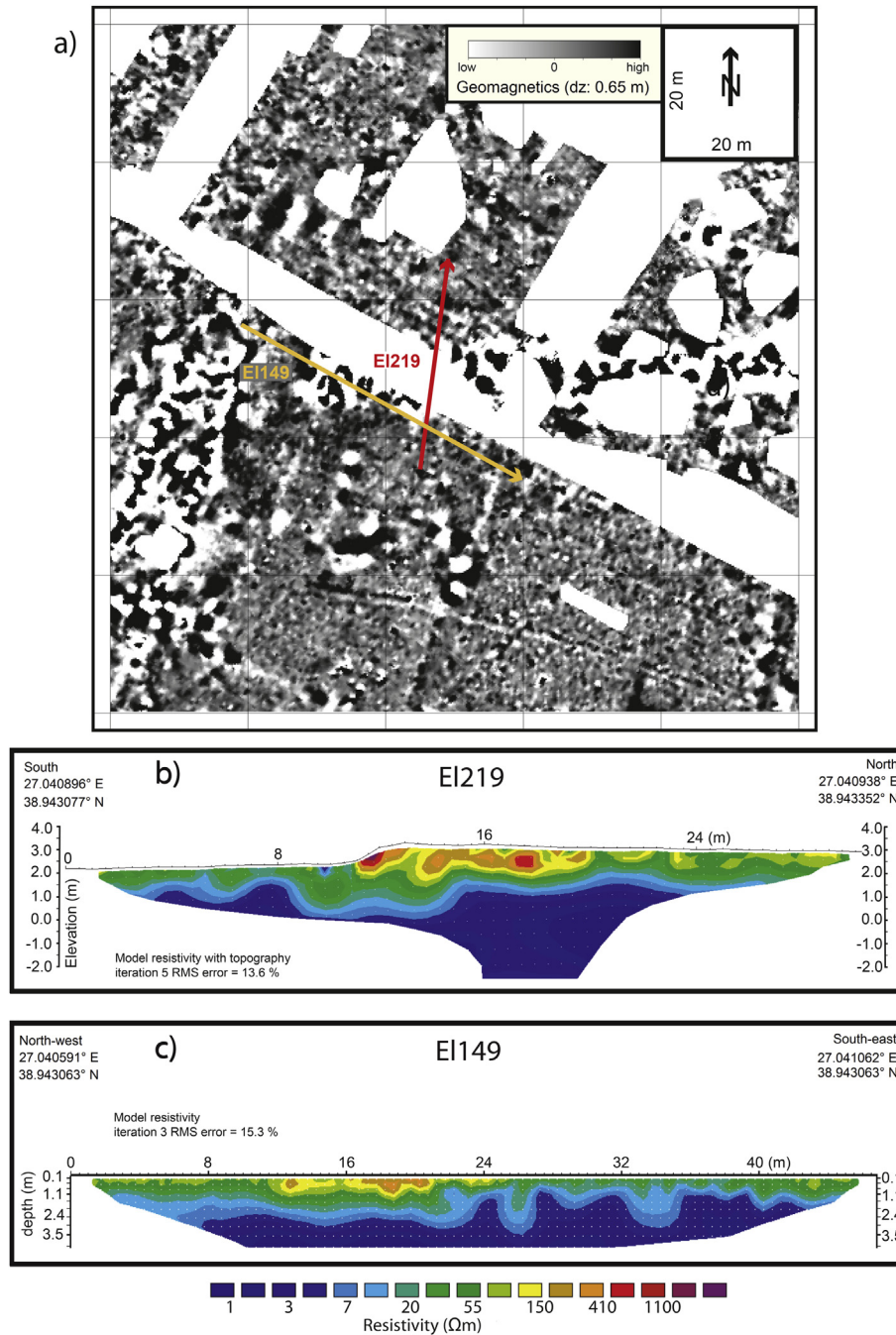


Fig. 5. Geomagnetic map (a), and results of 2D geoelectrical sections EI219 (b) and EI149 (c). For location of map and sites see Fig. 4.

lower Ti/Ca ratio and slightly higher proportion of silt and clay than before. The age of unit 5 is difficult to interpret, since the wide range of the lower age (731–299 cal BC) is due to a plateau effect of the ^{14}C calibration curve, and the upper ages are close to an age inversion (the 2σ errors overlap for 50 years in the 1st century BC). The silty sand containing marine shells is very similar to the sediment of the two precedent units but contains charcoal, wood and brick fragments in its upper part. The uppermost unit 6 comprises about 80 cm of sand with marine shells and anthropogenic particles followed by clayey and silty sand with charcoal, brick fragments, more and more angular stones and marks of oxidation.

5.3. Micropalaeontology

5.3.1. Taxa

Investigations of the eleven Recent samples and the core ELA 58 document 36 ostracod and 59 foraminifer taxa (Fig. 8; Tables A and B – Appendix A). Other organismic remains encountered are fragments of molluscs, which were not examined in detail. In general, the state of preservation of the microfossils is good.

5.3.2. Actualistic study

Nine sites around the inner Bay of Elaia and in its catchment were sampled for Recent meiofauna, i.e. mainly Ostracoda and

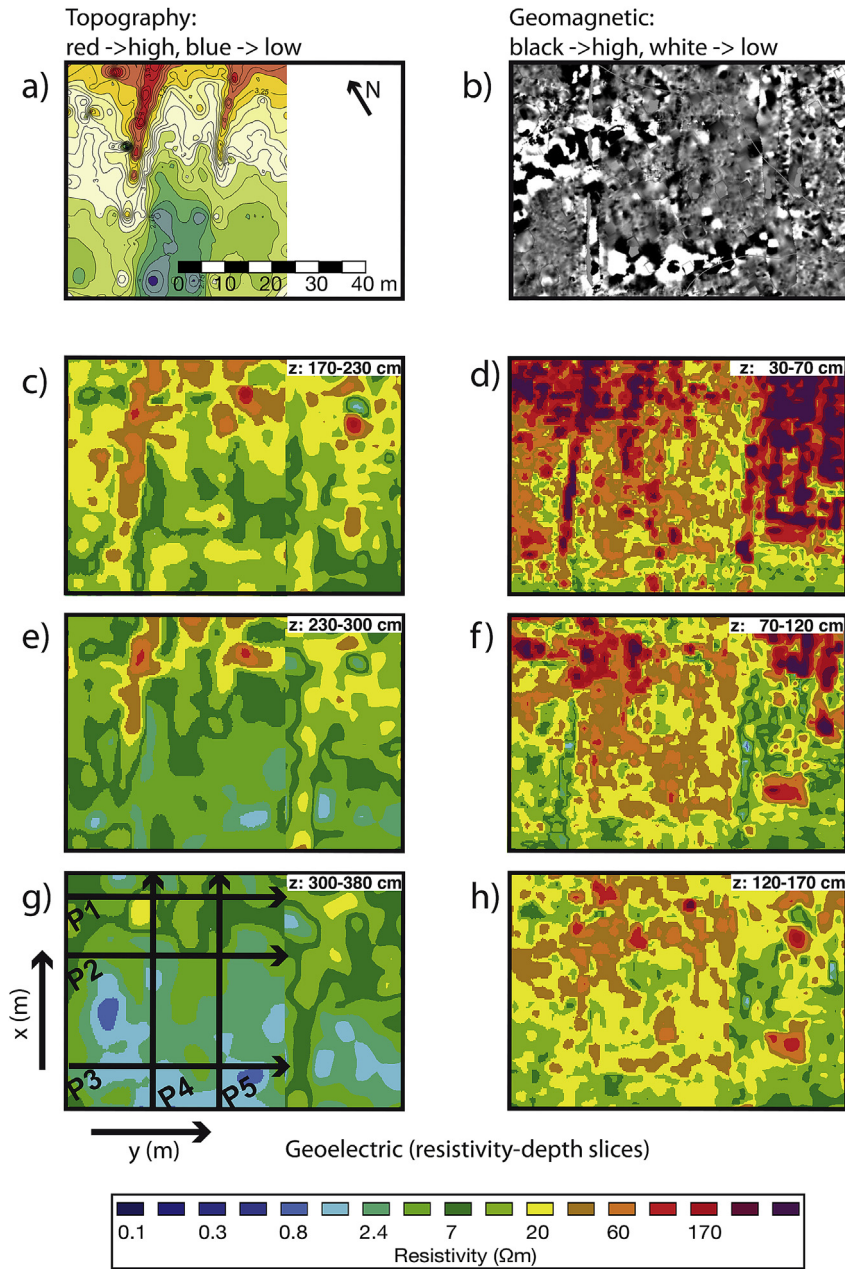


Fig. 6. Results of 3D geoelectrical resistivity imaging (for location see Fig. 4). (a) Topography; (b) geomagnetic map; (c)–(h) resistivity depth slices, the respective depth (z) of each slice is presented in the upper right corner. Note that the images are not oriented towards north.

Foraminifera (Fig. 2, Table 3). Based on similarities of meiofauna species distribution and species diversity three groups of sites could be distinguished reflecting the associated environments. The littoral environment (group 1) surrounding the sand spit (R2, R3) presents the highest diversity.

Except in the subtidal samples R4 and R6 (group 2), the dominant ostracod is the brackish water species *Cyprideis torosa*. Also common are species of the mostly brackish genera *Leptocythere*, *Loxoconcha* and *Xestoleberis*.

The littoral environment (group 1), represented by the sand spit samples R2 and R3, is mainly characterised by the marine foraminifer species *Elphidium macellum* as well as *Ammonia parkinsoniana*, *Quinqueloculina* spp. and *Ammonia* spp. are the dominant foraminifer taxa of the subtidal environment of the inner lagoon of Elaia (sites R4–R6, group 2). Sites R7–R11 (group 3) reflect

intertidal environments; they are dominated by the foraminifers *Ammonia tepida* and *Haynesina germanica*.

5.3.3. ELA 58

Twenty genera and 26 species of Ostracoda and 30 genera and 49 species of Foraminifera were identified in core ELA 58. In total 6597 tests and valves were counted. Based on the microfossil distribution the section was divided into two main parts: Zones 1–2 and Zone 3, separated by a microfossil-barren sandy layer (Table 2).

First microfossils appear at 8.17 m below surface (b.s.) and continue to 5.85 m below surface (units 1–3 in Fig. 7; see also Fig. 8). Above this is a 1.5 m thick sandy layer that does not contain any microfossils or shell fragments (unit 4 in Fig. 7). From 4.30 m to 3.23 m b.s. two main parts are different in faunal composition: The

Coring ELA 58 - In front of the ship sheds
(27°02'30.25" E; 38°56'34.26" N)

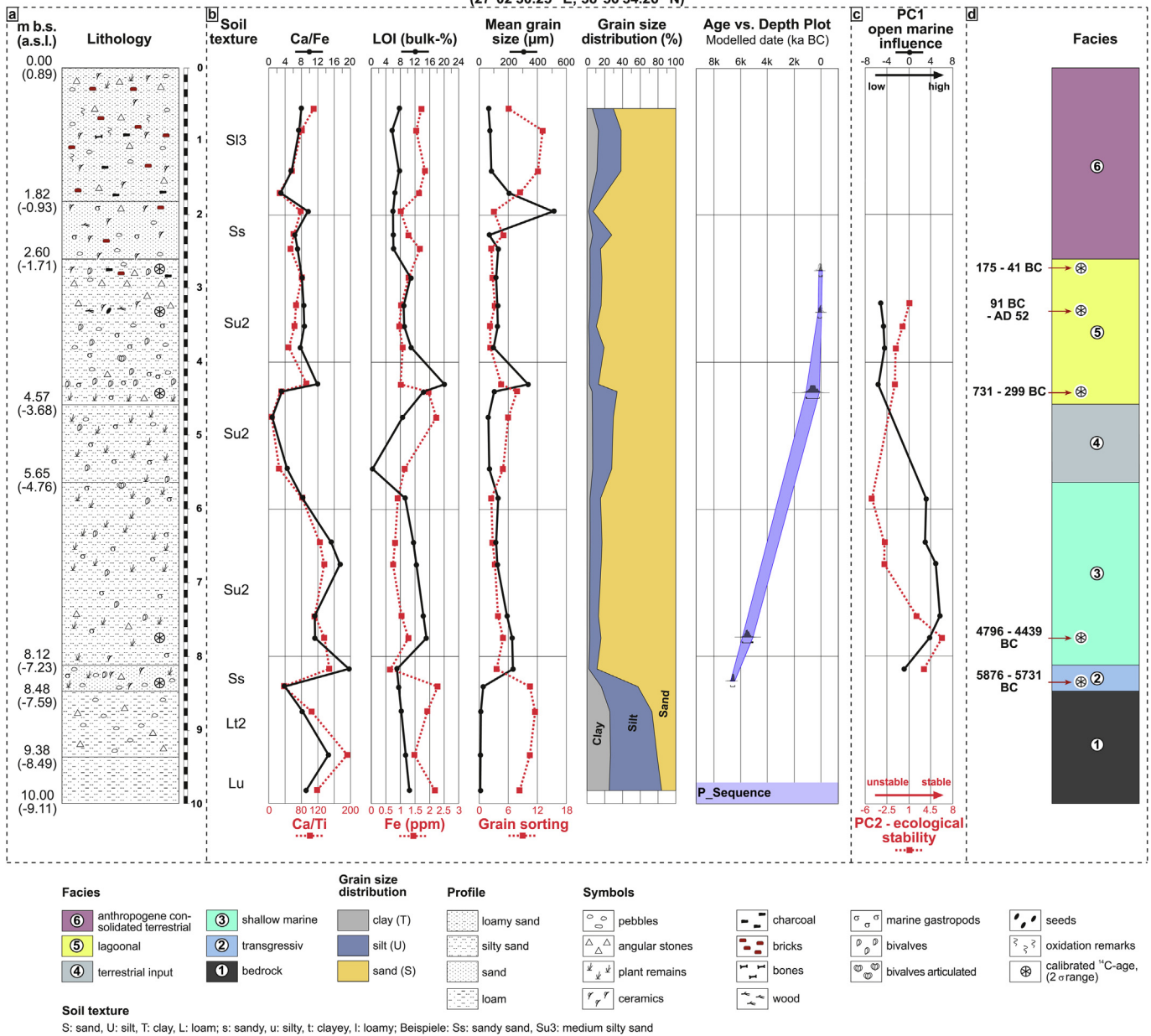


Fig. 7. Sediment core ELA 58 with geochemical and sedimentological parameters (a and b). The age/depth plot is based on the Oxcal 4.2 Software using a P-Sequence. (c) Microfaunal data. (d) Facies interpretation and dating results.

lower part of Zones A–B is dominated by the Ostracoda *Loxoconcha bairdi* and *Aurila convexa*, and the Foraminifera *Lobatula lobatula*, *Rosalina floridana* and *Cibicides advenum*. This part of the core may be further subdivided into two subzones. In contrast to the lower

zone A, the upper Zone B shows a markable increase in diversity of Ostracoda and Foraminifera and slight differences in association. Zone C is dominated by the Ostracoda *Loxoconcha stellifera* and *Aurila convexa*, and the Foraminifera *Ammonia tepida*, *Ammonia*

Table 2
Lithological units and micropalaeontological zonation of core ELA 58.

Core depth [m below surface]	Unit	Zone	Lithology	Characteristic Ostracoda	Characteristic Foraminifera
2.60–0.00	6		Colluvial facies with anthropogenic influence	–	–
4.57–2.60	5	C	Well sorted silty sand	<i>Loxoconcha stellifera</i> <i>Aurila convexa</i>	<i>Ammonia tepida</i> <i>Ammonia beccarii</i>
5.65–4.57	4		Well sorted sand with rounded gravels	–	–
8.12–5.65	3	A, B	Well sorted silty sand	<i>Loxoconcha bairdi</i> <i>Aurila convexa</i>	<i>Lobatula lobatula</i> <i>Rosalina floridana</i> <i>Ammonia compacta</i>
8.48–8.12	2	A	Sand with well -rounded gravels	–	<i>Lobatula lobatula</i>
10.00–8.48	1		Reddish yellow calcare-ous sandstone (bedrock)	–	–

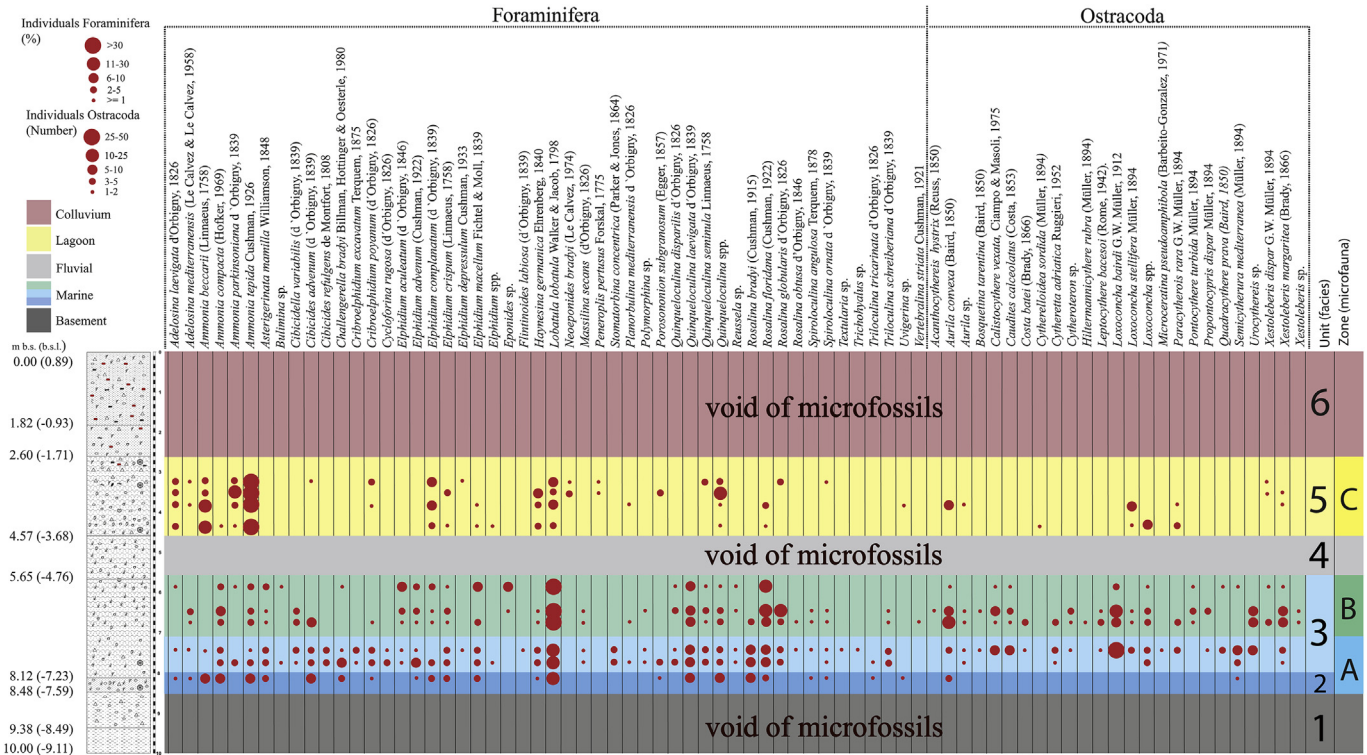


Fig. 8. Microfossil distribution. Zonal division based on microfossil distribution over core ELA 58. Sedimentation units: 1–5; microfossil zones: A–C. The presentation of the abundance of the ostracods and the dominance of the foraminifers are given semi-quantitatively.

beccarii and *Adelosina laevigata*. The diversity is significantly reduced compared to the lower parts of the core.

The dataset of the core ELA 58 includes abundances and diversity indices (Figs. 9a,b). The preparation of the data implied the exclusion of taxa present in less than three samples, and the pairwise exclusion of taxa with a high correlation (Spearman Rank correlation of more than $|\pm 0.9|$). Thus, a total of 39 taxa were excluded. The abundances are $\log(x + 1)$ transformed and then standardised together with diversity indices (Fig. 9a). To compare ELA 58 with Recent associations, the Renkonen index ($PS = \sum \min(p1 i, p2 i)$) is used (Renkonen, 1938). For that, the lower relative abundances of the species (i) common in two samples (p) are

summarised. Note: By adding relative abundances of Foraminifera and Ostracoda, two identical samples would produce a Renkonen index of 200 % (Fig. 10).

6. Discussion

6.1. Site evolution of core ELA 58

6.1.1. Changing depositional contexts

Following the zonation of the core (Figs. 7 and 10) and based on microfaunistic and sedimentological characteristics, we interpret the site evolution of core ELA 58 as follows:

Table 3
Recent sample sites and their most frequent microfossil taxa.

Group	Site	Location	Coordinates	Most frequent Ostracoda	Most frequent Foraminifera
Group 1	R2	Exposed side of the sand spit of Elaia	38.92962 N 27.04752 E	<i>Xestoleberis</i> sp. <i>Cyprideis torosa</i>	<i>Elphidium macellum</i> , <i>Ammonia parkinsoniana</i>
	R3	Sheltered side of the sand spit of Elaia	38.92962 N 27.04752 E		<i>Ammonia tepida</i> <i>Elphidium</i> spp.
Group 2	R4	Subtidal zone of the open inner lagoon of Elaia	38.93781 N 27.04558 E	<i>Xestoleberis</i> sp. <i>Cyprideis torosa</i>	<i>Haynesina germanica</i> <i>Quinqueloculina</i> spp.
	R5		38.93781 N 27.04558 E	<i>Cyprideis torosa</i> <i>Loxococoncha</i> spp.	<i>Ammonia tepida</i> <i>Quinqueloculina</i> spp.
	R6		38.93781 N 27.04558 E	<i>Loxococoncha</i> spp. <i>Cyprideis torosa</i>	<i>Ammonia tepida</i>
Group 3	R7	Tidal flat/salt marsh	38.94223 N 27.04036 E	<i>Cyprideis torosa</i>	<i>Ammonia tepida</i>
	R8		38.94182 N 27.03970 E	<i>Cyprideis torosa</i> <i>Leptocythere</i> sp.	<i>Haynesina germanica</i>
	R9		38.94180 N 27.03935 E	<i>Cyprideis torosa</i>	<i>Haynesina germanica</i> <i>Ammonia tepida</i>
	R11	Mouth of a distributary arm of the Bakırçay (Kaikos river)	38.921167 N 26.982972 E		<i>Quinqueloculina</i> spp. <i>Ammonia</i> spp.

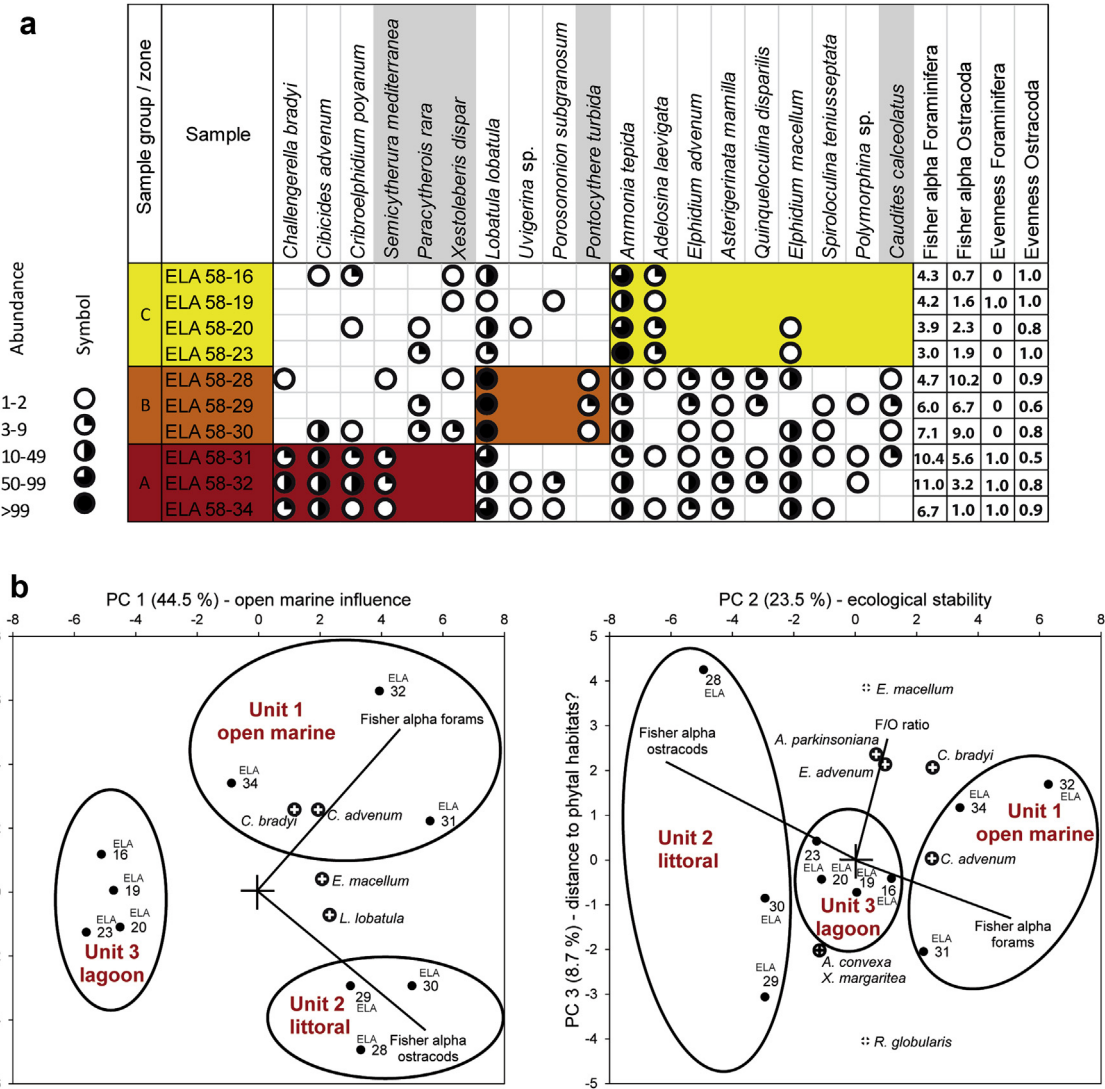


Fig. 9. a: Statistical analyses of the microfauna of sediment core ELA 58. Associations based on a hierarchical cluster analysis and on presence/absence of taxa, i.e. missing of frequent taxa partly also describes characteristic associations. Grey – ostracod species; red – sample group/unit and taxa characteristic of association 1 interpreted as living in an open marine habitat; orange – sample group/unit and taxa characteristic of association 2 interpreted as reflecting a littoral habitat; yellow – sample group/unit and taxa characteristic of association 3 interpreted as lagoonal. b: Statistical analyses of the microfauna of sediment core ELA 58. Principal Component Analysis. Faunistic loadings *10; all taxa with absolute loadings <0.2 are omitted for clarity. PC 1 is interpreted as open marine influence, PC 2 as ecological stability, PC 3 is supposed to reflect the distance to phytal habitats. (For interpretation of the references to colour in this figure legend, the reader is referred to the web version of this article.)

Unit 1: Basement (10.00–8.48 m b.s.). The reddish yellow calcareous sandstone likely belongs to a Pre-Quaternary formation. Due to the lack of microfossils, neither a precise chronology nor a palaeoecological interpretation is available.

Unit 2: Littoral layer (transgressive horizon; 8.48–8.12 m b.s.). The sand dominated sediment contains well rounded gravels that indicate the first shoreline migration during the marine transgression after the Last Glacial Maximum. The low organic

		ELA 58			Renkonen Index	Site/Unit	Habitat		
		open marine	littoral	lagoon					
		Unit 1	Unit 2	Unit 3					
Recent sites	Group 1	exposed spit	R2	31	37	Renkonen Index	Site/Unit	Habitat	
		sheltered spit	R3	23	26				23
	Group 2	subtidal (open inner lagoon)	R4	19	21				32
		tidal zone (intertidal, open inner lagoon)	R5	30	23				40
		sublittoral (open inner lagoon)	R6	29	26				32
	Group 3	tidal flat/salt marsh	R7	7	5				30
		tidal flat/salt marsh	R8	10	8				28
		tidal flat/salt marsh	R9	8	6				24
		estuary, mouth of Bakircay	R11	8	6				7

Fig. 10. Comparison of ELA 58 with Recent sites using the Renkonen index. The higher the Renkonen Index, the more similar are both associations. Light grey: habitats and environments; medium grey: sites and units, dark grey: Renkonen Indices.

content of only 7 % is typical of a high-energy littoral environment. ^{14}C AMS dating gave an age of 5876–5731 cal BC (8.35 m b.s.). *L. lobatula* and *C. advenum* at a depth of 8.17 m b.s. indicate shallow marine conditions. The diversity of Ostracoda and Foraminifera increases distinctively, reaching a maximum at top of the unit.

Unit 3: Shallow marine layer (8.12–5.65 m b.s.). Higher ratios of Ca/Fe and Ca/Ti and lower values of Fe indicate sedimentation under marine conditions (Vött et al., 2002). The well sorted silty sand contains *L. lobatula*, *R. floridana* and *A. convexa*; they represent a marine-littoral environment (Handl et al., 1999; Meriç et al., 2004; Bergin et al., 2006; Ertekin and Tunoglu, 2008). The diversity remains as high as in the highest part of Unit 2 (Fig. 8). Dating of sea grass (7.75 m b.s.) yielded a ^{14}C -age of 4796–4439 cal BC, a timespan far beyond the first settling of Elaia and Pergamum.

Unit 4: Fluvial layer (5.65–4.57 m b.s.). Shifts in the Ca/Fe and Ca/Ti ratios in favour of iron and titan and the total lack of microfossils indicate a dominating terrestrial (fluvial) input of sediment (Vött et al., 2002). Well rounded gravel (4.60 m b.s.) and minimum values of LOI support this assumption.

Unit 5: Lagoonal layer (4.57–2.60 m b.s.). In comparison to unit 3, unit 5 shows lower ratios of Ca/Fe and Ca/Ti, but a similar percentage of iron. This indicates a stronger terrestrial influence, probably supported by a very low-energy wave climate or the lack of vegetation, due to enhanced sedimentation. The increased occurrence of Foraminifera preferring very shallow and protected coastal areas, e.g. *A. tepida* and *A. beccarii* (Murray, 2008) or the ostracod *L. stellifera* indicate the evolution of a sheltered embayment or a lagoon.

The distinct dominance of marine organisms suggests a permanent water exchange with the open sea. Therefore a harbour utilisation of the bay is conceivable. At that time (731–299 cal BC, 4.40 m b.s.; Table 1), Elaia was in its formative phase before its heyday. The lagoonal conditions continued until the Roman Imperial period. The construction of the two breakwaters of the closed harbour basin – dated to approx. 280 BP (Seeliger et al., 2013, Figs. 2 and 4) – led to increased sedimentation in the Bay of Elaia. The time of the final siltation seems to have been around the 1st century BC; however, this interpretation is problematic because of the nearly inverted ^{14}C ages in the upper part of the section. Considering the younger time interval of 91 cal BC to 52 cal AD suggests the existence of lagoon-like conditions until the early Roman Imperial Period. If so, the ship sheds could still have been in use during the 1st century AD. In any case, the dating results (Fig. 7) reveal a much higher sedimentation rate in the lagoonal unit 5 than below in the transgressive and marine sequence of the core (units 2–3).

Unit 6: Colluvial and alluvial layer with anthropogenic influence (0–1.82 m below surface).

The uppermost part of the section contains colluvial and alluvial sediments with a huge number of pottery fragments dated to the Hellenistic and Roman Periods. In addition, pieces of carved bones are present in this section, which hints to diversified craftsmanship in the city of Elaia.

As we know from other parts of the city, the swampy parts of the dried up areas were intentionally made accessible by the deposition of stones and broken ceramics (Brückner et al., 2013; Seeliger et al., 2013). Later, the material was reworked by farming activities, evidenced by the wide distribution of ceramic finds in the uppermost part of the profile. With the seaward migration of the coast-line, the use of the ship sheds came to an end.

6.1.2. Comparison with the recent milieus in the Bay of Elaia

Comparing the studied Recent microfossil associations with those from ELA 58 using the Renkonen index for both Ostracoda and Foraminifera reveals considerable differences but also some similarities (Fig. 10): The highest similarity of microfaunal Zones A and B points to the exposed side of the Recent sand spit reflecting open shallow marine conditions; however, Zone A resembles more subtidal habitats and Zone B more intertidal ones. Zone C is most similar to the Recent intertidal environment, but without brackish water characteristics. As a result of these comparisons and in agreement with the palaeoecological analysis, the three zones are best classified as open marine (zone A), littoral (zone B), and marine-lagoonal (zone C) environments. The generally low agreement of the Recent microfauna as compared to the fossil samples may be caused by the presently very much protected milieu of the Bay of Elaia, whereas 5000 years BC, during the post glacial transgression, the coast was much more exposed.

In both the empirical and the statistical analyses (Fig. 9a, b) there is no evidence of a fully brackish water body, like a closed lagoon. *C. torosa* is the most frequent and most widely distributed ostracod species within the Recent samples indicating brackish water conditions (Frenzel and Boomer, 2005; Pint et al., 2012), but lives as an opportunistic species in nearly any other aqueous habitats as well. *C. torosa* and other typical brackish water ostracod species like *Loxoconcha elliptica* and some *Leptocythere* species, which could indicate a closed harbour basin (Mazzini et al., 1999; Morhange et al., 2003; Marriner and Morhange, 2007), are missing in the core ELA 58. On the other hand, the increasing sedimentation rate around 500 BC (Fig. 7) points to deposition of “harbour mud” due to the sheltered situation (Marriner and Morhange, 2007). Until its final and strong siltation, likely caused by anthropogenic soil erosion and intentionally deposited material, the microfaunal associations of ELA 58 indicate a subtidal environment of a few metres water depth only.

The evolution of a natural lagoon is recognisable when studying the succession of Foraminifera associations (Fig. 8). Unit 2 in Zone A is dominated by open marine species, whereas in both units of 3 (upper Zone A and Zone B) littoral species increase in proportion. Unit 5 (Zone C) is characterised by species preferring lagoonal conditions.

In contrast, the ostracod species show only variations in diversity and abundance but not in ecological preferences. Almost all ostracod species are epi-faunal and of marine origin, however, a distinction of coastal and open lagoonal environments seems to be possible (Mazzini et al., 1999, 2011, Marriner et al., 2008, 2010). A high similarity between more open marine and lagoon water quality is recognisable, particularly concerning the factor salinity. Therefore, we assume a lagoon widely open in offshore direction. The low diversity of Ostracoda from the lowermost and the uppermost part of the section may be caused in unfavourable ecological conditions. A high turbulence of water is considerable for the lower part, whereas the upper part may be characterised by low oxygen concentration.

6.1.3. Palaeoecologic consequence

The satellite image clearly shows the former extension of the sand spit to the north-west (Fig. 2, esp. 2e). The outer Bay of Elaia still hosts an island, which is the remnant of a bigger structure that had reached much more towards the east (Fig. 2). Both morphologic features represent secondary coastal spits or barriers that were built up by coastal long shore drift and the gyre which had once evolved in the Bay of Elaia. As an effect of their formation the innermost areas of the embayment – this holds in particular also true for coring site ELA 58 – turned more and more towards very calm conditions.

Why these features are nowadays drowned and partly eroded? As a result of our research about the drowned salt works of Elaia (Seeliger et al., 2014) we know that today's sea level is at least 1.7 m higher than during Hellenistic times (Seeliger et al., 2013). The reasons are the ongoing global warming, amplified by the subsidence of the graben ensemble. An earthquake may have caused a sudden subsidence of the whole terrain for a few decimetres. Another reason for the opening of the elongated sand spits and barriers may have been a severe storm. In any case, these secondary coastal features have been partly eroded since then.

As a result of our detailed studies we can state that core ELA 58 has very well archived these depositional changes in the micro-faunal record.

Except of the Hellenistic and Roman periods, the human impact on the landscape was negligible and no large-scale construction projects are known from antiquity. Unfortunately no investigations dealing with the progradation of the Kaikos River delta and the fluctuations of its sediment load have been conducted so far. Both processes may have influenced the Bay of Elaia as well.

A huge container port is under construction just between the river mouth of the Kaikos and the Bay of Elaia (Figs. 1a and 2a) since 2011. For that purpose, large amounts of building material is mined in the Yuntdağ mountain area. More process oriented sedimentological studies should be done to answer how this will change the appearance of the Bay of Elaia in future.

6.2. Archaeological implications

A natural lagoon or sheltered bay can offer favourable conditions for a harbour situation that implies a minimum of water depth and a connection to the open sea. The protected area of both, lagoon and harbour, produced very fine sediments, described as harbour mud and effected a rapid increase of the sedimentation rate that could mark harbour activity (Marriner and Morhange, 2007). Additionally, typical microfauna assemblages including brackish water and lagoonal species like the Ostracoda *C. torosa* and *Loxocochoa* spp. and the Foraminifera *H. germanica* and *A. tepida* are observable (Reinhardt et al., 1994; Stock et al., 2013). Spit-protected lagoons, used as harbours in the Mediterranean, like the Phoenician military harbour of Kition Bamboula (Cyprus), were already described by Morhange et al. (2000).

The open beach ending at the southernmost point of the fortification wall was only sparsely inhabited, which is backed by a very small quantity of finds during an enlarged ceramic survey (Pirson, 2011). A breakwater or a sea wall has not been detected. For this reason we assume that the beach may have been used as a landing place. The southern part of the city probably served as a multi-purpose military zone, where, e.g., allied ships could be beached, soldiers and sailors set up their camp and maintenance work on a large scale could be carried out (Pirson, 2011).

Regarding the open harbour zone the basic question is: What type of building was the structure with a size of c. 105 × 55 m² visible in the geophysical image and which kind of function did it have (see Figs. 4 and 5; chapter 5.1). The complex is largely aligned with its narrow side parallel to the southern breakwater. This may indicate a maritime orientation of the building. For the moorage of vessels, however, the right angles of the structure offered poor conditions; this section can therefore not have served as a quay. Rather, it was a large building structure that was divided more or less evenly into long rectangular compartments that were oriented to the waterfront at a right angle. Such a partition can be found in Classical and Hellenistic ship sheds. Those installations were needed, because ancient warships were always kept out of the water when not in action in order to avoid rot and the destructive shipworm (Morrison and Coates, 1996). The roof of the ship sheds

protected the warships from sun and rain (Blackman, 2003, 2008). Elementary for the interpretation of the structure as the ship sheds of Elaia, however, is the question whether or not there was a sufficient water depth on the seaward side so that the oared warships could be pulled inside.

The size and draught of Classical and Hellenistic oared warships were convincingly reconstructed by Morrison and Coates (1986, 1996) and Coates (1987). Their research demonstrates that the most common classes of warships of these eras had a draught between approx. 1.10 m for the so-called threes (*triere*) and of up to approx. 1.50 m for the fifths (*pentere*; Morrison and Coates, 1986, 1996). By far bigger in size and draught were the so-called sixes and sevens with a draught exceeding 1.50 m, not to speak of even larger ships (Morrison and Coates, 1996). However, those categories of ships were only rarely used in battle; there are no hints that the kings of Pergamum possessed ships of these classes. Resulting from those reconstructions of the ancient oared warships in Hellenistic times a water depth of at least 1.50 m is required on the seaward site at coring point ELA 58 to give a sufficient water depth that ships could have been pulled into the ship sheds.

The top of the closed harbour mole's basement acts as a sufficient palaeo-sea level indicator since it was more or less at sea level when the breakwater was erected in early Hellenistic times (first half of the 3rd century BC). Hence a palaeo-sea level about 1.7 m lower compared to the modern one can be postulated. In addition, sea-grass fibres (ELA 70/80H), which may more or less represent the palaeo-sea floor, were ¹⁴C dated to 650–181 cal BC (until Hellenistic times) at a core depth of 4.69 m below present day sea level (Seeliger et al., 2013). The sea grass in this unit of core ELA 70 is distributed over a 3.5 m thick layer and therefore can be assumed to be autochthonous (Seeliger et al., 2013). As a consequence, a maximum mean water depth of approx. 3 m during Hellenistic times can be stated for the closed harbour basin. If this very thick sea grass layer would represent an accumulation at the driftline, what we doubt, the reconstructed water would be even less. Regarding literature, dredging of ancient harbours was a common practice all over the Mediterranean (Marriner and Morhange, 2006; Kraft et al., 2007; Morhange and Marriner, 2010), but no literary nor sedimentological evidence for this action has so far been discovered from Elaia (Seeliger et al., 2013). Thus, the water depth of approx. 3 m can be extrapolated for the open harbour area as well. Bearing in mind that the tidal range in the Bay of Elaia is only c. 20 cm, the closed harbour basin was easily navigable by ship in those days. In addition, the microfossil analysis of ELA 58 situated in front of the assumed ship sheds leads to the conclusion that water depth was a few metres in Hellenistic times – i.e. enough for the draught of a warship of that era.

The ship sheds of Elaia may have housed about fourteen ships of the Pergamian royal fleet. This appears at first sight to be a fairly small number for a regional power such as the kingdom of Pergamum that had to act at sea in the 3rd and especially 2nd century BC. However, it can be assumed that the royal fleet was spread over several naval bases in the Eastern Mediterranean and not all ships were concentrated in the harbour of Elaia. Another naval base could have been located on the island of Aegina which belonged to the Attalids since 211 BC (Escher, 1894; Kalcyk, 1996). Other smaller contingents may have been stationed at smaller bases on the southern coast of Asia Minor or the Aegean coast.

The much larger fleet of the Hellenistic city of Rhodes can serve as a comparison to the different naval bases of the fleet of the kingdom of Pergamum: The ships were not only stationed in the extensive military harbour of the city, but smaller units were also based at outposts along the south-western coast of Asia Minor and on smaller islands northwest of Rhodes (Gabrielsen, 1997; Blackman, 2010).

The connection between a major inland city and a port at the coast cannot only be found at Hellenistic Pergamon with its maritime satellite Elaia (Pirson, 2004, 2008b), but also at Classical Athens with Piraeus or at Imperial Rome with Portus-Ostia. The acquisition of a port city was vital for the development of those inland metropolises.

After the end of the Pergamian Empire and the integration of its territory into the newly established Roman province of Asia, the ship sheds of Elaia had lost their function as naval bases. There are no literary or archaeological evidences that warships had been stationed there in Roman times.

The sediment core ELA 58 indicates that the regression of the sea in the 'wedge' between the southern breakwater, the seawall and the ship sheds had already begun in the 1st century BC. In the time of the early Roman Empire the colluvium-alluvium is intentionally covered with debris, stones and pottery up to a thickness of 1.50 m (unit 6 in Fig. 7). Apparently, this package was to consolidate the silted up area and make it accessible.

How the area was used during Roman Imperial times cannot be reconstructed with certainty. The closed harbour was surely still in use (Seeliger et al., 2013), but the area of the Hellenistic ship sheds could only have served as an anchorage for smaller boats by then.

7. Conclusion

The microfossil analysis of core ELA 58 from the Bay of Elaia primarily answers two questions. At first, variation in foraminifer distribution indicates a lagoonal development, and second, the marine ostracod assemblage points to a wide seaward opening of the lagoon. It is a marine microfauna of mostly subtidal conditions, without brackish water impact. In addition, the palaeontological research shows that the water depth of the open harbour was sufficient for navigation in Hellenistic times and even shortly before the final siltation.

As expected, typical environmental characteristics of closed harbours (Marriner and Morhange, 2007), like a brackish water fauna association, are missing in the open harbour zone of ELA 58. The sedimentation rate increased during the lagoonal period, likely induced by the immediate vicinity of the closed harbour.

The synopsis of the geophysical research and the analyses of core ELA 58 indicate that the structure in the harbour zone of Elaia with a size of about 105 × 55 m² can best be interpreted as the place of Hellenistic ship sheds. Water depth in the open harbour was sufficient for the draught of most of the Hellenistic oared warships, such as the so-called threes (*triere*), fourth (*tetrere*) and fifth (*pentere*) (Morrison and Coates, 1996).

Acknowledgements

The project presented here was conducted in the context of the DFG priority program (SPP) 1209 "The Hellenistic Polis as a Living Space – Urban Structures and Civic Identity Between Tradition and Innovation" (2008–2012). Financial support by the German Research Foundation is gratefully acknowledged (DFG ref. no. PI 740/1-3). Our research was part of the Elaia Survey Project, headed by Prof. Dr. Felix Pirson, Director of the DAI Istanbul and excavation director of Pergamum/Turkey. The studies would not have been possible without the support and hospitality of the Pergamum excavation team. We are thankful to Dr. Güler Ateş (Institute for Ancient Studies, Heidelberg University) for the determination of the ceramic finds, and to Dr. Harald Stümpel (Institute of Geosciences, Kiel University) for assisting with the interpretation of geophysical data. Melanie Müßle and Thomas Fuhrmann (Karlsruhe Institute of Technology) supported the DGPS data processing.

PD Dr. habil. Wolf-Rüdiger Teegen (ArchaeoBioCenter at the LMU, Munich) is thanked for the interpretation of carved bones pieces. The Ministry of Culture and Tourism of the Republic of Turkey kindly granted the research permits.

Appendix A

Table A

Foraminifera taxa from Recent and fossil samples of the Bay of Elaia.

Species	Recent associations	ELA 58 zone
Foraminifera		
<i>Adelosina laevigata</i> d'Orbigny, 1826		A–C
<i>Adelosina mediterraneensis</i> (Le Calvez & Le Calvez, 1958)		A–C
<i>Adelosina</i> spp.	2–9, 11	
<i>Ammonia beccarii</i> (Linnaeus, 1758)	2–3	A–C
<i>Ammonia compacta</i> (Hofker, 1969)		A–C
<i>Ammonia parkinsoniana</i> d'Orbigny, 1839	2–9, 11	A–C
<i>Ammonia tepida</i> Cushman, 1926	2–9, 11	A–C
<i>Asterigerinata mamilla</i> Williamson, 1848	2	A, B
<i>Bulimina</i> sp.		A, B
<i>Cibicides variabilis</i> (d'Orbigny, 1839)		A, B
<i>Cibicides advenum</i> (d'Orbigny, 1839)		A–C
<i>Cibicides refulgens</i> de Montfort, 1808		A
<i>Cibicides</i> sp.	2	
<i>Challengerella bradyi</i> Billman, Hottinger & Oesterle, 1980		A, B
<i>Criboelphidium excavatum</i> Terquem, 1875	2–7	A
<i>Criboelphidium poeyanum</i> (d'Orbigny, 1826)		A–C
<i>Cycloforina rugosa</i> (d'Orbigny, 1826)		A
<i>Elphidium aculeatum</i> (d'Orbigny, 1846)	2–7	A, B
<i>Elphidium advenum</i> (Cushman, 1922)		A, B
<i>Elphidium complanatum</i> (d'Orbigny, 1839)	2–6, 8–9	A–C
<i>Elphidium crispum</i> (Linnaeus, 1758)	2	A–C
<i>Elphidium depressulum</i> Cushman, 1933		A, C
<i>Elphidium macellum</i> Fichtel & Moll, 1839	2–6, 8, 11	A–C
<i>Elphidium</i> spp.	2–6	A, C
<i>Eponides</i> sp.		B
<i>Flintinoides labiosa</i> (d'Orbigny, 1839)		A
<i>Haynesina germanica</i> Ehrenberg, 1840	2–9	A–C
<i>Hemisphaerammina</i> sp.	2–7, 9	
<i>Jadammina macrescens</i> Brady, 1870	4, 6, 8–9	
<i>Lobatula lobatula</i> Walker & Jacob, 1798	2	A–C
<i>Neoponides bradyi</i> (Le Calvez, 1974)		C
<i>Nubecularia lucefuga</i> Defrance, 1825	2, 4	
<i>Massilina secans</i> (d'Orbigny, 1826)		A, B
<i>Peneroplis pertusus</i> Forskal, 1775	2–6	C
<i>Peneroplis planatus</i> Fichtel & Moll, 1798	2, 5–6	
<i>Stomatobina concentrica</i> (Parker & Jones, 1864)		A
<i>Planorbulina mediterraneensis</i> d'Orbigny, 1826	2, 4, 6	A–C
<i>Polymorphina</i> sp.		A, B
<i>Porosonion subgranosum</i> (Egger, 1857)		A, C
<i>Quinqueloculina disparilis</i> d'Orbigny, 1826		A, B
<i>Quinqueloculina seminula</i> Linnaeus, 1758		A–C
<i>Quinqueloculina</i> spp.	2–9, 11	A–C
<i>Reussella</i> sp.		A, B
<i>Rosalina bradyi</i> (Cushman, 1915)		A, B
<i>Rosalina floridana</i> (Cushman, 1922)		A–C
<i>Rosalina globularis</i> d'Orbigny, 1826		A–C
<i>Rosalina obtusa</i> d'Orbigny, 1846		A, B
<i>Rosalina</i> spp.	2–6, 8	
<i>Siphonaperta aspera</i> d'Orbigny, 1826	2, 4–6	
<i>Spiroloculina angulosa</i> Terquem, 1878	4, 6	A, B
<i>Spiroloculina ornata</i> d'Orbigny, 1839	4, 6	A–C
<i>Textularia</i> sp.		A
<i>Trichohyalus</i> sp.		A
<i>Triloculina schreiberiana</i> d'Orbigny, 1839		A, B
<i>Triloculina tricarinata</i> d'Orbigny, 1826		A
<i>Triloculina</i> spp.	2–5, 7, 9	
<i>Trochammina inflata</i> Montagu, 1808	2, 4–7, 9	
<i>Uvigerina</i> sp.		A, C
<i>Vertebralina striata</i> Cushman, 1921	2–6	B

Table B
Ostracod taxa from Recent and fossil samples of the Bay of Elaia.

Species	Recent associations	ELA 58 zone
Ostracoda (marine)		
<i>Acanthocythereis hystrix</i> (Reuss, 1850)		B
<i>Aurila convexa</i> (Baird, 1850)		A–C
<i>Aurila glyptica</i> Barbieto-Gonzalez, 1971	2, 3, 5, 6	
<i>Aurila prasina</i> Barbieto-Gonzalez, 1971	2, 3, 5, 6	
<i>Aurila woodwardii</i> Brady, 1868	2, 3, 5, 6	
<i>Aurila</i> sp.		A–C
<i>Bosquetina tarentina</i> (Baird, 1850)		A, B
<i>Calistocythere cf. badia</i> Norman, 1862	2, 3	
<i>Calistocythere vexata</i> Ciampo & Masoli, 1975		A, B
<i>Caudites calceolatus</i> (Costa, 1853)		A, B
<i>Costa batei</i> (Brady, 1866)		A, B
<i>Cytherelloidea sordida</i> (Müller, 1894)		C
<i>Cytheretta adriatica</i> Ruggieri, 1952		A, B
<i>Cythereis</i> spp.	2, 4, 8	
<i>Cytheropteron</i> sp.		A, B
<i>Hiltermannicythere rubra</i> (Müller, 1894)		B
<i>Heterocythereis</i> sp.	2	
<i>Leptocythere bacesoi</i> (Rome, 1942)		A, B
<i>Leptocythere</i> spp.	1	
<i>Loxococoncha bairdi</i> (Müller, 1894)		A, B
<i>Loxococoncha stellifera</i> Müller, 1894		A–C
<i>Loxococoncha</i> spp.		A–C
<i>Microceratina pseudoamphibola</i> (Barbeito-Gonzalez, 1971)		B
<i>Paracytherois rara</i> Müller, 1894		B, C
<i>Pontocythere turbida</i> Müller, 1894		B
<i>Pontocythere</i> sp.	2, 11	
<i>Propontocypris dispar</i> (Müller, 1894)		A, B
<i>Semicytherura mediterranea</i> (Müller, 1894)		A, B
<i>Tenedocythere prava</i> (Baird, 1850)		A, B
<i>Urocythereis</i> sp.	2, 3	A, B
<i>Xestoleberis dispar</i> Müller, 1894		B, C
<i>Xestoleberis margaritea</i> (Brady, 1866)		A–C
<i>Xestoleberis</i> sp.	2, 3, 4, 5, 6	B
Ostracoda (brackish)		
<i>Cyprideis torosa</i> (Jones, 1850)	1–9, 11	
Ostracoda (freshwater)		
<i>Candona</i> sp.	R8	
<i>Ilyocypris</i> sp.	R3	

Appendix B. Supplementary data

Supplementary data related to this article can be found at <http://dx.doi.org/10.1016/j.jas.2014.06.011>.

References

- AG Boden (Ed.), 2005. *Bodenkundliche Kartieranleitung*. Schweizerbart, Stuttgart.
- Aksu, A.E., Piper, D.J.W., Konuk, T., 1987. Late Quaternary tectonic and sedimentary history of outer Izmir and Çandarlı Bays, Western Turkey. *Mar. Geol.* 76, 89–104.
- Antonoli, F., Anzidei, M., Lambeck, K., Auriemma, R., Gaddi, D., Furlani, S., Orrù, P., Solinas, E., Gaspari, A., Karinja, S., Kovačić, V., Surace, L., 2007. Sea-level change during the Holocene in Sardinia and in the north-eastern Adriatic (central Mediterranean Sea) from archaeological and geomorphological data. *Quat. Sci. Rev.* 26 (19–21), 2463–2486.
- Anzidei, M., Antonoli, F., Benini, A., Lambeck, K., Sivan, D., Serpelloni, E., Stocchi, P., 2011. Sea level change and vertical land movements since the last two millennia along the coasts of southwestern Turkey and Israel. *Quat. Int.* 232, 13–20.
- Auriemma, R., Solinas, E., 2009. Archaeological remains as sea level change markers: a review. *Quat. Int.* 206, 134–146.
- Barillé-Boyer, A.L., Barillé, L., Massé, H., Razet, D., Héral, M., 2003. Correction for particulate organic matter as estimated by loss on ignition in estuarine ecosystems. *Estuarine Coast. Shelf Sci.* 58, 147–153.
- Bergin, F., Kucuksezgin, F., Uluturhan, E., Barut, I.F., Meric, E., Avsar, N., Nazik, A., 2006. The response of benthic foraminifera and ostracoda to heavy metal pollution in Gulf of Izmir (Eastern Aegean Sea). *Estuarine Coast. Shelf Sci.* 66, 368–386.
- Blackman, D.J., 2003. Progress in the study of ancient shipsheds: a review. In: Beltrame, C. (Ed.), *Boats, Ships and Shipyards*. Proceedings of the Ninth International Symposium on Boat and Ship Archaeology, Venice 2000. Oxbow Books, Oxford, pp. 81–90.

- Blackman, D.J., 2008. Roman Shipsheds. In: Hohlfelder, R.L. (Ed.), *The Maritime World of Ancient Rome*. University of Michigan Press, Ann Arbor, pp. 23–36.
- Blackman, D.J., 2010. The Rhodian Fleet and the Karian Coast. In: van Bremen, R., Carbon, J.-M. (Eds.), *Hellenistic Karia*, Proceedings of the First International Conference on Hellenistic Karia, Oxford, 29 June–2 July 2006. De Boccard, Bordeaux, pp. 379–392.
- Blott, S.J., Pye, K., 2001. GRADISTAT: a grain size distribution and statistics package for the analysis of unconsolidated sediments. *Earth Surf. Process. Landf.* 26, 1237–1248.
- Bonaduce, G., Ciampo, G., Masoli, M., 1975. Distribution of ostracoda in the Adriatic sea. *Pub. Staz. Zool. Napoli* 40 (Suppl.), 1–304.
- Brinkmann, R., 1976. *Geology of Turkey*. Elsevier, Stuttgart.
- Brückner, H., 1997. Geographische Forschungen in der Westtürkei – das Beispiel Ephesos. *Passau. Schriften zur Geogr.* 15, 39–51.
- Brückner, H., 2005. Holocene shoreline displacements and their consequences for human societies: the example of Ephesus in western Turkey. *Z. Geomorphol. N.F.* 137 (Suppl.), 11–22.
- Brückner, H., Müllenhoff, M., Gehrels, R., Herda, A., Knipping, M., Vött, A., 2006. From archipelago to floodplain – geographical and ecological changes in Miletus and its environs during the past six millennia (Western Anatolia, Turkey). *Z. Geomorphol. N.F.* 142 (Suppl.), 63–83.
- Brückner, H., Urz, R., Seeliger, M., 2013. Geomorphological and geoarchaeological evidence for considerable landscape changes at the coasts of western Turkey during the Holocene. *Geopedol. Landsc. Dev. Res. Ser.* 1, 81–104.
- Cartledge, P., 2004. *Alexander the Great. The Hunt for a New Past*. Overlook Press, New York.
- Cimerman, F., Langer, M.R., 1991. *Mediterranean Foraminifera*. Slovenska Akademija Znanosti in Umetnosti, Academia Scientiarum et Artium Slovenica, Ljubljana.
- Coates, J.F., 1987. Reconstructing the ancient Greek trireme warship. *Endeavour* 11 (2), 94–99.
- Dankers, N., Laane, R., 1983. A comparison of wet oxidation and loss on ignition of organic material in suspended matter. *Environ. Technol. Lett.* 4, 283–290.
- Engel, M., Knipping, M., Brückner, H., Kiderlen, M., Kraft, J.C., 2009. Reconstructing middle to late Holocene palaeogeographies of the lower Messenian plain (southwestern Peloponnese, Greece): coastline migration, vegetation history and sea level change. *Palaeogeogr. Palaeoclimatol. Palaeoecol.* 284 (3–4), 257–270.
- Ernst, W., 1970. *Geochemical Facies Analysis*. Elsevier, Amsterdam, London, New York.
- Ertekin, I.K., Tunoglu, C., 2008. Pleistocene-Holocene ostracods from Mersin offshore sediments, Turkey, Eastern Mediterranean. *Rev. Micropaléontol.* 51, 309–326.
- Escher, J., 1894. In: Aigina, S.V. (Ed.), *Paulys Real-Encyclopädie der classischen Altertumswissenschaft* 1/1. J. B. Metzler'sche Verlagsbuchhandlung, Stuttgart, pp. 964–968.
- Evelpidou, N., Pirazzoli, P., Vassilopoulos, A., Spada, G., Ruggieri, G., Tomasin, A., 2012. Late Holocene sea level reconstructions based on observations of Roman fish tanks, Tyrrhenian Coast of Italy. *Geoarchaeology* 27, 259–277.
- Flaux, C., Claude, Ch., Marriner, N., Morhange, Ch., 2013. A 7500-year strontium isotope record from the northwestern Nile delta (Maryut lagoon, Egypt). *Quat. Sci. Rev.* 78, 22–23.
- Flemming, N.C., 1978. Holocene eustatic changes and coastal tectonics in the Northeast Mediterranean: implications for models of crustal consumption. *Philos. Trans. R. Soc. Lond. Math. Phys. Sci.* 289, 405–458.
- Florida, E., Auriemma, R., Faivre, S., Radi Rossi, I., Antonoli, F., Furlani, S., 2011. Istrian and Dalmatian fish tanks as sea-level markers. *Quat. Int.* 232, 105–113.
- Folk, R.L., Ward, W.C., 1957. Brazos River bar: a study in the significance of grain size parameters. *J. Sediment. Petrol.* 27, 3–26.
- Frenzel, P., Boomer, I., 2005. The use of ostracods from marginal marine, brackish waters as bioindicators of modern and quaternary environmental change. *Palaeogeogr. Palaeoclimatol. Palaeoecol.* 225, 68–92.
- Gabrielsen, V., 1997. *The Naval Aristocracy of Hellenistic Rhodes*. Aarhus University Press, Aarhus.
- Gifford, J., Rapp, G., Vitali, V., 1992. Palaeogeography of Carthage (Tunisia): coastal change during the first millennium BC. *J. Archaeol. Sci.* 19, 575–596.
- Goiran, J.-P., Tronchère, H., Salomon, F., Carbonel, P., Djerbi, H., Ognard, C., 2010. Palaeoenvironmental reconstruction of the ancient harbours of Rome: Claudius and Trajan's marine harbours on the Tiber delta. *Quat. Int.* 216, 3–13.
- Goiran, J.-P., Salomon, F., Mazzini, I., Bravard, J.-P., Pleuger, E., Vittori, C., Boetto, G., Christiansen, J., Arnaud, P., Pellegrino, A., Pepe, C., Sadori, L., 2014. Geoarchaeology confirms location of the ancient harbour basin of Ostia (Italy). *J. Archaeol. Sci.* 41, 389–398.
- Hadler, H., Kissas, K., Koster, B., Mathes-Schmidt, M., Mattern, T., Ntageretis, K., Reicherter, K., Willershäuser, T., Vött, A., 2013. Multiple late-Holocene tsunami landfall in the eastern Gulf of Corinth recorded in the palaeotsunami geo-archive at Lechaion, harbour of ancient Corinth (Peloponnese, Greece). *Z. Geomorphol. N.F.* 57 (Suppl.), 139–180.
- Handl, M., Mostafawi, N., Brückner, H., 1999. Ostracodenforschung als Werkzeug der Paläogeographie. *Marb. Geogr. Schr.* 134, 116–153.
- Hansen, E., 1971. *The Attalids of Pergamon*. Cornell University Press, Ithaca.
- Heiri, O., Lotter, A.F., Lemcke, G., 2001. Loss on ignition as a method for estimating organic and carbonate content in sediments: reproducibility and comparability of results. *J. Paleolimnol.* 25, 101–110.
- Joachim, F., Langer, M., 2008. The 80 Most Common Ostracods from the Bay of Fetoveia, Elba Island (Mediterranean Sea). *Selbstverlag Universität Bonn*, Bonn.

- Kalcky, H., 1996. In: Aigina, S.V. (Ed.), *Der Neue Pauly. Enzyklopädie der Antike 1*. Verlag J. B. Metzler, Stuttgart, pp. 320–323.
- Kelterbaum, D., Brückner, H., Dikarev, V., Gerhard, S., Pint, A., Porotov, A., Zin'ko, V., 2012. Palaeogeographic changes at Lake Chokrak on the Kerch Peninsula, Ukraine, during the Mid- and Late-Holocene. *Geoarchaeology* 27 (3), 206–219.
- Kraft, J.C., Brückner, H., Kayan, I., Engemann, H., 2007. The geographies of ancient Ephesus and the Artemision in Anatolia. *Geoarchaeology* 22, 121–149.
- Livy: *Ab urbe condita*, 1991. Books 35–38. Translation and comments by Hans Jürgen Hillen and Josef Feix. Wissenschaftliche Buchgesellschaft, Darmstadt (Latin to German).
- Loke, M.H., Barker, R.D., 1995. Least-squares deconvolution of apparent resistivity pseudosections. *Geophysics* 60, 1682–1690.
- Marriner, N., Morhange, C., 2006. Geoarchaeological evidence for dredging in Tyre's ancient harbour. *Levant. Quat. Res.* 65, 164–171.
- Marriner, N., Morhange, C., 2007. Geoscience of ancient Mediterranean harbours. *Earth-Sci. Rev.* 80, 137–194.
- Marriner, N., Morhange, C., Carayon, N., 2008. Ancient Tyre and its harbours: 5000 years of human environment interactions. *J. Archaeol. Sci.* 35, 1281–1310.
- Marriner, N., Morhange, C., Goiran, J.-P., 2010. Coastal and ancient harbour geoarchaeology. *Geol. Today* 26 (1), 21–27.
- Marriner, N., Goiran, J.-P., Geyer, B., Matoian, V., al-Maqdissi, M., Lecante, M., Carbonel, P., 2012. Ancient harbors and Holocene morphogenesis of the Ras Ibn Hani peninsula (Syria). *Quat. Res.* 78 (1), 35–49.
- Mazzini, I., Anadon, P., Barbieri, M., Castorina, F., Ferrelli, L., Gliozzi, E., Mola, M., Vittori, E., 1999. Late quaternary sea-level changes along the Tyrrhenian coast near Orbetello (Tuscany, central Italy): palaeoenvironmental reconstruction using ostracods. *Mar. Micropaleontol.* 37, 345–364.
- Mazzini, I., Faranda, C., Giardini, M., Giraudi, C., Sadori, L., 2011. Late Holocene palaeoenvironmental evolution of the ancient harbour of Portus (Latium, Central Italy). *J. Paleolimnol.* 46, 243–256.
- McHugh, C.M., Seeber, L., Cormier, M., Dutton, J., Gagatay, N., Polonia, A., Ryan, W.B., Gorur, N., 2006. Submarine earthquake geology along the North Anatolia Fault in the Marmara Sea, Turkey: a model for transform basin sedimentation. *Earth Planet. Sci. Lett.* 248, 661–684.
- Merić, E., Avsar, N., Bergin, F., 2004. Benthic foraminifera of eastern Aegean Sea (Turkey); systematics and autoecology. *Turk. Mar. Res. Found.* 18, 1–306.
- Mook, D.H., Hoskin, C.M., 1982. Organic determinations by ignition, caution advised. *Estuarine Coast. Shelf Sci.* 15, 697–699.
- Morhange, C., Marriner, N., 2010. Roman dredging in ancient Mediterranean harbours. *Boll. Archeol. Online vol. spec. IAAC*, 23–32.
- Morhange, C., Goiran, J.-P., Bourcier, M., Carbonel, P., Le Campion, J., Rouchy, J.-M., Yon, M., 2000. Recent Holocene paleoenvironmental evolution and coastline changes of Kition, Larnaca, Cyprus, Mediterranean Sea. *Mar. Geol.* 26, 205–230.
- Morhange, C., Blanc, F., Bourcier, M., Carbonel, P., Prone, A., Schmitt-Mercury, S., Vivent, D., Hesnard, A., 2003. Bio-sedimentology of the late Holocene deposits of the ancient harbour of Marseilles (southern France, Mediterranean Sea). *Holocene* 13, 593–604.
- Morhange, C., Pirazzoli, P., Evlpidou, N., Marriner, N., 2012. Tectonic uplift and silting up of Lechaion, western harbour of ancient Corinth (Greece). *Geoarchaeology* 27, 278–283.
- Morhange, C., Marriner, N., Excoffon, P., Bonnet, S., Flaux, C., Zibrowius, H., Jean-Philippe Goiran, J.-P., El Amouri, M., 2013. Relative sea-level changes during Roman Times in the Northwest Mediterranean: the 1st century A.D. fish tank of Forum Julii, Fréjus, France. *Geoarchaeology* 28, 363–372.
- Morrison, J.S., Coates, J.F., 1986. *The Athenian Trireme: the History and Reconstruction of an Ancient Greek Warship*. Cambridge University Press, Cambridge.
- Morrison, J.S., Coates, J.F., 1996. *Greek and Roman Oared Warships*. Oxbow Books, Oxford.
- Mourtzas, N.D., 2012. Fish tanks of eastern Crete (Greece) as indicators of the Roman sea level. *J. Archaeol. Sci.* 39 (7), 2392–2408.
- Murray, J.W., 2008. *Ecology and Applications of Benthic Foraminifera*. Cambridge University Press, New York.
- Niwa, Y., Sugai, T., Saegusa, Y., Ogami, T., Sasao, E., 2011. Use of electrical conductivity to analyze depositional environments: example of a Holocene delta sequence on the Nobi Plain, central Japan. *Quat. Int.* 230, 78–86.
- Pint, A., Frenzel, P., Fuhrmann, R., Scharf, B., Wennrich, V., 2012. Distribution of *Cyprideis torosa* (Ostracoda) in Quaternary athalassic sediments in Germany and its application for palaeoecological reconstructions. *Int. Rev. Hydrobiol.* 97 (4), 330–355.
- Pint, A., Seeliger, M., Bartz, M., Kelterbaum, D., Brückner, H., 2013. Die Rekonstruktion der Paläoumwelt von Elaia anhand von mikropaläontologischen, sedimentologischen und geochemischen Daten. In: Pirson, F. (Ed.), *Pergamon. Bericht über die Arbeiten der Kampagne 2012*. *Archäol. Anzeiger* 2, 175–185.
- Pirson, F., 2004. Elaia, der maritime Satellit Pergamons. *Istanbuler Mittl.* 54, 197–213.
- Pirson, F., 2007. Elaia. In: Pirson, F. (Ed.), *Pergamon. Bericht über die Arbeiten der Kampagne 2006*. *Archäol. Anzeiger* 2, 47–58.
- Pirson, F., 2008a. Elaia. In: Pirson, F. (Ed.), *Pergamon. Bericht über die Arbeiten der Kampagne 2007*. *Archäol. Anzeiger* 2, 130–140.
- Pirson, F., 2008b. Das Territorium der hellenistischen Residenzstadt Pergamon – Herrschaftlicher Anspruch als raumbezogene Strategie. In: Jöchner, C. (Ed.), *Räume der Stadt – Von der Antike bis heute*. Reimer, Berlin, pp. 27–50.
- Pirson, F., 2009. Elaia. In: Pirson, F. (Ed.), *Pergamon. Bericht über die Arbeiten der Kampagne 2008*. *Archäol. Anzeiger* 2, 182–200.
- Pirson, F., 2010. Survey. In: Pirson, F. (Ed.), *Pergamon. Bericht über die Arbeiten der Kampagne 2009*. *Archäol. Anzeiger* 2, 195–201.
- Pirson, F., 2011. Elaia. In: Pirson, F. (Ed.), *Pergamon. Bericht über die Arbeiten der Kampagne 2010*. *Archäol. Anzeiger* 2, 166–174.
- Radt, W., 2011. *Pergamon – Geschichte und Bauten einer antiken Metropole*. Primus Verlag, Darmstadt.
- Ramsey, C.B., 2008. Deposition models for chronological records. *Quat. Sci. Rev.* 27, 42–60.
- Reimer, P.J., Bard, E., Bayliss, A., Beck, J.W., Blackwell, P.G., Bronk Ramsey, C., Buck, C.E., Cheng, H., Edwards, R.L., Friedrich, M., Grootes, P.M., Guilderson, T.P., Hafflidason, H., Hajdas, I., Hatt, C., Heaton, T.J., Hogg, A.G., Hughen, K.A., Kaiser, K.F., Kromer, B., Manning, S.W., Niu, M., Reimer, R.W., Richards, D.A., Scott, E.M., Southon, J.R., Turney, C.S.M., van der Plicht, J., 2013. IntCal13 and MARINE13 radiocarbon age calibration curves 0–50000 years calBP. *Radiocarbon* 55 (4), 1869–1887.
- Reinhardt, E.G.R., Patterson, T., Schröder-Adams, C.J., 1994. Geoarchaeology of the ancient harbour site of Caesarea Maritima, Israel: evidence from sedimentology and paleoecology of benthic foraminifera. *J. Foram. Res.* 24 (1), 37–48.
- Renkonen, O., 1938. Statistisch-ökologische Untersuchungen über die terrestrische Käferwelt der finnischen Bruchmoore. *Ann. Zool. Soc. Zool. Bot. Fenn. Vanamo* 6 (1), 1–231.
- Salehi, M.H., Hashemi, B.O., Bigi, H.H., Esfandiarpour, B.I., Motaghian, H.R., 2011. Refining soil organic matter determination by loss-on-ignition. *Pedosphere* 21 (4), 473–482.
- Schneider, S., Knitter, D., Schütt, B., 2011. Geoarchäologische Untersuchungen im westlichen Kaikostal. In: Pirson, F. (Ed.), *Pergamon – Bericht über die Arbeiten in der Kampagne 2010*. *Archäol. Anzeiger* 2, 160–166.
- Seeliger, M., Bartz, M., Brückner, H., 2012. Mauern im Meer – Geoarchäologische Untersuchungen in der Bucht von Elaia. In: Pirson, F. (Ed.), *Pergamon. Bericht über die Arbeiten der Kampagne 2010*. *Archäol. Anzeiger* 2, 175–185.
- Seeliger, M., Bartz, M., Erkul, E., Feuser, S., Kelterbaum, D., Klein, C., Pirson, F., Vött, A., Brückner, H., 2013. Taken from the sea, reclaimed by the sea: the fate of the closed harbour of Elaia, the maritime satellite city of Pergamum (Turkey). *Quat. Int.* 312, 70–83.
- Seeliger, M., Brill, D., Feuser, S., Bartz, M., Erkul, E., Kelterbaum, D., Vött, A., Klein, C., Pirson, F., Brückner, H., 2014. The purpose and age of underwater walls in the Bay of Elaia of western Turkey: a multidisciplinary approach. *Geoarchaeology* 29, 138–155.
- Siani, G., Paterne, M., Arnold, M., Bard, E., Metivier, B., Tisnerat, N., Bassinot, F., 2000. Radiocarbon reservoir ages in the Mediterranean Sea and Black Sea. *Radiocarbon* 42, 271–280.
- Stock, F., Pint, A., Horejs, B., Ladstätter, S., Brückner, H., 2013. In search of the harbours: new evidence of Late Roman and Byzantine harbours of Ephesus. *Quat. Int.* 312, 57–69.
- Strabon: *Geographica*, 2005. Translation and Comments by Albert Forbiger. Marix Verlag, Wiesbaden (Greek to German).
- Vita-Finzi, C., 1969. Late Quaternary continental deposits of central and western Turkey. *Man. New Ser.* 4, 605–619.
- Vött, A., 2007. Silting up Oiniadai's harbours (Acheloo River delta, NW Greece). *Geoarchaeological implications of late Holocene landscape changes. Géomorphologie* 1, 19–36.
- Vött, A., Brückner, H., 2006. Versunkene Häfen im Mittelmeerraum. *Antike Küstenstädte als Archive für die Kultur- und Umweltforschung. Geogr. Rundsch.* 58 (4), 12–21.
- Vött, A., Handl, M., Brückner, H., 2002. Rekonstruktion holozäner Umweltbedingungen in Akarnanien (Nordwestgriechenland) mittels Diskriminanzanalyse von geochemischen Daten. *Geol. Palaeontol.* 36, 123–147.
- Vött, A., Brückner, H., Schriever, A., Besonen, M., Van Der Borg, K., Handl, M., 2004. Holocene coastal evolution around the ancient seaport of Oiniadai, Achelooos alluvial plain, NW Greece. *Coast. Rep.* 1, 43–53.
- Vött, A., Bareth, G., Brückner, H., Lang, F., Sakellariou, D., Hadler, H., Ntageretzis, K., Willershäuser, T., 2011. Olympia's harbour site Pheia (Elis, Western Peloponnese, Greece) destroyed by tsunami impact. *Die Erde* 142 (3), 259–288.
- Zimmermann, M., 2011. *Pergamon: Geschichte, Kultur, Archäologie*. C. H. Beck, München.

Chapter 4

4 Elaia, Pergamon's maritime satellite – Rise and fall of an ancient harbour city due to shoreline migration

Journal Article (in review):

Seeliger, M., Pint, A., Feuser, S., Riedesel, S., Frenzel, P., Kelterbaum, D., Pirson, F., Bolten, A., Brückner, H. Elaia, Pergamon's maritime satellite – Rise and fall of an ancient harbour city due to shoreline migration. *Journal of Quaternary Science*.

Elaia, Pergamon's maritime satellite – Rise and fall of an ancient harbour city due to shoreline migration

Journal:	<i>Journal of Quaternary Science</i>
Manuscript ID	Draft
Wiley - Manuscript type:	Research Article
Date Submitted by the Author:	n/a
Complete List of Authors:	Seeliger, Martin; University of Cologne, Institute of Geography Pint, Anna; University of Cologne, Institute of Geography Feuser, Stefan; Universitat Rostock, Heinrich Schliemann-Institute for Ancient Studies Riedesel, Svenja; University of Cologne, Department of Geography Frenzel, Peter Kelterbaum, Daniel ; University of Cologne, Department of Geography Pirson, Felix; German Archaeological Institute (DAI) Istanbul Bolten, Andreas; University of Cologne, Department of Geography Brückner, Helmut; University Köln, Institute for Geography
Keywords:	Palaeogeography, ancient harbours, coastal evolution, Pergamon, Micropalaeontology

1 Martin Seeliger^{1*}, Anna Pint¹, Stefan Feuser², Svenja Riedesel¹, Peter Frenzel³, Daniel Kelterbaum¹,
2 Felix Pirson⁴, Andreas Bolten¹, Helmut Brückner^{1*}

3

4 **Elaia, Pergamon's maritime satellite – Rise and fall of an ancient harbour city due to shoreline**
5 **migration**

6

7 ¹ Institute of Geography, Universität zu Köln, Albertus-Magnus-Platz, D-50923 Köln (Cologne)/Germany

8 ² Heinrich Schliemann-Institute for Ancient Studies, Universität Rostock, D-18051 Rostock/Germany

9 ³ Institute of Earth Sciences, Friedrich-Schiller-Universität Jena, Burgweg 11, D-07749 Jena/Germany

10 ⁴ German Archaeological Institute (DAI) Istanbul, İnönü Caddesi 10, TK-34437 Istanbul/Turkey

11

12 * corresponding authors: martin.seeliger@uni-koeln.de (Martin Seeliger); h.brueckner@uni-koeln.de (Helmut Brückner)

13

14 **Keywords: Palaeogeography, ancient harbours, coastal evolution, Micropalaeontology,**
15 **Pergamon**

16

17 **Abstract**

18 During Hellenistic times (330–30 BC), when the Pergamenian kings were at the height of their power,
19 they were operating an important harbour, used for commercial and military purposes at the city of
20 Elaia on the eastern Aegean coast. The aim of this study is to reconstruct the coastal evolution,
21 particularly with regard to the harbour areas of Elaia, and to correlate these results with the
22 archaeological and historical findings. For that purpose, several sediment cores were investigated by
23 means of micropalaeontology, sedimentology and geochemistry. Around 1500 BC, the sea reached its
24 maximal extension in the Bay of Elaia and the later Acropolis hill stretched into the embayment as a
25 peninsula. Mostly due to human activities during the following centuries siltation led to a regression of
26 the sea. From approx. 300 BC onwards, the three harbours of Elaia – closed, open and beach harbour –
27 were in full use. Their ongoing siltation in addition to the shrinking political importance of Elaia in
28 late Roman times led to the city's abandonment soon after AD 500. The geoarchaeological results
29 confirm the archaeological and historical evidence of Elaia's heyday during Hellenistic and early
30 Roman times, and the city's decline during the late Roman period.

31

32 **1 Introduction**

33 Towards the end of the Holocene marine transgression around 6000 BC at the “dawn of civilisations”
34 (Lambeck and Purcell, 2007), a more or less stable sea level enabled ancient societies to settle the
35 Mediterranean shores (Murray-Wallace and Woodroffe, 2014; Khan *et al.*, 2015).

36 By observing history over thousands of years, the connection to the sea was an important factor in
37 order to establish a flourishing settlement for many civilisations. In the Aegean Sea, this statement is,
38 for example, evidenced by the Neolithic settlements of Hoca Çeşme in Thrace (Başaran, 2010; Özbek,
39 2010), Hamaylıtarla on the Gallipoli peninsula (Özbek, 2010) and Çukuriçi Höyük near ancient
40 Ephesus (Horejs, 2012; Horejs *et al.*, 2015; Stock *et al.*, 2015). All of them are situated in short

41 distance to the sea, which was closer during the time of their establishment than today (Ammerman *et*
42 *al.*, 2008).

43 There are many examples from the Aegean region that the fate of ancient settlements was closely
44 linked to migrating shorelines and the changing sea level. Troia, Miletus, Ainos and Ephesus in
45 Western Anatolia are the most prominent ones. Their rise and fall as harbour cities was dependent on
46 environmental changes, which is outlined in many geoarchaeological studies (Kraft *et al.*, 1977, 2007;
47 Brückner *et al.*, 2006, 2010a, 2013, 2015; Goodman *et al.*, 2008, 2009; Stock *et al.*, 2013, 2015; Delile
48 *et al.*, 2015).

49

50 This paper presents another case study: the city of Elaia, which hosted the former military and
51 commercial harbour of ancient Pergamon. Addressing the human-environment interactions in space
52 and time, we focus on (i) reconstructing the shoreline changes of the Bay of Elaia; and (ii) linking
53 these changes to the settlement periods of Elaia.

54

55 **2 Physical setting**

56 Elaia is located in the north-western part of modern Turkey between Izmir and ancient Troia
57 (Figures 1a, b). The study area is part of the westwards drifting Aegean-Anatolian microplate
58 (Brückner *et al.*, 2010b; Vacchi *et al.*, 2014). As a consequence of this drift, several E-W oriented rift
59 structures were formed in the late Miocene, such as the Bergama graben, and its tributary, the
60 Zeytindağgraben. This tectonic ensemble represents a fractured zone, which was favourable for the
61 evolution of the Kaikos valley (Vita-Finzi, 1969; Aksu *et al.*, 1987; Seeliger *et al.*, 2013; Figure 1a).

62 The whole area is still tectonically active. Besides historic earthquakes, this is evidenced by (i) a partly
63 submerged Roman thermal bath complex (Bademli Ilica) located on the western part of the Karadağ,
64 and (ii) the sagged and flooded underwater walls in the Bay of Elaia (Seeliger *et al.*, 2013, 2014;
65 Figure 1a). Regarding the transgressive contact in the closed harbour basin (Seeliger *et al.*, 2013), the
66 open harbour area of Elaia (Pint *et al.*, 2015) and the previous study of archaeological sea-level
67 markers, a subsidence rate of the graben of <1 m per 1000 years is estimated (Seeliger *et al.*, 2013;
68 Pint *et al.*, 2015; in contrast to Aksu *et al.*, 1987; Figure 2).

69

70 The Karadağ Mountains to the west and the Yuntdağ Mountains to the east borders the Gulf of Elaia
71 (Figures 1, 2). The wide alluvial plain and the cusped delta of the Bakır Çay (ancient name: Kaikos)
72 are located to the west of the Bay of Elaia, separated by the relatively flat ridge of Bozyertepe (approx.
73 40 m a.s.l. (above present sea level); Figures 2a, b).

74

75 In general, the Aegean Sea is dominated by a relatively short fetch and small swell, which is
76 attenuated in the Gulf of Elaia due to its elongated shape and its inland extension (Soukissian *et al.*,
77 2008). In addition, the Bay of Elaia, as well as the topography of the coastal plain, show a very low

78 vertical gradient with the 20 m isobaths being approx. 4 km offshore (Aksu *et al.*, 1987). In line with
79 this, our own DGPS measurements revealed a mean tidal range of ca. 20 cm, which is in good
80 accordance with the micro-tidal regime of other sites in the Aegean Sea (Flemming, 1978; Anzidei *et*
81 *al.*, 2011; Brückner *et al.*, 2013; Seeliger *et al.*, 2013, 2014; Vacchi *et al.*, 2014).

82 The Elaia coastal zone has a typically Mediterranean climate, Csa according to Koeppen and Geiger's
83 nomenclature, with hot and dry summers, and mild and humid winters. Heavy rain and torrential rivers
84 are major morphological agents (Brückner, 1994; Jeckelmann, 1996). Own observations have shown,
85 that the sea in the Bay of Elaia turns brownish due to excessive wash-down of colluvial
86 material during heavy rain.

87

88 **3 A brief history of Elaia and Pergamon**

89 Pergamon is one of the most famous ancient settlements in Turkey, mentioned in a row with Troia,
90 Miletus and Ephesus (Kraft *et al.*, 1980, 2003, 2007; Brückner, 2005; Brückner *et al.*, 2006, 2013).
91 Among others, Pergamon is known for its famous Hellenistic Great Altar presumably dedicated to
92 Zeus and Athena, and the invention of parchment, which is, however, as yet an unverified myth.
93 Thanks to various shifts of the settlement areas, its impressive monumental structures, its important
94 library and school of philosophers, Pergamon provides detailed insight into the urban structure of a
95 Hellenistic residence city (Kunze and Kästner, 1990; Radt, 2011). Therefore, it was included in the
96 UNESCO World Cultural Heritage List in 2014 (Pirson and Scholl, 2015).

97

98 Soon after Alexander the Great died 323 BC in Babylon, the so-called "Wars of the Diadochi" started
99 affecting wide parts of Alexander's empire (Cartledge, 2004). In a later stage of these fights, the
100 dynasty of the Attalids came to power in the Kaikos region and established – in alliance with Rome –
101 a powerful kingdom in Asia Minor, which, during its heyday under King Eumenes II (197–159 BC)
102 ruled the western half of today's Turkey. Finally, in 133 BC, their realm was integrated into the
103 growing Roman Empire (Hansen, 1971; Radt, 2011; Zimmermann, 2011; Pirson and Scholl, 2015;
104 Figure 1c).

105

106 Pergamon's location on top of the 330 m high Acropolis hill, surveying the surrounding Kaikos plain
107 (Figure 1a), was excellent for security reasons and defence, but complicated trade and transport.
108 Additionally, the Pergamenians were in need of a maritime harbour. They found it in the nearby city
109 of Elaia, located at the Aegean Sea approx. 26 km southwest of Pergamon (Figures 1a, 2a). According
110 to the current state of research, Elaia came under Pergamenian hegemony during the regency of king
111 Eumenes I (263–241 BC; Pirson, 2004; Radt, 2011). Strabo mentioned Elaia as the commercial
112 harbour of the Pergamenians and as the military base of the Attalids (Geographica XIII, 1, 67; XIII, 3,
113 5). Further evidence from literary sources and archaeological findings emphasise the close link
114 between Elaia and Pergamon (Pirson, 2004, 2008, 2010, 2011, 2014; Schneider *et al.*, 2015).

115

116 The harbour zone of Elaia is divided into three parts (Figure 2).

117 First, the closed harbour basin (I in Figure 2) within the fortification walls, which was built in early
118 Hellenistic times. It was protected against the sea and enemies by two massive breakwaters, one to the
119 west and one to the south; they are nowadays silted-in, but still visible. Geoarchaeological research
120 revealed that substantial siltation occurred between the 3rd and the end of the 4th century AD; thus,
121 from the 5th century AD onwards the closed harbour was no longer useable (Pirson, 2007, 2008;
122 Brückner *et al.*, 2013; Seeliger *et al.*, 2013, 2014; Pint *et al.*, 2015; Figure 2).

123 Second, an approx. 250 m long open harbour zone (II in Figure 2) stretched from the southern
124 breakwater of the closed harbour south-eastwards to the point where an internal wall reached the
125 waterfront. This so-called *diateichisma* divided the city area into a northern, densely populated part
126 and a southern one (Pirson, 2011; Pint *et al.*, 2015; Figure 2).

127 Third, an open beach harbour extended from south of the diateichisma to the south-eastern tip of the
128 city wall (III in Figure 2). Most presumably this area was used as a multifunctional military zone,
129 including dockyards where warships were beached and maintenance work was conducted (Pirson,
130 2011, 2014; Pint *et al.*, 2015; Figure 2).

131

132 **4 Material and methods**

133 Geoarchaeological fieldwork

134 Sediment coring with an Atlas Copco Cobra TT vibracorer was performed in the surroundings of the
135 Bay of Elaia, down to a maximal depth of 12 m b.s. (below surface). Open steel auger heads
136 (diameter: 6 and 5 cm, respectively) and closed steel auger heads with opaque 1 m long inliner PVC
137 tubes (external diameter: 5 cm) were chosen to gain the sediment cores.

138

139 On-site, sediments were described according to grain size, colour (Munsell Soil Color Charts),
140 and carbonate content (Ad-hoc-AG Boden, 2005); bulk samples for laboratory analyses were taken fr
141 om the open sediment cores (4-5 samples/metre). In contrast, corings gained by the closed
142 coring technique were only opened and sampled in the laboratory (every 5 cm).

143 All coring sites were measured with the Leica DGPS System 530 (accuracy of ≤ 2 cm in all
144 three dimensions; Seeliger *et al.*, 2013, 2014); they are stated in m above sea level (a.s.l.) and
145 m below surface (b.s.)

146

147

148 Sedimentology and geochemistry

149 Multi-proxy laboratory analyses were conducted (Ernst, 1970; Engel *et al.*, 2009; Kelterbaum *et al.*,
150 2012; Hadler *et al.*, 2013; Seeliger *et al.*, 2013). Samples were air-dried, ground with mortar
151 and pestle, and sieved to separate the ≤ 2 mm grain size fraction for further analyses.

152 For laser-based grain size analysis (Beckman Coulter LS13320;), the organic content was decomposed
153 using 15 % hydrogen peroxide (H₂O₂). Afterwards, sodium pyrophosphate (Na₄P₂O₇ concentration:
154 47 g/l) was taken as a dispersant. Each sample was measured three times in 116 classes, determining
155 grain-size distributions in a range from 0.04 to 2000 µm For the calculation of grain-size parameters
156 after Folk and Ward (1957), the GRADISTAT software (Blott and Pye, 2001) was applied.
157 To estimate the organic content, measurements of LOI (loss on ignition) were performed by
158 oven drying (105°C for 12 h to determine the water content) and combusting in a furnace (550°C for 4h
159 to determine the organic substance). Several chemical processes may cause substantial
160 uncertainties dealing with LOI; loss of structural water out of clay minerals (Dankers and
161 Laane, 1983), loss of carbon dioxide from carbonates consisting of inorganic material (Salehi *et al.*,
162 2011), and loss of sulphur compounds. These processes result in a weight reduction not
163 caused by loss of organic
164 substance (c.g. Mook and Hosin, 1982; Heiri *et al.*, 2001; Campos, 2010). Electric conductivity was
165 determined in an aqueous solution (5 g sediment in 25 ml deionised water) with a glass
166 electrode
167 connected to a Mettler Toledo InLab®731-2m instrument. To determine different sedimentary facies,
168 characteristic elements (e.g. Fe, K, Ca, Ti etc.) were measured using a portable XRF (X-ray
169 fluorescence) spectrometer (Niton XI3t 900 GOLDD; Vött *et al.*, 2011). To ensure comparability
170 within all XRF analyses and to reduce grain size dependency, each sample was ground to powder in a
171 ball triturator (Retsch PM 4001) and then pressed to pills to be measured. It is not possible to quantify
172 Sodium (Na) by XRF, which was therefore done by atomic absorption spectroscopy (Perkin Elmer A-
173 Analyst 300). For that purpose, the samples were digested with concentrated HCl (37 %).

174

175 Micropalaeontology

176 For microfaunal analysis, selected 1 cm³ samples were wet-sieved using a 100 µm mesh. Under
177 a stereoscopic microscope, at least 300 ostracods valves and foraminifer tests, respectively, were picked
178 from appropriate splits of the residues of every sample. If less than 300 specimens were present within
179 a sample all were picked. Species were mainly identified according to Bonaduce *et al.* (1975)
180 and Joachim and Langer (2008) for ostracods as well as Cimermann and Langer (1991) and Meriç *et al.*
181 *al.* (2004) and Murray (2006) for foraminifers and counted.

182

183 Chronology

184 The chronological framework is based on ¹⁴C-AMS age determinations. Depending on the δ¹³C value
185 each sample was calibrated using either the IntCal13 or the MARINE13 calibration curve of the recent
186 Calib 7.1 software (Reimer *et al.*, 2013) with a marine reservoir effect of 390±85 years and ΔR of
187 35±70 years (Siani *et al.*, 2000). All ages are presented in calendar years BC/AD and years BP
188 representing a 2σ-confidence interval (Table 1).

5 Results of Ela 57 and Ela 12

189 The coring profiles of the Elaia region – a selection of 19 is presented here (Figure 2a) – can be
190 divided into two groups: those, which reached bedrock and those that did not. In addition, the
191 sedimentation pattern in the western part of the Bay (transects A–A' and B–B') differs a lot from the
192 one in the eastern part (D–D', E–E' and F–F'). This shall be demonstrated by the detailed description
193 of two cores, one from each group (Ela 57 and Ela 12, respectively). In addition, core Ela 58 (Pint *et*
194 *al.*, 2015) is considered in order to present all of the sedimentary units (Figure 2a).

195

196 Sediment core Ela 57 representing the eastern part of the Bay of Elaia

197 Situated between Ela 55 (102 m distance) and Ela 56 (69 m distance), Ela 57 (27.046354° E;
198 38.940715° N; final depth: 6.00 m b.s.; elevation: 1.09 m a.s.l.) is the central coring of transect E–E'
199 (Figure 2a). It may act as an excellent example of the corings, which attained bedrock, and illustrates
200 the typical environmental conditions in the eastern part of the bay (Figures 3, 4).

201

202 The Neogene bedrock, compact calcareous sandstone, was reached at 5.42 m b.s. A piece of charcoal
203 dates the basal contact at 5.39 m b.s. to 2198–2035 cal BC (Ela 57/23H; Table 1). The overlaying
204 section reaches up to 3.45 m b.s. It consists of dark to olive grey moderately sorted sand (mean: 726–
205 878 μm) with well-rounded pebbles (max. 4 cm \varnothing) and fragments of marine gastropods. The Ca/Fe
206 ratio is the highest of the whole profile (20–31). In addition, seagrass (*Posidonia* sp.) is a remarkable
207 feature of this section. The dominating foraminifers are *Ammonia* spp., *Elphidium* spp., *Lobatula*
208 *lobatula* and *Rosalina* sp. and are accompanied by a marine ostracod fauna..

209 The upper 50 cm of this section show a gradual transition to the overlaying section, with decreasing
210 mean grain size and Ca/Fe values. This part is rich in macro remains (olive stones, seeds of grape and
211 melon) as well as debris of marine molluscs. A grape seed at 3.56 m b.s. dates to 165 cal BC–
212 1 cal BC/AD (Ela 57/17H; Table 1).

213 In the following section, macrofaunal and -floral remains are missing. The microfaunal association is
214 dominated by the foraminifers *Ammonia parkinsoniana*, *Cibicides advenum*, *Neoconorbina* sp. and
215 *Stomatorbina* sp., ostracods are very rare. Above an erosional disconformity at 2.70 m b.s., the next
216 section starts with poorly sorted brownish slightly loamy sand (mean: 135–148 μm) which contains
217 well-rounded pebbles and brick fragments (<2 cm). The increase of Fe/K and the decrease of Ca/Fe
218 are remarkable. Raised values of LOI reflect the large amount of plant fibres, seeds, charcoal and even
219 pieces of bones. Microfossils are absent. The upper border of this section dates to 38 cal BC–cal AD
220 116 (Ela 57/8H; Table 1).

221 The top section above 1.82 m b.s. consists of poorly sorted, fine-grained (mean: 37–119 μm) pale
222 brownish silty loam, which contains pieces of bricks, angular stones, pebbles and plant remains. The
223 uppermost 45 cm are dominated by bricks, stones, roots and ceramics.

224

225 Sediment core Ela 12 representing the western part of the Bay of Elaia

226 Ela 12 (27.029586° E; 38.943023° N; total depth: 10.00 m; elevation: 0.88 m a.s.l.) is part of transect
227 A–A', situated between Ela 11 and 14 at distances of 109 m and 145 m, respectively (Figure 2a). It did
228 not reach bedrock, but illustrates the typical environmental conditions in the western part of the Bay of
229 Elaia (Figures 5, 6).

230

231 Dark to light grey moderately sorted homogeneous clayey silt (mean: <50 µm) forms the lowermost
232 section. It is rich in debris of marine molluscs, but also contains intact valves (*Nucula* sp; 8.47 m b.s.)
233 and even an articulated specimen of *Cerastoderma glaucum* (2 cm in size; depth: 8.33 m b.s.). Fe/Na
234 shows low ratios, Na/K moderate ones, while LOI reaches its maximum of the entire profile due to
235 intercalated layers of *Posidonia* sp. Charcoal at a depth of 8.65 m b.s. dates to 803–568 cal BC (Ela
236 12/36H; Table 1). The microfossil association of this section mainly consists of the foraminifers
237 *Ammonia tepida*, *Aubignyna perlucida*, *Criboelphidium excavatum*, *Haynesina germanica* and some
238 *Elphidium* spp., and the ostracods *Xestoleberis* sp. and *Loxoconcha elliptica* amongst others.

239 The next section starts with a smooth transition at 5.49 m b.s. This one consists of poorly sorted
240 greyish sand with well-rounded pebbles, some fibres of sea weed and broken marine gastropods and
241 shells. This unit shows a coarsening-upward sequence. LOI and electric conductivity decrease, while
242 Fe/Na shows a remarkable increase. The microfauna is dominated by the foraminifers *Ammonia*
243 *parkinsoniana* and *Ammonia tepida*, and the ostracods *Cyprideis torosa* and *Loxoconcha elliptica*.

244 The uppermost section of the profile starts at 3.66 m b.s. It consists of poorly sorted, fine-grained pale
245 brownish loamy sand with some pebbles and pieces of wood, but without microfossils. The uppermost
246 55 cm show bricks, stones and recent plant remains.

247

248 **6 Interpretation**

249 **6.1 Introduction of sedimentary units**

250 The large number of sediment cores from the Elaia area is summarised by the classification in units of
251 typical environmental characteristics. Their definition is based on geochemical, granulometrical and
252 microfaunistic parameters as shown in chapter 5 for core Ela 57 and 12. This compilation is intended
253 to shorten the interpretation of the cores (Figure 7).

254

255 Unit 1 – bedrock

256 Neogene calcareous sandstone forms the bedrock in the Elaia region (Seeliger *et al.*, 2013; Pint *et al.*,
257 2015). In Hellenistic and Roman times, it was mined not far north of Elaia in the Bozvertepe area and
258 used for construction works, for example for the harbour breakwaters of Elaia (Figure 3c in Seeliger *et*
259 *al.*, 2013). The material sometimes turns reddish, while normally it is of whitish-yellowish colour. It
260 shows low mean grain size, poor sorting and high values of Ca. In addition, it is free of organics and
261 microfauna (Brückner *et al.*, 2013; Seeliger *et al.*, 2013; Pint *et al.*, 2015).

262

263 Unit 2 – littoral (transgressive)

264 Unit 2 originates from wave action due to the first transition of the shoreline in context of the
265 Holocene marine transgression. On top of the bedrock, poorly sorted pebbles in coarse sandy matrix
266 were deposited showing fining upwards tendency. The few plant remains are mostly fibres of sea
267 weed. The values of Fe/Na, K/Na and the electrical conductivity are quite moderate and variable. The
268 typical microfaunal association consists of the ostracods *Callistocythere vexata* and *Aurila* spp. and
269 the foraminifers *Ammonia beccarii*, *Lobatula lobatula* and *Elphidium aculeatum* typical for the marine
270 littoral zone (Murray, 2006). The high-energy wave environment, which dominated in the course of
271 the marine transgression, is the reason why only very robust and thick-walled specimens of the
272 foraminifers *Ammonia compacta* and *Elphidium crispum* occur at the base of this littoral unit.

273

274 Unit 3 – shallow marine

275 Deeper-water settings created a low-energy wave environment with the deposition of homogeneous,
276 light grey, well-sorted silty sands. They were the habitat for seagrass meadows. In the lowermost parts
277 of the unit, however, anoxic conditions prevailed, which is evidenced by the strong smell of hydrogen
278 sulphide (H₂S) still during sampling. Further characteristics of unit 3 are high values of electric
279 conductivity and, compared to the littoral zone, higher contents of organic matter. Low ratios of
280 Fe/Na, as well as high ratios of K/Na hint to strong marine and reduced terrestrial influence.

281 The microfossil association reveals a high diversity with marine ostracods such as *Pontocythere*
282 *turbida* and *Xestoleberis* spp., and marine foraminifers, e.g. *Ammonia parkinsoniana*, *Elphidium*
283 *advenum* and *Elphidium complanatum* (Murray, 2006). The malacofauna consists of articulated
284 specimens of *Nucula* sp., single valves of *Lasaea rubra* and the abundant occurrence of the gastropods
285 *Pirenella conica* and *Cerithideopsisilla conica* – all of these species live in a shallow marine
286 environment.

287

288 Unit 4 – stagnant water (connected to the open sea)

289 Unit 4 is similar to unit 3 concerning grain size, grain sorting and LOI (Figure 3).

290 However, lower Ca/Fe and Ca/Ti ratios, and higher K/Na ratios indicate a stronger terrestrial
291 influence (Pint *et al.*, 2015; Seeliger *et al.*, 2013). The microfauna is dominated by species
292 which prefer very shallow marine and confined coastal areas, e.g. the foraminifers *Ammonia*
293 *tepida*, *Aubignyna perlucida* and
294 *Criboelphidium* spp. (Murray, 2006) as well as the ostracods *Cyprideis torosa*, *Loxococoncha elliptica*
295 and *Leptocythere* spp. (Frenzel and Boomer, 2005).

296

297 Unit 5 – littoral (regressive)

298 For unit 5 nearly the same holds true as for unit 2. In case of the second transition of the shoreline,
littoral sediments may occur once again characterised by a similar microfaunal association as in unit 2.

299 However, while unit 2 shows an erosional disconformity to the underlying bedrock, this is missing in
300 unit 5. In addition, a coarsening-upward sequence becomes visible in most regressive littoral units.

301

302 Unit 6 – fluvial

303 Episodic flood events during the rainy winter season left their imprint by layers deposited by
304 ephemeral creeks. They are characterised by coarse grain size, pebbles, and a remarkably low
305 LOI.

306 The fining-upward sequence often starts with an erosional disconformity. Increased K/Na ratios hint to
307 stronger freshwater influence. Rising Fe contents in addition to the complete absence of microfauna
308 are further characteristics of this riverine sediment.

309 Unit 7a – colluvial (natural)

310 In this study, colluvium names loose terrestrial material, denuded from the hills and slopes, and
311 accumulated at the foothills and in small valleys. It is made up of a fine-grained matrix (brownish silt
312 or silty loam) and poorly rounded pebbles (calcareous sandstone and different volcanic rocks). While
313 Fe reaches its highest values due to weathering processes, Na values are the lowest in the
314 entire stratigraphic column. LOI

315 increases due to plant remains and roots. The uppermost part of unit 7 is the
316 plough horizon, which reaches a depth of 40–50 cm b.s. in the Elaia region. Therefore, more or less
317 recent roots from field crops occur. Unit 7 is void of microfossils.

318

319 Unit 7b – colluvial (anthropogenic)

320 For unit 7b the same holds true as for unit 7a. In addition, unit 7b contains fragments of ceramics and
321 bricks as well as bones and even metal objects. In a good case, this may allow dating the stratum. It is
322 evidence of settling, artisanship and commerce (Seeliger *et al.*, 2013; Pint *et al.*, 2015).

323

324 **6.2 Core-based reconstruction of palaeoenvironments**

325 Based on chapters 5 and 6.1 coring profiles Ela 57 and Ela 12 can be interpreted as follows:

326

327 Sediment core Ela 57 representing the eastern part of the Bay of Elaia

328 The palaeogeographical evolution of the eastern part of the Bay of Elaia is exemplified by
329 profile Ela 57 (Figures 2, 3, 4).

330 Neogene bedrock encountered in ELA 57 at 5.42 m b.s. (unit 1) forms the base of numerous cores in
331 the study area. The calcareous sandstone, outcropping nearby, was used to construct the harbour
332 breakwaters; later the blocks were reused as spolia when the saltworks were built in late
333 Antiquity (Seeliger *et al.*, 2013, 2014).

334 The overlying unit 2 represents the transgressive littoral facies in the course of the Holocene sea-level
335 rise. The high-energy environment is obvious from the amount of pebbles, the coarse grain size and
the patches of seagrass. The low biodiversity and the sole occurrence of robust foraminifers in the

336 lower part of unit 2, such as *Ammonia compacta* and *Elphidium crispum*, are evidence for the high
337 stress level of this littoral environment in which only a few species are able to survive. The fining-
338 upward sequence is due to the increase in water depth, which is also reflected in a higher biodiversity.
339 The Holocene transgression reached this area at the end of the 3rd millennium BC (2198–2035 cal BC),
340 which is long before the human occupation phase in the Bay of Elaia. A second age of core Ela 57
341 dates to late Hellenistic/ early Roman times (165 cal BC–1 cal BC/AD), the period when Elaia
342 flourished.

343 The rising sea level led to the forming of a shallow water body represented by unit 4. It shows a
344 fining-upward sequence due to the inland migration of the shoreline with the consequence of reduced
345 wave action. This results in a lower amount of shell debris and the occurrence of more preserved
346 valves. The microfaunal association indicates a shallow marine environment. Considering the results
347 gained inside the closed harbour, relative sea level at the turn of the eras was approx. 1.50 m deeper
348 than today. Thus, water depth during those days should not have exceeded more than 1.30–1.50 m
349 (Pint *et al.*, 2015).

350 By then, the environs of this part of the city area may have served as a beach harbour area where
351 foreign soldiers landed, repaired their ships and put up camps, thus staying outside the actual city area
352 (further details in Seeliger *et al.*, 2013; Pint *et al.*, 2015). This custom was normal for small to
353 medium-sized cities during those times, because it granted a higher level of security for the
354 inhabitants. Since the nearby coring Ela 56 does not show any marine or littoral sediments, the site of
355 Ela 57 was always at a nearshore position, close to the landing area for ships and smaller vessels.

356 The sharp contact at -1.61 m a.s.l. suggests a sudden end of this sheltered marine water body, possibly
357 due to a massive deposition by a torrential flood, triggered by catastrophic rainfall. Such kind of
358 events were favoured by the widespread clearing of forests in this area during Hellenistic and Roman
359 times and is reflected by results of a pollen profile (Brückner *et al.*, 2010a). The erosional contact at
360 the base, the fining-upward sequence, the fluvial character of the stratum with brick fragments, seeds,
361 charcoal and even bones, all washed down from the nearby slopes, as well as the absence of
362 microfauna supports this interpretation. The upper part of this unit dates to Roman Imperial times.
363 Since the dated olive stone (Ela 57/8H) is very robust and may have been reworked, the age should be
364 regarded as a minimum age only. It seems that the fluvial deposition most probably occurred during
365 the phase of settlement of Elaia in late Roman times.

366 Since the area of coring site Ela 57 suddenly became terrestrial, the second transition of the shoreline,
367 often indicated by a second littoral phase (unit 5), is missing. That the area was at least partly
368 influenced by human impact is evidenced by the anthropogenic colluvium (unit 7b), which forms the
369 top layer.

370

371

372

373 Sediment core Ela 12 representing the western part of the Bay of Elaia

374 The palaeogeographical evolution of the western Bay of Elaia is exemplified by profile Ela 12
375 (Figures 2, 5, 6).

376 At the bottom, the profile shows sediments of a sheltered embayment (unit 4) where *Posidonia*
377 meadows could settle the sea floor. Well-preserved marine bivalves support this assumption. The
378 geochemical fingerprint and the microfaunal association indicate a nearshore environment. Typically
379 open marine species are missing (Pint *et al.*, 2015). A radiocarbon age of 803–568 cal BC dates this
380 part of the profile to the first half of the 1st millennium (Geometric-Archaic times) – a period for which
381 not much is known about the history of the study area (Figure 1b). The shallow marine environment
382 prevailed for quite some time, until sediments from the nearby Bozyertepe were washed into the
383 embayment more and more. This caused a regression of the shoreline with decreasing water depth, and
384 the establishment of littoral unit 5, which is of regressive origin. Compared to the transgressive facies
385 of Ela 57, the regressive facies of Ela 12 has a similar microfaunal composition, but displays a
386 coarsening-upward sequence. The environmental stress led to low biodiversity, while the increased
387 occurrence of mollusc and shell debris acts as an evidence of high wave energy. It can be excluded,
388 that the advancing delta of the Kaikos (Bakır Çay; Figures 1, 2) played a role in the silting up of this
389 inner part of the Bay of Elaia, because neither Ela 12 nor the whole transects A–A' and B–B' contains
390 fluvial-deltaic sediments.

391 The littoral unit ends at -2.78 m a.s.l., when terrestrial processes become dominant. This is the onset of
392 the accumulation of colluvium (unit 7a). Since the transect A–A' is situated at quite a distance from
393 the settled area of the city of Elaia, it is not astonishing that no direct indicators of human impact, such
394 as ceramics, bricks and metal objects, were found in the colluvium.

395

396 **6.3 Landscape evolution based on coring transects**

397 After the detailed description of two representative sediment cores, five spatial transects and one
398 single coring are discussed in order to clarify the landscape evolution of the Bay of Elaia. These
399 transects are described from west to east (Figure 8; for detailed descriptions of the corings see
400 Brückner *et al.*, 2013; Seeliger *et al.*, 2013; 2014; Pint *et al.*, 2015).

401

402 Transect A-A'

403 The westernmost transect A–A' consists of three different types of profiles. The coastal corings Ela 11
404 and 12 show a typical regressive sedimentary sequence (Chapter 6.2; Brückner *et al.*, 2010b).
405 Increased sedimentation in the context of the settlement period of Elaia led to a silting up of a low
406 energy, shallow marine water body (unit 4), which turned to a littoral unit and later to a natural
407 colluvial environment (Unit 7a). Ela 14 and 20 reached the bedrock, which is topped by nearshore
408 littoral deposits (unit 2); they are overlain by natural colluvium. The rising bedrock towards
409 Bozyertepe caused the landward thinning of the littoral strata. Since coring Ela 19 did not contain

410 marine or littoral facies, the maximum marine transgression in A–A' is close to coring site Ela 20,
411 where it dates to the end of the 2nd millennium BC.

412

413 Transect B–B'

414 This transect represents the marine transgression into the valley between the Acropolis hill of Elaia to
415 the east and the Bozyertepe to the west. It provides results comparable to A–A'. Coastal corings Ela 1
416 and 2 demonstrate a regressive sediment sequence, similar to Ela 11 and 12. They represent a shallow
417 water body in this area of the bay at least since the first half of the 1st millennium BC. According to
418 these results, the areas of Ela 1 and 2 were still under marine influence during the main occupation
419 phase of Elaia (Figures 1, 2). Since Ela 9 only shows fluvial and colluvial sediments, coring Ela 3/17
420 marks the maximum marine transgression of B–B'. This dates to the end of the 3rd millennium BC.

421

422 Ela 58 ("C")

423 Ela 58 is the only coring of this area, which includes a shallow marine facies (unit 3) with high
424 biodiversity (Pint *et al.*, 2015). It dates to the 4th and 5th millennia BC. As in the eastern transects,
425 massive fluvial input terminated the shallow marine conditions, and started the establishment of a
426 sheltered water area (unit 4), which prevailed during the centuries of Elaia's heyday. Later, the
427 Elaitians dumped material in this area to consolidate the terrain (Pint *et al.*, 2015).

428

429 Transects in the area of the eastern city district

430 Transects D–D', E–E' and F–F' show similar results, wherefore they are presented together.

431 The nearshore coring profiles (Ela 59, 55 and 62) reach the bedrock. The transgressive littoral unit,
432 which starts with an erosional disconformity, is covered by facies of a stagnant marine water body.

433 The very low energy wave conditions prevailed because a regressive littoral zone is
434 missing; all of the profiles show a smooth transition to colluvial deposits.

435 The inland corings (Ela 60, 56 and 64) reveal a terrestrial sedimentation pattern interrupted by a layer
436 of fluvial sediments, most probably caused by torrential floods.

437 The central corings (Ela 61, 57 and 63) contain the most essential information about the marine
438 extension in this area. All of them display a typical stratigraphy: the bedrock is overlain by
439 transgressive littoral deposits; then facies of a low energy marine embayment follows as evidence of
440 the rising sea level. The shallow marine deposit is covered by the massive input of fluvial sediments,
441 which are topped by human-induced colluvium. Severe flooding can only be traced in the sediment
442 sequence of the central and inland corings.

443

444 Synopsis

445 With regard to the height above sea level in F–F' a similar age for the maximum marine ingression in
446 each transect of approx. 1500 BC is assumed.

447 Derived from the thickness of the marine strata of Ela 58 (“C”), the maximum transgressive shoreline
448 is to be located further inland, i.e. in the area of the later city (where, unfortunately, coring was not
449 possible). Coring Ela 61 indirectly proves this. Accordingly, the same as for the ancient cities of
450 Miletus, Ainos and Ephesus can be stated for Elaia. Parts of the city had been erected on formerly
451 marine sediments (Brückner, 2005; Brückner *et al.*, 2006, 2015; Seeliger *et al.*, 2013).

452 The eastern city district transects and Ela 58 (“C”) show thick sheet wash deposits which caused
453 massive siltation of the area. In case of Ela 58, this could have taken place at the beginning of the 1st
454 millennium BC. This is in good accordance with transect D–D’ where this event occurred at a similar
455 date (Ela 61/16; 1149–791 cal BC). In Ela 57 (E–E’) it is visible just around the turn of the eras,
456 whereas in Ela 63 (F–F’) it occurred in Classical or even Hellenistic times (Ela 63/10/H; 797–551 cal
457 BC). However, severe flood events do not occur in the western part of the embayment (transects A–A’
458 and B–B’). Summing up, torrential floods connected with sheet wash dynamics occur before and
459 during the intense human settlement activity; they do affect the eastern area of ancient Elaia (Figure
460 2). This is on the one hand a result of the increased relief energy of the nearby foothills of the steep
461 Yuntdağ Mountains, as compared to the flat Bozyertepe and the Acropolis hill (A–A’ and B–B’). On
462 the other hand, the human influence in the eastern area of the embayment was much more intense,
463 causing soil degradation and erosion. Furthermore, at the end of the 1st century BC and the beginning
464 of the 1st century AD the settlement pattern of the surroundings of Elaia changed when several of the
465 Hellenistic farmsteads were abandoned – maybe because of intense floods (Pirson, 2011).

466

467 **6.4 Scenarios of coastline changes**

468 Following these results, three palaeogeographical scenarios of shoreline displacements are established
469 for the Bay of Elaia (Figures 2, 9).

470

471 1500 BC: This is the time of the maximum marine extension in the Bay of Elaia. The coastal zone
472 reaches far northwards along the slopes of Bozyertepe, almost up to Ela 9. Near this coring site one of
473 Elaia’s graveyards was located (Pirson, 2010), which fits well to the finding that this area had never
474 been part of the sea during the Holocene.

475 During the maximum marine extension, the later Acropolis hill of Elaia protruded into the bay as a
476 peninsula; by then it was most probably uninhabited. The small embayment to the north of Ela 58 may
477 have acted as a preferred landing area; but as yet this assumption has not been verified by
478 archaeological criteria. The same holds true for the western flank of the Acropolis hill. In the eastern
479 city area, the shoreline reached close to the foothills of the Yuntdağ. Quite well identifiable are those
480 parts of the later city, which had once been shallow marine and littoral areas. When they had been
481 silted up and probably also partly intentionally filled in by the inhabitants of the area, they turned to
482 settled ground after approx. 500 BC (Figures 1b, 9).

483

484 300 BC: This scenario represents the period when Elaia started to prosper. Archaeological findings
485 document intense settlement activities on the Acropolis hill and in the eastern city district (Pirson,
486 2010). In addition, various crops and fruits are intensively cultivated in the surroundings of Elaia,
487 which is evidenced by palynological record (Brückner *et al.*, 2010a) and supported by linguistic
488 studies: “Elaia” means “olive” in the Greek language (Pirson, 2004), and the modern Turkish name of
489 the main village of the area is “Zeytindağ” in English: “Olive Mountain”.

490 Increased sediment load due to soil erosion from Bozyertepe and activities of the nameless episodic
491 creek between Bozyertepe and Acropolis hill caused a shoreline regression in the western part. None
492 of the corings of A–A’ and B–B’ show fluvial sediments of the nearby Kaikos delta. Therefore, its
493 influence concerning the siltation of the inner part of the Bay of Elaia can be neglected. Wide areas
494 between the Acropolis hill and Bozyertepe remained marine. Due to the ongoing seaward shift in the
495 shoreline, a harbour situation on the western flank of the Acropolis hill is improbable in those days.
496 However, immediately south of the Acropolis hill, two harbours were constructed: the terrain was
497 consolidated and transformed into a closed harbour basin by the erection of two harbour breakwaters
498 (Seeliger *et al.*, 2013). Similar considerations hold true for the area of the open harbour zone,
499 including the presumed Hellenistic ship sheds (Pirson, 2010; Pint *et al.*, 2015). During that time, both
500 harbours were fully accessible and used for military and commercial purposes (Pirson, 2004; Seeliger
501 *et al.*, 2013; Pint *et al.*, 2015).

502 The eastern city district experienced a slight regression of the shoreline caused by denudation
503 processes and human impact. The coastal area was ideal for landing warships while trading was most
504 probably processed in the closed and the open harbours (Pirson 2011, 2014). Torrential floods will
505 have been a temporary common nuisance for the area, but nothing is known about this topic from
506 literature.

507 Further south the shoreline leaves a narrow passage between the slopes of Yuntdağ and the sea.
508 This underlines Elaia’s strategic position: the city did not only serve as the main harbour of Pergamon,
509 it was also a defensive stronghold, which secured the southern entrance to the inner realm of the lower
510 Kaikos area (Seeliger *et al.*, 2013; Pirson, 2014). This topographic setting is comparable to the one at
511 Thermopylae in central Greece, where in 480 BC the legendary 300 Spartans were able to withstand
512 the far larger Persian army for quite a long battle due to their strategic use of the landscape (Kraft *et*
513 *al.*, 1987).

514 It is reasonable to assume that a defence turret fortified the southern end of the city wall
515 (Pirson, 2010). A turret would have been in need of a solid foundation when being constructed in a near
516 shore position; however, nothing of that kind was detected by coring; in Ela 65 (Figures 2a, 9) only litt-
517 oral sediments for the late Hellenistic to Roman periods were revealed.

518

519 AD 500: This scenario represents the time, when Elaia was at or near the end of its heyday. In several
520 areas, the shoreline is close to its present position. All corings present terrestrial sedimentation patterns

521 for those days. The closed harbour basin was out of use and nearly silted up (Seeliger *et al.*, 2013).
522 The area of the former ship sheds was not accessible by ship anymore. Since the harbour was no
523 longer usable, the people left the city. Most probably also in fear of pirate attacks, they moved to the
524 landward settlement of Püsküllü Tepeler (Pirson, 2010; Seeliger *et al.*, 2014). As documented in the
525 pollen chart, the natural vegetation reoccurred and wide areas became woodland again (Brückner *et*
526 *al.*, 2010a). Saltworks were constructed, mostly built by spolia, about 2 km south of the city far out in
527 the shallow bay. Salt was of great economic value, not only in those times; and it was quite easily
528 harvested by only a few men. Very shallow marine conditions and very low energy wave conditions in
529 the bay favoured its use as a saltworks (Pirson, 2014; Seeliger *et al.*, 2014).

530

531 **8 Conclusion**

532 Around 1500 BC the marine extension in the Bay of Elaia was at its maximum. The sea protruded far
533 inland in the northern and western area; thus, the later Acropolis hill was transformed into a peninsula.
534 Due to the adjacent Yuntdağ Mountains, the extension of the sea in the area of the later eastern part of
535 the city of Elaia was far less as compared to the western part. Mostly due to human activities during
536 the following centuries (Brückner *et al.*, 2010a), siltation led to a continuing regression of the
537 shoreline.

538 During Hellenistic and Roman times, approx. from ~300 BC onwards, three harbour areas were in full
539 operation: the closed harbour, the open harbour and the beach harbour. While the closed harbour was
540 used for commercial as well as military purposes, the open harbour was most presumably the place of
541 the ship sheds housing the warships of the Pergamenian kings. The eastern city district with its beach
542 harbour served as a place of temporal residence for foreign merchants, sailors and soldiers (Pirson,
543 2010; Seeliger *et al.*, 2014; Pint *et al.*, 2015).

544 The siltation of the harbours in addition to the declining political importance of the city in late Roman
545 times led to its abandonment (soon after AD 500). Later, much of the building material of the city was
546 reused as spolia (Seeliger *et al.*, 2014). In sum, the geoarchaeological results confirm the
547 archaeological and historical evidence of Elaia's heyday during the Hellenistic and early Roman
548 periods, and the city's decline during late Roman times.

549

550 **9 Acknowledgements**

551 The project presented here was conducted in the context of the DFG priority program (SPP) 1209 "*The*
552 *Hellenistic Polis as a Living Space – Urban Structures and Civic Identity between Tradition and*
553 *Innovation*" (2008–2011). Financial support by the German Research Foundation is gratefully
554 acknowledged (DFG ref. no. PI 740/1–3). Our research was part of the greater Elaia Survey Project,
555 headed by Prof. Dr. Felix Pirson, Director of the DAI Istanbul and excavation director of Pergamon.
556 The studies would not have been possible without the hospitality and support of the excavation team in
557 Pergamon. We are thankful to Dr. Güler Ateş (Celal Bayar University, Manisa/Turkey) for

558 determining the ceramic finds. The Ministry of Culture and Tourism of the Republic of Turkey kindly
559 granted the research permits.

560 **References:**

- 561 Ad-Hoc-AG Boden. 2005. *Bodenkundliche Kartieranleitung*. Schweizerbart: Stuttgart.
- 562 Aksu AE, Piper DJW, Konuk T. 1987. Late Quaternary tectonic and sedimentary history of outer
563 İzmir and Çandarlı Bays, Western Turkey. *Marine Geology* **76**: 89–104.
- 564 Ammerman AJ, Efstratiou N, Ntinou M, Pavlopoulos K, Gabrielli R, Thomas KD, Mannino MA.
565 2008. Finding the early Neolithic in Aegean Thrace: the use of cores. *Antiquity* **315**: 139–150.
- 566 Anzidei M, Antonioli F, Benini A, Lambeck K, Sivan D, Serpelloni E, Stocchi P. 2011. Sea level
567 change and vertical land movements since the last two millennia along the coasts of southwestern
568 Turkey and Israel. *Quaternary International* **232**: 13–20.
- 569 Başaran S. 2010. *Ainos (Enez)*. University İstanbul Press: İstanbul.
- 570 Blott SJ, Pye K. 2001. GRADISTAT: a grain size distribution and statistics package for the analysis of
571 unconsolidated sediments. *Earth Surface Processes and Landforms* **26**: 1237–1248.
- 572 Bonaduce G, Ciampo G and Masoli M. 1975. Distribution of Ostracoda in the Adriatic Sea.
573 *Pubblicazioni della Stazione zoologica di Napoli* **40** (Suppl.): 1–304.
- 574 Brückner H. 1994. Das Mittelmeergebiet als Naturraum. In *Das Alte Rom*, Martin J (ed). Bertelsmann:
575 München; 13–29.
- 576 Brückner H. 2005. Holocene shoreline displacements and their consequences for human societies: the
577 example of Ephesus in western Turkey. *Zeitschrift für Geomorphologie N.F.* **137** (Suppl): 11–22.
- 578 Brückner H, Müllenhoff M, Gehrels R, Herda A, Knipping M, Vött A. 2006. From archipelago to
579 floodplain - geographical and ecological changes in Miletus and its environs during the past six
580 millennia (Western Anatolia, Turkey). *Zeitschrift für Geomorphologie N.F.* **142** (Suppl): 63–83.
- 581 Brückner H, Seeliger M, Knipping M. 2010a. Ergebnisse der geoarchäologischen Arbeiten in der
582 Bucht von Elaia aus der Geländekampagne 2009. *Archäologischer Anzeiger* **2010(2)**, 208–220.
- 583 Brückner H, Kelterbaum D, Marunchak O, Porotov A, Vött A. 2010b. The Holocene sea level story
584 since 7500 BP - Lessons from the Eastern Mediterranean, the Black and the Azov Seas.
585 *Quaternary International* **225**: 160–179.
- 586 Brückner H, Urz R, Seeliger M. 2013. Geomorphological and geoarchaeological evidence for
587 considerable landscape changes at the coasts of western Turkey during the Holocene. *Geopedology
588 and Landscape Development Research Series* **1**: 81–104.
- 589 Brückner H, Schmidts T, Bücherl H, Pint A, Seeliger M. 2015. Die Häfen und ufernahen
590 Befestigungen von Ainos - eine Zwischenbilanz. In: *Häfen im ersten Millennium AD. Bauliche
591 Konzepte, herrschaftliche und religiöse Einflüsse*, Schmidts T, Vučetić MM (eds). Verlag des
592 Römisch-Germanischen Zentralmuseums: Mainz; 53–76.
- 593 Campos AC. 2010. Analyzing the relation between loss-on-ignition and other methods of soil organic
594 carbon determination in a tropical cloud forest (Mexico). *Communications in Soil Science and
595 Plant Analysis* **41**: 1454–1462.
- 596 Cartledge P. 2004. *Alexander the Great. The Hunt for a New Past*. Overlook Press: New York.
- 597 Cimerman F, Langer MR. 1991. *Mediterranean foraminifera*. Slovenska Akademija Znanosti in
598 Umetnosti, Academia Scientiarum et Artium Slovenica: Ljubljana.

- 599 Dankers N, Laane R. 1983. A comparison of wet oxidation and loss on ignition of organic material in
600 suspended matter. *Environmental Technology Letters* **4**: 283–290.
- 601 Delile H, Blichert-Toft J, Goiran JP, Stock F, Arnaud-Godet F, Bravard JP, Brückner H, Albarède F.
602 2015. Demise of a harbor: A geochemical chronicle from Ephesus. *Journal of Archaeological*
603 *Science* **53**: 202–213.
- 604 Engel M, Knipping M, Brückner H, Kiderlen M, Kraft JC. 2009. Reconstructing middle to late
605 Holocene palaeogeographies of the lower Messenian plain (southwestern Peloponnese, Greece):
606 Coastline migration, vegetation history and sea level change. *Paleogeography, Paleoclimatology,*
607 *Paleoecology* **284(3–4)**: 257–270.
- 608 Ernst W. 1970. *Geochemical facies analysis*. Elsevier: Amsterdam, London, New York.
- 609 Flemming NC. 1978. Holocene eustatic changes and coastal tectonics in the Northeast Mediterranean:
610 Implications for models of crustal consumption. *Philosophical Transactions of the Royal Society of*
611 *London. Mathematical and Physical Sciences* **289**: 405–458.
- 612 Folk RL, Ward WC. 1957. Brazos River bar: a study in the significance of grain size parameters.
613 *Journal of Sedimentary Petrology* **27**: 3–26.
- 614 Frenzel P, Boomer I. 2005. The use of ostracods from marginal-marine, brackish waters as
615 bioindicators of modern and Quaternary environmental change. *Palaeogeography,*
616 *Palaeoclimatology, Palaeoecology* **225(1–4)**: 68–92.
- 617 Goodman B, Reinhardt E, Dey H, Boyce J, Schwarcz H, Sahoglu V, Erkanal H, Artzy M. 2008.
618 Evidence for Holocene marine transgression and shoreline progradation due to barrier development
619 in Iskele, Bay of Izmir, Turkey. *Journal of Coastal Research* **24(5)**: 1269–1280.
- 620 Goodman B, Reinhardt E, Dey H, Boyce J, Schwarcz H, Sahoglu V, Erkanal H, Artzy M. 2009. Multi-
621 proxy geoarchaeological study redefines understanding of the paleocoastlines and ancient harbours
622 of Liman Tepe (Iskele, Turkey). *Terra Nova* **21(2)**: 97–104.
- 623 Hadler H, Kissas K, Koster B, Mathes-Schmidt M, Mattern T, Ntageretzis K, Reicherter K,
624 Willershäuser T, Vött A. 2013. Multiple late-Holocene tsunami landfall in the eastern Gulf of
625 Corinth recorded in the palaeotsunami geo-archive at Lechaion, harbour of ancient Corinth
626 (Peloponnese, Greece). *Zeitschrift für Geomorphologie N.F.* **57(4)** (Suppl): 139–180.
- 627 Hansen E. 1971. *The Attalids of Pergamon*. Cornell University Press: Ithaca.
- 628 Heiri O, Lotter AF, Lemcke G. 2001. Loss on ignition as a method for estimating organic and
629 carbonate content in sediments: reproducibility and comparability of results. *Journal of*
630 *Paleolimnology* **25**: 101–110.
- 631 Horejs B. 2012. Çukuriçi Höyük. A Neolithic and Bronze Age Settlement in the Region of Ephesos. In
632 *The Neolithic in Turkey. New Excavations & New Research*, Özdoğan M, Başgelen N, Kuniholm P
633 (eds). Archaeology and Art Publications: İstanbul; 117–131.
- 634 Horejs B, Milić B, Ostmann F, Thanheiser B, Weninger B, Galik K. 2015. The Aegean in the Early 7th
635 Millennium BC: Maritime Networks and Colonization. *Journal of World Prehistory* **28(4)**: 289–
636 330.
- 637 Jeckelmann C. 1996. *Genese lokaler Thermalwasservorkommen in der Region Bergama/W-Türkei -*
638 *Hydrochemie, Gas- und Isotopenanalysen zur Korrelation tiefer Grundwasserzirkulation und*
639 *aktiver Tektonik*. PhD-Thesis, University of Zürich, Switzerland.
- 640 Joachim F, Langer M. 2008. *The 80 most common ostracods from the Bay of Fetoveia, Elba Island*
641 *(Mediterranean Sea)*. University Bonn Press: Bonn.

- 642 Kelterbaum D, Brückner H, Dikarev V, Gerhard S, Pint A, Porotov A, Zin'ko V. 2012.
643 Palaeogeographic changes at Lake Chokrak on the Kerch Peninsula, Ukraine, during the Mid- and
644 Late-Holocene. *Geoarchaeology* **27(3)**: 206–219.
- 645 Khan NS, Ashe E, Shaw TA, Vacchi M, Walker J, Peltier WR, Kopp R, Horton BP. 2015. Holocene
646 relative sea-level changes from near-, intermediate-, and far-field locations. *Current Climate*
647 *Change Reports* **1(4)**: 247–262.
- 648 Kraft JC, Aschenbrenner SE, Rapp G Jr. 1977. Paleogeographic reconstructions of coastal Aegean
649 archeological sites. *Science* **195**: 941–947.
- 650 Kraft JC, Brückner H, Kayan I, Engelmann H. 2007. The geographies of ancient Ephesus and the
651 Artemision in Anatolia. *Geoarchaeology* **22**: 121–149.
- 652 Kraft JC, Kayan I, Erol O. 1980. Geomorphic reconstructions in the environs of ancient Troy. *Science*
653 **209**: 776–782.
- 654 Kraft JC, Kayan I, Luce JV. 2003. Harbor areas at ancient Troy: sedimentology and geomorphology
655 complement Homer's Iliad. *Geology* **31(2)**: 163–166.
- 656 Kraft JC, Rapp G, Szemler GJ, Tziavos C, Kase EW. 1987. The pass at Thermopylae, Greece. *Journal*
657 *of Field Archaeology* **14**: 181–198.
- 658 Kunze M, Kästner V. 1990. *Der Altar von Pergamon – Hellenistische und römische Architektur*.
659 Henschelverlag Kunst und Gesellschaft: Berlin.
- 660 Lambeck K, Purcell A. 2007. Palaeogeographic reconstructions of the Aegean for the past 20,000
661 years: Was Atlantis on Athens doorstep? In *The Atlantis Hypothesis: Searching for a Lost Land*,
662 Papamarinopoulos SP (ed). Heliotos Publications: Santorini; 241–257.
- 663 Meriç E, Avşar N, Bergin F. 2004. Benthic foraminifera of eastern Aegean Sea (Turkey); systematics
664 and autoecology. *Turkish Marine Research Foundation* **18**: 1–306.
- 665 Mook DH, Hoskin CM. 1982. Organic determinations by ignition, caution advised. *Estuarine, Coastal*
666 *and Shelf Science* **15**: 697–699.
- 667 Murray JW, 2006. *Ecology and Applications of Benthic Foraminifera*. Cambridge University Press:
668 New York.
- 669 Murray-Wallace CV, Woodroffe CD. 2014. *Quaternary Sea-Level Changes: A Global Perspective*.
670 Cambridge University Press: Cambridge.
- 671 Özbek O. 2010. Hamaylitarla reconsidered: a Neolithic site and its environmental setting in southern
672 Thrace. *Anatolia Antiqua* **18(1)**: 1–21.
- 673 Pint A, Seeliger M, Frenzel P, Feuser S, Erkul E, Berndt C, Klein C, Pirson F, Brückner H. 2015. The
674 environs of Elaia's ancient open harbour - a reconstruction based on microfaunal evidence. *Journal*
675 *of Archaeological Science* **54**: 340–355.
- 676 Pirson F. 2004. Elaia, der maritime Satellit Pergamons. *Istanbuler Mitteilungen* **54**: 197–213.
- 677 Pirson F. 2007. Elaia. *Archäologischer Anzeiger* **2007(2)**: 47–58.
- 678 Pirson F. 2008. Das Territorium der hellenistischen Residenzstadt Pergamon – Herrschaftlicher
679 Anspruch als raumbezogene Strategie. In *Räume der Stadt - Von der Antike bis heute*, Jöchner C
680 (ed). Reimer: Berlin; 27–50.
- 681 Pirson F. 2010. Survey. *Archäologischer Anzeiger* **2010(2)**: 195–201.
- 682 Pirson F. 2011. Elaia. *Archäologischer Anzeiger* **2011(2)**: 166–174.

- 683 Pirson F. 2014. Elaia, der (maritime) Satellit Pergamons. In *Harbor Cities in the Eastern*
684 *Mediterranean from Antiquity to the Byzantine Period*, Ladstätter S, Pirson F, Schmidts T (eds).
685 Ege Yayinlari: İstanbul; 339–356.
- 686 Pirson F, Scholl A. 2015. *Pergamon. A Hellenistic Capital in Anatolia*. Ege Yayinlari: İstanbul.
- 687 Poppe GT, Goto Y. 2000. *European Seashells*. ConchBooks: Harxheim.
- 688 Radt W. 2011. *Pergamon – Geschichte und Bauten einer antiken Metropole*. Primus Verlag:
689 Darmstadt.
- 690 Reimer PJ, Bard E, Bayliss A, Beck JW, Blackwell PG, Bronk Ramsey C, Buck CE, Cheng H,
691 Edwards RL, Friedrich M, Grootes PM, Guilderson TP, Haflidason H, Hajdas I, Hatt C, Heaton TJ,
692 Hogg AG, Hughen, KA, Kaiser KF, Kromer B, Manning SW, Niu M, Reimer RW, Richards DA,
693 Scott EM, Southon JR, Turney CSM, van der Plicht J. 2013. IntCal13 and MARINE13 radiocarbon
694 age calibration curves 0-50000 years calBP. *Radiocarbon* **55(4)**: 1869–1887.
- 695 Salehi MH, Hashemi BO, Bigi HH, Esfandiarpour BI, Motaghian HR. 2011. Refining soil organic
696 matter determination by loss-on-ignition. *Pedosphere* **21(4)**: 473–482.
- 697 Schneider S, Matthaei A, Schlöffel M, Kronwald M, Pint A, Schütt B. 2015. A geoarchaeological case
698 study in the chora of Pergamon, Western Turkey to reconstruct the late Holocene landscape
699 development and settlement history. *Quaternary International* **367**: 62–76.
- 700 Seeliger M, Bartz M, Erkul E, Feuser S, Kelterbaum D, Klein C, Pirson F, Vött A, Brückner H. 2013.
701 Taken from the sea, reclaimed by the sea: The fate of the closed harbour of Elaia, the maritime
702 satellite city of Pergamum (Turkey). *Quaternary International* **312**: 70–83.
- 703 Seeliger M, Brill D, Feuser S, Bartz M, Erkul E, Kelterbaum D, Vött A, Klein C, Pirson F, Brückner
704 H. 2014. The purpose and age of underwater walls in the Bay of Elaia of western Turkey: A
705 multidisciplinary approach. *Gearchaeology* **29**: 138–155.
- 706 Siani G, Paterne M, Arnold M, Bard E, Metivier B, Tisnerat N, Bassinot F. 2000. Radiocarbon
707 reservoir ages in the Mediterranean Sea and Black Sea. *Radiocarbon* **42**: 271–280.
- 708 Stock F, Ehlers L, Horejs B, Knipping M, Ladstätter S, Seren S, Brückner H. 2015. Neolithic
709 settlement sites in Western Turkey - palaeogeographic studies at Çukuriçi Höyük and Arvalya
710 Höyük. *Journal of Archaeological Science: Reports* **4**: 565–577.
- 711 Stock F, Pint A, Horejs B, Ladstätter S, Brückner H. 2013. In search of the harbours - New evidence
712 of Late Roman and Byzantine harbours of Ephesus. *Quaternary International* **312**: 57–69.
- 713 Strabo. 2005. *Geographica*. Translation and comments by Albert Forbiger. Marix Verlag: Wiesbaden.
714 (Greek to German).
- 715 Soukissian T, Prospathopoulos A, Hatzinaki M, Kabouridou M. 2008. Assessment of the wind and
716 wave climate of the Hellenic seas using 10-year hindcast results. *The Open Ocean Engineering*
717 *Journal* **1**: 1–12.
- 718 Vacchi M, Rovere A, Chatzipetros A, Zouros N, Firpo M. 2014. An updated database of Holocene
719 relative sea level changes in NE Aegean Sea. *Quaternary International* **328-329**: 301–310.
- 720 Vita-Finzi C. 1969. Late Quaternary continental deposits of central and western Turkey. *Man New*
721 *Series* **4(4)**: 605–619.
- 722 Vött A, Bareth G, Brückner H, Lang F, Sakellariou D, Hadler H, Ntageretzis K, Willershäuser T.
723 2011. Olympia's harbour site Pheia (Elis, Western Peloponnese, Greece) destroyed by tsunami
724 impact. *Die Erde* **142(3)**: 259–288.

725 Zimmermann M. 2011. *Pergamon: Geschichte, Kultur, Archäologie*. C. H. Beck: München.

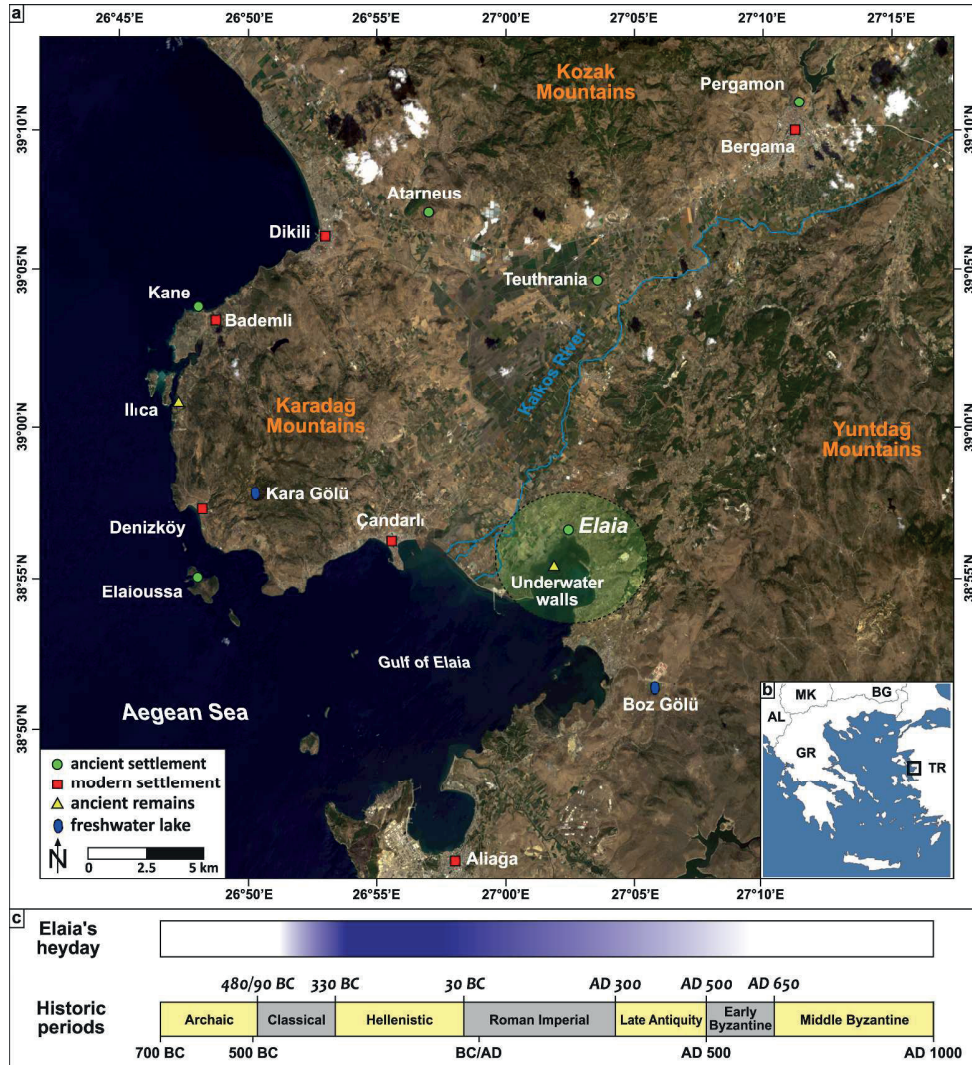


Figure 1: The area of research at the Aegean coast of Turkey. (a) Landsat 8 satellite image (acquired 23 September 2013; RGB composite based on bands 4, 3, 1), with locations mentioned in the text. Insert: (b) General map of the Aegean Sea; the area of research is indicated. (c) Timeline of the historical periods, linked with the period of Elaia's heyday (based on: Radt, 2011; Pirson and Scholl, 2015). 981x1075mm (96 x 96 DPI)

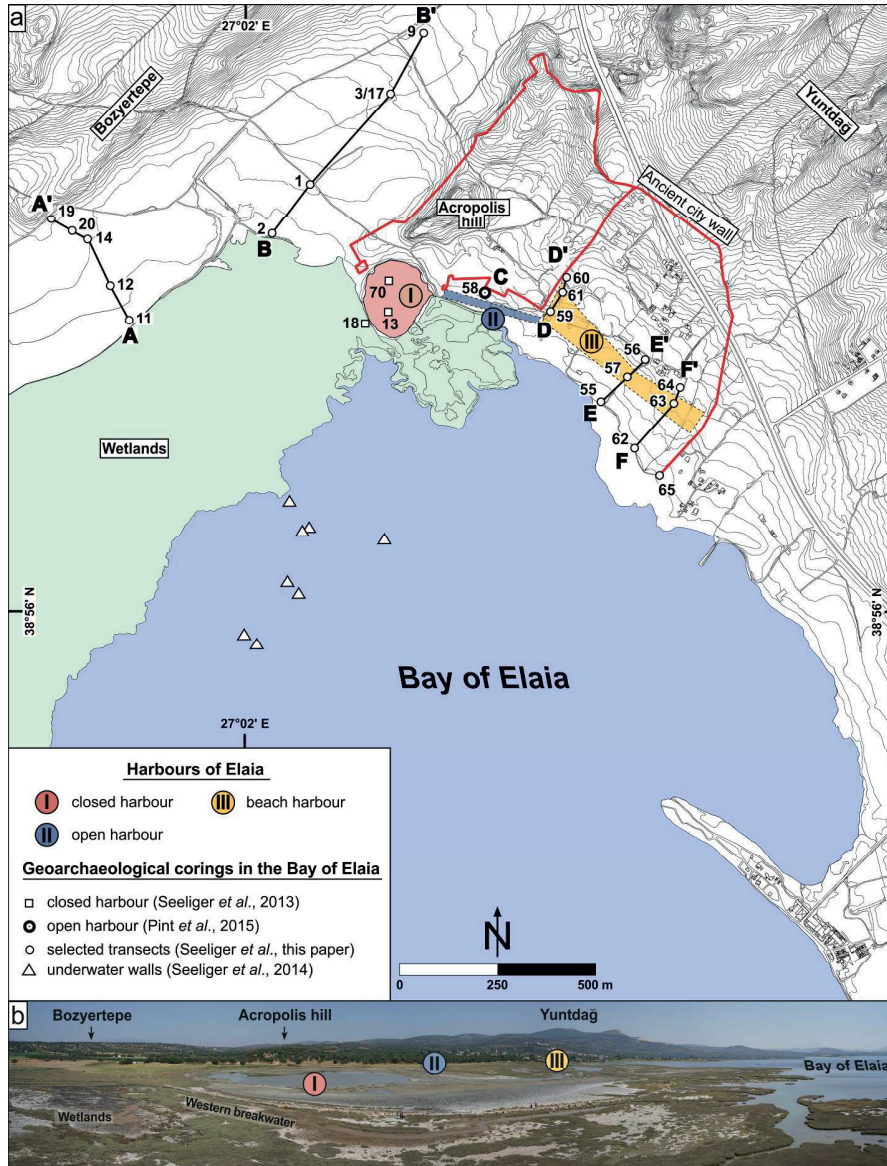


Figure 2: Locations of selected vibracores taken in the Bay of Elaia. (a) Locations of coring transects A–A', B–B', D–D', E–E' and F–F', and "C" (coring Ela 58). (b) Panoramic view of the research area (UAV image; taken on 1 September 2015 by Andreas Bolten) with location of harbour areas. 145x190mm (600 x 600 DPI)

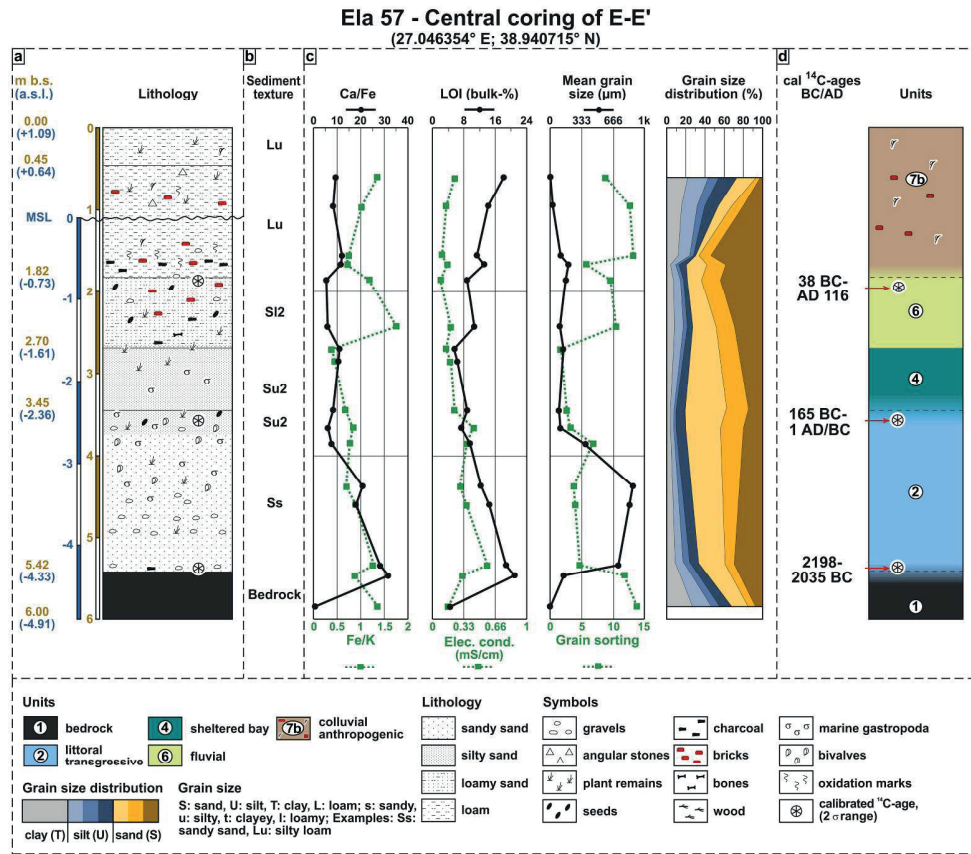


Figure 3: Sediment core Ela 57 with geochemical and sedimentological parameters (a, b, c). (d) Interpretation of sedimentary units and dating results. 121x106mm (600 x 600 DPI)

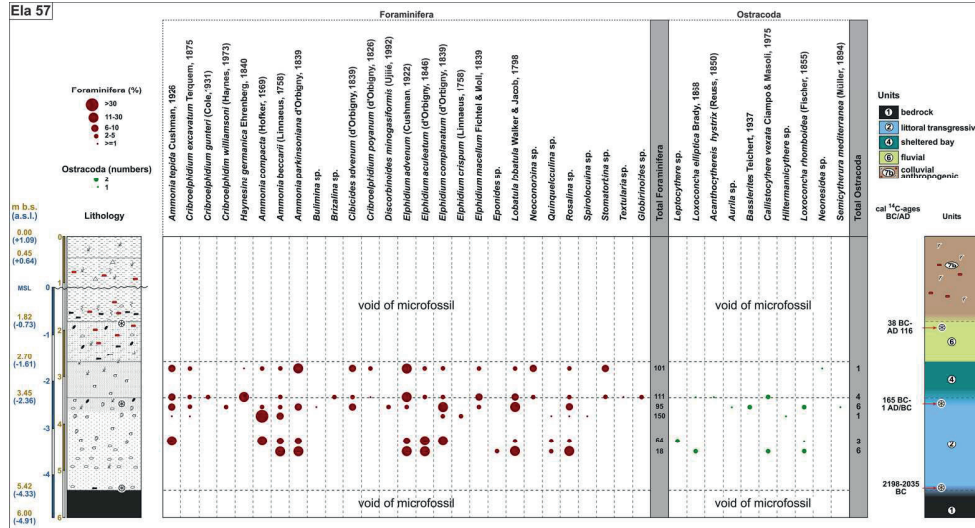


Figure 4: Sedimentary units of core Ela 57, based on microfauna. Relative abundance of ostracods and foraminifers is given semi-quantitatively. 96x52mm (600 x 600 DPI)

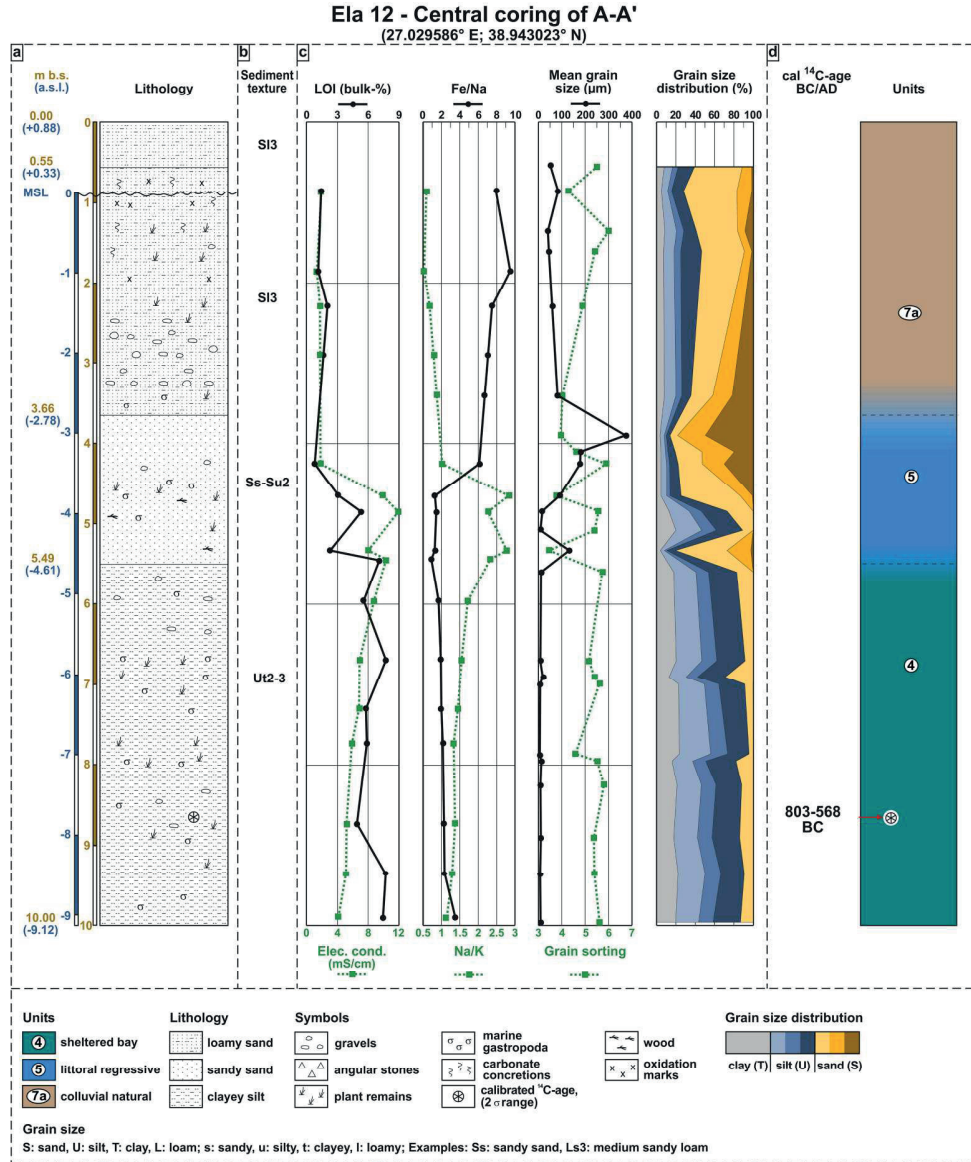


Figure 5: Sediment core Ela 12 with geochemical and sedimentological parameters (a, b, c). (d) Interpretation of sedimentary units and dating result. 124x150mm (600 x 600 DPI)

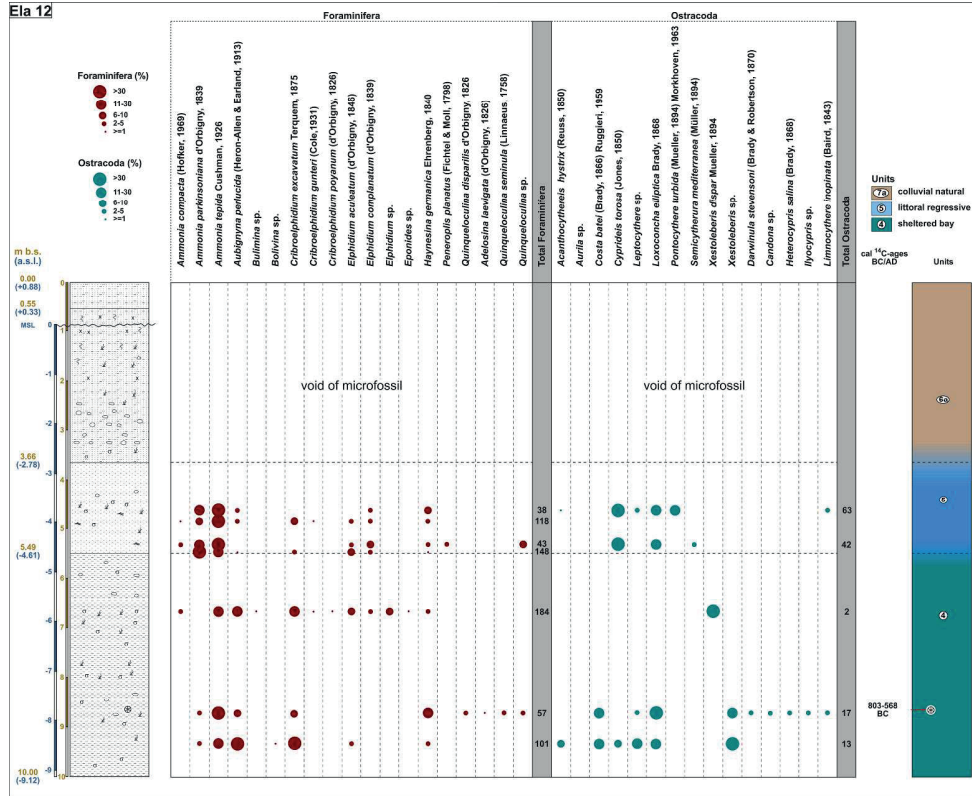


Figure 6: Sedimentary units of core Ela 12, based on microfauna. Relative abundance of ostracods and foraminifers is given semi-quantitatively.
138x113mm (600 x 600 DPI)

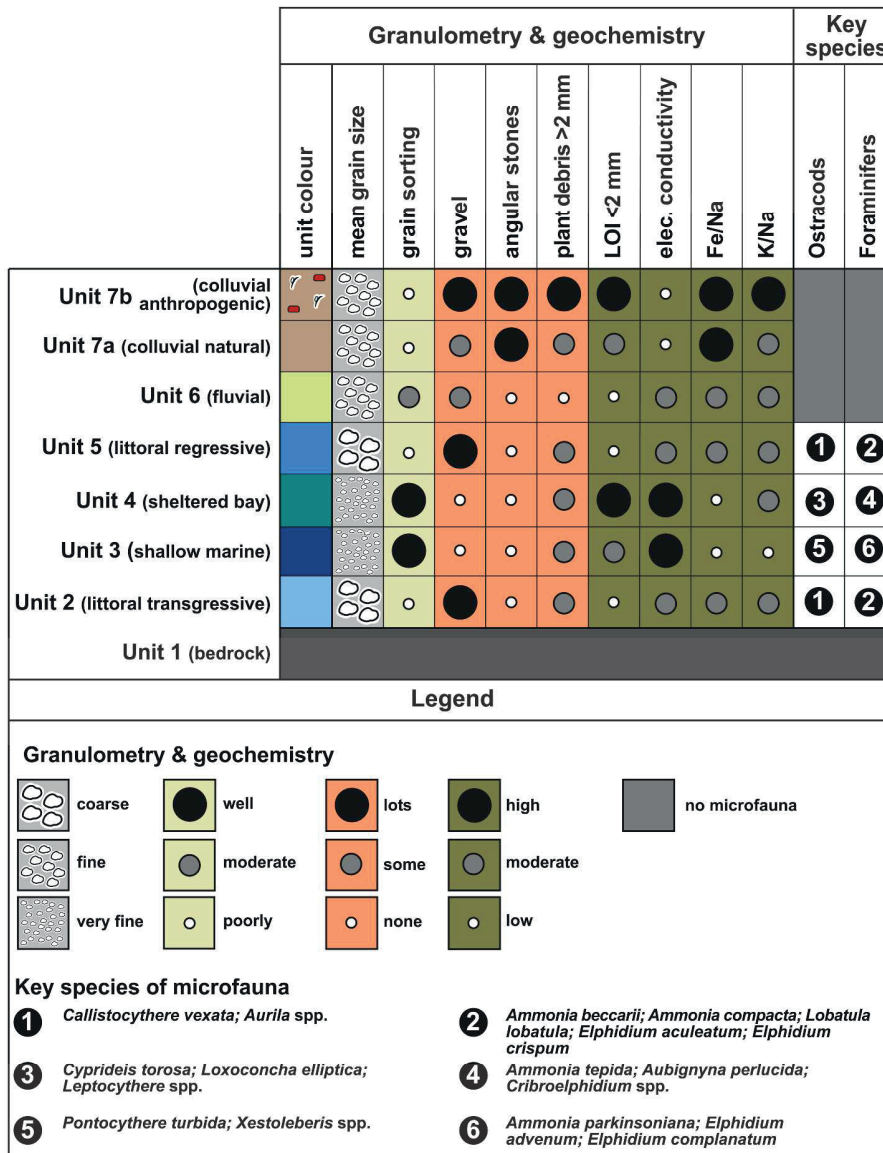


Figure 7: Microfaunal, granulometrical and geochemical characteristics of the sedimentary units of the corings in the Bay of Elaia.
227x293mm (600 x 600 DPI)

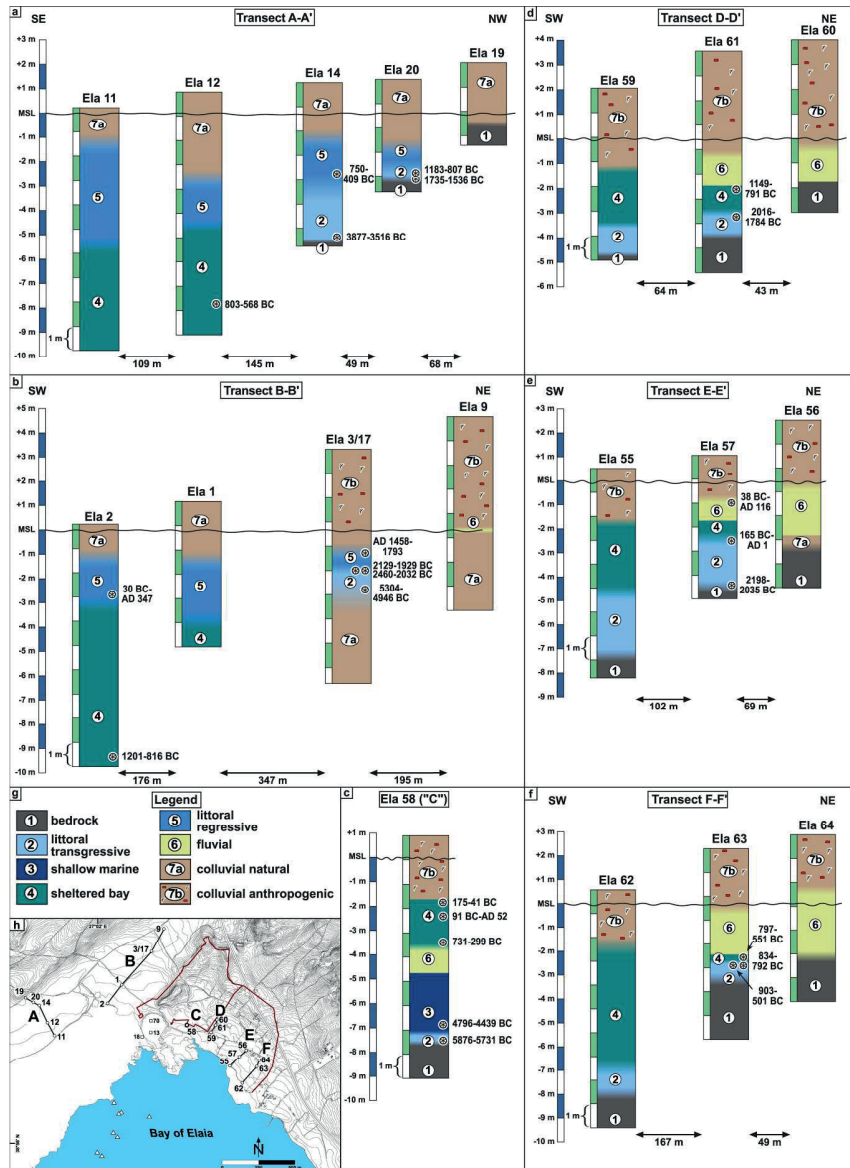


Figure 8: Synopsis of the coring transects (a) A-A', (b) B-B', (d) D-D', (e) E-E', and (f) F-F', as well as (c) (Ela 58); (g) legend; (h) locations of corings and transects. 133x182mm (600 x 600 DPI)

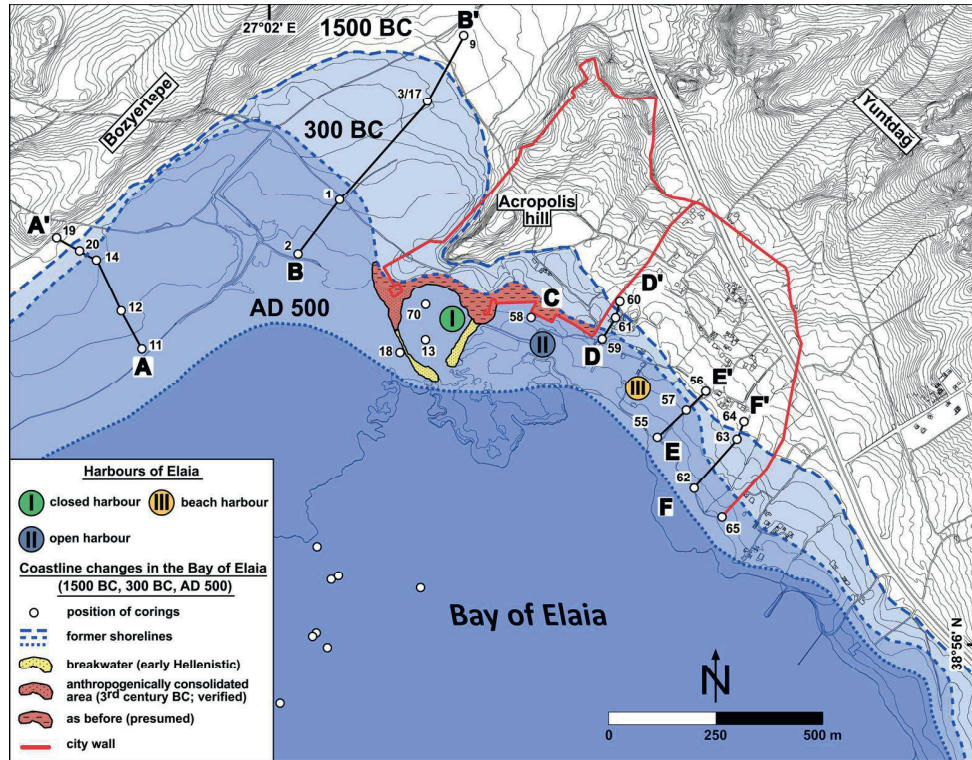


Figure 9: Coastline changes in the area of the Bay of Elaia in time slices: 1500 BC, 300 BC and AD 500. The scenarios are based on the results of this paper.
84x65mm (600 x 600 DPI)

Sample code	Lab code	Material	Depth b.s.	Depth a.s.l.	$\delta^{13}C$ (‰)	Libby-age	Calibrated ^{14}C -ages cal BC/cal AD (2 σ)	Calibrated ^{14}C -ages cal BC/cal AD (2 σ) with relative probability	Calibrated ^{14}C -ages cal BP (2 σ)	Calibrated ^{14}C -ages cal BP (2 σ) with relative probability
Ela 2/9	UGAMS 4148	shell (<i>nucula</i> sp.)	2.94 m	-2.71 m	4.20	2236±27	30 BC-AD 347	30 BC-AD 347 (100 %)	1603-1979 BP	1606-1979 BP (100 %)
Ela 2/225G	UGAMS 4150	sea grass	9.56 m	-9.33 m	-12.72	3194±28	1201-816 BC	1201-816 BC (100 %)	2765-3150 BP	2765-3150 BP (100 %)
Ela 3/7H	UGAMS 4151	wood	4.28 m	-0.47 m	-24.4	305±52	AD 1458-1793	AD 1458-1665 (98.6 %) AD 1785-1793 (1.4 %)	157-492 BP	157-165 BP (1.4 %) 285-492 BP (98.6 %)
Ela 3/12H	UGAMS 4152	sea grass	4.98 m	-1.17 m	-13.6	4176±30	2460-2032 BC	2460-2032 BC (100 %)	3981-4409 BP	3981-4409 BP (100 %)
Ela 3/15	UGAMS 4153	shell (<i>Lasaea rubra</i>)	5.80 m	-1.99 m	2.4	6606±31	5304-4946 BC	5304-4946 BC (100 %)	6895-7253 BP	6895-7253 BP (100 %)
Ela 12/36H	UGAMS 6039	charcoal	8.65 m	-7.77 m	-26.7	2560±25	803-568 BC	803-749 BC (82.9 %) 683-668 BC (5.4 %) 638-589 BC (10.5 %) 577-568 (1.2 %)	2517-2752 BP	2517-2526 BP (1.2 %) 2538-2587 BP (10.5 %) 2617-2632 BP (5.4 %) 2698-2752 BP (82.9 %)
Ela 14/10H	UGAMS 6035	wood	3.75 m	-2.49 m	-25.8	2440±25	750-409 BC	750-684 BC (25.2 %) 667-638 BC (8.5 %) 590-409 BC (66.4 %)	2358-2699 BP	2358-2539 BP (66.4 %) 2587-2616 BP (8.5 %) 2633-2699 BP (25.2 %)
Ela 14/18	UGAMS 6034	sea grass	6.36 m	-5.10 m	-14.3	5300±25	3877-3516 BC	3877-3868 BC (0.6 %) 3864-3516 BC (99.4 %)	5465-5826 BP	5465-5813 BP (99.4 %) 5817-5826 BP (0.6 %)
Ela 17/14H	UGAMS 6033	charcoal	4.90 m	-1.57 m	-24	3640±25	2129-1929 BC	2129-2088 BC (13 %) 2047-1937 BC (86.4 %) 1933-1929 (0.6 %)	3878-4078 BP	3878-3882 BP (0.6 %) 3886-3996 BP (86.4 %) 4037-4078 BP (13 %)
Ela 18/7HK	UGAMS 6031	charcoal	1.38 m	-1.20 m	-24.5	1740±25	AD 240-380	AD 240-358 (94.2 %) AD 363-380 (5.8 %)	1570-1710 BP	1570-1587 (5.8 %) 1592-1710 BP (94.2 %)
Ela 20/15	UGAMS 6028	sea grass	3.85 m	-2.47 m	-15.9	3180±25	1183-807 BC	1183-807 BC (100 %)	2756-3132 BP	2756-3132 BP (100 %)
Ela 20/16SG	UGAMS 6027	plant remain	4.04 m	-2.66 m	-14.5	3350±25	1735-1536 BC	1735-1717 BC (3.7 %) 1693-1606 BC (88.4 %) 1583-1545 BC (7.7 %) 1537-1536 BC (0.1 %)	3485-3684 BP	3485-3486 BP (0.1 %) 3494-3532 BP (7.7 %) 3555-3642 BP (88.4 %) 3666-3684 BP (3.7 %)
Ela 57/8H	UGAMS 11900	olive seed	1.95 m	-0.86 m	-26.6	1960±25	38 BC-AD 116	38 BC-AD 85 (91.8 %) 109-116 AD (1.0 %)	1834-1987 BP	1834-1841 BP (1.0 %) 1865-1953 BP (91.8 %) 1957-1987 BP (7.2 %)
Ela 57/17H	UGAMS 11901	grape seed	3.56 m	-2.47 m	-25.3	2060±25	165 BC-1 BC/AD	165-18 BC (95.4 %) 14 BC-1 BC/AD (4.6 %)	1949-2114 BP	1949-1963 BP (4.6 %) 1967-2114 BP (95.4 %)
Ela 57/23H	UGAMS 11441	charcoal	5.39 m	-4.30 m	-27.4	3720±25	2198-2035 BC	2198-2162 BC (20.1 %) 2152-2035 BC (79.9 %)	3984-4101 BP	3984-4101 BP (79.9 %) 4111-4147 BP (20.1 %)
Ela 58/14HK	UGAMS 11442	charcoal	2.73m	-1.84 m	-26.7	2080±25	175-41 BC	175-41 BC (100 %)	2124-1990 BP	2124-1990 BP (100 %)
Ela 58/17H	UGAMS 11443	melon seed	3.30 m	-2.41 m	-25.0	2020±25	91 BC-AD 52	91-69 BC (5.3 %) 60 BC-AD 52 (94.7 %)	2040-1898 BP	2040-2018 BP (5.3 %) 2009-1898 BP (94.7 %)
Ela 58/24Po	UGAMS 11444	sea grass	4.40 m	-3.51 m	-10.8	2740±25	731-299 BC	731-299 BC (100 %)	2680-2248 BP	2680-2248 BP (100 %)
Ela 58/32	UGAMS 11445	sea grass	7.75 m	-6.86 m	-16.2	6170±30	4796-4439 BC	4796-4439 BC (100 %)	6745-6388 BP	6745-6388 BP (100 %)
Ela 58/38F	UGAMS 11446	charcoal	8.35 m	-7.46 m	-26.1	6920±30	5876-5731 BC	5876-5856 BC (5.4 %) 5852-5731 BC (94.6 %)	7825-7680 BP	7825-7805 (5.4 %) 7801-7680 (94.6 %)
Ela 61/16	UBA 28500	bulk of marine ostracoda	5.60 m	-2.34 m	0.1	3154±23	1149-791 BC	1149-791 BC (100 %)	2740-3098 BP	2740-3098 BP (100 %)
Ela 61/19	UGAMS 11448	charcoal	6.70 m	-3.34 m	-27.4	3570±25	2016-1784 BC	2016-1996 BC (4.4 %) 1980-1877 BC (92.3 %) 1840-1825 BC (2.2 %) 1793-1784 BC (1.0 %)	3733-3965 BP	3733-3742 BP (1.0 %) 3774-3789 BP (2.2 %) 3826-3929 BP (92.3 %) 3945-3965 BP (4.4 %)
Ela 63/10H	UGAMS 11903	charcoal	4.54 m	-2.23 m	-28.0	2540±25	797-551 BC	797-744 BC (52.9 %) 686-665 BC (11.5 %) 644-551 BC (35.7 %)	2500-2746 BP	2500-2593 BP (35.7 %) 2614-2635 BP (11.5 %) 2693-2746 BP (52.9 %)
Ela 63/485	UBA 28499	bulk of marine ostracoda	4.85 m	-2.54 m	8.0	2952±27	903-501 BC	903-501 BC (100 %)	2450-2852 BP	2450-2852 BP (100 %)
Ela 63/11	UGAMS 11904	charcoal	4.88 m	-2.57 m	-28.0	2640±25	834-792 BC	834-792 BC (100 %)	2741-2783 BP	2741-2783 BP (100 %)

Table 1: Radiocarbon data sheet. ^{14}C -AMS dating was carried out at the Centre for Applied Isotope Studies (CAIS) of the University of Georgia at Athens, USA (lab code: UGAMS), and the ^{14}C Chrono Centre for Climate, the Environment, and Chronology, Queen's University Belfast, UK (lab code: UBA). All ages were calibrated with IntCal13 or MARINE13 calibration curves using the Calib 7.1 software (Reimer et al., 2013). A marine reservoir effect of 390 ± 85 years and a ΔR of 35 ± 70 years (Siani et al., 2000) was applied. The calibrated ages are presented in calendar years BC/AD and years BP (before AD 1950) with 2 σ confidence interval.

210x170mm (300 x 300 DPI)

Chapter 5

5 The purpose and age of underwater walls in the Bay of Elaia of Western Turkey: A multidisciplinary approach

Journal Article (2014):

Seeliger, M., Brill, D., Feuser, S, Bartz, M., Erkul, E., Kelterbaum, D., Vött, A., Klein, C., Pirson, F., Brückner, H., 2014. The purpose and age of underwater walls in the Bay of Elaia of Western Turkey: A multidisciplinary approach. *Geoarchaeology: An International Journal* 29, 138–155.

The Purpose and Age of Underwater Walls in the Bay of Elaia of Western Turkey: A Multidisciplinary Approach

Martin Seeliger,^{1,*} Dominik Brill,¹ Stefan Feuser,² Melanie Bartz,¹ Ercan Erkul,³ Daniel Kelterbaum,¹ Andreas Vött,⁴ Christina Klein,³ Felix Pirson,⁵ and Helmut Brückner^{1,*}

¹Institute of Geography, University of Cologne, Köln, (Cologne), Germany

²Heinrich Schliemann-Institute for Ancient Studies, University of Rostock, Rostock, Germany

³Institute of Geoscience, University of Kiel, Kiel, Germany

⁴Institute for Geography, Johannes Gutenberg-Universität Mainz, Mainz, Germany

⁵German Archaeological Institute, Istanbul Department, Istanbul, Turkey

Correspondence

*Corresponding authors; E-mail: martin.seeliger@uni-koeln.de; h.brueckner@uni-koeln.de

Received

23 September 2013

Accepted

21 November 2013

Scientific editing by Jamie Woodward and Gary Huckleberry

Published online in Wiley Online Library (wileyonlinelibrary.com).

doi 10.1002/geo.21471

Pergamum (modern: Bergama) was operating an important harbour used by military forces and merchants at the city of Elaia during Hellenistic and Roman Imperial times. Harbour-related facilities such as warehouses, breakwaters and wharfs document the importance of this harbour site not only for the Pergamenians. This paper focuses on the purpose and age of six submerged wall structures situated approximately 1 km south of the ancient closed harbour basin of Elaia. Geoelectric cross-sections and semi-aquatic coring near these walls failed to detect any solid basement under the walls which excludes their possible use as breakwaters or wharfs. Instead, the walls were most likely delineating and separating evaporation ponds of salt works, which compares well with similar structures from other periods and places around the Mediterranean. Combined OSL and ¹⁴C-dating determined the construction age of the installation between the 4th and 6th centuries A.D. Subsequent (re-)uses are likely and are in agreement with findings from archaeological surveys. © 2014 Wiley Periodicals, Inc.

INTRODUCTION

Several Mediterranean harbour cities have been studied over the last years dealing with regard to landscape history, utilisation of harbour basins in general, as well as harbour-related facilities such as breakwaters and wharfs (e.g., Reinhardt & Raban, 1999; Brückner, 2003; Morhange et al. 2003; Galili, Zviely, & Weinstein-Evron, 2005; Brückner et al., 2006; Kraft et al., 2007; Marriner & Morhange, 2007; Vött et al., 2007; Marriner, Morhange, & Saghieh-Beydoun, 2008; Bini et al., 2009; Algan et al., 2011; Kızıldağ, Özdağ, & Uluğ, 2012; Stanley & Bernasconi, 2012; Brückner et al., 2013; Hadler et al., 2013; Özdağ & Kızıldağ, 2013; Seeliger et al., 2013). For most of human history—from the Stone Age to modern times—harbours have played important roles in terms of trade, travelling, maritime traffic and economic centres. Other than cities in the hinterland, harbour settlements have been exposed to risks from the sea, such as extreme wave events (storms, tsunamis) and sea level rise

or fall. Harbours are also prone to siltation and abandonment. Any negative impact on harbours entails repercussions on inhabitants of the settlement and the hinterland (Knoblauch, 1981; Marriner & Morhange, 2007; Morhange & Marriner, 2010).

Archaeological and geoarchaeological fieldwork at Pergamum's harbour city started in 2006 (Pirson, 2007, 2008a, 2009, 2010, 2011; Brückner & Seeliger, 2009; Seeliger et al., 2011, 2012, 2013; Brückner et al., 2013). During Hellenistic times, when the Pergamenian kingdom was dominating Asia Minor, the Pergamenians were in need of a harbour for military and economic purposes due to the fact that the city was situated approx. 26 km inland. A site was found in the city of Elaia (Figure 1A), an insignificant harbour settlement during pre-Hellenistic times located on the Gulf of Elaia (modern: Gulf of Çandarlı) (Hansen, 1971; Radt, 1999; Cartledge, 2004; Pirson, 2004, 2008b, 2012; Zimmermann, 2011).

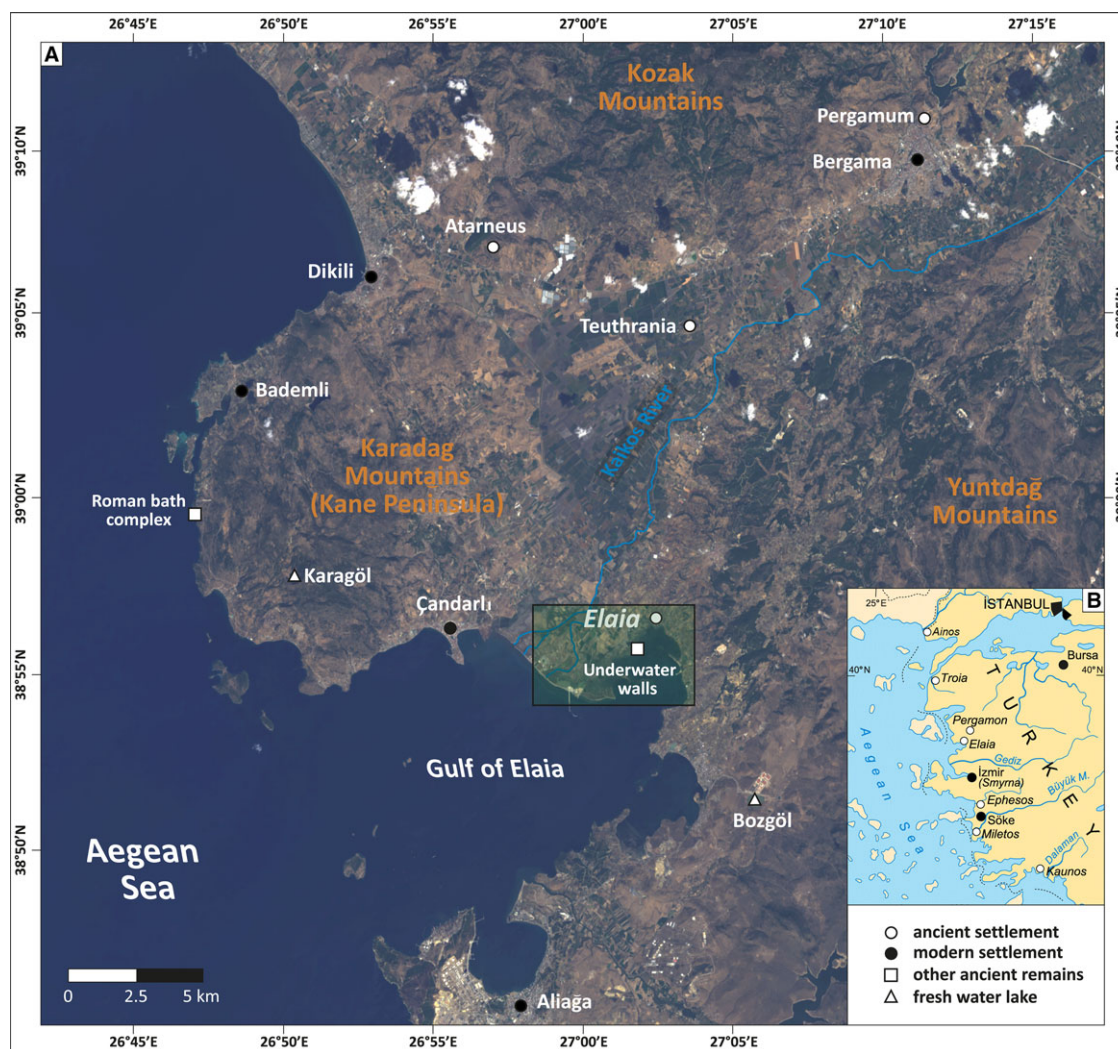


Figure 1 Area of research at the Aegean coast of Turkey. (A) Overview based on Landsat 8 (acquired September 23, 2013; composition based on bands 4, 3, 1) with locations mentioned in the text; (B) General map of western Turkey with a selection of ancient and modern settlements.

While most archaeological structures of Elaia's harbour have already been described and dated (Pirson, 2007, 2008a; Brückner & Seeliger, 2009; Seeliger, Bartz, & Brückner, 2012; Seeliger et al. 2013; Brückner et al., 2013) the purpose and age of several underwater wall structures in shallow marine waters about 1 km to the south of the closed harbour basin of Elaia remained unknown (Figure 2). In addition to the harbour breakwaters and parts of the city wall (Figure 2A), the underwater walls are the only preserved and visible remains of ancient Elaia. It has been speculated that they represent additional harbour infrastructures or shipyards far out in the embayment, breakwaters along the coast, or the remains of drowned salt works. Their age is difficult to determine because the underwater walls' blocks represent

re-used building material that makes dating by archaeological criteria impossible (Pirson, 2010).

This paper presents the results of geoarchaeological, geophysical and geochronological research on six underwater wall structures in order to (i) provide a chronological framework based on luminescence and radiocarbon dating constraining their construction time and (ii) to decipher their former purpose.

AREA OF INVESTIGATION

Physical Setting

The Gulf of Elaia is situated between the Karadağ Mountains (Kane Peninsula) to the west and the Yuntdağ

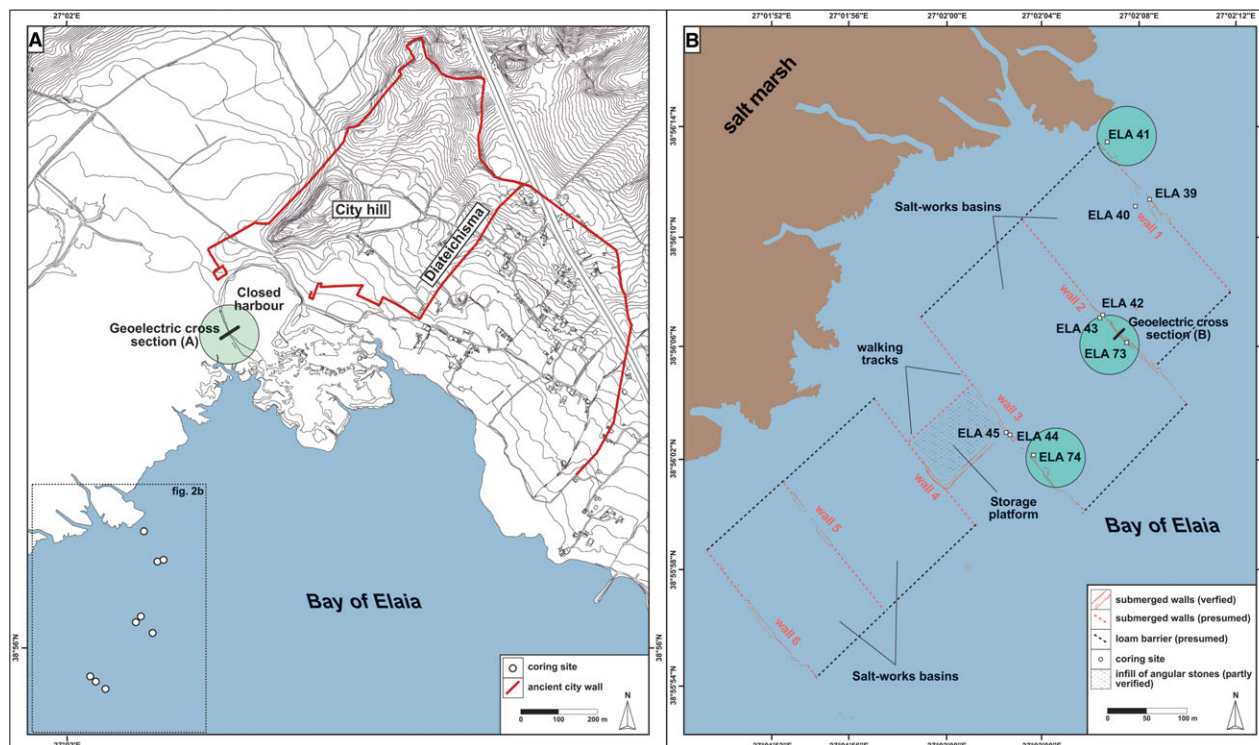


Figure 2 Location of vibracores carried out in the surroundings of the underwater walls in the Bay of Elaia. The maps are based on DGPS data levelled by the Pergamum excavation team. (A) Synoptic view with the area of the city of Elaia; (B) Location of underwater structures with associated sediment cores and geoelectric cross-sections.

mountain complex to the east (Figure 1A). It represents an area of low energy marine wave climate, even during extreme weather events during the winter season, due to its distance from the open Aegean Sea. The topography of the coastal plain as well as the bathymetry of the Bay of Elaia are relatively flat; the 20 m isobath lies ca. 4 km offshore (Aksu et al., 1987). The estimated tidal range of 20 cm determined by our DGPS (Differential Global Positioning System) surveys (Leica GPS System 530) in 2010 and 2011 are comparable to other sites in the eastern Aegean region, although wind surges may increase the sea level during the winter season (Flemming, 1978; Anzidei et al., 2011; Seeliger, Bartz, & Brückner, 2012; Seeliger et al., 2013). The modern Bakır Çay (translated: Copper River; ancient: Kaikos) forms a cusped delta between the Kane Peninsula and the Bay of Elaia before entering the Aegean Sea (Figure 1A).

The Bay of Elaia is located on the westwards drifting Aegean–Anatolian microplate. An ensemble of several E–W-oriented late Miocene rift structures (e.g., Bergama and Zeytinadağ grabens) serves as a drainage channel for the Bakır Çay, which filled the Bergama Graben with sediments (Vita-Finzi, 1969; Brinkmann, 1976; Aksu et al., 1987; McHugh et al., 2006; Schneider et al., 2011). Sev-

eral archaeological sites bear witness to ongoing subsidence of the graben system, namely (i) a partly drowned Roman thermal bath situated on the western Kane Peninsula (Figure 1A) and (ii) the sunken harbour breakwaters and drowned underwater wall structures in the Bay of Elaia (Figure 1A; Seeliger, Bartz, & Brückner, 2012; Seeliger et al., 2013). Our investigations of the transgressive contact in the closed harbour area of Elaia and the study of archaeological sea level markers resulted in an estimated subsidence rate of the graben ensemble of far less than 1 m per 1000 years (Seeliger et al., 2013, in contrast to Aksu et al., 1987).

Historical Background

Pergamum is one of the most prominent ancient settlements in western Turkey mentioned in connection with Troy or Miletus (Figure 1B; Brückner et al., 2013). The city is known for the Pergamum Altar (exhibited on the Museumsinsel in Berlin, Germany) and Aelius Galenus, a famous physician in the 2nd century A.D. (Radt, 1999). As a result of the so-called Wars of the Diadochi after the death of Alexander the Great in 323 B.C., the House of the Attalids came to power in the Kaikos



Figure 3 Combined investigations at the underwater structures with geophysical measurements and coring. (A) Overview facing north; (B) Zoomed view of the wall structures (length of scale: 1 m); (C) Boat-based geoelectric measurements was done with a floating electrode cable and the RESECS instrument of the company GEOSERVE; (D) Recovering a sediment core in the shallow marine waters by using a wooden table construction. The two persons beside the zodiac are standing in the surroundings of the underwater walls.

region. The Pergamenians established their Hellenistic kingdom, which on its heyday—under king Eumenes II (197–159 B.C.)—covered most of the western part of modern Turkey. In 133 B.C. the Pergamenian kingdom was absorbed by the Roman Empire (Hansen, 1971; Radt, 1999; Cartledge, 2004; Zimmermann, 2011).

Relation Between Pergamum and Elaia

Pergamum occupies a prominent strategic location at the 330 m high city hill dominating the surrounding Kaikos plain (Figure 1A) that was optimal for defence but restricted traffic and trade. Access to the Mediterranean Sea was provided through the acquisition of nearby Elaia, situated at the Aegean Sea some 26 km southwest of Pergamum, under Eumenes I (reign: 263–241 B.C.; Pirson, 2004). Strabo mentioned Elaia as the commercial harbour of the Pergamenians and as the military base of

the Attalids (Strabon: *Geographica* XIII, 1, 67 & XIII, 3, 5). Further literary as well as archaeological evidence underscore the close relations between Elaia and Pergamum (Pirson, 2004, 2008a, 2009, 2010).

Archaeological Setting of Underwater Wall Structures

Approx. 1 km south of the closed harbour basin (Figure 2A) six underwater wall structures trend parallel in northwest-southeast direction covering an area of ca. $1150 \times 265 \text{ m}^2$ (Figure 2B; Pirson, 2008a). Each structure has a preserved length between 80 and 265 m and a width of 4.8 to 5.0 m (Figures 3A and B). Between the third and fourth wall a U-shaped structure has been discovered which is constructed in the same fashion. Geomagnetic measurements revealed that a similar U-shaped structure had been in place between

the first and second wall (Pirson, 2010). Wave action and possible clearing of blocks may have reduced the original dimensions of the wall structures. Situated in shallow marine waters at depths of 0.5–2.0 m, the blocks rise above the silty-sandy subsoil by just a few decimetres (Figures 3A, B, and D). Well-preserved parts of walls exemplify the construction style as two parallel rows of ashlar in size of up to $0.9 \times 0.4 \text{ m}^2$ in addition to quarry stones (Figures 3A and B). The space between the rows is filled up with smaller quarry stones and debris. Ashlars exhibit dowel holes on their upper sides. However, the holes of adjacent blocks are not aligned with each other and the dowels, probably originally made of bronze, are not preserved (Pirson, 2008a).

Dating of these submerged walls by archaeological or historical means has not yet been possible. The dowel holes suggest the use of recycled building material (*spolia*). The *spolia* may indicate a construction date of the walls in late Antiquity (Müller, 2003), but *spolia* usage is also known to have occurred in Roman Imperial times (Höcker, 2001). Based on archaeological or historical criteria, wall construction in Antiquity seems to be as plausible as in Byzantine or even Ottoman times.

METHODS

Geophysical and Geoarchaeological Fieldwork

Lateral and vertical changes of the archaeological and underlying sedimentary stratigraphy of the underwater wall structures were studied by interpreting sediment cores (punctual data) and geophysical measurements (cross-sections). The position and elevation of each coring site and geophysical transect was measured by using DGPS (Leica GPS System 530), with a vertical resolution of less than 2 cm. All measured altitudes are based on the gauge of Izmir and were corrected by -0.875 m to account for an inaccuracy of the PergSys05 reference system established in 2005. The resulting elevations are accurate in relation to the present sea level (Seeliger, Bartz, & Brückner, 2012, Seeliger et al., 2013).

Sediment coring was performed with an Atlas Copco Cobra pro vibracorer. A wooden platform facilitated coring in shallow marine waters (Figure 3D). Closed steel auger heads with opaque 1 m long PVC tube liners with an external diameter of 5 cm preserved cores ELA 73 and ELA 74 aphotically for OSL dating. ELA 41 was cored using open steel auger heads (diameters of 6 and 5 cm). Preliminary stratigraphies based on AG Boden (2005) were determined in the field, including characterisation of grain size, texture, roundness, colour (Munsell Soil Colour Charts), sedimentary structure, carbonate content

(10 % hydrochloric acid) and macrofauna. Bulk samples of discrete sediment layers, as well as macrofossils and ceramic fragments were taken from open sediment cores for further laboratory analyses.

Earth electrical resistivity was determined with an RESECS multi-electrode system to reconstruct the thickness and shape of the closed harbour's western breakwater of Elaia (Figure 2A), and to investigate the linear underwater stone settings (electrode spacing: 1 m at the western breakwater, 2 m for cross-sections at underwater structures; Figures 2B and 3C). Several electrode arrangements were applied such as Dipole–Dipole and Wenner & Schlumberger. The apparent electrical resistivity was determined as a function of electrode geometry by the measuring instrument. Using the inversion software RESINV2D (Loke & Barker, 1995), a resistivity to depth distribution was inverted from the field data for each measured profile.

Sediment Analyses

Multi-proxy analyses were conducted in the laboratory to augment on-site facies interpretation (cf. Ernst, 1970; Vött, Handl, & Brückner, 2002, 2004; Brückner et al., 2006; Engel et al., 2009; Niwa et al., 2011; Kelterbaum et al., 2012). Samples were air-dried, ground with mortar and pestle and sieved to separate the $\leq 2 \text{ mm}$ grain size fraction for further analyses. OM was decomposed via treatment with hydrogen peroxide, followed by laser-based grain size analysis with a Beckman Coulter LS13320 instrument. The calculation of grain-size parameters after Folk and Ward (1957) utilised the GRADISTAT software (Blott & Pye 2001).

Geochemical analyses included the weight LOI. Oven-dried (105°C for 12 h) samples were combusted in a furnace at 550°C for 4 h. Electric conductivity was determined in an aqueous slurry consisting of 15 g sediment in 75 mL deionised water with a glass electrode connected to a Mettler Toledo InLab[®]731–2m instrument. The concentrations of 30 elements were measured with a portable XRF spectrometer (Niton XL3t 900 GOLDD; Vött et al., 2011). Sodium (Na) could not be quantified by XRF and was determined via atomic absorption spectrometry (Perkin Elmer A-Analyst 300).

Geochronological Techniques

^{14}C accelerator mass spectrometric (AMS) age determinations based on wood and charcoal were performed at the Center for Applied Isotope Studies (CAIS) of the University of Georgia, USA and at the ^{14}C Chrono Centre for Climate, the Environment, and Chronology at the Queen's University Belfast, UK. All ^{14}C -dated materials

Table I Radiocarbon data set. AMS-¹⁴C measurements were carried out at the Center for Applied Isotope Studies (CAIS) of the University of Georgia at Athens, USA (labcode: UGAMS) and ¹⁴Chrono Centre for Climate, The Environment, and Chronology at the Queen's University Belfast, UK (labcode: UB). For calibration the Calib 7.0 software was used (Reimer et al., 2013).

Sample	Labcode	Depth (bsf)	Material	$\delta^{13}\text{C}$ (‰)	Libby-age (a)	cal A.D. (1 σ)	cal A.D. (2 σ)
ELA 41/5H	UGAMS 8216	1.27 m	Wood	-27.2	1780 ± 20	228–322 cal A.D.	142–332 cal A.D.
ELA 41/6H	UGAMS 8217	1.40 m	Wood	-29.5	1900 ± 25	77–126 cal A.D.	32–209 cal A.D.
ELA 41/12H	UGAMS 8219	4.50 m	Wood	-24.2	1750 ± 25	248–330 cal A.D.	232–379 cal A.D.
ELA 73/1H	UBA-22412	0.33 m	Wood	-23.4	1120 ± 37	891–974 cal A.D.	777–1013 cal A.D.
ELA 73/8H	UBA-22415	1.22 m	Charcoal	-28.5	1699 ± 29	264–391 cal A.D.	254–407 cal A.D.

bsf, below see floor.

were of terrestrial origin with relatively negative $\delta^{13}\text{C}_{\text{VPDB}}$ (‰) values (cf. Table I), wherefore a marine reservoir correction is not needed (McCormac et al., 1994). All ages were calibrated with IntCal calibration curves using Calib 7.0 software (Reimer et al., 2013) and are presented in calendar years A.D. with a 2 σ range (i.e., 95.4% probability, Table I).

OSL measurements include determinations of burial doses and dose rates. The latter were estimated based on the uranium (U), thorium (Th) and potassium (K) contents in the surrounding material within a ca. 30 cm radius. U, Th and K were determined via high-resolution gamma spectrometry. The *in situ* concentrations of pore water and OM (determined by LOI) were considered for dose rate attenuation. The cosmic dose rate contribution was estimated based on geographic position, altitude above sea level, and burial depth (Prescott & Hutton, 1994). Handling and burial dose measurements of samples were performed under dimmed red light. Pre-processing included wet sieving to separate grain-size fractions of 40–63 μm , as well as chemical pre-treatment with hydrochloric acid, hydrogen peroxide and sodium oxalate to remove carbonates, OM and clay. Quartz grains were selectively preserved via etching in concentrated hexafluoro silicic acid (H_2SiF_6). Equivalent dose (D_e) measurements on a Risø TL/OSL device with a ⁹⁰Sr/⁹⁰Y beta radiation source, stimulation by blue LEDs (40 s) and

signal detection through a Hoya U340 filter (7.5 mm) followed the SAR protocol of Murray and Wintle (2003). Small aliquots of 1 or 2 mm were measured for all samples with D_e -values between 40 and 70, using an empirically selected preheating temperature of 200°C. The calculation of burial doses was based on aliquots of samples that passed SAR acceptance criteria in terms of (i) a recycling ratio from 0.85 to 1.15, (ii) <5% recuperation of D_e , (iii) a depletion ratio of 0.9 to 1.1, and (iv) a signal-to-noise ratio above 3. Depending on the degree of signal resetting, the central age model (CAM) or the minimum age model (MAM) of Galbraith et al. (1999) were applied, using empirical σ_b -values for young coastal sediments of 15% in case of MAM (e.g., Arnold & Roberts, 2009; Brill et al., 2012). All ages were calculated with ADELE software and reflect a 1 σ error (68.3%; Kulig, 2005; Table II).

RESULTS AND INTERPRETATION

Core Stratigraphies

The sedimentary context of Elaia's underwater structures was constrained by three sediment cores. Cores ELA 73 and ELA 74 were drilled directly on the archaeological structures (i.e., walls 2 and 3) between adjacent blocks, whereas core ELA 41 represents the sediment adjacent to wall 1 (Figure 2B).

Table II Luminescence data. depth b.s., sampling depth below surface; W, *in situ* water content; U, uranium; Th, thorium; K, potassium; d. rate, dose rate; \emptyset , aliquot size; $N_{\text{a/m}}$, number of accepted/measured aliquots; OD, over-dispersion; Sk, skewness; D_e (mean), burial dose, ^a calculated with CAM, ^b calculated with MAM. The OSL measurements were carried out in the Cologne Luminescence Lab (CLL).

Location		Dosimetry						Dose						
Sample	Labcode	Depth b.s. [m]	W [%]	U [ppm]	Th [ppm]	K [%]	d. rate [Gy/ka]	\emptyset [mm]	$N_{\text{a/m}}$	OD [%]	Sk	D_e (mean) [Gy]	Age [years]	Age [B.C./A.D.]
ELA 74/1	CL-3160	0.22	63	2.6 ± 0.1	12.7 ± 0.7	2.0 ± 0.1	2.3 ± 0.1	1	34/68	32.9	1.9	3.68 ± 0.22	1575 ± 133 ^b	A.D. 307–578
								2	57/68	24.5	0.6	3.97 ± 0.24	1696 ± 145 ^a	
ELA 74/2	CL-3161	0.69	51	3.3 ± 0.2	13.7 ± 0.8	2.1 ± 0.1	2.7 ± 0.1	1	34/42	13.5	0.1	6.60 ± 0.18	2406 ± 164 ^a	558–230 B.C.
ELA 73/1	CL-3156	0.43	45	4.4 ± 0.2	13.6 ± 0.8	2.1 ± 0.1	3.0 ± 0.3	2	33/44	30.9	0.4	5.81 ± 0.47	1944 ± 220 ^b	147 B.C.–A.D. 283
ELA 73/2	CL-3157	0.82	41	3.7 ± 0.2	14.7 ± 0.9	2.2 ± 0.1	3.1 ± 0.3	2	41/56	24.6	1.2	6.19 ± 0.63	1984 ± 240 ^b	213 B.C.–A.D. 270
ELA 73/3	CL-3158	1.42	51	3.0 ± 0.2	14.3 ± 0.9	2.2 ± 0.1	2.7 ± 0.2	1	43/72	36.6	1.2	4.79 ± 0.23	1770 ± 140 ^b	363 B.C.–A.D. 77
								2	37/48	21.7	1.4	4.63 ± 0.08	1712 ± 111 ^b	

Sediment Core ELA 41

Core ELA 41 (Figures 2B and 4B) was drilled adjacent to the northernmost edge of the first underwater wall (27°02'19.04" E, 38°56'35.34" N, 0.60 m below present mean sea level, bsl) and reached a depth of 5.00 m below sea floor (bsf).

Homogeneous dark grey sand between 5.00 and 1.60 m bsf form unit 1a, with loamy silt being intercalated from 4.75 to 4.66 m bsf (Figure 4A). The Fe/Na and Na/K elemental ratios as well as LOI values express only minor fluctuations, while the electric conductivity tends to decrease upwards from 15.36 mS/cm at 4.57 m bsf to 5.87 mS/cm at 1.85 m bsf. Fragments of seagrass (*Posidonia oceanica*), wood and charcoal were encountered throughout the section. Dark greenish grey clayey silts represent unit 1b above 1.60 m bsf, with the exception of intercalating brown silty clay at 1.12 to 0.49 m bsf. (unit 2). This special clayey layer is missing in all other sediment cores described in this paper. In spite of the finer grain size at more shallow depth, the electric conductivity drops to a minimum value of 3.91 mS/cm. In addition, the sodium concentration decreases to negligible values resulting in low Na/K and high Fe/Na ratios. The finding of terrestrial plant remains, oxidation spots and lime precipitations hint to a palaeosol formation under subaerial conditions.

The cumulative sedimentological, geochemical and geophysical evidence from core ELA 41 infers deposition in a shallow marine environment for units 1a and 1b, which were interrupted temporarily by semi-terrestrial deposition (unit 2) when dry conditions exposed the accumulating sediment to terrestrial weathering and oxidation.

Sediment Core ELA 73

In contrast to ELA 41, sediment core ELA 73 (Figures 2B and 4B) was drilled through the central debris of underwater wall 2 (27°02'08.49" E, 38°56'06.81" N, 0.95 m bsl) reaching a depth of 2 m bsf. The basal section between 2.00 m and 1.73 m bsf is homogeneous grey sand (unit 1a) that is coarser (mean grain size 386 μm), better sorted (2.60) and has lower values of LOI (2.16%) and electric conductivity (3.95 mS/cm) compared to the rest of the profile. Silty sand between 1.75 and 1.80 m bsf indicates a depositional environment with temporarily reduced wave energy.

The section between 1.73 m and 0.51 m bsf consists of grey loamy silt with uniform geochemical and grain size characteristics that are comparable to those of the underlying stratum. Seagrass (*P. oceanica*) and mostly fragmented marine gastropods occur sporadically. From 0.51

to 0.16 m bsf the silty sediment includes abundant angular stones (unit 3). In contrast to the underlying sediment, almost all parameters trend towards the characteristics of modern sedimentation.

The profile of core ELA 73 indicates sedimentation under shallow marine conditions during deposition of units 1a and 1b. In contrast to core ELA 41, the shallow marine deposition in core ELA 73 was not interrupted by semi-terrestrial conditions, which may be due to the greater distance of ELA 73 from the shoreline. Instead, the blocks of the underwater structure (unit 3) were placed directly into shallow water strata.

Sediment Core ELA 74

Core ELA 74 (Figures 2B and 4C) was drilled through the central debris of underwater wall 3 (27°02'03.52" E, 38°56'02.15" N, 0.81 m bsl) and reached a depth of 1.00 m bsf. The entire profile consists of grey loamy silt expressing upward trends of decreasing Ca/K and Ca/Fe ratios that suggest a declining marine influence. Except for a thin silty sand layer at 0.35–0.38 m bsf, the grain size data show little variation. Similar to cores ELA 41 and ELA 73, the lower part of core ELA 74 includes occasional seagrass and marine gastropods. The blocks of underwater wall 3 extend from 0.35 m bsf to the seafloor (unit 3).

The profile of core ELA 74 suggests a similar scenario of sedimentation like core ELA 73. A persistent shallow marine environment seems to have extended to the time period when the blocks of underwater wall 3 (unit 3) were placed directly into the water.

Geoelectric Cross-Sections

The vertical and horizontal extent of buried parts of the underwater structures was investigated by cross-sections of electric resistivity data that ran perpendicular to the wall structures. A similar application has been successful for reconstructing the shape and penetration depth of the breakwater in Elaia's western harbour (Seeliger et al., 2013).

Geoelectric Cross-Section of the Western Harbour's Breakwater

A 46-m-long geoelectric cross-section was measured on top of the western breakwater of the closed harbour basin (cross-section A in Figures 2A and 5A). Using this field data a resistivity to depth distribution down to a depth of approx. 5 m bsf was inverted. The boulders of the breakwater are located in the central position of the profile. The calculated electrical resistivity has a bandwidth of less than 0.1–2 Ωm . Low resistivity of $\leq 0.3 \Omega\text{m}$ at the outer

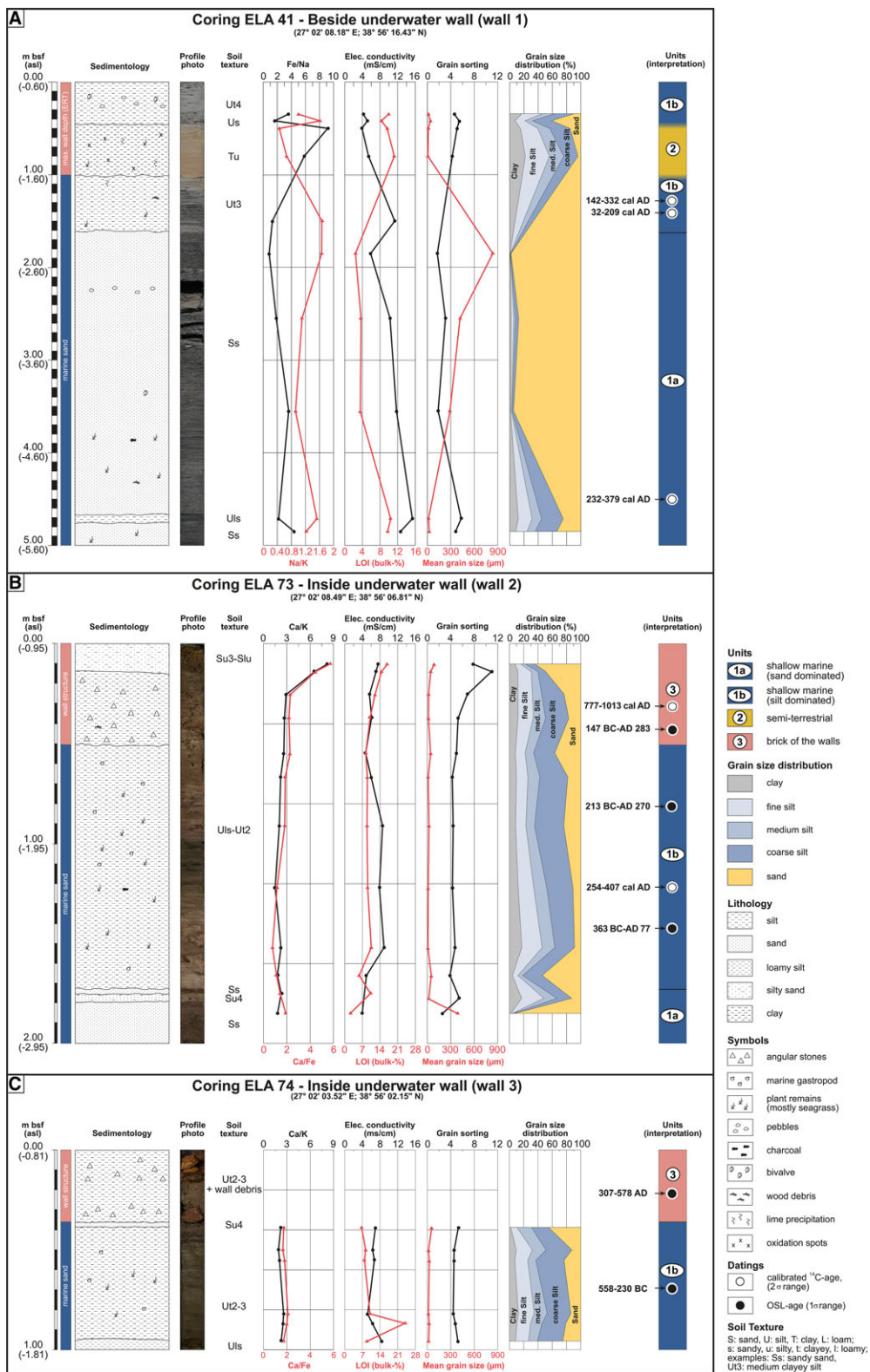


Figure 4 Stratigraphical record, facies distribution and chronological classification of cores ELA 41 (A), ELA 73 (B), and ELA 74 (C). For location of the sediment cores see Figures 2A, B.

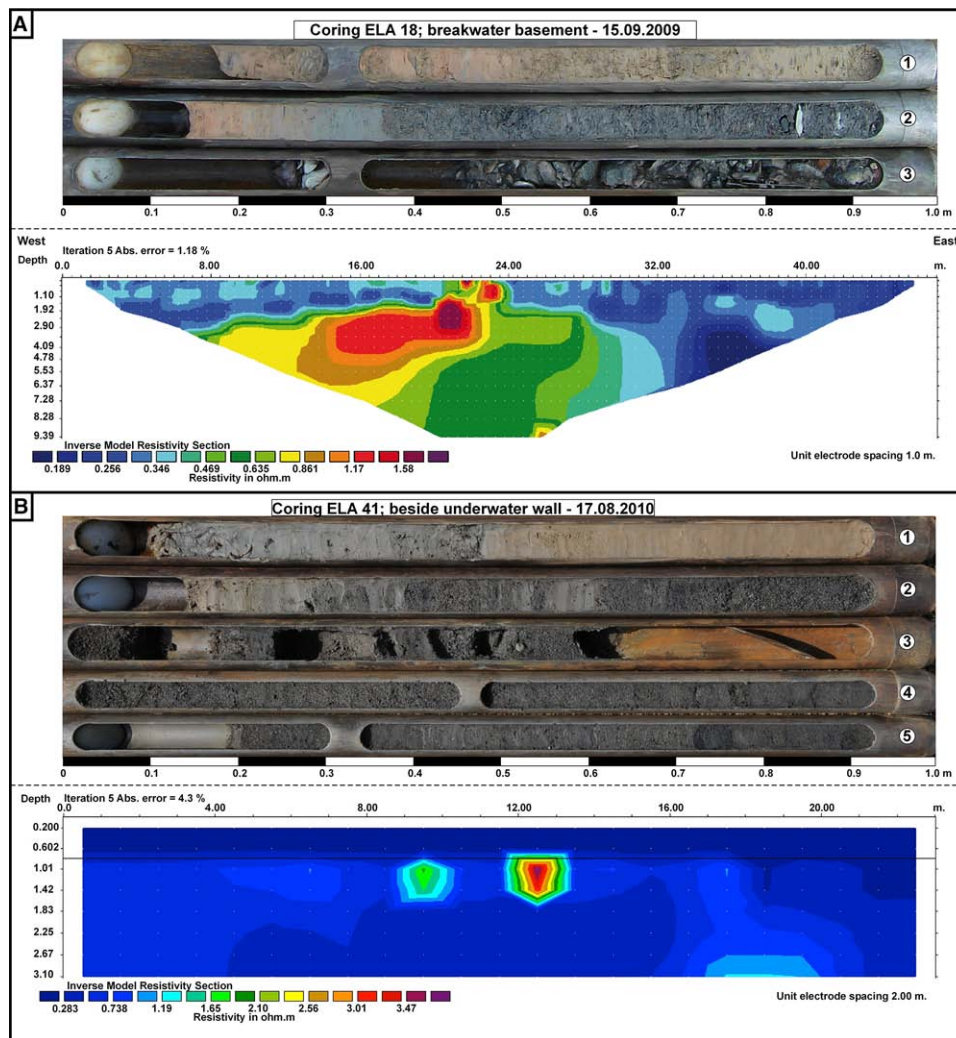


Figure 5 Earth resistivity transects for cross-sections A and B, and coring profiles of ELA 18 and 41 (for location see Figures 2A, B; Seeliger et al., 2013). The simplified inverse model section of earth resistivity measurements that were carried out by Klein and Erkul in 2010. While A shows the massive construction of the Hellenistic breakwater which even stopped the coring process at a depth of 3 m, B shows that the wall structures have no solid foundation at all; coring between two blocks only penetrated fine-grained sediments.

parts of the cross-section near the surface contrasts with highest resistivity of $\geq 2 \Omega\text{m}$ in the centre along a zone of nearly 8 m lateral and 2 m vertical extension between approx. 2 and 4 m bsf. The measured resistivity values are low compared with measurements on land because much of the electrical conductivity in marine environments is caused by dissolved salts.

Geoelectric Cross-Section of Underwater Wall 2

As a representative example for several measured profiles of underwater structures, Figure 5B illustrates a 23 m long geoelectric cross-section along the top of underwater wall 2 (cross-section B in Figure 2B). The cal-

culated electrical resistivity reflects a bandwidth between 0.3 and $3.5 \Omega\text{m}$ down to a depth of approx. 2 m bsf. The wall structure is located in the central position of the cross-section about 0.8 m below the present sea surface and features the highest resistivity $\geq 3.5 \Omega\text{m}$. The electrical resistivity decreases concentrically from the centre to the periphery down to $\leq 1.6 \Omega\text{m}$. A dislocated small boulder is discernible to the left of the centre. The width and depth of the structures stretch no more than 1 m.

Geochronology

Samples for dating were taken (i) from sediment below wall structures to establish an upper age limit of

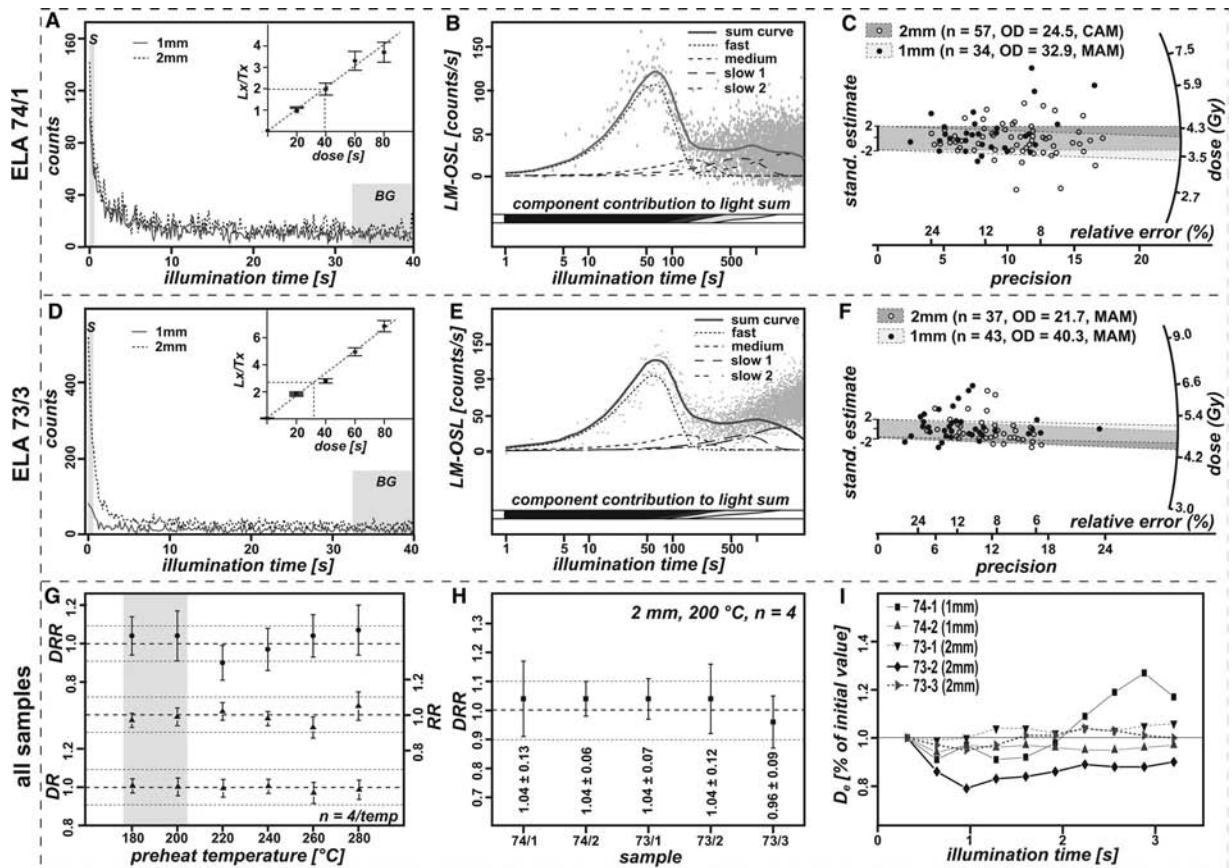


Figure 6 Luminescence properties. For cores ELA 74 and ELA 73 representative shine-down- and growth curves (A and D), LM-OSL curves (B and E) and equivalent dose distributions of 1 mm and 2 mm aliquots (C and F) are shown. While a combined dose-recovery-preheat-plateau test is shown for ELA 74/1 only (G), dose recovery tests with 200°C (H) and $D_e(t)$ plots (I) are documented for all samples. S, signal interval; BG, background interval; OD, over-dispersion; DRR, dose recovery ratio; RR, recycling ratio; DR, depletion ratio.

construction, and (ii) from within building layers to attempt a direct dating of the construction. Two marine sediment samples in unit 1 of core ELA 41, directly below the semi-terrestrial stratum (unit 2), were radiocarbon-dated (ELA 41/5H and ELA 41/6H, see Table I). Another ^{14}C date from the same core (ELA 41/12H) chronostratigraphically constrains the bottom of the profile (unit 1; Figure 4A). Core ELA 73 features two radiocarbon ages and three luminescence ages (Figure 4B). OSL sample ELA 73/1OSL and ^{14}C sample ELA 73/1H provide direct age estimates for the wall structure (unit 3), whereas OSL samples ELA 73/2OSL and ELA 73/3OSL, as well as ^{14}C sample ELA 73/8H were taken from the underlying marine unit 1. Core ELA 74 provided one luminescence sample (ELA 74/1OSL) from between the blocks of the wall (unit 3) and another one (ELA 74/2OSL) from marine sediment directly below the basement of the wall (unit 1; Figure 4C).

Luminescence Properties

Quartz grains in cores ELA 73 and ELA 74 generally show weak luminescence signals of no more than 100–500 counts (Figure 6). Although the low background of 10–30 counts still allows for D_e determination even for small 1 or 2 mm aliquots, individual measurements are afflicted by relatively large uncertainty. However, in spite of low sensitivity of quartz grains, linear modulated luminescence (LM-OSL) of samples in cores ELA 73 and ELA 74 proved the existence of a dominating fast component with a photoionisation cross-section of $\sim 1.15\text{--}1.19 \times 10^{-17} \text{ cm}^2$ that is comparable to common empirical values (e.g., Singarayer & Bailey, 2003). More or less constant luminescence signals with increasing illumination time in $D_e(t)$ plots indicate that the fast component is thermally stable (e.g., Bailey, 2003) and may be used for equivalent dose determination.

Dose recovery tests performed on all samples yield ratios of measured dose versus laboratory dose of 0.96 ± 0.09 to 1.04 ± 0.13 ($n = 4$) and hence indicate that the applied SAR protocol for luminescence dating of quartz from both cores is appropriate. Although signal recovery was not significantly influenced by the temperature of preheating, combined tests of dose-recovery and preheating plateau revealed that performance of the SAR protocol is best for low preheating temperatures, in accordance with other studies on young marine sediments (e.g., Kiyak & Canel, 2006; Brill et al., 2012). A preheating temperature of 200°C was adopted for all routine measurements.

In case of core ELA 74, aliquots of 1 mm were favoured over 2 mm aliquots for D_e determination, since smaller aliquots are more appropriate to detect partial bleaching (Duller, 2008). Weaker signals in core ELA 73 from 1 mm aliquots with unacceptably large errors and high rejection rates prompted the use of 2 mm aliquots for D_e determination. Generally, two types of D_e distributions were observed: (i) Samples ELA 74/1OSL, 73/1OSL, 73/2OSL and 73/3OSL yielded significantly positively skewed (1.2 to 1.9) and over-dispersed ($OD = 21.7$ to 32.9) D_e distributions, as well as significantly higher D_e values and lower scatter for 2 mm aliquots compared to 1 mm aliquots (e.g., for ELA 74/1OSL), and point to incompletely bleached signals during deposition, prompting the use of MAM. (ii) Sample ELA 74/2OSL revealed normally distributed (skewness = 0.1) D_e values with low over-dispersion ($OD = 13.5$), indicating complete resetting of the luminescence signal and allowing for the use of CAM for calculating the burial dose.

Chronostratigraphy

A radiocarbon-dated fragment of wood at 4.50 m bsf in sediment core ELA 41 (Figure 4A) yielded an age of 232 to 379 cal A.D. for the base of the marine deposits (unit 1) reached in this core. Since core ELA 41 was drilled adjacent to underwater wall 1 (Figure 2B), the core lacks direct evidence of the wall structures (unit 3), such as bricks or stone fragments. However, considering the results of the geoelectric cross-section along profile B (Figure 5B), the underwater structures do not penetrate the sediment to depths of more than 1 m. Thus, the brown silty clay of unit 2 seems to be related to the construction of the walls. The two ^{14}C -dated fragments of wood from the top of unit 1 at 1.27 m bsf (sample ELA 41/5H) and at 1.40 m bsf (sample ELA 41/6H), that is, immediately below unit 2, are indicating a maximum age estimate for the underwater structures. Sample ELA 41/6H yielded an age of 32 to 209 cal A.D., whereas

sample ELA 41/5H dates from 142 to 332 cal A.D. (Table I).

Core ELA 73 (Figure 4B) is chronologically constrained by five ages (Tables I, II). Marine sediments of unit 1 have been dated by two luminescence samples at 1.42 m bsf (sample ELA 73/3OSL) and 0.82 m bsf (sample ELA 73/2OSL) and by a radiocarbon-dated piece of charcoal at 1.22 m bsf (sample ELA 73/8H). The three dates yield maximum ages for the underwater structure of 363 B.C. to 77 A.D., 213 B.C. to 270 A.D., and 254–407 cal A.D., respectively. Direct age information for the emplacement of the wall structures is provided by a third OSL sample at 0.43 m bsf (sample ELA 73/1OSL) with an age of 147 B.C. to 283 A.D., and by a fragment of ^{14}C -dated wood at 0.33 m bsf (sample ELA 73/1H) implying an age of 777 to 1013 cal A.D.

The underwater structure documented in sediment core ELA 74 (Figure 4C) is chronologically constrained by two luminescence ages. A first OSL sample from the marine deposits at 0.69 m bsf (unit 1b) yields a maximum limiting age of 558–230 B.C. (sample ELA 74/2OSL), and a second luminescence date (sample ELA 74/1OSL) from 0.22 m bsf (unit 2) provides a direct age of 307–578 A.D. for underwater structure 3 (Table II).

DISCUSSION

Time of Construction

Geochronological results from core ELA 41 and geoelectric profile B (Figures 2B and 5B) suggest the construction of the walls to have occurred shortly after 142–332 cal A.D. (Figure 7) during the Roman Imperial to the Late Antique period or later. The lowermost ^{14}C age of 232–379 cal A.D. (sample ELA 41/12H) is somewhat confusing. Acceptance of all three ^{14}C ages would mandate rapid sedimentation during the 3rd and 4th century A.D., which could be explained by increased sediment load of the Kaikos (Bakır Çay) due to intensified farming in its catchment area (Pirson, 2009, 2010). Unfortunately, no research concerning the late Holocene evolution of the delta has been carried out to date.

The interpretation of core ELA 74 (Figures 2B and 7) leads to similar results, indicating that the walls could have been built in the Late Antique period. According to the OSL age of sample ELA 74/1OSL, the sediment between the blocks of the walls (unit 3) was deposited between A.D. 307 and A.D. 578 (Figure 7). Thus, the erection of the walls during the Late Antique period seems to be most likely. With an age of 558–230 B.C. (sample ELA 74/2OSL), the depositional age of the shallow marine sediments immediately below the wall structure (unit 1) is in agreement with the assumed age of the

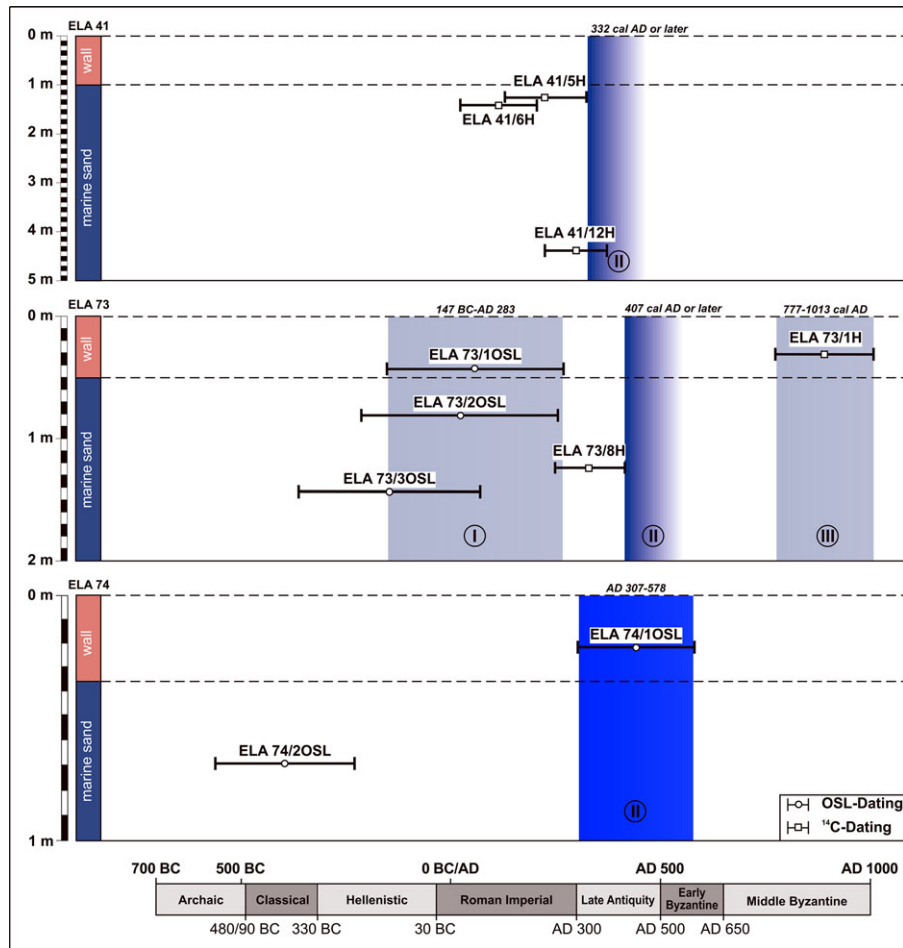


Figure 7 Synoptic chronostratigraphy of cores ELA 41, 73 and 74 (based on all measured OSL- and ¹⁴C-ages) with age estimates for the time of wall construction (shaded areas). Probability II is drawn in dark blue cause it is the most likely time for the erection. Full colour shading was used for ages gained out of the wall section whereas shaded colours were used for limiting ages gained out of the marine substratum. Note that a re-use of parts of the installation is also a possible explanation for the age scatter.

structure and with results from other cores in the Bay of Elaia (Seeliger et al., 2013). Core ELA 74 features a more moderate sedimentation rate to the higher sedimentation rate of core ELA 41. It is likely that the sedimentation rate at the site of core ELA 74 was significantly less affected by the prograding Bakır Çay delta (Figures 1A and 2B).

In contrast to the similar interpretations of ages of the underwater walls based on cores ELA 41 and ELA 74, the interpretation of core ELA 73 (Figures 2B and 7) is more complicated. Although all three luminescence ages are in stratigraphically correct order, they are in conflict with the radiocarbon ages from the same profile, as well as with the chronostratigraphies of cores ELA 41 and ELA 74 (Figure 7). Three different interpretations are possible if only information from core ELA 73 is taken into account (Figure 7):

- (i) If the luminescence ages are correct, the date of 147 B.C. to A.D. 283 from the lower part of unit 3 (sample ELA 73/1OSL), as well as the limiting ages of 363 B.C. to A.D. 270 from unit 1 (samples ELA 73/2OSL and ELA 73/3OSL) point to wall construction in Hellenistic to Roman Imperial times.
- (ii) Acceptance of the lowermost ¹⁴C age (sample ELA 73/8H) makes the wall structure younger than 254–407 cal A.D. The origin of the ¹⁴C sample from nearly the same depth (1.22 m bsf) as samples ELA 41/5H (1.27 m bsf) and ELA 41/6H (1.40 m bsf) provides ages completely in agreement with the chronology of this core.
- (iii) Acceptance of the uppermost ¹⁴C age from within unit 3 (sample ELA 73/1H) dates the construction of wall 2 to A.D. 777–1013 A.D., that is, the Middle Byzantine

times. However, this is significantly younger than postulated on the basis of cores ELA 41 and ELA 74, and relocation of the dated fragment of wood by wave action or during the coring process cannot be excluded.

Considering the fact that cores ELA 41 and ELA 74 are both pointing to a construction of the walls within the 4th to 6th centuries A.D., we consider the second interpretation to be the most likely one. The slightly older construction date of 147 B.C. to A.D. 283 proposed by the first interpretation might be influenced by inadequate assessment of partial bleaching due to insensitive samples and their weak luminescence signals. The third interpretation can be excluded if we assume relocation of the dated plant material. However, it is also possible that the wall structures 1 to 3 are not strictly contemporaneous, and that the underwater wall 2 is slightly older than structures 1 and 3. Nevertheless, the preponderance of the combined information and geochronological data of all three cores indicate a construction of the walls between the 4th and 6th centuries A.D. (Figure 7).

The Purpose of Elaia's Underwater Walls

What was the function of the underwater structures?

Most harbour infrastructures, such as shipyards or breakwaters, rely on a solid foundation to withstand heavy wave action during storms. The foundation of shipyards needs to support the weight of additional installations and ships. The closed harbour's western breakwater is an example of solidly constructed marine installations built in Hellenistic times (Figure 5A; Seeliger et al., 2013). The 8 m wide and 2 m thick foundation of the breakwater is clearly visible in geoelectric cross-section A as indicated by high values of electric resistivity (red colours in Figure 5A). The foundation is gently sloping towards the sea, whereas its harbour side shows a sharp edge with a precipitous drop to facilitate the mooring of ships (Figure 5A). The anthropogenic character of the breakwater's foundation was confirmed by sediment core ELA 18 (Figure 5A; Seeliger et al., 2013) featuring mainly rounded and angular stones, ceramics, remains of *P. oceanica* and shell debris. Based on fragments of pottery and ceramics, the structure was dated to the Hellenistic to Roman era (Seeliger et al., 2013). Massive boulders stopped the coring progress at a depth of 3 m.

In contrast to the above mentioned, the geoelectric profile B (Figure 5B) shows that Elaia's underwater wall structures are far smaller in size and are limited to approximately 1 m depth and 1 m width (Figures 2B and 5B; note the different scales of the depths axis). The lack of any extended foundation was documented by core

ELA 41 (Figure 4A, 5A) and by nine sediment cores that explored the sedimentary context of the underwater structures (Figure 2B). Furthermore, the absence of dowels to fixate and link adjacent blocks indicates that the walls are lacking robust construction. We conclude that a utilisation as harbour infrastructures, shipyards, breakwaters or other solid structures can be excluded. An interpretation as *piscinae*—artificial fish ponds—is also improbable as those installations are by far smaller, of another layout and a different building technique than the wall structures in the Bay of Elaia (Higginbotham, 1997; Grüner, 2006; Evelpidou et al., 2012; Morhange et al., 2013). Plus, considering the palaeo-ecologic setting, anoxic conditions with the emission of hydrogen sulphide (H₂S) would have endangered fish farming.

Instead, similar walls have been found at several other places along the shores of the Mediterranean for compartmentalisation of evaporative ponds within marine salt works (Figure 2B). The construction design has changed little from Antiquity to modern times (Traina, 1992; Thonemann, 2011; Asencio, 2013). Additionally, the contemporaneous occurrence of semi-terrestrial conditions (unit 2 in core ELA 41; Figure 4A) in parts of the bay fits well with the assumption of salt works that would have worked only in shallow water conditions. Salt works in a shallow marine area rely on ponds that can be intermittently flooded with sea water, followed by pond closure, evaporation of sea water and harvesting of sea salt. It is known that sediments of former brines or salt pits are characterised by a higher level of calcium and magnesium compared to adjacent natural soil (Flad et al., 2005). Most probably due to leaching caused by constant water coverage over the last centuries this was not preserved in the sediments of the salt works of Elaia.

In the Bay of Elaia the former, typically rectangular wall structures of ancient salt works have mostly disappeared probably due to intentional clearing, demolition or recycling of building blocks and/or due to the weathering and destruction by wave action after the desertion of the site. Today's drowned position of the structures is incompatible with functional salt works, but can be explained by relative sea level rise or the impact of subsidence caused by eustatic, tectonic and geomorphological factors in this earthquake-prone area (Vött, 2007). At Elaia, the relative sea level has risen by approximately 1.67 m since the construction of the closed harbour's breakwater in Early Hellenistic times (Seeliger et al., 2013). Moreover, it may be assumed that the blocks have sunken into the soft substratum beneath them, especially during strong seismic events which can cause liquefaction of underlying, water-logged and unconsolidated sediment (Figure 3). Since most of the walls were demolished by human impact or partly destroyed by wave action

their functional height cannot be reconstructed precisely; thus, it is impossible to use the walls as reliable sea level markers.

Does the historical background support the assumption of salt works in Elaia?

Dietary salt intake is essential for humans, especially in the warm Mediterranean climate. Salt is also needed for the well-being of livestock. Pre-modern societies frequently relied on salt for the preservation of food such as meat, cheese and fish. Literary sources of the Greek and Roman periods testify to the widespread use of salt (Blümner, 1920; Moinier, 2011). Up to the 19th century, the production of salt was limited to sea salt, mining, salt lakes and saline springs. Salt from the sea was best extracted in shallow coastal areas with hot climatic conditions. Although the climate in the Mediterranean is ideal for much of the year, there are only few favourable locations for the production of sea salt along its shorelines (Giovannini, 2000; Di Rita, Celant, & Magri, 2010). The shallow Bay of Elaia with its small tidal range of approximately 20 cm (Seeliger et al., 2013) was eminently suitable for the production of sea salt.

In the beginning of the 5th century A.D. the Roman magistrate Rutilius Namatianus describes *salinae* at Vada Volaterrana along the Etruscan coast of northern Italy (Rutilius Namatianus, *De reditu suo*, 470–475). Similar to the Bay of Elaia, the maritime topography of this Etruscan town is characterised by an alluvial plain deposited by two rivers. Vada Volaterrana's salt works were located near a salt marsh and represented a system of numerous canals and ponds that seems to resemble the layout of the almost contemporary salt works in the Bay of Elaia. The latter were probably built soon after the rapid aggradation of parts of the bay between the 3rd and 4th century A.D. replacing the newly evolved salt marshes. The salt works' construction was straight forward and economical with parallel rows of re-used ashlar and a fill of smaller stones in between, obviating the need for any foundation or substructure.

In Late Antiquity and Early Byzantine times of the 5th and 6th centuries the usage of the salt works in the Elaia region may have declined. In those days the population of Elaia shrank dramatically and most of the former farmland lay fallow. Elaia and its salt works were eventually abandoned and the Elaiaians seem to have founded a more secure settlement further inland in the area nowadays called Püsküllü Tepeler. The new settlement was separated from the sea by the foothills of the Bozyertepe, a mountain ridge that separates the Bay of Elaia from the Kaikos delta area (Pirson, 2010).

After having lain fallow for several centuries, the salt works seem to have been revived in the Late Byzantine period of the 13th century, as witnessed by a rectangular building approx. 40 m long and 20 m wide that was located on the western foothills of the Bozyertepe, at a short distance to the north-west of the Bay of Elaia (Pirson, 2009). The building is oriented towards the sea, and the approx. 1.4 km distance to the salt works could be covered easily by crossing the salt marsh (Pirson, 2009). Written sources of the 13th century describe similar salt works in the estuary region of the Büyük Menderes River near ancient Miletus that were in possession of the monastery of the island of Patmos (Thonemann, 2011).

Nothing is known from literature about the possible use of the salt works in Elaia during the subsequent Ottoman period. Production of salt in the Bay of Elaia was reported in the early 19th century by Prokesch von Osten (1837) while travelling from Pergamum to Smyrna (modern: Izmir). He observed salt works and piles of salt in the marshland area in the vicinity of the ancient city. In addition, expansive salt works are operating in the region today, for example in the coastal zone of Ayvalık north of Kaikos area (Seeliger, Bartz, & Brückner, 2012).

CONCLUSIONS

The area of the later underwater walls had been part of a shallow marine embayment when Elaia was prospering under the rule of the Pergamenians in Hellenistic and early Roman Imperial times. The water depth must have been sufficient for typical Hellenistic and later Roman ships—most maritime vessels did not require water depths in excess of 1.60 m—to reach the harbour of ancient Elaia (Coates, 1987; Beltrame & Gaddi, 2007; Marriner & Morhange, 2007; Auriemma & Solinas, 2009; Boetto, 2010; Seeliger et al., 2013). Increasing settlement activities in the hinterland seems to have caused progradation of the Bakır Çay delta and began filling the Bay of Elaia with sediment from a westerly direction since the turn of the eras. As a result, water depth decreased and a salt marsh developed (Brückner, Knipping, & Seeliger, 2010; Pirson, 2010; Seeliger, Bartz, & Brückner, 2012). Although this development was a disadvantage for shipping and trade, it offered an opportunity for the production of economically valuable sea salt.

Therefore, the underwater wall structures detected in the Bay of Elaia are best interpreted as the remains of salt works. Detailed geophysical and geoarchaeological surveys proved them to consist of blocks with a width and depth of maximally 1 m each. The walls cannot have functioned as breakwaters, piers, wharfs or any other kind of durable construction that would have needed

to occasionally resist rough wave action during storms. The construction design, building technique, size and the palaeo-ecologic setting exclude a usage as fish tanks.

According to ^{14}C and OSL age estimates and in agreement with archaeological data, the walls were installed between the 4th and 6th centuries A.D. Blocks from demolished city buildings were recycled and emplaced into the salt marsh in the south-west of the bay to construct architecturally simple walls without foundation. The walls delineated and compartmentalised evaporation ponds as part of salt works. In Early Byzantine times the city of Elaia declined and was eventually abandoned, most probably because (i) the harbour's functionality became too limited, and (ii) a more secure settlement was established further inland.

Within the uncertainty of applied geochronological dating methods of this study, it is possible that not all of the wall structures have been built simultaneously. A later (re-)use and maintenance of some parts of salt works is probable as well. The eventual drowning of the walls, which makes them useless for salt works, can be attributed to eustatic sea level rise during the last ca. 1500 years, to tectonic subsidence, and to partial sinking of heavy building blocks into unconsolidated sediment when severe earthquakes may have caused sediment liquefaction.

Summing up, salt production in the region of ancient Elaia can be stated for the time soon after A.D. 300 up to the 5th or 6th centuries A.D., as well as for the 19th century A.D. The salt-works of the Late Antique period supplied Elaia, its immediate surroundings as well as the city of Pergamum with salt. There are hints given that the salt production was also in use during Late Byzantine times.

This research was conducted under the umbrella of the German Research Foundation (DFG) priority program (SPP) 1209 "The Hellenistic Polis as a Living Space – Urban Structures and Civic Identity Between Tradition and Innovation" (2008–2012). Financial support is gratefully acknowledged (DFG ref. no. PI 740/1-3). This work was part of the Elaia Survey headed by Felix Pirson, Director of the German Archaeological Institute (DAI), İstanbul Department, and excavation director in Pergamum. The investigations would not have been possible without the support and hospitality of the Pergamum excavation team. The discovery and survey of the underwater wall structures benefited from the help of Yüksel Afşin from Zeytindağ-Kazıkbağları (Turkey). Anja Zander and Nicole Klasen (both Institute of Geography, University of Cologne) helped to carry out the OSL measurements in the Cologne Luminescence Lab (CLL). Harald Stümpel (Institute of Geoscience, University of Kiel) assisted in the interpretation of geophysical data. The Geoserve company provided the electrical resistivity instrument RESECS with underwater components. The Ministry of Culture and Tourism of the Republic of Turkey

kindly granted research permits. We also thank four anonymous referees for their helpful comments on an earlier version of this paper. Finally, we thank Arndt Schimmelmann (Department of Geological Sciences, Indiana University at Bloomington, USA) and Christine Seeliger (European Bioinformatics Institute, University of Cambridge, UK) for improving the manuscript language.

REFERENCES

- A.G. Boden, Ed. (2005). *Bodenkundliche Kartieranleitung*. Stuttgart: Schweizerbart.
- Algan, O., Namık Yalçın, M., Özdoğan, M., Yılmaz, Y., Sarı, E., Kırıcı-Elmas, E., Yılmaz, I., Bulkan, Ö., Ongan, D., Gazioğlu, C., Nazik, A., Polat, M.A., & Meriç, E. (2011). Holocene coastal change in the ancient harbor of Yenikapı-İstanbul and its impact on cultural history. *Quaternary Research*, 76(1), 30–45.
- Aksu, A.E., Piper, D.J.W., & Konuk, T. (1987). Late Quaternary tectonic and sedimentary history of outer İzmir and Çandarlı Bays, Western Turkey. *Marine Geology*, 76, 89–104.
- Anzidei, M., Antonioli, F., Benini, A., Lambeck, K., Sivan, D., Serpelloni, E., & Stocchi, P. (2011). Sea level change and vertical land movements since the last two millennia along the coasts of southwestern Turkey and Israel. *Quaternary International*, 232, 13–20.
- Arnold, L.J., & Roberts, R.G. (2009). Stochastic modelling of multi-grain equivalent dose (D_e) distributions: Implications for OSL dating of sediment mixtures. *Quaternary Geochronology*, 4, 204–230.
- Ascencio, A.D. (2013). Permanent salt evaporation ponds in a semi-arid Mediterranean region as model systems to study primary production processes under hypersaline conditions. *Estuarine, Coastal and Shelf Science*, 124, 24–33.
- Auriemma, R., & Solinas, E. (2009). Archaeological remains as sea level change markers: A review. *Quaternary International*, 206, 134–146.
- Bailey, R.M. (2003). The use of measurement-time dependent single-aliquot equivalent-dose estimates from quartz in the identification of incomplete signal resetting. *Radiation Measurements*, 37, 673–683.
- Beltrame, C., & Gaddi, D. (2007). Preliminary analysis of the hull of the Roman ship from Grado Gorizia, Italy. *International Journal of Nautical Archaeology*, 36, 138–147.
- Bini, M., Chelli, A., Durante, A.M., Gervasini, L., & Pappalardo, M. (2009). Geoarchaeological sea-level proxies from a silted up harbour: A case study of the Roman colony of Luni (northern Tyrrhenian Sea, Italy). *Quaternary International*, 206, 147–157.
- Blott, S.J., & Pye, K. (2001). GRADISTAT: A grain size distribution and statistics package for the analysis of unconsolidated sediments. *Earth Surface Processes and Landforms*, 26, 1237–1248.

- Blümner, H. (1920). s. v. Salz. In J. B. Metzler'sche (Ed.), *Paulys Real-Encyclopädie der classischen Altertumswissenschaft A 1*. (Sp. 2075–2099) Stuttgart: Verlagsbuchhandlung.
- Boetto, G. (2010). Le port vu de la mer: l'apport de l'archéologie navale à l'étude des ports antiques. In S. Keay, G. Boetto (Eds.), *Portus, Ostia and the Ports of the Roman Mediterranean. Contributions from Archaeology and History* (pp. 112–128). Rome: Ministero per i Beni e le Attività Culturali.
- Brill, D., Klasen, N., Brückner, H., Jankaew, K., Scheffers, A., Kelletat, D., & Scheffers, S. (2012). OSL dating of tsunami deposits from Phra Thong Island, Thailand. *Quaternary Geochronology*, 10, 224–229.
- Brinkmann, R. (1976). *Geology of Turkey*. Stuttgart: Enke.
- Brückner, H. (2003). Delta evolution and culture – aspects of geoarchaeological research in Miletos and Priene. In G.A. Wagner, E. Pernicka, & H.P. Uerpmann (Eds.), *Troia and the Troad. Scientific approaches* (pp. 121–144). Berlin, Heidelberg, New York: Springer Series: Natural Science in Archaeology.
- Brückner, H., Müllenhoff, M., Gehrels, R., Herda, A., Knipping, M., & Vött, A. (2006). From archipelago to floodplain – geographical and ecological changes in Miletus and its environs during the past six millennia (Western Anatolia, Turkey). *Zeitschrift für Geomorphologie N.F., Suppl. Vol. 142*, 63–83.
- Brückner, H., & Seeliger, M. (2009). Geoarchäologische Untersuchungen. In Pirson, F. (Ed.), *Pergamon. Bericht über die Arbeiten der Kampagne 2008. Archäologischer Anzeiger*, 2009(2), 194–199.
- Brückner, H., Knipping, M., & Seeliger, M. (2010). Geoarchäologische Untersuchungen in der Bucht von Elaia. In Pirson, F. (Ed.), *Pergamon. Bericht über die Arbeiten der Kampagne 2009. Archäologischer Anzeiger*, 2010(2), 208–219.
- Brückner, H., Urz, R., & Seeliger, M. (2013). Geomorphological and geoarchaeological evidence for considerable landscape changes at the coasts of western Turkey during the Holocene. *Geopedology and Landscape Development Research Series*, 1, 81–104.
- Cartledge, P. (2004). *Alexander the Great. The Hunt for a New Past*. New York: Overlook Press.
- Coates, J.F. (1987). Reconstructing the ancient Greek trireme warship. *Endeavour*, 11(2), 94–99.
- Di Rita, F., Celant, A., & Magri, D. (2010). Holocene environmental instability in the wetland north of the Tiber delta (Rome, Italy): Sea-lake-man interaction. *Journal of Paleolimnology*, 44, 51–67.
- Duller, G.A.T. (2008). Single-grain optical dating of Quaternary sediments: Why aliquot size matters in luminescence dating. *Boreas*, 37, 589–612.
- Engel, M., Knipping, M., Brückner, H., Kiderlen, M., & Kraft, J.C. (2009). Reconstructing middle to late Holocene palaeogeographies of the lower Messenian plain (southwestern Peloponnese, Greece): Coastline migration, vegetation history and sea level change. *Palaeogeography, Palaeoclimatology, Palaeoecology*, 284(3–4), 257–270.
- Ernst, W. (1970). *Geochemical facies analysis*. Amsterdam, London, New York: Elsevier.
- Evelpidou, N., Pirazzoli, P., Vassilopoulos, A., Spada, G., Ruggieri, G., & Tomasin, A. (2012). Late holocene sea level reconstructions based on observations of Roman fish tanks, Tyrrhenian coast of Italy. *Geoarchaeology*, 27, 259–277.
- Flad, R., Zhu, J., Wang, C., Chen, P., von Falkenhausen, L., Sun, Z., & Li, S. (2005). Archaeological and chemical evidence for early salt production in China. *Proceedings of the National Academy of Sciences of the United States of America*, 102(35), 12618–12622.
- Flemming, N.C. (1978). Holocene eustatic changes and coastal tectonics in the Northeast Mediterranean: Implications for models of crustal consumption. In: *Philosophical Transactions of the Royal Society of London. Mathematical and Physical Sciences*, 289, 405–458.
- Folk, R.L., & Ward, W.C. (1957). Brazos River bar: A study in the significance of grain size parameters. *Journal of Sedimentary Petrology*, 27, 3–26.
- Galbraith, R.F., Roberts, R.G., Laslett, G.M., Yoshida, H., & Olley, J.M. (1999). Optical dating of single grains of quartz from Jinmium rock shelter, northern Australia. Part I: Experimental design and statistical models. *Archaeometry*, 41, 339–364.
- Galili, E., Zviely, D., & Weinstein-Evron, M. (2005). Holocene sea level changes and landscape evolution on the northern Carmel coast (Israel). *Méditerranée*, 104, 79–86.
- Giovannini, A. (2000). s. v. Salz. II. Griechisch-Römische Antike. In: *Der Neue Pauly. Enzyklopädie der Antike 11*, Verlag J. B. Metzler, Stuttgart, Sp. 1275–1278.
- Grüner, A. (2006). Architektur und Ästhetik römischer Fischzuchtanlagen. Zur Wahrnehmung und Funktion gattungübergreifender Dekorationssysteme in der spätrepublikanischen Villenarchitektur. *Archäologischer Anzeiger*, 2006(1), 31–60.
- Hadler, H., Kissas, K., Koster, B., Mathes-Schmidt, M., Mattern, T., Ntageretzi, K., Reicherter, K., Willershäuser, T., & Vött, A. (2013). Multiple late-Holocene tsunami landfall in the eastern Gulf of Corinth recorded in the palaeotsunami geo-archive at Lechaion, harbour of ancient Corinth (Peloponnese, Greece) – *Zeitschrift für Geomorphologie N.F., Supplementary Issue*, 4, 139–180.
- Hansen, E. (1971). *The Attalids of Pergamon*. Ithaca: Cornell University Press.
- Higginbotham, J.A. (1997). *Piscinae. Artificial fishponds in Roman Italy*. Chapel Hill: The University of North Carolina Press.
- Höcker, Ch. (2001). s. v. Spolien. In: *Der Neue Pauly. Enzyklopädie der Antike 11*, Verlag J. B. Metzler, Stuttgart, Sp. 834–836.
- Kelterbaum, D., Brückner, H., Dikarev, V., Gerhard, S., Pint, A., Porotov, A., & Ziřko, V. (2012). Palaeogeographic

- changes at Lake Chokrak on the Kerch Peninsula, Ukraine, during the Mid- and Late-Holocene. *Geoarchaeology*, 27(3), 206–219.
- Kiyak, N.G., & Canel, T. (2006). Equivalent dose in quartz from young samples using the SAR protocol and the effect of preheat temperature. *Radiation Measurements*, 41, 917–922.
- Kızıldağ, N., Özdaş, A.H., & Uluğ, A. (2012). Late Pleistocene and Holocene Sea Level Changes in the Hisarönü Gulf, Southeast Aegean Sea. *Geoarchaeology*, 27, 220–236.
- Knoblauch, P. (1981). Die Rolle der Strandverschiebungen bei der Rekonstruktion antiker Hafenanlagen. In J. Schäfer & W. Simon (Eds.), *Strandverschiebungen in ihrer Bedeutung für Geowissenschaften und Archäologie* (pp. 91–114). Heidelberg: Esprint.
- Kraft, J.C., Brückner, H., Kayan, I., & Engelmann, H. (2007). The geographies of ancient Ephesus and the Artemision in Anatolia. *Geoarchaeology*, 22, 121–149.
- Kulig, G. (2005). Erstellung einer Auswertesoftware zur Altersbestimmung mittels Lumineszenzverfahren unter spezieller Berücksichtigung des Einflusses radioaktiver Ungleichgewichte in der 238-U-Zerfallsreihe. Bachelorthesis, TU Freiberg, Freiberg.
- Loke, M.H., & Barker, R.D. (1995). Least-squares deconvolution of apparent resistivity pseudosections. *Geophysics*, 60, 1682–1690.
- Marriner, N., & Morhange, C. (2007). Geoscience of ancient Mediterranean harbours. *Earth-Science Reviews*, 80, 137–194.
- Marriner, N., Morhange, C., & Saghieh-Beydoun, M. (2008). *Geoarchaeology of Beirut's ancient harbour, Phoenicia*. *Journal of Archaeological Science*, 35(9), 2495–2516.
- McCormac, F.G., Baillie, M.G.L., Pilcher, J.R., Brown, D.M., & Hoper, S.T. (1994). $\delta^{13}\text{C}$ Measurements from the Irish Oak Chronology. *Radiocarbon*, 36(1), 27–35.
- McHugh, C.M., Seeber, L., Cormier, M., Dutton, J., Cagatay, N., Polonia, A., Ryan, W.B., & Gorur, N. 2006. Submarine earthquake geology along the North Anatolia Fault in the Marmara Sea, Turkey: A model for transform basin sedimentation. *Earth and Planetary Science Letters*, 248, 661–684.
- Moinier, B. (2011). Salt in Antiquity: A quantification essay. In Alexianu, M., Weller, O., & Curcă, R.-G. (Eds.), *Archaeology and anthropology of salt: A diachronic approach*. Proceedings of the International Colloquium, 1–5 October 2008, Al. I. Cuza University (pp. 137–148). Iași, Romania: Oxford.
- Morhange, C., Blanc, F., Bourcier, M., Carbonel, P., Prone, A., Schmitt, S., Vivent, D., & Hesnard, A. (2003). Bio-sedimentology of the late Holocene deposits of the ancient harbor of Marseilles (Southern France, Mediterranean sea). *The Holocene*, 13(4), 593–604.
- Morhange, C., & Marriner, N. (2010). Palaeo-hazards in the coastal Mediterranean: A geoarchaeological approach. In Martini, I., & Chesworth, P.W. (Eds.), *Landscapes and Societies* (pp. 223–234).
- Morhange, C., Marriner, N., Excoffon, P., Bonnet, S., Flaux, C., Zibrowius, H., Goiran, J.-P., & Amouri, M.E. (2013). Relative sea-level changes during Roman times in the northwest Mediterranean: The 1st century A.D. fish tank of Forum Julii, Fréjus, France. *Geoarchaeology*, 28, 363–372.
- Müller, R. (2003). s. v. Spolien (RWG), In: *Der Neue Pauly. Enzyklopädie der Antike* 15/3, Verlag J. B. Metzler, Stuttgart, Sp. 195–208.
- Murray, A.S., & Wintle, A.G. (2003). The single aliquot regenerative dose protocol: Potential for improvements in reliability. *Radiation Measurements*, 37, 377–381.
- Niwa, Y., Sugai, T., Saegusa, Y., Ogami, T., & Sasao, E. (2011). Use of electrical conductivity to analyze depositional environments: Example of a Holocene delta sequence on the Nobi Plain, central Japan. *Quaternary International*, 230, 78–86.
- Özdaş, H., & Kızıldağ, N. (2013). Archaeological and geophysical investigation of submerged coastal structures in Kekova, Southern Coast of Turkey. *Geoarchaeology*, 28, 504–516.
- Pirson, F. (2004). Elaia, der maritime Satellit Pergamons. *Istanbuler Mitteilungen*, 54, 197–213.
- Pirson, F. (2007). Elaia. In Pirson, F. (Ed.), *Pergamon. Bericht über die Arbeiten der Kampagne 2006*. *Archäologischer Anzeiger*, 2007(2), 47–58.
- Pirson, F. (2008a). Elaia. In Pirson, F. (Ed.), *Pergamon. Bericht über die Arbeiten der Kampagne 2007* (pp. 130–140). *Archäologischer Anzeiger*, 2008(2), 130–140.
- Pirson, F. (2008b). Das Territorium der hellenistischen Residenzstadt Pergamon – Herrschaftlicher Anspruch als raumbezogene Strategie. In Jöchner, C. (Ed.), *Räume der Stadt – Von der Antike bis heute* (pp. 27–50). Berlin: Reimer.
- Pirson, F. (2009). Elaia. In Pirson, F. (Ed.), *Pergamon. Bericht über die Arbeiten der Kampagne 2008*. *Archäologischer Anzeiger*, 2009(2), 182–200.
- Pirson, F. (2010). Survey. In Pirson, F. (Ed.), *Pergamon. Bericht über die Arbeiten der Kampagne 2009* (pp. 195–201). *Archäologischer Anzeiger*, 2010(2), 195–201.
- Pirson, F. (2011). Elaia. In Pirson, F. (Ed.), *Pergamon. Bericht über die Arbeiten der Kampagne 2010*. *Archäologischer Anzeiger*, 2011(2), 166–174.
- Pirson, F. (2012). Hierarchisierung des Raumes? Überlegungen zur räumlichen Organisation und deren Wahrnehmung im hellenistischen Pergamon und seinem Umland. In Pirson, F. (Ed.), *Manifestationen von Macht und Hierarchien in Stadtraum und Landschaft*, BYZAS, 13, 187–232. Istanbul.
- Prescott, J.R., & Hutton, J.T. (1994). Cosmic ray contributions to dose rates for luminescence and ESR dating: Large

- depths and long-term time variations. *Radiation Measurements*, 23, 497–500.
- Prokesch von Osten, A. (1837). *Denkwürdigkeiten und Erinnerungen aus dem Orient III*, Stuttgart 1837.
- Radt, W. (1999). *Pergamon – Geschichte und Bauten einer antiken Metropole*. Darmstadt: Wissenschaftliche Buchgesellschaft.
- Reimer, P.J., Bard, E., Bayliss, A., Beck, J.W., Blackwell, P.G., Bronk Ramsey, C., Buck, C.E., Cheng, H., Edwards, R.L., Friedrich, M., Grootes, P.M., Guilderson, T.P., Hafflidson, H., Hajdas, I., Hatt, C., Heaton, T.J., Hogg, A.G., Hughen, K.A., Kaiser, K.F., Kromer, B., Manning, S.W., Niu, M., Reimer, R.W., Richards, D.A., Scott, E.M., Southon, J.R., Turney, C.S.M., & van der Plicht, J. (2013). IntCal13 and MARINE13 radiocarbon age calibration curves 0–50000 years calBP. *Radiocarbon*, 55(4), 1869–1887.
- Reinhardt, E.G., & Raban, A. (1999). Destruction of Herod the Great's harbor at Caesarea Maritima, Israel – geoarchaeological evidence. *Geology*, 27, 811–814.
- Rutilius Namatianus, *De reditu suo*. Translation and comments by Ernst Doblhofer I. II. Carl Winter Universitätsverlag, Heidelberg 1972 (Latin to German).
- Schneider, S., Knitter, D., & Schütt, B. (2011). Geoarchäologische Untersuchungen im westlichen Kaikostal. In Pirson, F. (Ed.), *Pergamon – Bericht über die Arbeiten in der Kampagne 2010*. *Archäologischer Anzeiger*, 2011(2), 160–166.
- Seeliger, M., Schneider, S., Brückner, H., Schütt, B., Horjes, B., Feuser, S., Zimmermann, M., & Pirson, F. (2011). Studying Pergamon's environs – geoarchaeological research in Elaia and Bakircay valley. *Proceedings of the International Bergama Symposium*, 7–9 April 2011, vol. I: 48–65. Izmir.
- Seeliger, M., Bartz, M., & Brückner, H. (2012). Mauern im Meer – Geoarchäologische Untersuchungen in der Bucht von Elaia. In Pirson, F. (Ed.), *Pergamon. Bericht über die Arbeiten der Kampagne 2010*. *Archäologischer Anzeiger*, 2011(2), 175–185.
- Seeliger, M., Bartz, M., Erkul, E., Feuser, S., Kelterbaum, D., Klein, C., Pirson, F., Vött, A. & Brückner, H. (2013). Taken from the sea, reclaimed by the sea: The fate of the closed harbour of Elaia, the maritime satellite city of Pergamum (Turkey). *Quaternary International*, 312, 70–83.
- Singarayer, J.S., & Bailey, R.M. (2003). Further investigations of the quartz optically stimulated luminescence components using linear modulation. *Radiation Measurements*, 37, 451–458.
- Stanley, J.-D., & Bernasconi, M.P. (2012). Buried and submerged Greek archaeological coastal structures and artifacts as gauges to measure late Holocene Seafloor Subsidence off Calabria, Italy. *Geoarchaeology*, 27, 189–205.
- Strabon: *Geographica*. Translation and comments by Albert Forbiger. Marix Verlag, Wiesbaden 2005 (Greek to German).
- Thonemann, P. (2011). *The Maeander valley. A historical geography from Antiquity to Byzantium*. Cambridge University Press.
- Traina, G. (1992). Sale e saline nel Mediterraneo antico. *La parola del passato*, 47, 363–378.
- Vita-Finzi, C. (1969). Late Quaternary continental deposits of central and western Turkey. *Man, New Series*, 4, 605–619.
- Vött, A. (2007). Relative sea level changes and regional tectonic evolution of seven coastal areas in NW Greece since the mid-Holocene. *Quaternary Science Reviews*, 26, 894–919.
- Vött, A., Handl, M., & Brückner, H. (2002). Rekonstruktion holozäner Umweltbedingungen in Akarnanien (Nordwestgriechenland) mittels Diskriminanzanalyse von geochemischen Daten. *Geologica et Palaeontologica*, 36, 123–147.
- Vött, A., Brückner, H., Schriever, A., Handl, M., Besonen, M., & van der Borg, K. (2004). Holocene coastal evolution around the ancient seaport of Oiniadai, Acheloos alluvial plain, NW Greece. *Coastline Reports*, 1, 43–53.
- Vött, A., Schriever, A., Handl, M., & Brückner, H. (2007). Holocene palaeogeographies of the central Acheloos River delta (NW Greece) in the vicinity of the ancient seaport Oiniadai. *Geodinamica Acta*, 20(4), 241–256.
- Vött, A., Bareth, G., Brückner, H., Lang, F., Sakellariou, D., Hadler, H., Ntageretzis, K., & Willershäuser, T. (2011). Olympia's harbour site Pheia (Elis, Western Peloponnese, Greece) destroyed by tsunami impact. *Die Erde*, 142(3), 259–288.
- Zimmermann, M. (2011). *Pergamon: Geschichte, Kultur, Archäologie*. C. H. Beck, München.

Chapter 6

6 The harbour of Elaia: A palynological archive for human/environmental interactions during the last 7500 years

Journal Article (accepted):

Shumilovskikh, L.S., **Seeliger, M.**, Feuser, S., Novenko, E., Schlütz, F., Pint, A., Brückner, H., 2016. The harbour of Elaia: A palynological archive for human/environmental interactions during the last 7500 years. *Quaternary Science Reviews*.



The harbour of Elaia: A palynological archive for human/environmental interactions during the last 7500 years

Lyudmila S. Shumilovskikh^{a, b, *}, Martin Seeliger^c, Stefan Feuser^d, Elena Novenko^e, Frank Schlütz^f, Anna Pint^c, Felix Pirson^g, Helmut Brückner^c

^a Department of Palynology and Climate Dynamics, Georg-August-University Göttingen, Göttingen, Germany

^b Laboratory of Taxonomy and Phylogeny of Plants, Tomsk State University, Russia

^c Institute of Geography, University of Cologne, Köln (Cologne), Germany

^d Heinrich Schliemann-Institute of Ancient Studies, University of Rostock, Rostock, Germany

^e Moscow State University, Moscow, Russia

^f Lower Saxony Institute for Historical Coastal Research, Wilhelmshaven, Germany

^g DAI Department Istanbul, Turkey

ARTICLE INFO

Article history:

Received 5 April 2016

Received in revised form 11 July 2016

Accepted 12 July 2016

Available online xxx

Keywords:

Vegetation history

Maritime trade

Erosion

Non-pollen palynomorphs

Helminth eggs

Fungal spores

Dinoflagellate cysts

Pergamon

Turkey

Holocene

ABSTRACT

Elaia, the harbour city for ancient Pergamon (western Turkey), was investigated using geoarchaeological methods. The rise and fall of Elaia were closely linked to the flourishing period of Pergamon, which ruled wide parts of today's western Turkey in Hellenistic times. In the framework of this research, the palynological analysis of a 9 m sediment core, Ela-70, retrieved from the enclosed harbour of the city, was carried out to reconstruct the vegetation and environmental history of the wider Gulf of Elaia region. An age-depth model, based on 11 calibrated radiocarbon ages, starting from 7.5 ka BP, provides the basis for the high resolution study of sediments from the Hellenistic period, as well as before and after. The lower part of the pollen diagram is characterised by high percentages of deciduous oaks and pines, suggesting the dominance of open forests close to the coring site. The change from oak forests to a cultural landscape, with olive, pistachio, walnut, and grape, started around 850 BC, reaching a maximum ca. 250 BC, and continuing to ca. AD 800. This period is characterised by increase of fire activity, soil erosion intensity, and pastoral farming. Such long-lasting intensive land use likely led to the climax ecosystem turnover from open deciduous oak forests to pine stands, while salt marshes developed around the coring site. The discovery of the dinoflagellate cyst of *Peridinium ponticum*, a Black Sea endemic species, in the harbour of Elaia evidences maritime trade between the Aegean Sea and the Black Sea during the time of the Mithridatic Wars (1st century BC). In conclusion, palynological data, in addition to historical and archaeological records, provide a deeper insight into human/environmental interactions, as derived from the geoarchaeological archive of the harbour of Elaia.

© 2016 Published by Elsevier Ltd.

1. Introduction

Today, the hills of Zeytindağ (Turkish for olive mountain) and the area surrounding Elaia are covered with olive groves (Fig. 1), playing an important role in the regional economy. Linguistic and numismatic evidence attests to the importance of olive oil production at Elaia in antiquity. Even the name of the city “Elaia” means “oily” in local Luwisch and “olive” in Greek (Pirson, 2004). On the reverse side of coins from Elaia, minted from the 5th/4th century BC until Roman period, olive branches are depicted (Fig. 2b). Elaia has been famous for its olives for centuries, but there are no historical records that bear witness to the onset of olive cultivation.

Archaeological records reveal a continuous occupation of the Elaia region since prehistoric times (Fig. 1b). Ceramics from Elaia indicate settlement activities from the early Bronze Age (Knitter et al., 2013; Pirson, 2007, 2008), while ancient historical accounts provide

very little information about Elaia. Strabo (2005) attributes the foundation of the city to Menestheus in the context of the Trojan War (Pirson, 2004). Later, Elaia paid the lowest tributes to the Athenian-dominated Delian League (454–425 BC; Pirson, 2004). However, the city gained fame during the period of the Pergamenian Empire (282–133 BC), when it was a naval station for the Pergamenian fleet and was important for military transport and trade, especially during the flourishing period of the Pergamon (Pirson, 2014).

Pergamon, the capital of the Pergamenian Empire, was located on a 330 m high hill on the Kaikos plain at a distance of 26 km to the sea, which provided a perfect defensive position for the city. However, the lack of direct access to the sea restricted traffic and trade. Being the capital city, Pergamon was in need of a harbour, which was constructed in the nearby Elaia (Pirson, 2004). In 133 BC the Pergamenian Empire came under Roman rule (Pirson and Scholl, 2015). During Roman and Byzantine times, historical documents from the region are very sparse, indicating the shrinking role of Elaia. The long period of human occupation had a continuous impact on the environment, forming a cultural landscape.

* Corresponding author. Department of Palynology and Climate Dynamics, Georg-August-University Göttingen, Göttingen, Germany.

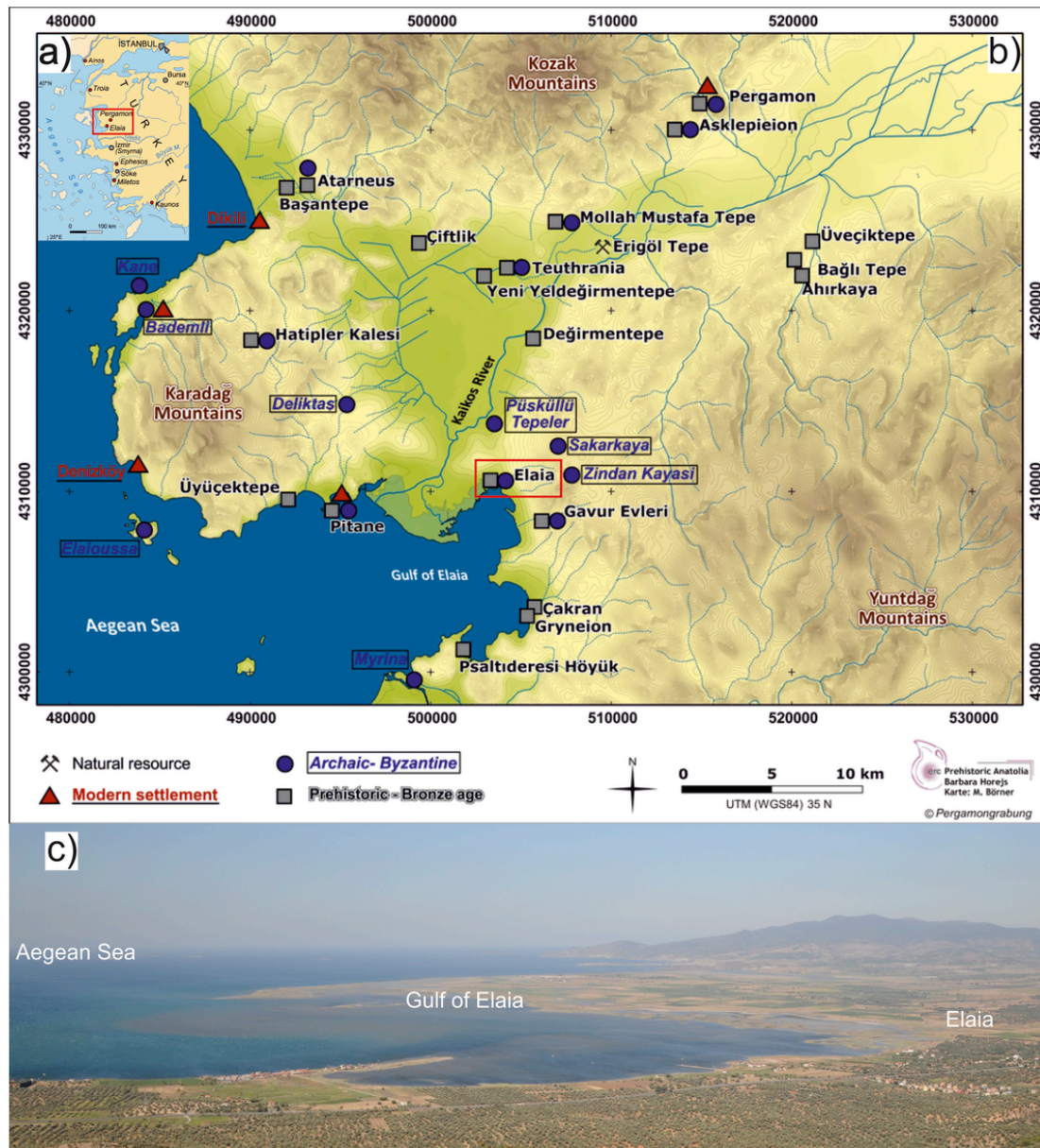


Fig. 1. Location of the ancient city of Elaia: a) Elaia's position in western Anatolia (ancient settlements in italics); b) archaeological sites of the region around Elaia and Pergamon (based on Horjes, 2010); c) view from Yuntdağ Mts. on the Gulf of Elaia and olive groves (photo: M. Seeliger, 2010).

In order to reconstruct the environmental changes in the Elaia region, corings were carried out in the Bay of Elaia and in the so-called closed harbour (Seeliger et al., 2013). Ancient harbour basins are of particular geoarchaeological interest, because, as economic centres and points for naval navigation, they are important archives of geological, biological, and archaeological information that can be amalgamated in multi-temporal landscape scenarios (Morhange et al., 2014). Based on corings around and within the harbours of Elaia, the paleogeographical (Seeliger et al., 2013) and hydrological (Pint et al., 2015) changes can be reconstructed (Fig. 2a). In this paper, we present a model for environmental change based on the palynological analysis of the core Ela 70 from the basin of the harbour of Elaia.

2. Geographical settings

The Gulf of Elaia is located south of the Bakır Çay delta (transl.: “Copper River”, ancient name “Kaikos”) between the granitic mountain ranges of Karadağ to the west and Zeytindağ to the east. During the late Miocene, the westward drift of the Anatolian Plate formed several E-W-oriented rift structures, such as the Bergama graben and Zeytindağ graben, which later were filled with sediments of the Bakır Çay (Seeliger et al., 2013; Schneider et al., 2015).

The Bergama region experiences the climate of the summer-dry subtropics, with hot and dry summers, and mild and humid winters (Csa climate, according to the Koeppen and Geiger classification; average annual precipitation: 755 mm; average annual temperature: 16.1 °C, with 6.1 °C in January and 26.1 °C in July; Meyer and Aksoy, 1986).

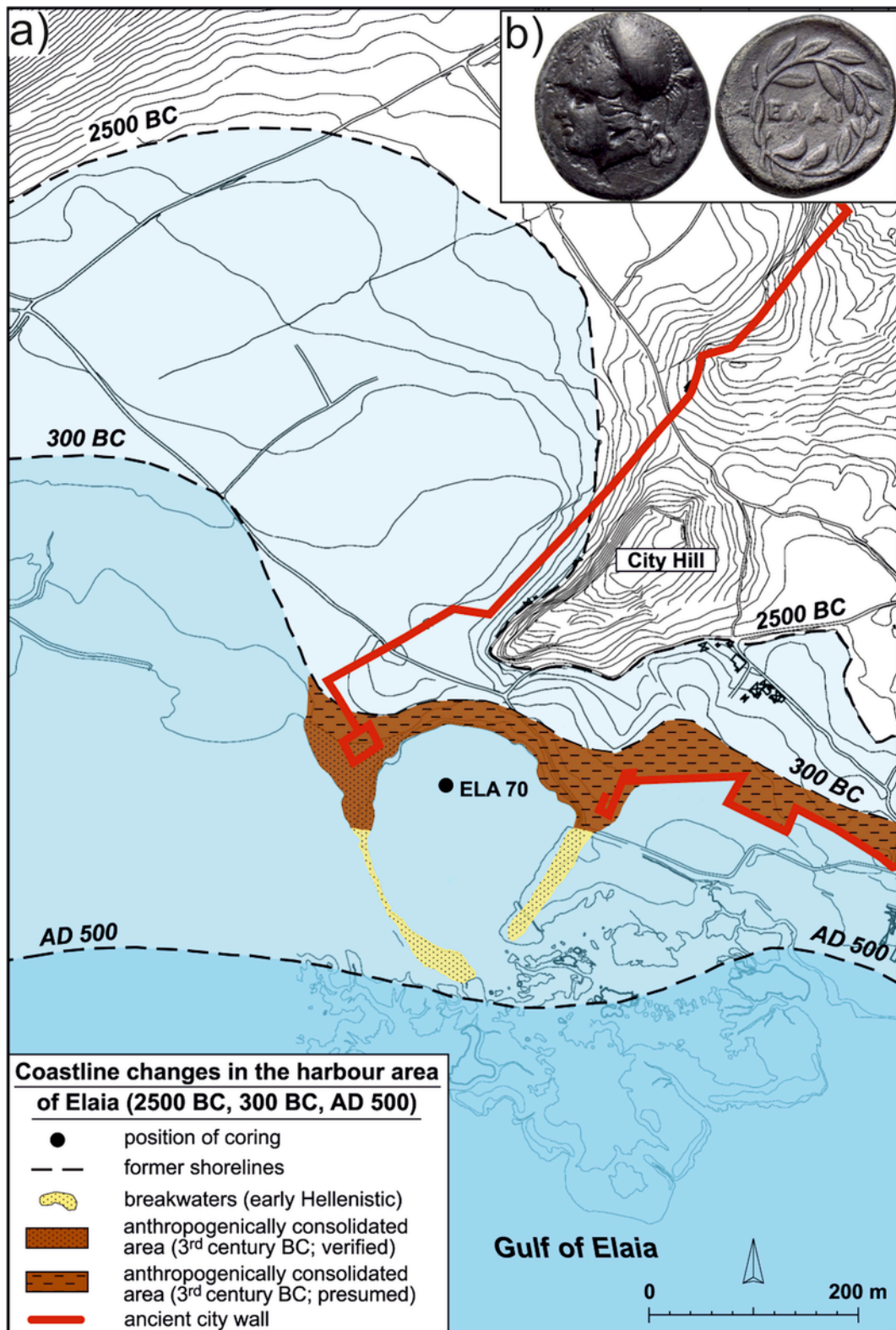


Fig. 2. The enclosed harbour of Elaia: a) position of shoreline ~2500 BC, 300 BC, and AD 500 according to Seeliger et al., 2013 (location of coring site Ela-70 is indicated; b) coins from Elaia showing two olive branches (Classical epoch, late 5th – 4th cent. BC) (www.pecunem.com).

According to the maps of the supposedly natural vegetation (Quezel and Barbero, 1985; Zohary, 1973), the vegetation around

Elaia belongs to Mesomediterranean or Eu-Mediterranean zone, with *Quercetalia ilicis* formations, including evergreen (*Quercus coc-*

cifera) and deciduous (*Quercus infectoria*, *Quercus macrolepis*) oaks, and Pistacio-Rhamnietalia formations in coastal areas. Both formations are of the macchia-type, with numerous species such as *Pistacia terebinthus*, *Rhamnus alaternus*, *Cistus*, *Arbutus andrachne*, *Erica arborea*, *Myrtus communis*, *Olea*, *Phillyrea*, *Laurus*, and *Juniperus* (Hütteroth and Höhfeld, 2002; Walter, 1956; Zohary, 1973). *Pinus brutia* forests occupy lowlands to the northeast and east from Elaia. Supramediterranean or Oro-Mediterranean formations include *Quercus cerris*, *Quercus frainetto*, and *Quercus ithaburensis* on non-calcareous or alluvial soils, and *Ostrya carpinifolia*, *Carpinus orientalis*, and *Quercus pubescens* on calcareous soils. Native *Pinus pinea* appear north of Bergama in the Kozak Mountains. *Fagus orientalis* and *Abies equi-trojani* represent southern outposts of Euxinian forests in the Kaz Mountains (Meyer and Aksoy, 1986). Riverine forests are formed by *Platanus orientalis*, *Alnus*, *Fraxinus angustifolia*, *Salix*, *Vitex agnus-castus*, and *Nerium oleander*.

At present, the marginal parts of the Bay of Elaia are silted-up; they are covered with salt marshes consisting of salt-tolerant Amaranthaceae, such as *Salicornia* sp. and *Atriplex* sp. The area of Elaia is intensively used for olive groves (Fig. 1c) and cereal fields. In general, due to the intensive exploitation of the natural vegetation for agriculture, pasture, and lumbering over the past several millennia, only patches of semi-natural vegetation have survived today between the cultural landscapes. Depending on the intensity of anthropogenic pressure at a given locus, the degraded natural vegetation occurs as semi-natural forests, bushes, or macchia between agricultural and urban areas (Hütteroth and Höhfeld, 2002).

3. Historical and archaeological context

During the time span 2006–2011, an archaeological survey was conducted in the area of ancient Elaia, which was part of an interdisciplinary research project headed by Felix Pirson, Director of the DAI's Istanbul branch (German Archaeological Institute). The aim of the survey was to gain more insight into the settlement history of the Hellenistic-Roman city and its surroundings as a sub-centre of Pergamon. The multi-disciplinary project integrated archaeological and architectural surveys, small-scale excavations, as well as the application of geophysical and geoarchaeological methods. The settlement phases were dated based on an intensive ceramic survey within the city. Smaller settlements and farmsteads were detected during survey, collectively covering an approximately 5 km area around the city (Pirson, 2014). Excavations in parts of a Hellenistic cemetery and in a late Classic/early Hellenistic grave mound (tumulus) both to the north of Elaia enhanced our knowledge of the ancient settlement (Pirson, 2008, 2009).

Archaeological surveys have shown that the Kaikos valley was settled since prehistoric times (Fig. 1b; Horjes, 2010). Excavations at Yeni Yeldeğirmentepe demonstrated the cultural connection of this tell with Troia I and Çukuriçi IV, suggesting the foundation of the settlement at the end of the 4th to the first half of the 3rd millennium BC (Pirson, 2009). In Elaia, the earliest ceramics date from the late Chalcolithic/Early Bronze Age (~3000 BC), and persist, reaching their maximum density during the Hellenistic-Roman period with the dominance of material from Pergamon (Pirson, 2009, 2014). In the middle of the 3rd century BC, the infrastructure of Elaia was greatly enhanced. The enclosed harbour basin and an open harbour zone with ship sheds were erected as well as a fortification wall surrounding the settlement (Pirson, 2014). During that time, farmsteads were established in the immediate vicinity of the city. To the north, north-east, and south of Elaia, cemeteries flanked the main roads in and out of the city. In the late Roman period the city declined, as demonstrated by the sparsity of archaeological material. In early Byzantine times,

Elaia was abandoned for a more inland settlement on the so-called Püsküllü Tepeler – most probably in fear of pirate attacks (Pirson, 2009, 2010, 2014). For the middle and late Byzantine periods the archaeological record reveals that the area was populated only sparsely by minor farmsteads – neither Elaia nor the settlement on the Püsküllü-Tepeler were still inhabited.

4. Material and methods

4.1. Geoarchaeological field-work

In 2008–2012, several cores were collected in the environs of ancient Elaia by the geoarchaeological research project (Seeliger et al., 2013, 2014). Core Ela-70 was extracted from within the silted-up basin of the enclosed harbour (Fig. 2a; coordinates: 38.94315° N; 27.038622° E; core length: 9 m; coring device: Atlas Copco Cobra TT vibracorer; closed steel auger heads with opaque 1 m long PVC inliner tubes; external diameter: 5 cm).

All coring sites were levelled with DGPS (Leica GPS System 530; accuracy of ≤ 2 cm in all three dimensions). The altitudes are referenced to present sea level (Seeliger et al., 2013, 2014). They are stated in m a.s.l. (m above present sea level) and m b.s. (m below present terrain surface at the coring site).

4.2. Chronology

The chronology is based on AMS- ^{14}C age estimates (for details see Table 1). The ages are presented in years cal BP and in calendar years BC/AD with a 2σ confidence interval (Table 1). Since the spatio-temporal variation of the marine reservoir effect for the Aegean Sea is still not well known, ^{14}C -ages of marine carbonates should be interpreted carefully. To estimate the sedimentation rate of the core, an age vs. depth plot was calculated using the clam module of R (Fig. 3; Blaauw, 2010).

4.3. Sedimentology and geochemistry

Multi-proxy laboratory analyses were conducted (cf. Ernst, 1970; Rae, 1997; Vött et al., 2002, 2011; Brückner et al., 2006; Niwa et al., 2011; Kelterbaum et al., 2012; Seeliger et al., 2013; Hadler et al., 2013). Samples were air-dried, ground with mortar and pestle, and sieved to separate the ≤ 2 mm grain size fraction for further analyses (Fig. 4).

The organic content was decomposed using hydrogen peroxide (H_2O_2), followed by laser-based grain size analysis with a Beckman Coulter LS13320 device. For the calculation of grain-size parameters after Folk and Ward (1957), the GRADISTAT software (Blott and Pye, 2001) was applied.

XRF analysis was done with an Itrax Core Scanner (Cox analytical system; exposure time of 10 s; element range Al to Pb; resolution 2 mm; Croudace et al., 2006). Measurements of the electrical conductivity were performed in an aqueous solution consisting of 15 g of sediment and 75 ml distilled water with a glass electrode (Mettler Toledo InLab[®]731-2m) (Beck et al., 1995).

4.4. Palynology

A total of 42 subsamples were collected from sediment core Ela-70, at 10–40 cm intervals. The laboratory treatment included demineralization with cold hydrochloric acid (10%), followed by cold hydrofluoric acid (70%) overnight, then sieving at 1–2 μm nylon mesh using ultrasound bath (less than 1 min). Acetolysis (Erdtman, 1960) was avoided because it destroys peridinoïd dinoflagellate cysts.

Table 1

AMS-¹⁴C data of sediment core Ela-70. UGAMS: Centre for Applied Isotope Studies (CAIS), University of Georgia at Athens, USA; UBA: ¹⁴Chrono Centre for Climate, the Environment, and Chronology, Queen's University Belfast, UK; ERL: AMS C14-Labor Erlangen, University Erlangen-Nürnberg, Germany. Sample Ela70/395: enriched terrestrial pollen. Depending on the $\delta^{13}\text{C}_{\text{VPDB}}$ value each sample was calibrated either using the IntCal13 or MARINE13 calibration curve of the recent Calib 7.1 software (Reimer et al., 2013), with a marine reservoir effect of 390 ± 85 years and a ΔR of 35 ± 70 years (Siani et al., 2000). The 2σ confidence interval is presented.

Sample codes	Lab code	Material	Depth b.s.	$\delta^{13}\text{C}$ (‰)	Libby-age	Calibrated ¹⁴ C ages cal BC/cal AD (2σ)	Calibrated ¹⁴ C ages cal BC/cal AD (2σ) with relative probability	Calibrated ¹⁴ C ages cal BP (2σ)	Calibrated ¹⁴ C ages cal BP (2σ) with relative probability
Ela 70/190	UBA-23841	wooden piece	1.90 m	-26.1	1730 ± 29	AD 244–385	AD 244–385 (100%)	1565–1706 BP	1565–1706 BP (100%)
Ela 70/250	UBA-23840	wooden piece	2.50 m	-27.3	1699 ± 29	AD 254–407	AD 254–303 (23%) AD 314–407 (77%)	1543–1696 BP	1543–1636 BP (77%) 1647–1696 (23%)
Ela 70/275	UBA-23839	wooden piece	2.75 m	-28.1	1772 ± 29	AD 139–341	AD 139–198 (10.5%) AD 207–341 (89.5%)	1609–1811 BP	1609–1743 BP (89.5%) 1752–1811 BP (10.5%)
Ela 70/377	UGAMS-11130	charcoal	3.77 m	-27.0	1960 ± 30	39 BC–AD 120	39 BC–AD 87 (96.3%) AD 105–120 (3.7%)	1830–1988 BP	1830–1845 BP (3.7%) 1863–1988 BP (96.3%)
Ela 70/395	ERL-18675	terr. pollen	3.95 m	-26.0	2253 ± 42	398–204 BC	398–340 BC (33.3%) 327–204 BC (66.7%)	2153–2347 BP	2153–2276 BP (66.7%) 2289–2347 BP (33.3%)
Ela 70/457	UGAMS-11131	seaweed	4.57 m	-18.2	2680 ± 30	650–181 BC	650–181 BC (100%)	2130–2599 BP	2130–2599 BP (100%)
Ela 70/480	UBA-23837	seed	4.80 m	-8.2	2659 ± 31	895–794 BC	895–867 BC (10.5%) 858–794 BC (89.5%)	2743–2844 BP	2743–2807 BP (89.5%) 2816–2844 BP (10.5%)
Ela 70/585	UBA-23836	seaweed	5.85 m	-12.7	4274 ± 34	2597–2155 BC	2597–2155 BC (100%)	4104–4546 BP	4104–4546 BP (100%)
Ela 70/672	UGAMS-11132	seaweed	6.72 m	-17.7	5920 ± 30	4529–4203 BC	4529–4203 BC (100%)	6152–6478 BP	6152–6478 BP (100%)
Ela 70/695	UBA-23835	seaweed	6.95 m	-12.7	6616 ± 37	5316–4948 BC	5316–4948 BC (100%)	6897–7265 BP	6897–7265 BP (100%)
Ela 70/782	UGAMS-11133	bivalve	7.82 m	-0.7	7040 ± 30	5690–5421 BC	5690–5421 BC (100%)	7370–7639 BP	7370–7639 BP (100%)

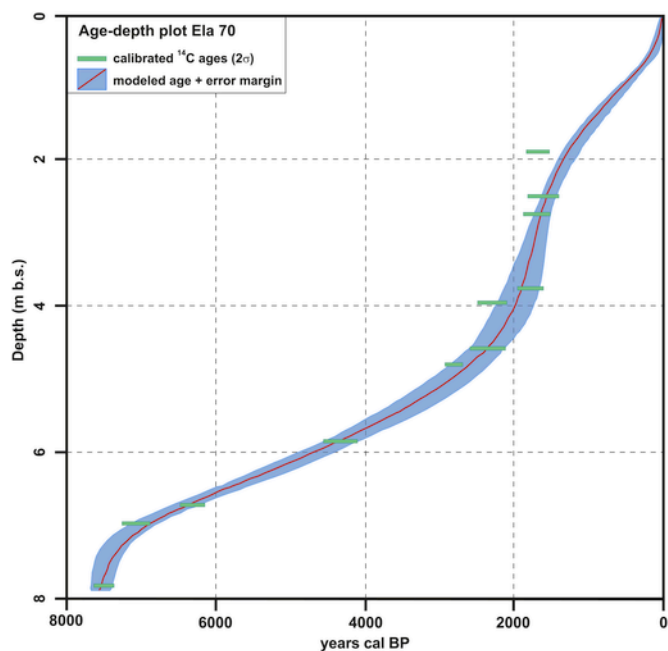


Fig. 3. Age-depth model of the sediment core Ela-70.

One tablet with a known number of *Lycopodium* spores (Batch number 1031) was added at the beginning of the preparation in order to calculate the concentration of microfossils (Stockmarr, 1971). Prepared subsamples were stored in glycerin and counted under 400× or 1000× magnification. As long as there were sufficient pollen concentration, counts of 300–500 pollen grains per sample were made; in case of low concentration (<800 cm³), pollen grains were counted up to 100. Pollen identification and taxonomy follows Beug (2004) and Moore et al. (1999). Beside pollen and plant spores, non-pollen paly-

nomorphs (NPP), including fungal spores, animal remains and dinoflagellate cysts as well as charcoal particles, were identified and counted. For NPP identification we mostly used biological literature and made a comparison to described NPP types (Table 2, Plates 1–3). Description of several NPP types is given in accordance to the modern biological literature and taxonomy (Section 5.2.1). Pollen and NPP are expressed as percentages of the total sum of identified pollen. The diagrams (Figs. 5–7) were constructed using C2 version 1.5.6 (Juggins, 2007). Counts of pollen, spores and NPP have been submitted to PAN-GAEA. Pollen and NPP were grouped by their ecological meaning (Table 3; Fig. 9).

The delimitation of local pollen assemblage zone boundaries was aided visually and supported by multivariate analyses, such as stratigraphically constrained incremental sum-of-squares cluster analysis (CONISS: Grimm, 1987) and principal component analysis (PCA). Calculation and plotting of the CONISS dendrogram (Supplementary 1) was carried out in R with package 'rioja' (Juggins, 2015) for pollen taxa, exceeding an abundance of 5%. The number of CONISS zones was statistically proven by the broken stick model (Bennett, 1996). To investigate interactions among the identified taxa along the studied core in a temporal context PCA was carried out in C2 (Juggins, 2007) for pollen taxa exceeding 1% using a square root transformation (Figs. 5 and 8).

Changes of the total woody coverage were reconstructed from the pollen data using the Best Modern Analogue (BMA) technique (Fig. 5). This approach, first developed by Overpeck et al. (1985) for climate reconstructions and extended by Guiot (1990) and Nakagawa et al. (2002), has been successively applied for forest cover reconstructions (Tarasov et al., 2007; Novenko et al., 2014). In BMA analyses we used squared-chord distances (SCD) (Overpeck et al., 1985) as the index of dissimilarity between pollen assemblages: two spectra were judged analogous if their SCD's were less than a threshold T (in our study T = 0.4). BMA estimates of woody cover are then calculated as weighted averages of the modern woody cover variables of

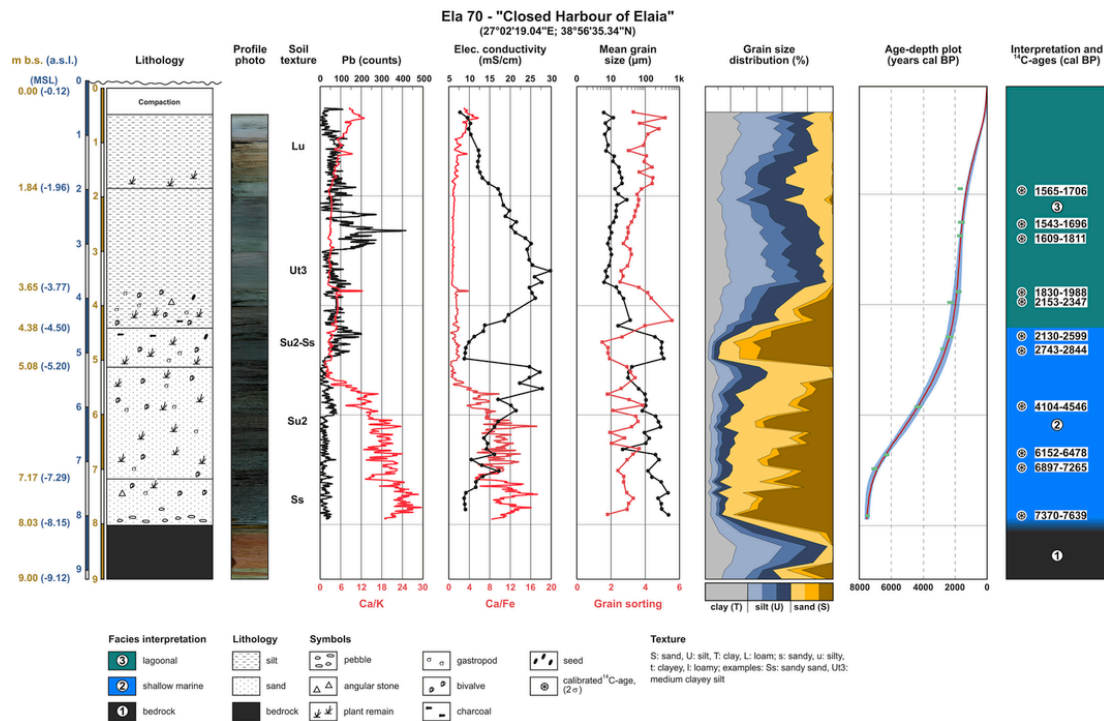


Fig. 4. Sedimentological and geochemical characteristics of sediment core Ela-70. The definite change from shallow marine to lagoonal facies is due to the construction of the harbour basin around 260 BC. Meanwhile, the basin is silted up. MSL = mean sea level, tidal range is around 20–30 cm.

the 8 best analogues, with the inverse SCD as weights (Nakagawa et al., 2002). BMA calculations were done with Polygon 1.5 (<http://dendro.naruto-u.ac.jp/nakagawa/>).

As modern analogues for reconstruction, we used 1100 pollen datasets originating from a wide variety of landscapes in Europe, the south-eastern Mediterranean region, and the Middle East. Modern surface samples were derived from the European Pollen Database (EPD) (<http://www.europeanpollendatabase.net>) and from the Russian pollen data base (<http://pollendata.org>). We used MODIS satellite images and the VCF (Vegetation Continuous Fields) estimates of modern tree cover (Hansen et al., 2003), which detail the proportion of each 500×500 m pixel that is covered by trees, herbs, and bare ground, for the entire world. The proportion of tree vegetation was estimated in a radius 20 km around each site from the reference dataset of modern pollen assemblages. The test of the accuracy of the applied method using a database of surface pollen assemblages shows that this method can reproduce present day characteristics of wood cover in Europe quite accurately ($R^2 = 0.57$, $SEE = 10.8\%$), and it is sufficient for reconstructing major changes of the woodland vegetation in the past (Novenko et al., 2014).

5. Results

5.1. Sedimentology and geochemistry

The Ela-70 core was taken from inside the harbour basin of Elaia (Fig. 2a). Here, the general features of the sediment core are presented (further details in Seeliger et al., 2013).

The sediment core is divided into three main units (Fig. 4). Unit 1 (900–803 cm) is composed of the common Neogene bedrock of the area of Elaia; it is mined close by in the Bozyertepe region and used for building purposes (Seeliger et al., 2013, 2014).

The overlaying unit 2 (803–438 cm) starts with a fining-upward sequence of sands and pebbles, representing the transgressive facies

of the postglacial sea-level rise (803–717 cm). The remaining part consists of shallow marine facies. Seagrass (*Posidonia oceanica*) and shell debris, e.g. *Dosinia lupinus* and gastropods, are common in unit 2. High values of Ca/Fe and Ca/K hint to shallow marine conditions. Six radiocarbon age estimates provide a chronological framework, ranging from ~7500 BP to ~2300 BP (Table 1, Fig. 4).

Unit 3 (438 cm to surface) follows, with a sharp contrast. It is composed of fine-grained sediments (medium clayey silt and silty loam). The lowermost part of this unit (438–365 cm) is rich in finds: charcoal, seeds, seagrass, mollusc shells, and angular stones.

The low Ca/Fe and Ca/K ratios hint to an increased input of freshwater and terrestrial sediments. Thus, a lagoon environment may be expected to have contributed to the formation of unit 3 (Seeliger et al., 2013). The rapid change from open marine to lagoon conditions was caused by the construction of the harbour breakwaters during early Hellenistic times. This is backed by high values of the heavy metal lead (Pb) between ~300 and ~200 cm, i.e. during the Hellenistic and Roman periods according to the age-depth model (Fig. 3). In this context, lead is a clear indicator of human influence (Delile et al., 2014). According to the age-depth model this unit started in Hellenistic times (extending through modern times Table 1, Fig. 4). This fits well to the archaeological evidence, because it was the time when the moles of the enclosed harbour were erected (Seeliger et al., 2013).

5.2. Palynology

5.2.1. Description and identification of some new NPP types

5.2.1.1. *Glomosporium leptideum* (Plate 2: 11–12)

Spore balls are ovoid, $37.3 \times 40 \mu\text{m}$ in size, brownish yellow, composed of numerous spores. Spores are angular on their free outer side of $7\text{--}9 \times 9\text{--}11 \mu\text{m}$, having a verrucate surface. They taper towards the middle of the spore ball, are $19\text{--}20 \mu\text{m}$ in length, with smooth inner walls. Morphologically the spore balls refer to the ba-

Table 2

List of NPP from Ela-70 with reference to identification literature and to corresponding NPP form types.

Documented palynomorphs	Taxonomical group	ID reference	NPP form-type with reference
<i>Botryococcus</i>	Green algae	Jankovská and Komárek (2000)	
<i>Mougeotia</i>	Green algae	van Geel (2001)	
<i>Pediastrum</i>	Green algae	Jankovská and Komárek (2000)	
Zygnemataceae	Green algae	van Geel (2001)	
<i>Brigantedinium</i> sp. <i>Brigantedinium</i> sp. <i>Brigantedinium</i> sp.	Dinoflagellate cyst	Rochon et al. (1999)	
<i>Echinidinium zonneveldiae</i>	Dinoflagellate cyst	Rochon et al. (1999)	
<i>Gymnodinium</i> sp. <i>Gymnodinium</i> sp. <i>Gymnodinium</i> sp.	Dinoflagellate cyst	Rochon et al. (1999)	
<i>Lejeunecysta</i> cf. <i>sabrina</i> <i>Lejeunecysta</i> cf. <i>sabrina</i> <i>Lejeunecysta</i> cf. <i>sabrina</i>	Dinoflagellate cyst	Rochon et al. (1999)	
<i>Lingulodinium machaerophorum</i>	Dinoflagellate cyst	Rochon et al. (1999)	
<i>Operculodinium centrocarpum</i>	Dinoflagellate cyst	Rochon et al. (1999)	
<i>Pentapharsodinium dalei</i>	Dinoflagellate cyst	Rochon et al. (1999)	
<i>Peridinium ponticum</i>	Dinoflagellate cyst	Wall et al. (1973)	
<i>Polykrikos schwarzii</i>	Dinoflagellate cyst	Rochon et al. (1999)	
<i>Pyxidinospis reticulata</i>	Dinoflagellate cyst	Rochon et al. (1999)	
<i>Quinquecuspis concreta</i>	Dinoflagellate cyst	Rochon et al. (1999)	
<i>Spiniferites bentorii</i>	Dinoflagellate cyst	Rochon et al. (1999)	
<i>Spiniferites membranaceus</i>	Dinoflagellate cyst	Rochon et al. (1999)	
<i>Spiniferites mirabilis</i>	Dinoflagellate cyst	Rochon et al. (1999)	
<i>Spiniferites ramosus</i>	Dinoflagellate cyst	Rochon et al. (1999)	
<i>Tectatodinium pellitum</i>	Dinoflagellate cyst	Rochon et al. (1999)	
<i>Tuberculodinium vancampoae</i>	Dinoflagellate cyst	Rochon et al. (1999)	
<i>Cymatiosphaera globulosa</i>	Prasinophyte	Mudie et al. (2010)	HdV 116 by Pals et al. (1980)
<i>Pseudoschizaea circula</i>	Acritarch	Mudie et al. (2010)	
<i>Radiosperma</i> -type <i>Radiosperma</i> -type <i>Radiosperma</i> -type	Tintinnid	Mudie et al. (2010)	
Foraminifer linings	Foraminifera	Mudie et al. (2010)	
<i>Ascaris</i>	Nematoda	Lardín and Pacheco (2015)	
<i>Capillaria</i>	Nematoda	Lardín and Pacheco (2015)	
<i>Trichuris</i>	Nematoda	Lardín and Pacheco (2015)	

Table 2 (Continued)

Documented palynomorphs	Taxonomical group	ID reference	NPP form-type with reference
<i>Arnim-type</i> <i>Arnim-type</i>	Fungi	Bell (2005), Doveri (2007)	<i>Arnim-type</i> (HdV 261) by Van Geel et al. (2003)
<i>Cercophora-type</i> <i>Cercophora-type</i>	Fungi	Bell (2005), Doveri (2007)	<i>Cercophora-type</i> (HdV 112) by Van Geel et al. (1981)
<i>Apiosordaria</i>	Fungi	Bell (2005), Doveri (2007)	<i>Zopfiella/ Apiosordaria</i> (HdV 169) by Van Geel et al. (1983)
<i>Chaetomium</i>	Fungi	Bell (2005), Doveri (2007)	<i>Chaetomium</i> sp. (HdV 7A) by Van Geel (1978)
<i>Coniochaeta ligniaria</i>	Fungi	Van Geel et al. (1983)	<i>Coniochaeta</i> cf. <i>ligniaria</i> (HdV 172) by Van Geel et al. (1983)
<i>Delitschia</i>	Fungi	Bell (2005), Doveri (2007)	<i>Delitschia</i> sp. by Cugny et al. (2010)
<i>Diporothea</i>	Fungi	Van Geel et al. (1986)	HdV 143 by Van der Wiel (1982)
<i>Gelasinospora</i>	Fungi	Van Geel (1978)	<i>Gelasinospora-type</i> by Van Geel (1978) new type
<i>Glomosporium leptideum</i>	Fungi	Ellis and Ellis (1997)	
<i>Glomus-type</i> <i>Glomus-type</i>	Fungi	Kolaczek et al. (2013)	<i>Glomus</i> cf. <i>fasciculatum</i> (HdV 207) by Van Geel et al. (1989)
<i>Helicoma</i>	Fungi	Ellis and Ellis (1997)	–
<i>Helicoon fuscosporum/ ellipticum</i>	Fungi	Ellis and Ellis (1997)	new type
<i>Pithomyces chartarum</i>	Fungi	Ellis 1971	<i>Pithomyces chartarum</i> by Pirozynski et al. (1984)
<i>Podospora curvispora</i>	FUNGI	Mirza and Cain (1969)	<i>Podospora curvispora</i> by Shumilovskikh et al. (2015)
<i>Podospora decipiens-type</i> <i>Podospora decipiens-type</i>	Fungi	Bell (2005), Doveri (2007)	<i>Podospora-type</i> (HdV 368) by Van Geel et al. (1981)
<i>Podospora group</i> <i>Podospora group</i>	Fungi	Bell (2005), Doveri (2007)	<i>Sordaria-type</i> (HdV 55A) by Van Geel (1978)
<i>Mediaverrinites (Potamomyces)</i>	Fungi	Schlütz and Shumilovskikh (2013)	<i>Mediaverrinites</i> by Jarzen and Elsik (1986), Sancay (2014)
<i>Puccinia</i>	Fungi	Grove (1913)	<i>Puccinia</i> sp. (HdV 357) by Van Geel et al. (1981) new type
<i>Saccobolus minimus-type</i> <i>Saccobolus minimus-type</i>	Fungi	Bell (2005), Doveri (2007)	
<i>Sordaria-type</i>	Fungi	Bell (2005), Doveri (2007)	<i>Sordaria-type</i> (HdV 55A) by Van Geel (1978)
<i>Sphaerodes retispora</i>	Fungi	García et al. (2004)	New type
<i>Sporormiella-type</i>	Fungi	Bell (2005), Doveri (2007)	<i>Sporormiella-type</i> (HdV 113) by Van Geel et al. (2003)
<i>Sporoschisma saccardoii</i>	Fungi	Ellis and Ellis (1997)	<i>Sporoschisma</i> spp. (HdV 1002) by Gelorini et al. (2011)
<i>Thecaphora</i>	Fungi	Vanki (1994)	<i>Thecaphora</i> sp. (HdV 364) by Van Geel et al. (1981)

Table 2 (Continued)

Documented palynomorphs	Taxonomical group	ID reference	NPP form-type with reference
Uredospores	Fungi	Grove (1913)	Uredospores by McAndrews and Turton (2010)
<i>Urocystis</i>	Fungi	Vanki (1994)	<i>Urocystis</i> (UG 1079) by Gelorini et al. (2011)
<i>Xylaria</i>	Fungi	Dennis (1981)	cf. <i>Xylaria</i> (EMA 17) by Barthelmes et al. (2006)
<i>Zopfia rhizophila</i> stomata	Fungi Conifers	Ellis and Ellis (1997) Hansen (1995)	New type Stomata (HdV 391, 505) by van Geel et al. (1981, 1986)

sidiospores of the smut fungus *Glomsporidium leptideum*, infecting the seeds of different species of *Chenopodium* (Vanky, 1994, 1998). Finding of this spores in Ela-70 (180 cm) confirms presence of *Chenopodium* (Amaranthaceae) in Elaia surroundings.

5.2.1.2. *Helicoon ellipticum/fuscosporum* (Plate 2: 5–6)

Parts of coiled spores, 25 µm in diameter, multiseptate, brown filaments 5 µm brought, are similar to spores of the recent fungus *Helicoon ellipticum* (32–40 × 20–30 µm) and *H. fuscosporum*

(25–30 × 20–30 µm) (Ellis and Ellis, 1997). *Helicoon* is a genus of saprophytic hyphomycetes. *H. ellipticum* was found on rotten, mainly coniferous, wood, and *H. fuscosporum* on dead stems of *Rubus idaeus* (Ellis and Ellis, 1997).

5.2.1.3. *Mediaverrunites* (*Potamomyces*) (Plate 2: 9–10, 13–14)

Spores attributed to the fossil from-taxa *Mediaverrunites* (Elsik, 1976; Nandi and Sinha, 2007) are ascospores of the extant genus *Potamomyces* (Hyde, 1995). While several types of *Mediaverrunites* spores are known from fossil material the genus *Potamomyces* comprises until now *Potamomyces armatisporus* (Cai et al., 2006) and a second species provisional named *P. nepalensis* only known from its spores (Schlütz and Shumilovskikh, 2013). Spores with three meridional verrucae (plate 2: 13–14) of *Mediaverrunites pontidiensis* (Sancay, 2014) as well as spores of *Mediaverrunites elsikii* (plate 2: 9–10) occurred. Both groups are aggregated in the diagram under the genus name *Mediaverrunites* (*Potamomyces*).

5.2.1.4. *Pithomyces chartarum* (Plate 2: 17)

Pithomyces is a genus of the dematiaceous Hyphomycetes (Ellis, 1971) and actually placed into the ascomycete family Montagnulaceae of the large order Pleosporales (Da Cunha Et Al., 2014). The genus *Pithomyces* comprises today about 15 species (Ellis et al., 2007). Ellis (1971, 1976) provide a spore-based key to most of them.

The conidiospores of *Pithomyces chartarum* are muriform, broadly ellipsoid, 18–29 × 10–17 µm, medium to dark brown with an

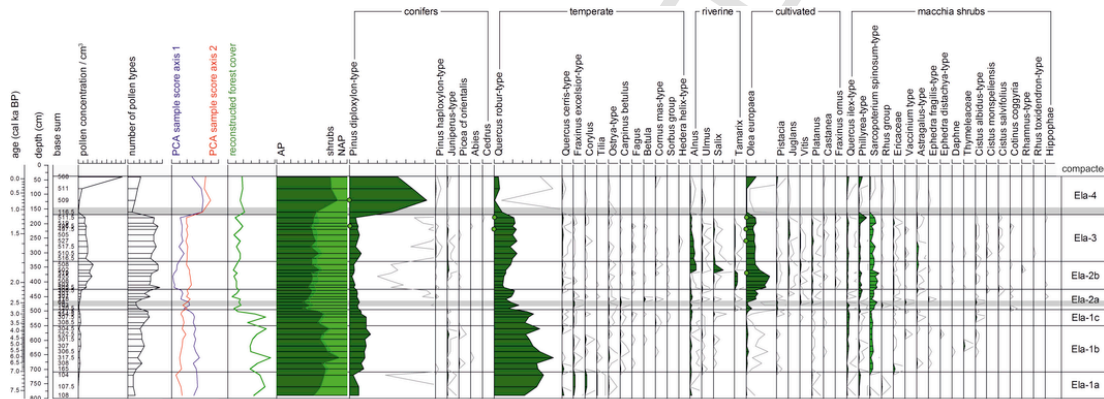


Fig. 5. Arboreal pollen (trees and shrubs; AP) diagram of sediment core Ela-70. Green circles indicate the presence of pollen clumps. (For interpretation of the references to colour in this figure legend, the reader is referred to the web version of this article.)

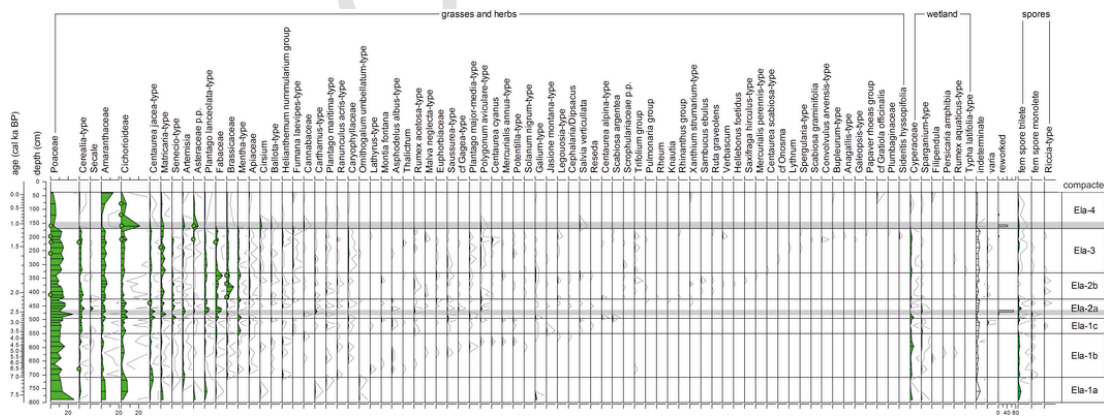


Fig. 6. Non-arboreal pollen (NAP) diagram of sediment core Ela-70. Green circles indicate the presence of pollen clumps. (For interpretation of the references to colour in this figure legend, the reader is referred to the web version of this article.)

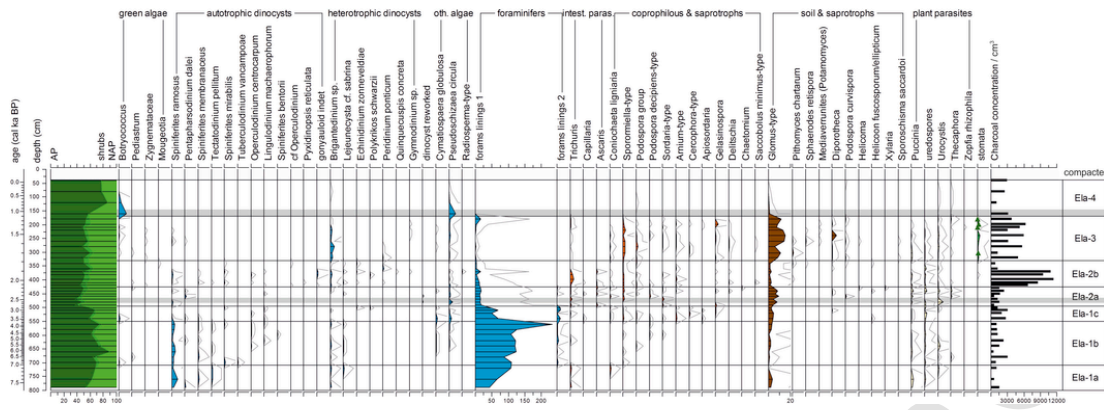


Fig. 7. Non-pollen palynomorphs (NPP) diagram of sediment core Ela-70. Green triangles indicate *Pinus* stomata. (For interpretation of the references to colour in this figure legend, the reader is referred to the web version of this article.)

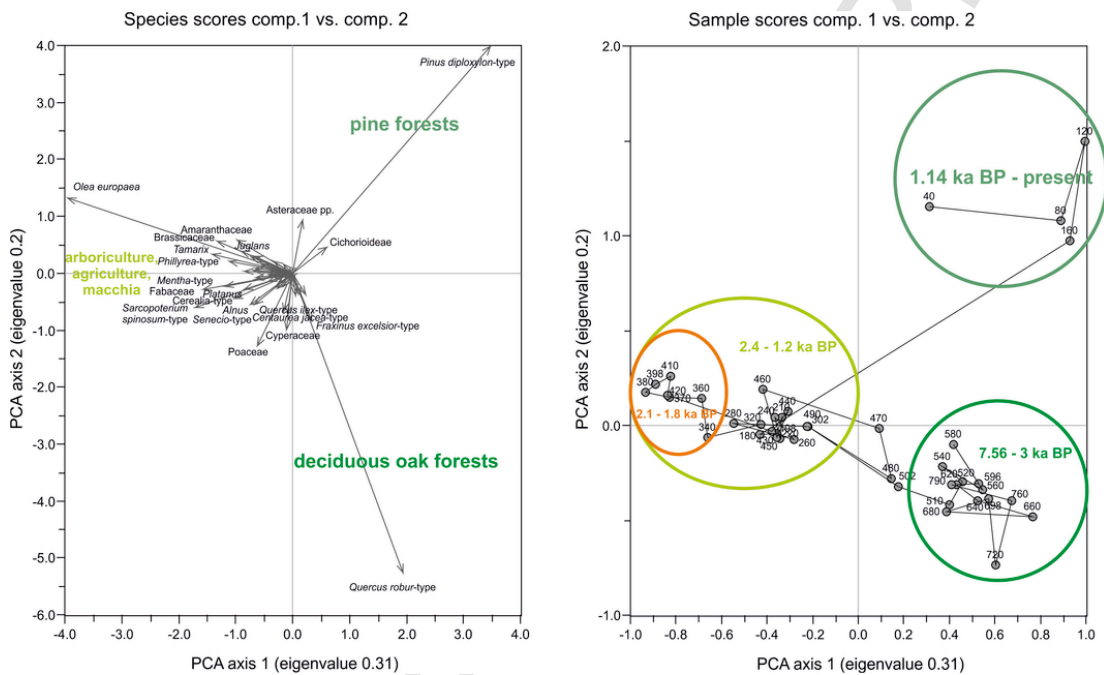


Fig. 8. PCA plots of the pollen record Ela-70.

echinulate to verrucose surface, slightly constricted at the septa (Ellis, 1971). They are distinguished from other muriform spores in the genus by their high number of 3–4 transverse septa (Ellis, 1971, 1976; Marasas et al., 1972). The middle cells are divided each by a longitudinal septum. The apical cell is obtuse; the basal cell bear a small remain of the denticle that attached the conidiospore to the mycelium (Ellis, 1971; Ellis et al., 2007). The surface might be also smooth (Watanabe, 2010).

P. chartarum is a wide spread largely saprophytic fungus isolated from different kind of substrates but mostly from decaying leaves of a wide variety of plants (Ellis, 1971), in high priority from grasses (Ellis and Ellis, 1997; Caretta et al., 1999). The fungus prefers the warm temperate climates of the tropics and subtropics but also inhabits temperate regions (Di Menna et al., 2010; Gregory et al., 1964; Marasas and Schumann, 1972).

P. chartarum is also a pathogen of cereals (Chong et al., 1982; Tóth et al., 2007), but the more for ruminants. Many isolates of *P. chartarum* produce the mycotoxin sporidesmin causing facial eczema

(Collin et al., 1998). In New Zealand, facial eczema of sheep is known for over 100 years and appears when *P. chartarum* sporulates profusely after rain in late summer and autumn (Di Menna et al., 2010). Lately van Wuijckhuise et al. (2006) described facial eczema by *P. chartarum* from Europe.

P. chartarum can be also isolated from soils (Domsch et al., 2007; Watanabe, 2010), dung pellets collected from the ground (Kuthubutheen and Webster, 1986) and occurs in air traps (Lacey and West, 2006). Fossil spores are reported for the late Pleistocene from lake sediments and dung (Murad, 2011; Pirozynski et al., 1984).

5.2.1.5. *Podospora curvispora* (Plate 2: 8)

The ascospores of *Podospora curvispora* are dark-brown 11–13 (17) × 8–10 μm, strongly curved, concave on one side and convex on the other, with an apical germ pore of 1 μm in diameter (Mirza and Cain, 1969). In contrast, morphologically similar ascospores of *Podospora selenospora* have a germ pore on the convex side of the spore (Stchigel et al., 2002). Shumilovskikh et al. (2015) reported

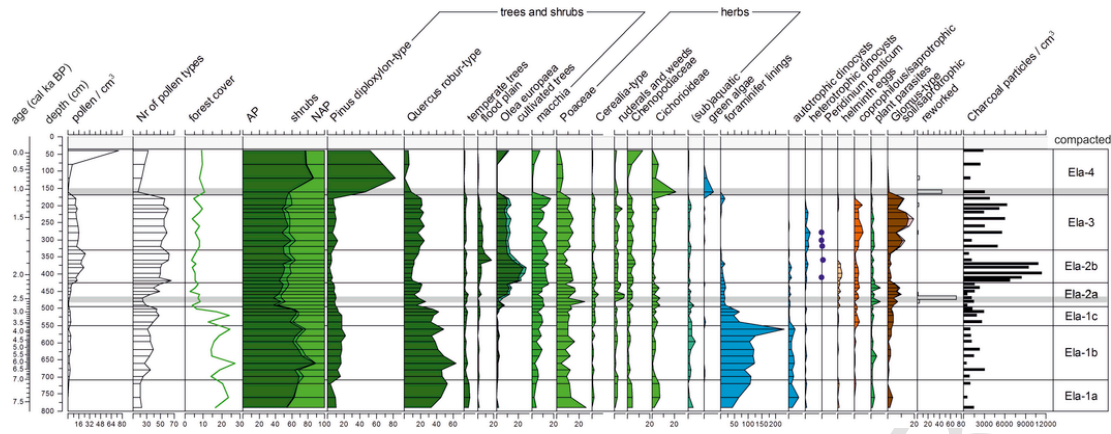


Fig. 9. Summary diagram of vegetation and environmental changes in Elaia.

about the similarity of *Podospora curvispora* to NPP type IBB-18 (Montoya et al., 2010). *P. curvispora* grows on decaying plant substrates, burnt soil and dung in subtropical and tropical regions (Krug and Khan, 1989; Mirza and Cain, 1969; Wicklow, 1975).

5.2.1.6. *Saccobolus minimus*-type (Plate 2: 4)

Saccobolus is a wide spread genus of the Ascobolaceae (Ascomycetes) covering about 30 mainly coprophilous species (van Brummelen, 1967; Kirk et al., 2008). The spores are characterised by a violet to purple-brownish pigmentation and their arrangement in firmly clustered bundles (Bell, 2005; Doveri, 2014). The spores found in core Ela-70 (Plate 2: 4) have a size of $13\text{--}14 \times 7\text{--}8 \mu\text{m}$. They resemble very much those of *Saccobolus minimus* ($13.5\text{--}16 \times 7\text{--}8 \mu\text{m}$), *S. truncatus* ($14.8\text{--}15.3 \times 7.2\text{--}7.6 \mu\text{m}$) and *S. depauperatus* ($12.5\text{--}15 \times 6.5\text{--}7 \mu\text{m}$) (Doveri, 2007 p. 441) and are therefore included in the herewith erected *S. minimus*-type.

5.2.1.7. *Sphaerodes retispora* (Plate 2: 18)

The ascospores in *Sphaerodes* are usually coarsely reticulate with the two protruding apical germ pores (Cannon and Hawksworth, 1982). The genus covers about a dozen species isolated from soils from different parts of the world (Garcia et al., 2004; Guarro et al., 2012). An updated spore based key is given by Vujanovic and Goh (2009). Spores found in Elaia (Plate 2: 18) are $19\text{--}21 \times 14\text{--}15 \mu\text{m}$ in size with broad reticulate surface characteristic for *Sphaerodes retispora* (Garcia et al., 2004).

5.2.1.8. *Zopfia rhizophila* (Plate 2: 1, 2)

The parasitic genus *Zopfia* (Zopfiaceae, Ascomycetes) covers 3 species (Cannon and Kirk, 2007; Zhang et al., 2012) that differ in spore morphology, geographical distribution and plant hosts. The ascospores found in Ela-70 (Plate 2: 1–2) are one-septate, $71 \times 49 \mu\text{m}$ in size, dark-brown to black with a verrucate surface, tapered ends and very thick wall. Morphologically and in size they are similar to spores of *Zopfia rhizophila* ($60\text{--}80 \times 30\text{--}45 \mu\text{m}$), a plant parasite, which can be found on decaying roots of *Asparagus* (Ellis and Ellis, 1997), indicating possible presence of asparagus in the vicinity of Elaia.

5.2.2. Palynological diagram

Based on main changes in pollen and NPP assemblages (Figs. 5–7), changes in the two first PCA axes (Figs. 5 and 8) and CONISS dendrogram (Supplementary 1), the diagram was divided into four main local pollen zones (LPZ).

LPZ Ela-1 (800–495 cm, $\sim 7.56\text{--}2.8$ ka BP = 5600–850 BC) is characterised by the dominance of *Quercus robur*-type (35–64%), *Pinus diploxylon*-type (4–22%) and Poaceae (4–27%). Pollen concentrations vary between 350 and 4500 pollen/cm³. Samples of this zone contain a lot of foraminiferal linings (43–107%) and autotrophic dinocysts (up to 7%), decreasing towards the end of the zone, whereas spores of coprophilous/saprotrophic and soil/saprotrophic fungi increase in its upper part up to 4–5%. The zone is subdivided in 3 sub-zones.

LPZ Ela-1a (800–710 cm, $\sim 7.56\text{--}7$ ka BP = 5600–5100 BC) is characterised by the lowest pollen concentration (350–620 pollen/cm³) and number of pollen taxa (20–23) in the record. Pollen spectra are dominated by *Quercus robur*-type (32–53%) and *Pinus diploxylon*-type (4–10%). Pollen of temperate trees *Tilia*, *Ostrya*-type, *Corylus*, and *Fraxinus excelsior*-type occur regularly (1–2%). NAP is mainly presented by Poaceae (12–27%), Cichorioideae (2–7%) and Amaranthaceae (5%). Foraminifer linings increase from 43 to 108%, autotrophic dinocysts (*Spiniferites ramosus*, *Spiniferites membranaceus*, *Tectatodinium pellitum*) and *Glomus*-type show maxima of 7 and 4%. Eggs of intestinal parasites *Trichuris* and *Capillaria* are present.

LPZ Ela-1b (710–550 cm, $\sim 7\text{--}3.66$ ka BP = 5100–1700 BC) is indicated by the dominance of *Quercus robur*-type (34–64%), *Pinus diploxylon*-type (13–23%), and an increase of macchia shrubs (2.5–8.5%), especially *Sarcopoterium spinosum*-type. Pollen concentration increased up to 4.000 pollen/cm³ and spectra get more diverse, with the number of pollen taxa ranging from 25 to 39. Foraminiferal linings have maximum of 233%, and *Glomus*-type increase up to 3% at the end of the zone.

LPZ Ela-1c (550–495 cm, $\sim 3.66\text{--}2.8$ ka BP = 1700–850 BC) is characterised by a decrease of *Quercus robur*-type (35%) and *Pinus diploxylon*-type (12%), and an increase of *Olea europaea* (2%), Cerealia-type (3.6%), macchia indicators (5–10%) and generally NAP (31–38%). Pollen concentrations remain similar to the previous zone, while the number of pollen taxa reaches its maximum of 45 types. The marine indicators, such as foraminiferal linings and autotrophic dinoflagellate cysts, decrease in the total amount of microfossils, while the role of fungal spores increase due to more abundant and diverse assemblages of coprophilous/saprotrophic and soil/saprotrophic fungi.

LPZ Ela-2 (495–330 cm, $\sim 2.8\text{--}1.77$ ka BP = 850 BC–AD 180) is dominated by *Olea europaea* (6–25%), *Quercus robur*-type (10–26%), *Pinus diploxylon*-type (3–10%), with increased percentages of macchia shrubs, Cerealia-type, and weeds. The total microfossil assemblage is characterised by an increased role of fungal

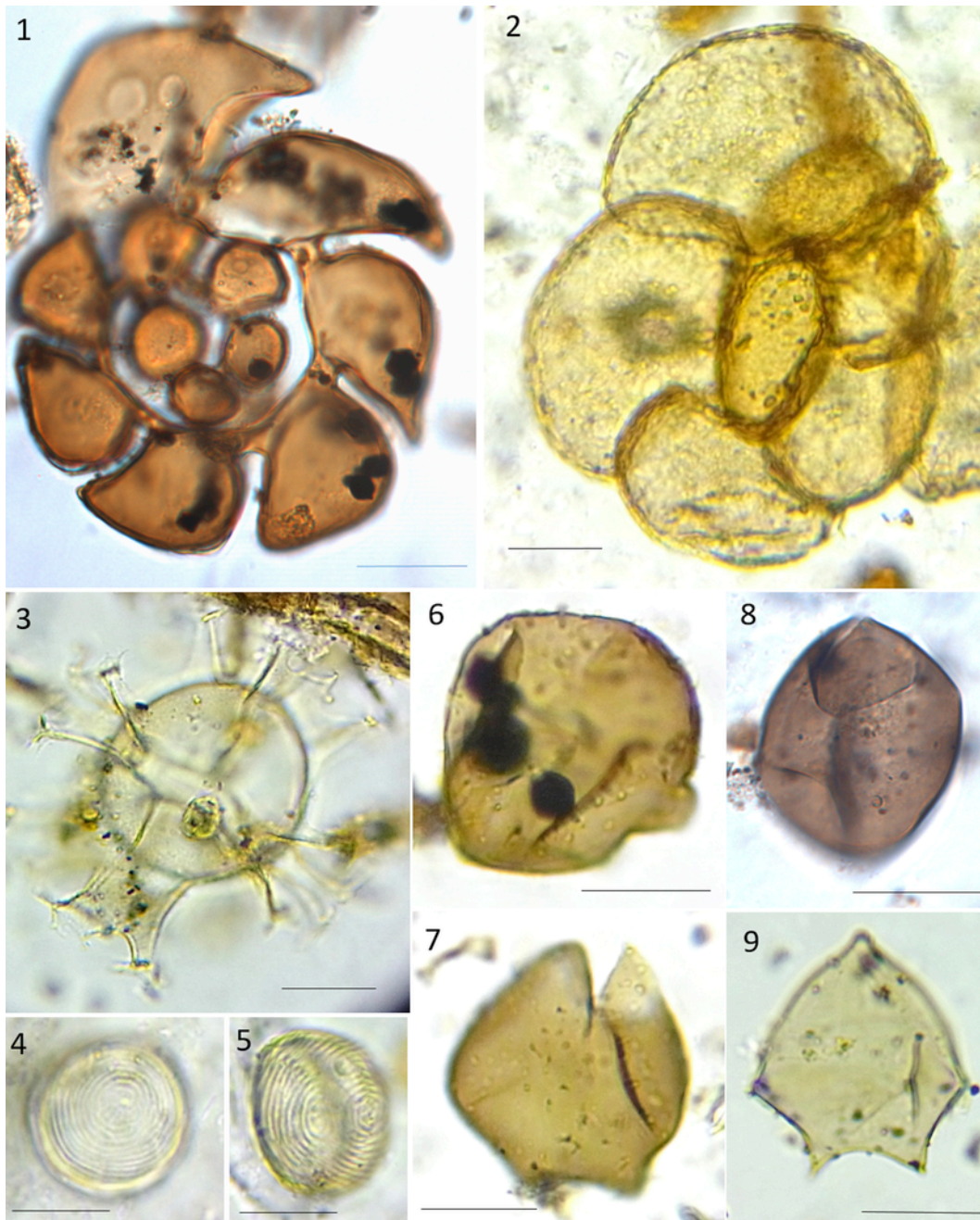


Plate 1. Foraminifer remains and dinocysts: 1) foraminifer lining 1a (680 cm), 2) foraminifer lining 1b (180 cm); 3) *Spiniferites mirabilis* (560 cm); 4) *Pseudoschizaea circula* (180 cm); 5) *Pseudoschizaea circula* (460 cm); 6–7) *Peridinium ponticum* (360 cm, 320 cm); 8) *Brigantedinium* sp. (420 cm); 9) *Lejeunecysta* cf. *sabrina* (720 cm). Scale bar 20 μm .

spores and eggs of intestinal parasites, and a reduction of marine indicators.

In comparison to the previous zone, in LPZ Ela-2a (495–425 cm, ~2.8–2.12 ka BP = 850–170 BC) *Quercus robur*-type (12–26%) and *Pinus diploxylon*-type (8–10%) continue to decrease, while *Olea europaea* (2–25%) and macchia shrubs increased further. Percentages of Cerealia-type, *Platanus*, *Pistacia*, and *Vitis* are higher than before, and *Juglans* increases at the end of the zone. NAP show a maximum of 45–58%, dominated by Poaceae (8–25%) and presented by a very diverse assemblage with Asteraceae (Cichorioideae, *Centaurea jacea*-type, *Matricaria*-type, *Senecio*-type, *Artemisia*,

Carthamus-type, *Saussurea*-type), Fabaceae, *Plantago lanceolata*-type etc. Pollen concentrations are similar to the previous zone (800–5200 pollen/cm³) and the number of pollen types reaches 49. NPP assemblages are still dominated by foraminifer linings, which, however, decrease to 16–17%. *Glomus*-type and spores of plant parasites reach their maxima densities in this zone (9 and 8%, respectively). Eggs of intestinal parasites occur regularly in the sediment, while *Ascaris* appears for the first time. The core depth 480–470 cm differs from other samples in this zone by low concentration (800–1600 pollen/cm³), decreased number of pollen types (24–25),

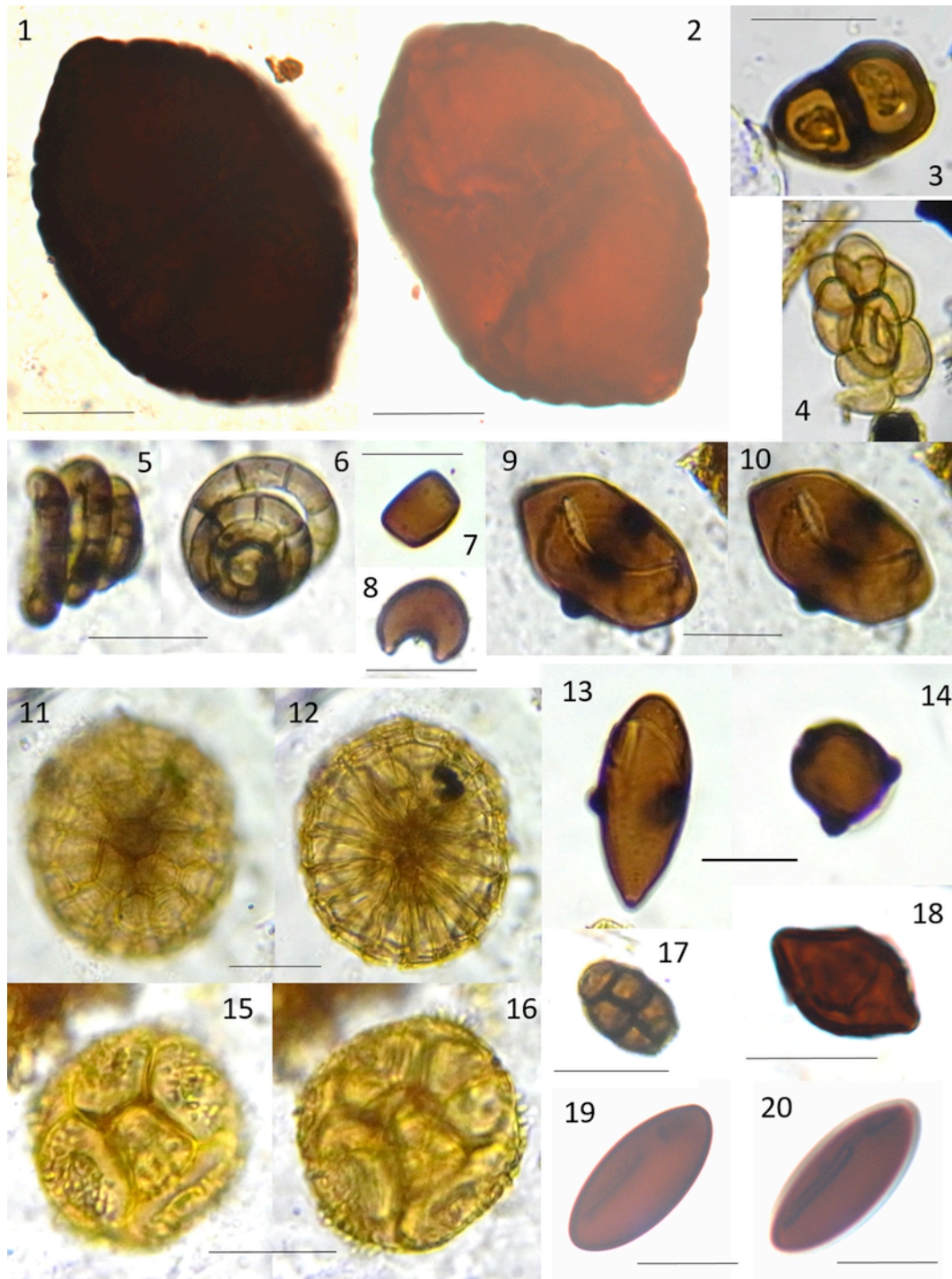


Plate 2. Fungal spores: 1–2) *Zopfia rhizophila* (210 cm); 3) *Puccinia* (302 cm); 4) *Saccobolus minimus*-type (280 cm); 5–6) *Helicoon fuscosporum/ellipticum* (440 cm); 7) *Sporormiella*-type (280 cm); 8) *Podospora curvispora* (180 cm); 9) *Mediaverrucites pontiadiensis* (240 cm); 11–12) *Glomosporium leptideum* (180 cm); 13–14) *Mediaverrucites el-sikii* (198 cm); 15–16) *Thecaphora* (180 cm); 17) *Pithomyces chartarum* (302 cm); 18) *Sphaerodes retispora* (260 cm); 19–20) *Xylaria* (340 cm). Scale bar 20 μ m.

the lowest abundance of *Olea europaea* (1.5–2%), and high amount of reworked pollen (5–72%).

LPZ Ela-2b (425–330 cm, \sim 2.12–1.77 ka BP = 170 BC–AD 180) is characterised by maximum of *Olea europaea* (25%), accompanied by *Platanus*, *Pistacia*, *Vitis*, *Juglans*, and *Fraxinus ornus*. Cerealia-type pollen reaches a maximum of 5% and decreases towards the end of the zone. Riverine taxa increase here with maxima of *Tamarix* (3.5%) and later *Alnus* (6%) and *Salix* (10%). NAP is dominated by

Poaceae (6–15%), Amaranthaceae (3–7%), Brassicaceae (3–8%), and Fabaceae (0.6–8%). The zone is characterised by the highest pollen concentration, varying between 13,000 and 26,000 pollen/cm³, and highest numbers of pollen types (48–66). The foraminiferal linings decreases from 12 to 3% of the assemblage in the end of the zone. Dinocysts are represented by autotrophic (3%) and heterotrophic (2.5%) species equally. Notifiable is the occurrence of *Peridinium ponticum* at 410 cm. *Trichuris* has the maximum of 3% and is accom-

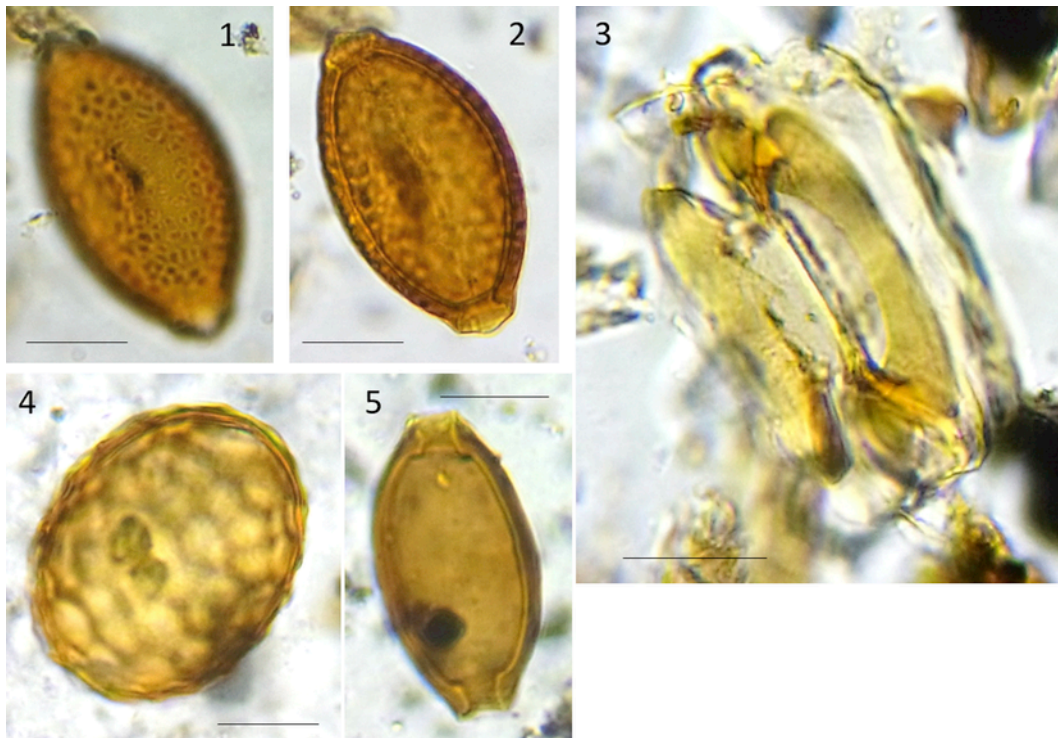


Plate 3. Conifer stomata and helminth eggs: 1, 2) *Capillaria* egg (540 cm); 3) conifer stomata (302 cm); 4) fertilized *Ascaris* egg (490 cm); 5) *Trichuris* egg (490 cm). Scale bar 20 μm .

panied by *Ascaris*. *Glomus*-type does not exceed 2.5%. The charcoal concentration is the highest (6.7×10^5 – 11.4×10^5 particles/ cm^3) at 420–370 cm; it decreases towards the end of the zone.

In the LPZ Ela-3 (330–170 cm, ~ 1.77 – 1.14 ka BP = AD 180–800), *Quercus robur*-type and *Pinus diploxylon*-type increase up to 25 and 12%, respectively, whereas *Olea europaea* and *Alnus* decline. NAP is again dominated by Poaceae, Asteraceae (Cichorioideae, *Matricaria*-type, *Senecio*-type, *Centaurea jacea*-type, *Artemisia*, *Cirsium*), and Amaranthaceae, similar to the LPZ Ela-2a. Macchia shrubs vary between 4 and 15%, weeds and overgrazing indicator species slightly decrease. Pollen concentration (10,000–15,000 pollen/ cm^3) and number of types (50–62) slightly decrease. Foraminiferal linings occur sporadically, dinocysts are mainly represented by heterotrophic species (0.2–3.8%). A strong increase in the abundance and diversity of coprophilous fungi (*Sporormiella*-type, *Podospora* group, *Podospora decipiens*-type, *Saccobolus*), soil (*Glomus*-type, *Sphaerodes retispora*), and saprotrophic fungi (*Mediaverrucites/Potamomyces*, *Pithomyces chartarum*, *Diporothea*, *Helicoma*, *Helicoon fuscospirium/ellipticum*, *Podospora curvispora*, *Sporoschisma saccardoii*) is noticeable. Plant parasites slightly increase. Charcoal concentrations vary between 1.2×10^5 and 6.4×10^5 particles/ cm^3 .

LPZ Ela-4 (170–40 cm, ~ 1.14 ka BP-present = AD 800-present) differs from the previous zones by the absolute dominance of *Pinus diploxylon*-type (46–83%), whereas *Quercus robur*-type does not exceed 8.5%. *Olea europaea* remains low (<1%), but increases in the uppermost sample (10%), similar to macchia shrubs. Temperate and riverine trees appear in low abundance (<1%). In NAP, Asteraceae and Poaceae dominate the lower part, and Amaranthaceae and Poaceae the upper part. Pollen concentrations increase from 500 pollen/ cm^3 at the beginning and up to 75,000 pollen/ cm^3 at the top sample. Number of types increases from 17 to 32. The sample from

the core depth 160 cm differs from the upper part of the zone by the high abundance of reworked pollen, low pollen concentration (500 pollen/ cm^3), and low number of types (17). Microfossil spectra are very poor and represented by green algae *Botryococcus* and *Pseudoschizaea circula* in the lower part of the zone, whereas *Glomus*-type decrease to <1%. The top core sample contains almost exclusively pollen, lacking other palynomorphs.

PCA (Fig. 8) contains 54 variables exceeding the abundance of 1% and 42 samples. The first two principal components explain 51% of the total variance. The first PC axis (eigenvalue 0.31) is oriented between positive species score values of *Quercus robur*-type (1.94) and *Pinus diploxylon*-type (3.46), and negative of *Olea europaea* (–3.9), *Phillyrea*-type (–1.1), *Tamarix* (–1.4), Brassicaceae (–1.3), Cerealia-type (–1), Fabaceae (–1.56), *Mentha*-type (–1.19) and *Sarcopoterium spinosum*-type (–1.7). The second PC axis (eigenvalue 0.2) is oriented between positive species score values of *Olea europaea* (1.3), *Pinus diploxylon*-type (3.97), and negative of *Quercus robur*-type (–5.25) and Poaceae (–1.3). Plotted PCA sample scores divide all depths into three well recognisable groups: group 1 is presented by 790–510 cm and several transitional samples between 502 and 470 cm; group 2 (460–180 cm) includes a significant subgroup 2a (420–340 cm); and group 3 (160–40 cm).

The reconstructions of areas covered by tree vegetation using the BMA approach for the study area near the ancient city of Elaia (Fig. 5) shows a variation in the total woodland coverage of 15–25% during the period between ca. 7.56–2.8 ka BP (5600–850 BC). An abrupt decrease in woodland coverage from 17 to 6% occurred around 2.8 ka BP (850 BC). In the pollen diagram this event corresponds to changes in the composition of the pollen assemblages at the boundary between LPZ Ela-1 and 2 (495 cm). Later on, areas covered by forests remained sparse. During the period ~ 2.8 – 1.77 ka BP (850

Table 3
Pollen and non-pollen palynomorphs ordered to different ecological groups.

Vegetation groups	Pollen types
Cultivated trees	<i>Castanea</i> , <i>Fraxinus ornus</i> , <i>Juglans</i> , <i>Olea europaea</i> , <i>Pistacia</i> , <i>Platanus</i> , <i>Vitis</i>
Macchia	<i>Astragalus</i> -type, <i>Cistus albidus</i> -type, <i>Cistus monspeliensis</i> , <i>Cistus salviifolius</i> , Ericaceae, <i>Daphne</i> , <i>Mentha</i> -type, <i>Salvia verticillata</i> , <i>Sarcopoterium spinosum</i> -type, <i>Rhus</i> group, Thymelaeaceae, <i>Vaccinium</i> -type, <i>Quercus ilex</i> -type, <i>Phillyrea</i> , <i>Ephedra distachya</i> -type, <i>Ephedra fragilis</i> -type, <i>Rhamnus</i> -type, <i>Hippophae</i> , <i>Cotinus coggygria</i> , <i>Juniperus</i> -type
Temperate trees	<i>Carpinus betulus</i> , <i>Corylus</i> , <i>Fagus</i> , <i>Fraxinus excelsior</i> , <i>Hedera helix</i> -type, <i>Tilia</i> , <i>Sorbus</i> group, <i>Ostrya</i> -type, <i>Quercus cerris</i> -type, <i>Betula</i> , <i>Cornus mas</i> -type
Flood plain	<i>Alnus</i> , <i>Salix</i> , <i>Ulmus</i> , <i>Tamarix</i>
Ruderals and weeds	<i>Artemisia</i> , <i>Centaurea cyanus</i> , <i>Papaver rhoeas</i> group, <i>Plantago lanceolata</i> -type, <i>Plantago major-media</i> -type, <i>Polygonum aviculare</i> -type, <i>Ranunculus acris</i> -type, <i>Rumex acetosa</i> -type, <i>Xanthium strumarium</i> -type
(Sub)aquatic	Cyperaceae, <i>Sparganium</i> -type, <i>Typha latifolia</i> -type, <i>Rumex aquaticus</i> -type, <i>Filipendula</i>
Green algae	<i>Botryococcus</i> , <i>Pediastrum</i> , <i>Mougeotia</i> , Zygnemataceae
Dinocyst groups	Dinocyst species
Autotrophs	<i>Lingulodinium machaerophorum</i> , <i>Operculodinium centrocarpum</i> , <i>Pentaparsodinium dalei</i> , <i>Pxydinopsis reticulata</i> , <i>Spiniferites bentorii</i> , <i>Spiniferites membranaceus</i> , <i>Spiniferites mirabilis</i> , <i>Spiniferites ramosus</i> , <i>Tectatodinium pellitum</i> , <i>Tuberculodinium vancampoae</i>
Heterotrophs	<i>Lejeunecysta cf. sabrina</i> , <i>Brigantedinium</i> sp., <i>Peridinium ponticum</i> , <i>Gymnodinium</i> sp., <i>Echinidinium zonneveldiae</i> , <i>Quinquecuspis concreta</i>
Fungal spore groups	Fungal spore types
Soil/saprotrophic	<i>Glomus</i> -type, <i>Pithomyces chartarum</i> , <i>Sphaerodes</i> , <i>Potamomyces</i> , <i>Diporothea</i> , <i>Helicoma</i> sp., <i>Podospora curvispora</i> , <i>Xylaria</i> , <i>Sporoschisma saccardoii</i>
Coprophilous/saprotrophic	<i>Arniium</i> -type, <i>Coniochaeta ligniaria</i> , <i>Delitschia</i> -type, <i>Podospora</i> -type, <i>Podospora decipiens</i> -type, <i>Saccobolus</i> , <i>Ascobolus</i> , <i>Sordaria</i> -type, <i>Sporormiella</i> -type, cf. <i>Apiosordaria</i> , <i>Gelasinospora</i> , <i>Chaetomium</i>
Plant parasites	<i>Puccinia</i> -type, <i>uredospores</i> , <i>Urocystis</i> , <i>Thecaphora</i> , <i>Zopfia rhizophila</i>
Intestine parasites	<i>Trichuris</i> , <i>Capillaria</i> , <i>Ascaris</i>

BC-180 AD), the woodland coverage shrank to 5%. After ~1.77 ka BP (AD 180), it became slightly extended up to 10% (LPAZ Ela-3).

It seems that the woodland coverage reconstructed on the base of pollen data of the upper part of the core (LPAZ Ela-3, ~1.14 ka BP-present = AD 800-present) is underestimated. In assemblages of the LPAZ Ela-3 the pollen value of *Pinus* is high while other trees are not abundant. In the surface pollen spectra from the Mediterranean region these were taken as analogues for reconstructions using the BMA technique. Pine pollen is transported by wind, often over hundreds of kilometres. Relatively high percentages of *Pinus* pollen are often recorded in pollen assemblages from tree-less territories, clearly affecting the reconstructions.

6. Interpretation

6.1. Sedimentology versus Palynology

The sediment record of Ela-70 starts at ~7.5 ka BP, when the rising level of the Aegean Sea reached the Bay of Elaia, creating a beach environment at the coring site (Fig. 4). The littoral environment then changed to shallow marine conditions, which abruptly changed into lagoon conditions when the harbour was constructed. Thus, the depositional environment changed several times during the

past seven millennia (Seeliger et al., 2013). Such considerable changes might have influenced the pollen source area, pollen preservation conditions, and therefore, pollen concentrations and spectra of the record.

The lowermost part of the core (803-717 cm), composed by sands with pebbles, indicates that a high energy wave climate (beach) existed up to 7 ka BP. This may have caused selective pollen destruction, low concentrations and possibly very mixed pollen assemblages in LPZ Ela-1a (Fig. 5).

The change of the sedimentary conditions after 7 ka is to be explained by the further rise in sea-level, leading to the transition from a littoral to a shallow marine environment with *Posidonia oceanica*. *Posidonia oceanica* (L.) Delile is a seagrass species endemic to the Mediterranean Sea. It grows on the surface or up to a depth of 40 m and plays a major ecological role through forming a “mantle” of horizontal and vertical rhizomes, entrapping the sediment (Montefalcone, 2009). Due to the stabilizing conditions in the shallow marine milieu, finer grained material (silts, loam) was deposited (Fig. 4), providing better conditions for pollen preservation. This is reflected in increased pollen concentrations in zones LPZ Ela-1b, Ela-1c and Ela-2a (Fig. 5). Open water conditions allow the transport and mixing of pollen from insect-pollinated plants growing in the surrounding areas, providing a general picture of the local and regional vegetation in the pollen spectra.

An important sediment change from sands to medium clayey silt occurs at 4.38 cm (~2.22 ka BP = ~260 BC), very likely due to the construction of harbour breakwaters (Fig. 4). This triggered siltation process led to an increase in the accumulation rate to 15–44 mm/yr as well as higher pollen concentration and better pollen preservation in zones Ela-2a and Ela-3 (Fig. 5).

In the upper part (184-0 cm), the sediment consists of silty loam (Fig. 4), deposited after AD 800 when the coastline moved south of the silted-in harbour (Fig. 2a). Pollen concentrations are quite low at 160-80 cm but increase in the upper part of the core (Fig. 5), indicating the development of the vegetation directly at the coring site. An increase in the pollen concentration by a factor 12 (Fig. 5) is very likely due to the compacting of the upper 40 cm caused by the vibracoring technique. The siltation of the Bay of Elaia might have led to a change of the pollen source area, so that pollen spectra are represented here by local vegetation and wind-pollinated plants.

Two unusual deposition events, derived from the pollen analysis (Figs. 5–7) and coinciding with an increased amount of sand fraction in the sediment (Fig. 4). The first one, at a depth of 480–470 cm, is characterised by low pollen concentration, decreased number of pollen types, the presence of reworked pollen and dinocysts. According to the age/depth model this is more or less the time when the harbour basin was constructed; thus, it may represent a building activity in connection with these measures or a strong storm event. The second one at ~160 cm is characterised by a low pollen concentration, a decreased number of pollen types, and the presence of reworked pollen. After the second event, the pollen spectra changed considerably, suggesting a possible hiatus in sedimentation between 180 and 160 cm. This occurred during in the Byzantine time. By then the harbour was out of use, but its usage as saltworks is known from that time (Seeliger et al., 2014). It is interesting to note that palynological data provide the first indication of both events.

6.2. Vegetation and environmental development

According to the age-depth model (Fig. 3), the Holocene sedimentation of the Bay of Elaia started at ~7.56 ka BP (at least at the coring site), allowing for the reconstruction of vegetation and environmental changes since that time. The natural vegetation was represented

mainly by open deciduous *Quercus* forests with *Pinus*, *Tilia*, *Fraxinus excelsior*, *Corylus*, and *Carpinus betulus*, with total woodland coverage around 15–25% as well as by open grassland and macchia at dry habitats (Ela-1a). In general, in the Mediterranean region macchia is represented by thorny and unpalatable plant species such as *Quercus ilex*, *Phillyrea*, *Sarcopoterium*, *Astragalus*, Cistaceae, and Thymelaeaceae that spread in response to high pasture pressure. In the given profile, macchia indicators increase after ~7 ka BP (Ela-1b), suggesting an increase in pastures. Foraminiferal linings and the dinocysts *Spiniferites ramosus*, *S. membranaceus*, *Tectatodinium pellitum*, *Brigantodinium* sp., and *Lejeunecysta* cf. *sabrina* are evidence of the marine environment.

Between 7 and 2.8 ka BP (Ela-1b, Ela-1c), a general decrease of oak, a development of macchia and an increase of *Olea*, *Platanus*, *Pistacia*, and ruderal plants indicate an intensification of the human impact on the environment. Anthropogenic pressure was not constant, alternating between reforestation periods, notably from around 3.6 to 2.9 ka BP (1900 and 1000 BC, Ela-1c). The rise of spores of coprophilous fungi such as *Sporormiella*-type, *Podospora decipiens*-type, *Podospora* group, *Sordaria*-type, *Delitschia*, *Gelasinospora*, and *Cercophora* suggest increased pastoral activities around Elaia since ~3.4 ka BP (1500 BC). Coprophilous fungi usually grow on dung of herbivores, but some species also on decaying organic matter. They are usually used as indicators of the presence of herbivores close to the site (van Geel et al., 2003).

At ~2.8 ka BP (850 BC) a definite phase of landscape use with intensive olive cultivation started (Ela-2a). Natural open oak forests were degraded and replaced by macchia. The areas covered by tree vegetation decreased to ca. 5%. Apparently, the territory surrounding the ancient city of Elaia was treeless or covered by olive groves. Natural forest remains were not located near Elaia, but possibly situated on higher hills. Strong impact on vegetation with high pasture pressure led to increased soil erosion, as indicated by the frequent presence of the *Glomus*-type (Glomeromycota) spores. Glomeromycota is a group of mycorrhizal fungi, growing symbiotically on plant roots. The complete life cycle of Glomeromycota species occurs in the soil; therefore, the presence of their chlamydospores in the lacustrine or marine sediment indicates soil erosion (van Geel et al., 1989).

The most intensive phase of human impact on the ecosystems around Elaia occurred between 2.12 and 1.77 ka BP (170 BC-AD 180, Ela-2b), corresponding to the construction of the breakwaters of the harbour around 260 BC. Arboriculture with olives, walnut, plane tree, pistachio, and grapes, as well as agriculture and pastoralism dominated the landscape around the city. During the peak of Elaia's occupation, the frequent occurrence of eggs of intestinal parasites (*Ascaris* and *Trichuris*) suggests the presence of a sewerage in the city. The harbour activities, the highly populated city and the sewage led to the nitrification of the harbour waters, which is suggested by an increase of heterotrophic dinocysts. Since 2.3 ka BP (~80 BC), the endemic Black Sea dinocyst *Peridinium ponticum* occur regularly in the sediment, suggesting naval trade to the Black Sea and/or the Sea of Marmara.

From 1.77 to 1.14 ka BP (AD 180–800, Ela-3), olive cultivations decreased and pastoral pressure strongly increased. This occurred during the demise of Elaia in the late Roman period. Because of a reduction in the intensity of agricultural and arboricultural pursuits, the natural vegetation spread out in the landscape, first with macchia and later with oaks. However, with not more than 10% the woodland coverage maintained relatively low. The increased pasture, indicated by increased spores of coprophilous fungi, led to a further increase of soil erosion, suggested by high percentages of soil/saprotrophic fungi. Interesting to note the presence of *Mediaverrucites/Potamomyces* in

this zone (Fig. 7). *M. pontiidiensis* and *M. elsikii* (Plate 2) were described from Miocene sediments in the Black Sea and northern Turkey and possibly indicate deep sediment erosion in the vicinity of Elaia (Sancay, 2014). The erosion effect was the rapid siltation of the harbour, the sediments of which do not have any remains of foraminifers or dinocysts after AD 800.

After 1.14 ka BP (AD 800, Ela-4), the dominance of *Pinus* in the pollen spectra suggests an expansion of the pine forests, possibly with *Pinus brutia* close to the site; it may also indicate open landscapes. Pine produces large amounts of pollen, which can dominate the pollen spectra of open regions, even if no pine grows in the immediate vicinity. Human impact is identifiable in these sediments, but it is less blatant than before. The reconstructions of woodland cover show that arboreal vegetation occupied about 10% of the territory, but these assessments are probably underestimated. Towards the present situation, an increase of *Amaranthaceae* indicates the development of salt marshes with *Salicornia* and *Atriplex* in the silted harbour area, whereas an increase of *Olea* reflects modern olive cultivation on the surrounding hills of Elaia.

PCA axis 1 reflects a difference between oak or pine dominated forests to human-made olive groves and macchia shrubs, whereas PCA axis 2 reveals a dissimilarity between oak forests at the beginning of the record and pine forests at the end. The PCA clearly reflects the general evolution of the vegetation from natural deciduous oak forests, dominating during the time span 7.56–3 ka BP (5600–1000 BC), to human-made olive groves and grazed macchia shrubs, dominating during the period 2.4–1.2 ka BP (440 BC-AD 730), with a maximum at 2.09–1.84 ka BP (170 BC-AD 160), and back to semi-natural forests dominated by pine later than ~1.14 ka BP (AD 800). It is notable that after a decrease of the anthropogenic pressure, lasting for ~1200 years, the vegetation did not return into the original stage with the dominance of oak but transformed to a new stage: the pine forest.

7. Discussion

7.1. From natural to human-made landscapes and ecosystems

The mid- to late Holocene shift from natural to cultural landscapes is evidenced by many records in Mediterranean (e.g. Brückner et al., 2006; Zanchetta et al., 2013). Pollen data from Ela-70 reveals that the natural vegetation around Elaia was represented by open pine and deciduous oak forests with ash, hazel, and linden (Figs. 5 and 9). Dry habitats remained open or were occupied by macchia shrubs. Temporary human impact alternated with reforestation of natural open oak forests. Similar vegetation of open pine and oak forests during the mid-Holocene is evidenced by other palynological studies from western and south-western Turkey: Bafa Gölü (Knipping et al., 2008), Gölhisar Gölü (Eastwood et al., 1999; Bottema and Woldring, 1984), and Süğüt (Roberts, 1990).

At ~850 BC the continuous human impact on the environment, starting in Elaia, lasted for ~1600 years until ~800 AD. Progressive deforestation, cultivation of olives, walnut, plane trees, and vineyards, cereal fields and pasture land occupied the surrounding cultural landscapes (Fig. 9). Such visible anthropogenic impact, corresponding to so-called Beyşehir occupation phase (Bottema et al., 1986), started rather late in Elaia in comparison to south-western pollen records. For example in the Gölhisar Gölü area (Eastwood et al., 1999), this occupation phase lasted from ~1240 BC until ~665–783 AD and was characterised by *Olea*, *Juglans*, *Castanea*, and *Pistacia*.

A prominent feature of the pollen diagram from Elaia is the rapid increase in pine pollen from 7–10% to 46–83% at the core depth 160–180 cm (Figs. 5 and 9), coinciding with the abandonment of the city. A rapid increase in *Pinus* pollen after the long-lasting intensive land-use phase, lasting for two thousand years (Beyşehir Occupation phase), seems to be a general feature for the eastern Mediterranean region, also documented in sediments from Bafa Gölü at ~ AD 700 (Knipping et al., 2008), marsh of Gravgaz at ~ AD 700 (Vermeore et al., 2000) and Gölhisar Gölü at ~ AD 700 (Eastwood et al., 1999). Such an increase of pine in the pollen spectra is explained by one of two hypotheses: (i) the spread of pine forests over abandoned farming areas and pastureland (Knipping et al., 2008); and (ii) overrepresentation of pine due to high pollen production, its ability to long-distance transport, and open character of vegetation, implying strong human impact like intensive pasture. Pine is absent from the surroundings of the city today (Fig. 1b) and overrepresentation is evidenced by the top core sample, with 50% of the pollen grains being from pine (Fig. 9). The reconstruction of the reforestation (Fig. 9) also show an open environment around Elaia, leading to higher deposition of wind-transported pollen.

At present, *Pinus brutia* is a good indicator of Mediterranean conditions in Turkey. The wide distribution of *P. brutia* forests has been a topic of discussion. Schwarz (1936) and Louis (1939) signified *P. brutia* forests with sclerophyllous understory as climax formation typical for the Mediterranean zone. In contrast, Walter (1956) and Zohary (1973) argued that *P. brutia* forests represent a degradation stage of the macchia and the broad-leaved summer-green forests. Indeed, macchia-forming species *Q. coccifera*, *Q. ilex*, *P. lentiscus*, *P. terebinthus*, *Ceratonia siliqua*, *Phillyrea media*, and *Laurus nobilis* as well as broad-leaved summer-green oaks are able to grow as big trees on well-developed soils, in the absence of herbivores and lumbering (Walter, 1956). Wherever the undergrowth is protected against destruction, it grows into dense brushwood, which shadow light-demanding pine seedlings, which are unable to grow causing their disappearance (Zohary, 1973). Therefore, in the absence of anthropogenic pressure *P. brutia* would be restricted to sandstone or limestone rocks, which are less permeable to the deep roots of the broad-leaved trees. Palynological data from south-western Turkey reveal that the spread of pine occurred after a long-lasting human impact of more than one thousand years with enhanced soil erosion due to forest clearing, intensive agriculture and pasture. Such a destruction of the abiotic component possibly exceeds the ecosystem's carrying capacity, resulting in irreversible ecosystem changes, which in turn lead to the change of climax societies (Perevolotsky and Geligman, 1998). The recovery of the original oak forests around Elaia occurred after a short and less intensive disturbance period, before ~850 BC, but the climax species changed after AD 800 to predominantly pine forests. To sum up, large areas of modern pine forests in western and southern Turkey very likely are part of human-made landscapes.

Human influence in Elaia can also be identified in the marine ecosystem. *Posidonia oceanica* (L.) Delile is endemic to the Mediterranean Sea (Vassalo et al., 2013; Telesca et al., 2015). The destruction of seagrass habitat is today a worldwide phenomenon and fragmentation of the seagrass meadows is strongly influenced by human impact (Montefalcone, 2009, 2010; Telesca et al., 2015). Presents of vegetative remains of *Posidonia oceanica* in sedimentological record from Elaia reveal that seagrass was present in the Bay of Elaia from the beginning of the marine phase around 7 ka BP (Seeliger et al., 2013), but disappeared after the harbour construction, most possibly affected by harbour activities such as coastal constructions and anchoring (Montefalcone, 2009), as well as changed water quality (Vacchi et al., 2012). The example of Elaia demonstrates that human-induced fragmentation of *Posidonia oceanica* habitats started long ago, connected

to harbour constructions. In addition to historical records covering the last 50 years (Telesca et al., 2015), anthropogenic long-term influence on seagrass can be traced based on sedimentological records from other harbours.

7.2. Olive cultivation in Elaia

Cultivated olives, an emblematic tree of the entire Mediterranean region, expanded from the eastern borders of the Mediterranean Sea to the west in the 1st millennium BC (Loumou and Giourga, 2003; Engel et al., 2009). Palynological studies on core Ela-70 reveal that olive cultivation in Elaia started around ca. 850 BC and continued until AD 800 with the largest expansion between 170 BC and AD 180 (zone Ela-2b), during the period when the harbour was in use (Figs. 5 and 9). After a period of abandonment, olive cultivations started again and at present there are many olive groves in the environs of the former city of Elaia (Fig. 1c).

Olive ecosystems are quite stable, since they are very similar to the semi-natural Mediterranean ecosystems of the evergreen macchia vegetation (Loumou and Giourga, 2003). Such patterns of long-term coexistence of olive groves and highly diverse macchia vegetation can be suggested around Elaia between 850 BC and AD 800 (Figs. 5 and 9). At present, abandoned olive groves transform into species diverse cistus shrubs with the dominance of *Cistus creticus*, *Cistus salvifolius*, *Erica verticillata*, *Anthyllis hermanniae*, *Genista acanthoclada*, *Plantago bellardii*, *Trifolium stellatum*, *T. campestre*, *Asphodelus microcarpus*, *Tuberaria guttata*, *Filago gallica*, *Hypochaeris aetnensis*, *Tolpis virgata*, and *Hymenocarpus circinatus*, and later into the natural Mediterranean forests (Loumou and Giourga, 2003). The modern situation at Elaia with modern olive groves, which lack macchia vegetation, possibly because of intensive agricultural management, is well reflected by the top core sample.

7.3. Land-use and soil erosion

Arbuscular mycorrhizal fungi (AMF) colonize plant roots and sporulate under the earth. As previous studies have shown, the occurrence of Glomeromycota chlamydo spores in lacustrine context (Anderson et al., 1984; van Geel et al., 1989; Argant et al., 2006; Marinova and Atanassova, 2006) and coastal areas (López-Sáez et al., 2002; Kouli, 2012) is an important indicator of soil erosion, if absence of the local vegetation at the coring site is verified (Kołaczek et al., 2013).

The presence of marine indicators, such as foraminifer linings and marine dinocysts, strongly suggests that the sediment was deposited in open-water conditions, at least for the sediments deposited before the 180 cm mark of the core depth (Fig. 7). Moreover, the absence of *Glomus*-type in the upper part of the record proves the absence of mycorrhiza on modern roots of *Salicornia* sp., which now grows on-site. This is in agreement with new molecular studies on *Salicornia europaea*, reported as non-mycorrhizal plant, demonstrating the presence of mycorrhiza, but they lack arbuscules, due to salt stress (Sonjak et al., 2009). Therefore, the occurrence of chlamydo spores of Glomeromycota in Ela-70 below 180 cm very likely indicates soil erosion.

The presence of *Glomus*-type spores in zone Ela-1 indicates that soil erosion in the coastal areas occurred since the beginning of the sedimentation ~7.56 ka BP. This might be related to natural wave activity and/or terrestrial influx. An increase of *Glomus*-type at 490 cm (2.7 ka BP) coincides with an increase of anthropogenic indicators and plant parasitic fungi (Figs. 7 and 9), suggesting enhanced soil erosion due to deforestation, agriculture, and pastoral activities. This interpretation is confirmed by a significant increase in sedimentation

rates from 480 cm (2.6 ka BP) upwards. In general, the increase in sedimentation rates in the late Holocene is very likely human-induced and can be attributed to deforestation, agriculture, change of catchment of the supplying rivers, erosion of urban constructions with loam bricks and the use of the harbour basin as *ad hoc* waste dumps (Morhange et al., 2014). Landscape reconstruction around Elaia show continual silting up of the marine gulf since 2500 BC (Fig. 2a; Brückner et al., 2013; Seeliger et al., 2013). Furthermore, the archaeological survey indicates intensive settlement activity with small farmsteads in the surroundings of Elaia in Hellenistic times (250–50 BC), several of which were abandoned at the end of the 1st century BC (Pirson, 2011).

Surprisingly, the percentage of *Glomus*-type spores decreases during the use of Elaia's harbour (410–340 cm; Figs. 7 and 9), possibly due to the protection of the urban shore around the harbour and/or managed soil protection around the city.

After the decline of the harbour activities, *Glomus*-type spores increase again. This coincides with the decrease of *Olea* and other anthropogenic pollen and an increase of spores of coprophilous fungi (Fig. 9). The most probable scenario implies a change in land-use from an urban harbour with olive groves in environs of the city to intensive grazing, possibly by sheep and goats. It is well known that such a change in land-use can strongly affect the vegetation and soils (Loumou and Giourga, 2003). Experimental studies in Greece demonstrate that plant coverage and the number of woody species decrease from 81.2% and eleven species to 29.6% and five species already after 30 years of change from olive cultivation to pasture. Moreover, a lack of protection by the plant roots and plant coverage intensifies erosional processes and the soil thickness decreases from 30 cm to 6 cm within 30 years (Margaris et al., 1988 in Loumou and Giourga, 2003). It is reasonable to assume similar processes were taking place at Elaia when the arboriculture shifted toward grazing. Goat browsing is especially devastating for ecologically sensitive Mediterranean landscapes.

7.4. Maritime trade

Today, oceanic shipping and aquaculture are the main vectors of species distribution around the world (Streftaris et al., 2005). For example, the Mediterranean Sea receives one exotic species every four weeks (Streftaris et al., 2005; Zenetos et al., 2005). In the past, an accidental anthropogenic introduction of marine organisms within the bilge water was already considered for the Black Sea basin (Jones, 1993; Marret et al., 2009). During Hellenistic times, ships had no ballast water containers; however, during stays in ports organisms may have had an opportunity to settle on a ship and due to slow speed they could not be washed away in transit. In addition, during travelling water with planktonic organisms could easily get into the ship and be transported as bilge water for a long distances to other ports. By this way Jones (1993) explains the introduction and spread of the coccolithophorid *Emiliania huxleyi* in the Black Sea, the first (2.7 ka BP) and final invasions (1.7 ka BP) of which are well known and used as a stratigraphic marker for the deep-sea sediments of the Black Sea (Shumilovskikh et al., 2012). Marret et al. (2009) explore this idea, explaining the distribution of dinocyst *Gymnodinium catenatum/nolleri* in the Black Sea basin. So far, only the introduction of Mediterranean species into the Black Sea have been reported.

The palynological record from the Bay of Elaia presents the first evidence of an introduction in the reverse direction: the introduction of a Black Sea species into the Mediterranean Sea. The most prominent feature of the dinocyst assemblages of Ela-70 is the presence of *Peridinium ponticum* (Plate 1: 6–7). This species is restricted to the

brackish Black Sea, occurring rarely in the Marmara Sea. It prefers mesotrophic to eutrophic water conditions (Zonneveld et al., 2013). *P. ponticum* occurs in the Bay of Elaia for the first time at 2.3 ka BP (~80 BC), i.e., when the harbour was in full operation. The occurrence can be attributed to the passive transport by merchant ships. *P. ponticum* appears several times in the record, indicating either the establishment of its population and formation of new resting cysts, or the repeated introduction of cysts from the Black Sea, or both. As *P. ponticum* is restricted to brackish waters, a low salinity in Elaia's basin was required for its existence.

As already stated, the occurrence of *P. ponticum* in Elaia's harbour implies trading with the Black Sea. Elaia was a trade centre during the Hellenistic and Roman periods, as revealed by seals from Rhodes, Chios, Thasos, Pamphylia, and Knidos (Pirson, 2008, 2010, 2012). The first occurrence of *P. ponticum*, documented at 2.3 ka BP (~80 BC), corresponds well with the so-called first Mithridatic War 89–85 BC, during which Mithridates VI of Pontus (134–63 BC), in alliance with several Greek cities, rebelled against Roman supremacy. As Mithridates VI temporarily established his headquarter in Pergamon (Zimmermann, 2011), he most likely based part of his fleet in the harbour of Elaia. It is reasonable to assume that he received supplies from his Pontic Kingdom situated on the southern shore of the Black Sea. Thus, the *P. ponticum* might have reached Elaia by one of the Mithridatic ships.

Another vector for the spread of *P. ponticum* might have been the transport of marble from the island of Prokonnesos (modern Marmara Adasi) in the Sea of Marmara to Pergamon *via* the harbour of Elaia. This is attested for the marble of the friezes of the Pergamon Altar (Cramer et al., 2002), which was built in the first half of the 2nd century BC, i.e., approximately 100 years earlier than the first appearance of *P. ponticum* in Elaia. However, such a date can be explained by the age-depth model uncertainty. Moreover, sea-faring between the Black Sea and the Sea of Marmara and Elaia had a long-standing tradition even before and after that time.

7.5. Helminth eggs and sewerage in Elaia

Even if the most ancient finds of the helminths date back to hunter/gatherer communities during the last glacial period, parasites were wide spread since the Neolithic due to the introduction of agriculture (Brinkkemper and van Haaster, 2012; Reinhard et al., 2013). Therefore, the human parasitological picture since the 1st millennium BC comprises a broad species range. Already Hippocrates (460–370 BC) described echinococcosis (Daikos, 2007). Palaeoparasitological studies in the Near East from the 6/7th century BC to the 2nd century AD reveal the presence of whipworm (*Trichuris trichiura*), roundworm (*Ascaris lumbricoides*), dog tapeworm (*Echinococcus granulosus*), beef/pork tapeworm (*Taenia* spp.), pinworm (*Enterobius vermicularis*), and, in the medieval context, *Diphyllobothrium latum* (Mitchell et al., 2011). Thereby, *Ascaris lumbricoides* and *Trichuris trichiura* are very common in archaeological sites in Europe due to the use of human faeces as agricultural fertilizer, leading to the proliferation of fecal-borne parasites (Reinhard et al., 2013).

In the sediment core Ela-70, eggs of *Ascaris*, *Trichuris*, and *Capillaria* are present (Plate 3). The genus, *Ascaris*, consists of the two species, *A. lumbricoides* (egg dimensions 45–75 × 35–50 μm) and *A. suum* (50–70 × 40–60 μm), infecting humans and pigs, respectively. The size and morphology of these eggs overlap, making it impossible to identify the eggs to species without knowledge of the substrate (Brinkkemper and van Haaster, 2012). In the harbour sediments, both eggs could easily be deposited. The genus, *Trichuris*, consists of four species: *T. trichiura* (egg dimensions 50–58 × 22–27 μm) on human;

T. suis (50–68 × 21–31 µm) on pigs; *T. vulpis* (70–88 × 25–30 µm) on fox, dog, and cat; and *T. ovis* (70–80 × 30–42 µm) on sheep, goat, and cattle (Brinkkemper and van Haaster, 2012). Based on morphology and size, an identification of *T. trichiura/suis* and *T. vulpis/ovis* is possible. In Ela-70, all *Trichuris* findings belong to the first group and in the harbour sediment of Elaia eggs from pigs and humans could be deposited. *Capillaria* has a complicated taxonomy and includes several genera, infecting domestic animals, birds, and reptiles.

The eggs of *T. trichiura/suis* are present in the record starting around 7.56 ka BP, indicating the prehistorical presence of human and/or pigs and their parasites in the surroundings of Elaia. Since 2.7 ka BP (800 BC) the parasitic assemblage is more abundant and diverse (*Ascaris* and *Capillaria*), correlating with increased settlement activities in the surroundings of the city (LPZ Ela-2). The maximum density of intestinal parasite eggs in the sediments occurs during the active harbour phase between 2 and 1.87 ka BP (50 BC-AD 80). Since the terrestrial input from the coastal zone was quite low (see Section 7.3), the maximum of eggs might indicate the influx of wastewater from the city or even a canalisation with sewerage pipes going into the enclosed harbour. Such a connection was shown in the Roman harbour of Ephesus, where the maximum amount of *Trichuris* and *Ascaris* eggs correlates with the presence of a canalisation in the city (Stock et al., 2016).

8. Conclusions

The palynological record from a sediment core from the long since silted-up basin of the harbour of Elaia, provides insight into the vegetation dynamics and the long-term human impacts on terrestrial and lagoon ecosystems of the Bay of Elaia since prehistorical times. Around 7500 years ago, the landscape was covered with open oak forests, which later experienced several phases of deforestation alternating between natural forest recovery phases. At about 850 BC, the intensification of the land-use is evidenced by the appearance of olive groves, agriculture, arboriculture, increased pasture pressure, and soil erosion. The strongest impact is documented during the phase when Elaia's harbour was in full operation. The phase of very intensive land-use and possibly over-use of the ecosystems lasted for more than 1500 years. This seems to have led to a change of the climax plant communities from open oak forests to an even more open vegetation and pine forest. Humans influenced the lagoon ecosystem by construction of the harbour with two prominent moles around 260 BC. This led to a destruction of the marine habitats and local disappearance of *Posidonia*, while Elaia's harbour experienced eutrophication, changing dinocyst and foraminifer communities. The occurrence of eggs of human intestinal parasites in the sediments hints to the use of the harbour as a sewer for the city. Marine contacts with the Black Sea or Marmara Sea are attested by the detection of the Black Sea species *Peridinium ponticum*. Overall, we suggest that humans were the major factor of environmental changes during the last 3000 years in Elaia and especially during the city's flourishing periods in Hellenistic and Roman times.

Uncited reference

Bakker and van Smeerdijk, 1982.

Acknowledgements

We thank Bas van Geel for valuable reviewing of the manuscript and Robert Spengler for polishing the English. The project presented here was conducted in the context of the DFG priority program (SPP) 1209 "The Hellenistic Polis as a Living Space – Urban Structures and

Civic Identity between Tradition and Innovation" (2008–2011). Financial support by the German Research Foundation is gratefully acknowledged (DFG ref. nos. PI 740/1-3 and BR 877/32-1). The study was partially supported by the D. I. Mendeleev Scientific Fund Program of Tomsk State University and RFBR (16-35-60083 and 16-36-00293). Our research was part of the greater Elaia Survey Project, headed by Prof. Dr. Felix Pirson. The studies would not have been possible without the hospitality and support of the Pergamon excavation team. The Ministry of Culture and Tourism of the Republic of Turkey kindly granted the research permits.

Appendix A. Supplementary data


Supplementary data related to this article can be found at <http://dx.doi.org/10.1016/j.quascirev.2016.07.014>.

References

- Anderson, R.S., Homola, R.L., Davis, R.B., Jacobson, G.L., 1984. Fossil remains of the mycorrhizal fungal *Glomus fasciculatum* complex in postglacial lake sediments from Maine. *Can. J. Bot.* 62, 2325–2328.
- Argant, J., López-Sáez, J.A., Bintz, P., 2006. Exploring the antient occupation of a high altitude site (Lake Lauzon, France): comparison between pollen and non-pollen palynomorphs. *Rev. Palaeobot. Palynology* 141, 151–163.
- Bakker, R., van Smeerdijk, D.G., 1982. A palaeological study of a late Holocene section from 'het ilperweld', W. Netherlands. *Rev. Palaeobot. Palynology* 36, 95–163.
- Beck, R., Burger, D., Pfeiffer, K.-H., 1995. Laborskript. Kleinere Arb. aus dem Geogr. Inst. Univ. Tübingen 11, (in German).
- Bell, A., 2005. An illustrated Guide to the Coprophilous Ascomycetes of Australia. *Studies in Mycology* 58. CBS Biodiversity Series No. 3, Centraalbureau Voor Schimmelcultures, Utrecht, The Netherlands.
- Bennett, K., 1996. Determination of the number of zones in a biostratigraphic sequence. *New Phytol.* 132, 155–170.
- Beug, H.-J., 2004. Leitfaden der Pollenbestimmung. Verlag Dr. Friedrich Pfeil, München (in German).
- Blaauw, M., 2010. Methods and code for 'classical' age-modelling of radiocarbon sequences. *Quat. Geochronol.* 5, 512–518.
- Blott, S.J., Pye, K., 2001. GRADISTAT: a grain size distribution and statistics package for the analysis of unconsolidated sediments. *Earth Surf. Process. Landforms* 26, 1237–1248.
- Bottema, S., Woldring, H., 1984. Late quaternary vegetation and climate of southwest Turkey II. *Palaeohistoria* 26, 123–149.
- Bottema, S., Woldring, H., Aytuğ, B., 1986. Palynological investigations on the relations between prehistoric man and vegetation in Turkey: the Beyşehir Occupation Phase. In: *Proceedings of the 5th Optima Congress, Istanbul*. pp. 315–328.
- Brinkkemper, O., van Haaster, H., 2012. Eggs of intestinal parasites whipworm (*Trichuris*) and mawworm (*Ascaris*): non-pollen palynomorphs in archaeological samples. *Rev. Palaeobot. Palynology* 186, 16–21.
- Brückner, H., Müllenhoff, M., Gehrels, R., Herda, A., Knipping, M., Vött, A., 2006. From archipelago to floodplain - geographical and ecological changes in Miletus and its environs during the past six millennia (Western Anatolia, Turkey). *Z. für Geomorphol.* 142, 63–83.
- Brückner, H., Urz, R., Seeliger, M., 2013. Geomorphological and geoarchaeological landscape changes at the coasts of western Turkey during the Holocene. In: Raab, T., Raab, A., Gerwin, W., Schopper, F. (Eds.), *Landschaftswandel – Landscape Change. Geopedology and Landscape Development Research Series*, 1, pp. 81–104.
- Cai, L., Hyde, K.D., Tsui, C.K.M., 2006. *Genera in Freshwater Fungi*. Fungal Diversity Research Series 8. Fungal Diversity Press, Hong Kong.
- Cannon, P.F., Hawksworth, D.L., 1982. A re-evaluation of *Melanospora* Corda and similar Pyrenomycetes, with a revision of the British species. *Botanical J. Linn. Soc.* 84, 115–160.
- Cannon, P.F., Kirk, P.M., 2007. *Fungal Families of the World*. CAB International, Oxfordshire, UK, 456.
- Caretta, G., Piontelli, E., Picco, A., Del Frate, G., 1999. Some filamentous fungi on grassland vegetation from Kenya. *Mycopathologia* 145 (3), 155–169. <http://dx.doi.org/10.1023/A:1007038112075>.
- Chong, L.M., Sheridan, J.E., 1982. Mycoflora of barley (*Hordeum vulgare* L.) seed in New Zealand. *N. Z. J. Bot.* 20 (2), 187–189. <http://dx.doi.org/10.1080/0028825X.1982.10428839>.
- Collin, R.G., Odriozola, E., Towers, N.R., 1998. Sporidesmin production by *Pithomyces chartarum* isolates from Australia, Brazil, New Zealand and Uruguay.

- Micol. Res. 102 (2), 163–166. <http://dx.doi.org/10.1017/S0953756297004905>
- Cramer, T., Germann, K., Heilmeyer, W.-D., 2002. Petrographic and geochemical characterization of the Pergamon altar (telephos frieze) marble in the Pergamon museum, Berlin. In: Lazzarini, L. (Ed.), *Interdisciplinary Studies on Ancient Stone. ASMOSIA VI, Proceedings of the Sixth International Conference of the 'Association for the Study of Marble and Other Stones in Antiquity'*, Venice, June 15–18, 2000. pp. 285–291.
- Croudace, I.W., Rindby, A., Rothwell, R.G., 2006. ITRAX: description and evaluation of a new multi-function X-ray core scanner. In: Rothwell, R.G. (Ed.), *New Techniques in Sediment Core Analysis*. Geological Society, 267. Special Publication, London, pp. 51–63.
- Da Cunha, K.C., Sutton, D.A., Gené, J., Cano, J., Capilla, J., Madrid, H., Decock, C., Wiederhold, N.P., Guarro, J., 2014. Pithomyces species (Montagnulaceae) from clinical specimens: identification and antifungal susceptibility profiles. *Med. Mycol.* 52 (7), 748–757. <http://dx.doi.org/10.1093/mmy/myu044>
- Daikos, G.K., 2007. History of medicine: our Hippocratic heritage. *Int. J. Antimicrob. Agents* 29, 617–620.
- Delile, H., Blichert-Toft, J., Goiran, J.-P., Keay, S., Albarède, F., 2014. Lead in ancient Rome's city waters. *Proc. Natl. Acad. Sci. U. S. A.* 111 (18), 6594–6599.
- Dennis, R.W.G., 1981. *British Ascomycetes*. A.R. Gantner, Vaduz, 585.
- Di Menna, M.E., Smith, B.L., Miles, C.O., 2010. A history of facial eczema (pithomyctotoxicosis) research. *N. Z. J. Agric. Res.* 52 (4), 345–376. <http://dx.doi.org/10.1080/00288230909510519>
- Domsch, K.H., Gams, W., Anderson, T.-H., 2007. *Compendium of Soil Fungi*, revised by W. Gams ed second ed. Academic Press, London.
- Doveri, F., 2007. *Fungi Fimicoli Italiani*. A.M.B. Fondazione Centro Studi Micologici, Vicenza.
- Doveri, F., 2014. An update on the genera *Ascobolus* and *Saccobolus* with keys and descriptions of three coprophilous species, new to Italy. *Mycosphere* 5 (1), 86–135.
- Eastwood, W.J., Roberts, N., Lamb, H.F., Tibby, J.C., 1999. Holocene environmental change in southwest Turkey: a palaeoecological record of lake and catchment-related changes. *Quat. Sci. Rev.* 18, 671–695.
- Ellis, M.B., 1971. *Dematiaceous Hyphomycetes*. Commonwealth Mycological Institute.
- Ellis, M.B., 1976. *More Dematiaceous Hyphomycetes*. Commonwealth Mycological Institute. Kew, Eng.
- Ellis, D., Davis, S., Alexiou, H., Handke, R., Bartley, R., 2007. *Descriptions of Medical Fungi*, second ed. S. Aust, Adelaide.
- Ellis, M.B., Ellis, J.P., 1997. *Microfungi on Land Plants. An identification Handbook*. The Richmond Publishing, Slough, 868.
- Elsik, W.C., 1976. Microscopic fungal remains and cenozoic palynostratigraphy. *Geoscience Man* 15, 115–129.
- Engel, M., Knipping, M., Brückner, H., Kiderlen, M., Kraft, J.C., 2009. Reconstructing middle to late Holocene palaeogeographies of the lower Messenian plain (south-western Peloponnese, Greece): coastline migration, vegetation history and sea level change. *Palaeogeogr. Palaeoclimatol. Palaeoecol.* 248, 257–270.
- Erdtmann, G., 1960. The acetolysis method. *Sven. Bot. Tidskr.* 54, 561–564.
- Ernst, W., 1970. *Geochemical Facies Analysis*. Elsevier, Amsterdam, London, New York.
- Folk, R.L., Ward, W.C., 1957. Brazos River bar: a study in the significance of grain size parameters. *J. Sediment. Res.* 27, 3–26.
- García, D., Stchigel, A.M., Guarro, J., 2004. Two new species of *Sphaerodes* from Spanish soils. *Stud. Mycol.* 50, 63–68.
- Gregory, P.H., Lacey, M.E., 1964. The discovery of *Pithomyces chartarum* in Britain. *Trans. Br. Mycol. Soc.* 47 (1), 25–30. [http://dx.doi.org/10.1016/S0007-1536\(64\)80075-9](http://dx.doi.org/10.1016/S0007-1536(64)80075-9)
- Grimm, E.C., 1987. CONISS: a FORTRAN 77 program for stratigraphically constrained cluster analysis by the method of incremental sum of squares. *Comput. Geosciences* 13, 13–35.
- Grove, W.B., 1913. *The British Rust Fungi (Uredinales)*. University Press, Cambridge, 412.
- Guarro, J., Gene, J., Stchigel, A.M., Figueras, M.J., 2012. *Atlas of Soil Ascomycetes*. CBS-KNAW Fungal Biodiversity Centre. Utrecht, The Netherlands.
- Guiot, J., 1990. Methodology of the last climatic cycle reconstruction in France from pollen data. *Palaeogeogr. Palaeoclimatol. Palaeoecol.* 80, 49–69.
- Hadler, H., Kissas, K., Koster, B., Mathes-Schmidt, M., Mattern, T., Ntageretzi, K., Reichert, K., Willershäuser, T., Vött, A., 2013. Multiple late-Holocene tsunami landfall in the eastern Gulf of Corinth recorded in the palaeotsunami geo-archive at Lechaion, harbour of ancient Corinth (Peloponnese, Greece). *Z. für Geomorphol. N. F.* 57 (4), 139–180.
- Hansen, B.C.S., 1995. Conifer stomate analysis as a paleoecological tool: an example from the Hudson Bay Lowlands. *Can. J. Bot.* 73, 244–252.
- Hansen, M., De Fries, R.S., Townshend, J.R.G., Carroll, M., Dimiceli, C., Sohlberg, R.A., 2003. Global percent tree cover at a spatial resolution of 500 meters: first results of the MODIS vegetation continuous fields algorithm. *Earth Interact.* 7, 1–15.
- Horjes, B., 2010. Bronzezeitliche Besiedlungsmuster im Kaikostal. Interpretationen erster Surveyergebnisse im Umland von Pergamon (Türkei). In: In: Horejs, B., Kienlin, T.L. (Eds.), *Siedlung und Handwerk – Studien zu sozialen Kontexten in der Bronzezeit. Beiträge zu den Sitzungen der Arbeitsgemeinschaft Bronzezeit auf der Jahrestagung des Nordwestdeutschen Verbandes für Altertumsforschung in Schleswig 2007 und auf dem deutschen Archäologenkongress in Mannheim 2009*. Universitätsforschungen zur prähistorischen Archäologie, 194, pp. 47–67 (in German).
- Hütteroth, W.-D., Höhfeld, V., 2002. *Türkei*. Wissenschaftliche Buchgesellschaft, Darmstadt.
- Hyde, K.D., 1995. Tropical Australian freshwater fungi VII. New genera and species of Ascomycetes. *Nova Hedwig.* 61, 119–140.
- Jarzen, D.M., Elsie, W.C., 1986. Fungal palynomorphs recovered from recent river deposits, Luangwa Valley, Zambia. *Palynology* 10, 35–60.
- Jankovská, V., Komárek, J., 2000. Indicative value of *Pediastrum* and other green algae in Palaeoecology. *Folia Geobot.* 35, 59–82.
- Jones, G.A., 1993. Tales of Black Sea sedimentation, exploration and colonization. *AMS Pulse* 2 (1), 1–5.
- Juggins, S., 2007. *C2 Version 1.5 User Guide*. Software for Ecological and Palaeoecological Data Analysis and Visualisation. Newcastle University, Newcastle upon Tyne, UK.
- Juggins, S., 2015. *Rioja: Analysis of Quaternary Science Data*, R Package Version (0.9-5). <http://cran.r-project.org/package=rjoja>.
- Kelterbaum, D., Brückner, H., Dikarev, V., Gerhard, S., Pint, A., Porotov, A., Zin'ko, V., 2012. Palaeogeographic changes at lake Chokrak on the Kerch peninsula, Ukraine, during the mid- and late-holocene. *Geoarchaeology* 27 (3), 206–219.
- Kirk, P.M., Cannon, P., Minter, D.W., Stalpers, J., 2008. *Dictionary of the Fungi*, tenth ed. CAB International, Wallingford, UK.
- Knipping, M., Müllenhoff, M., Brückner, H., 2008. Human induced landscape changes around Bafa Gölü (western Turkey). *Veg. Hist. Archaeobotany* 17, 365–380.
- Knitter, D., Blum, H., Horejs, B., Nakoinz, O., Schütt, B., Meyer, M., 2013. Integrated centrality analysis: a diachronic comparison of selected Western Anatolian locations. *Quat. Int.* 312, 45–56.
- Kolaczek, P., Zubek, S., Blaszkowsky, Mleczo, P., Margielewski, W., 2013. Erosion or plant succession – how to interpret the presence of arbuscular mycorrhizal fungi (Glomeromycota) spores in pollen profiles collected from mires. *Rev. Palaeobot. Palynology* 189, 29–37.
- Kouli, K., 2012. Vegetation development and human activities in Attiki (SE Greece) during the last 5,000 years. *Veg. Hist. Archaeobotany* 21, 267–278.
- Krug, J.C., Khan, R.S., 1989. New records and new species of *Podospora* from east africa. *Can. J. Bot.* 67 (4), 1174–1182. <http://dx.doi.org/10.1139/b89-153>
- Kuthubtheen, A.J., Webster, J., 1986. Water availability and the coprophilous fungus succession. *Trans. Br. Mycol. Soc.* 86 (1), 63–76.
- Lacey, M.E., West, J.S., 2006. *The Air Spora: a Manual for Catching and Identifying Airborne Biological Particles*. Springer, Boston, MA.
- Lardín, C., Pacheco, S., 2015. *Helminths. Handbook for identification and Counting of Parasitic Helminths Eggs in Urban Wastewater*. IWA Publ., London, 115.
- López Sáez, J.A., López García, P., Sánchez, M.M., 2002. Palaeoecology and Holocene environmental change from a saline lake in South-West Spain: protohistorical and prehistorical vegetation in Cádiz Bay. *Quat. Int.* 93–94, 197–206.
- Louis, H., 1939. *Das natürliche Pflanzenkleid Anatoliens geographisch gesehen*. Geogr. Abh. Reihe 3. Heft 12, Stuttgart (in German).
- Loumou, A., Giourga, C., 2003. Olive groves: “The life and identity of Mediterranean”. *Agric. Hum. Values* 20, 87–95.
- Marasas, W.F.O., Schumann, I.H., 1972. The genus *Pithomyces* in South Africa. *Bothalia* 10 (4) <http://dx.doi.org/10.4102/abc.v10i4.1556>
- Margaris, N.S., Mardiris, Th, Chairopoulos, G., 1988. The “retreat” of olive groves-forest. In: *Proceedings of Scientific Meeting, the Aegean Olive Groves, February 25-27. Mytilini. Edition Elaiourgiki*, pp. 18–25 (in Greek).
- Marinova, E., Atanassova, J., 2006. Anthropogenic impact on vegetation and environment during the Bronze Age in the area of Lake Durankulak, NE Bulgaria: pollen, microscopic charcoal, non-pollen palynomorphs and plant macrofossils. *Rev. Palaeobot. Palynology* 141, 165–178.
- Marret, F., Mudie, P., Aksu, A., Hiscott, R.N., 2009. A Holocene dinocyst record of a two-step transformation of the Neoeuxinian brackish water lake into the Black Sea. *Quat. Int.* 197, 72–86.
- Meyer, H., Aksoy, H., 1986. *Wälder der Türkei*. Gustav Fischer Verlag, Stuttgart, New York, 289 (in German).
- Mirza, J.H., Cain, R.F., 1969. Revision of the genus *Podospora*. *Can. J. Bot.* 47, 1999–2048.

- Mitchell, P.D., Anastasiou, E., Syon, D., 2011. Human intestinal parasites in crusader Acre: evidence for migration with disease in the medieval period. *Int. J. Paleopathol.* 1, 132–137.
- Montefalcone, M., 2009. Ecosystem health assessment using the Mediterranean seagrass *Posidonia oceanica*: a review. *Ecol. Indic.* 9, 595–604.
- Montefalcone, M., 2010. Human influence on seagrass habitat fragmentation in NW Mediterranean Sea. *Estuarine. Coast. Shelf Sci.* 86, 292–298.
- Montoya, E., Rull, V., van Geel, B., 2010. Non-pollen palynomorphs from surface sediments along an altitudinal transect of the Venezuelan Andes. *Palaeogeogr. Palaeoclimatol. Palaeoecol.* 297 (1), 169–183.
- Moore, P.D., Webb, J.A., Collinson, M.E., 1999. *Pollen Analysis*. Blackwell Science, Oxford.
- Morhange, C., Marriner, N., Carayon, N., 2014. The geoarchaeology of ancient Mediterranean harbours. In: Arnaud-Fassetta, G., Carcaud, N. (Eds.), *French Geoarchaeology in the 21st Century*. CNRS Editions. pp. 281–290.
- Murad, W., 2011. *Late Quaternary Vegetation History and Climate Change in the Gobi Desert, South Mongolia*. (Dissertation/PhD-Thesis).
- Nakagawa, T., Tarasov, P., Kotoba, N., Gotanda, K., Yasuda, Y., 2002. Quantitative pollen-based climate reconstruction in Japan: application to surface and late Quaternary spectra. *Quat. Sci. Rev.* 21, 2099–2113.
- Nandi, B., Sinha, A., 2007. Validation of the Miocene fungal spore *Mediaverrucites* from Mizoram, India. *Palynology* 31 (1), 95–100.
- Niwa, Y., Sugai, T., Saegusa, Y., Ogami, T., Sasao, E., 2011. Use of electrical conductivity to analyze depositional environments: example of a Holocene delta sequence on the Nobi Plain, central Japan. *Quat. Int.* 230, 78–86.
- Novenko, E.Yu., Eremeeva, A.P., Chepurayeva, A.A., 2014. Reconstruction of Holocene vegetation, tree cover dynamics and human disturbances in central European Russia, using pollen and satellite data sets. *Veg. Hist. Archaeobotany* 23, 109–119.
- Overpeck, J.T., Webb III, T., Prentice, I.C.A., 1985. Quantitative interpretation of fossil pollen spectra: dissimilarity coefficients and the method of modern analogs. *Quat. Res.* 23, 87–108.
- Pals, J.P., van Geel, B., Delfos, A., 1980. Paleocological studies in the Klokkewiel bog near Hoogkarspel (prov. of Noord-Holland). *Rev. Palaeobot. Palynology* 30, 371–418.
- Perevolotsky, A., Seligman, N.G., 1998. Role of grazing in Mediterranean rangeland ecosystems. *BioScience* 48, 1007–1017.
- Pint, A., Seeliger, M., Frenzel, P., Feuser, S., Erkul, E., Berndt, C., Klein, C., Pirson, F., Brückner, H., 2015. The environs of Elaia's ancient open harbour – a reconstruction based on microfaunal evidence. *J. Archaeol. Sci.* 54, 340–355.
- Pirozynski, K.A., Carter, A., Day, R.G., 1984. Fungal remains in Pleistocene ground squirrel dung from Yukon Territory, Canada. *Quat. Res.* 22 (3), 375–382. <http://www.sciencedirect.com/science/article/B6WPN-4DV0V55-1H/2/8c80252cb83588573331860008a92e68>.
- Pirson, F., 2004. Elaia, der maritime Satellit Pergamons. *Istanbuler Mittl.* 54, 197–213 (in German).
- Pirson, F., 2007. Pergamon – bericht über die Arbeiten in der Kampagne 2006. *Archäologischer Anz.* 2, 13–69 (in German).
- Pirson, F., 2008. Pergamon – bericht über die Arbeiten in der Kampagne 2007. *Archäologischer Anz.* 2, 83–155 (in German).
- Pirson, F., 2009. Pergamon – bericht über die Arbeiten in der Kampagne 2008. *Archäologischer Anz.* 2, 129–213 (in German).
- Pirson, F., 2010. Pergamon – bericht über die Arbeiten in der Kampagne 2009. *Archäologischer Anz.* 2, 139–236 (in German).
- Pirson, F., 2011. Pergamon – bericht über die Arbeiten in der Kampagne 2010. *Archäologischer Anz.* 2, 81–212 (in German).
- Pirson, F., 2012. Hierarchisierung des Raumes? Überlegungen zur räumlichen Organisation und deren Wahrnehmung im hellenistischen Pergamon und seinem Umland. *Byzas* 13, 187–232.
- Pirson, F., 2014. Elaia, der (maritime) Satellit Pergamons, in: S. Ladstätter – F. Pirson – Th. Schmidts (edd.), *Häfen und Hafenstädte im östlichen Mittelmeerraum von der Antike bis in byzantinischer Zeit*. Bericht Kolloquium Istanbul 2011. *Istanbul, Ege Yayınları*. *Byzas* 19, 339–356 (in German).
- Pirson, F., Scholl, A., 2015. Pergamon. *Anadolu'da Hellenistik Başkent (A Hellenistic Capital in Anatolia)*. (Istanbul, Ege Yayınları).
- Quezel, P., Barbero, M., 1985. *Carte de la végétation potentielle de la région Méditerranéenne*. Éditions du Centre National de la Recherche Scientifique, Paris, 69 (in French).
- Rae, J.E., 1997. Trace metals in deposited intertidal sediments. In: Jeckells, T.D., Rae, J.E. (Eds.), *Biogeochemistry of Intertidal Sediments*. New York. pp. 16–41.
- Reinhard, K.J., Ferreira, L.F., Bouchet, F., Sianto, L., Dutra, J.M.F., Iniguez, A., Leles, D., Le Bailly, M., Fugassa, M., Pucu, E., Araújo, A., 2013. Food, parasites, and epidemiological transitions: a broad perspective. *Int. J. Paleopathol.* 3, 150–157.
- Reimer, P.J., Bard, E., Bayliss, A., Beck, J.W., Blackwell, P.G., Bronk Ramsey, C., Buck, C.E., Cheng, H., Edwards, R.L., Friedrich, M., Grootes, P.M., Guilderson, T.P., Hafliadason, H., Hajdas, I., Hatt, C., Heaton, T.J., Hogg, A.G., Hughen, K.A., Kaiser, K.F., Kromer, B., Manning, S.W., Niu, M., Reimer, R.W., Richards, D.A., Scott, E.M., Southon, J.R., Turney, C.S.M., van der Plicht, J., 2013. *IntCal13 and MARINE13 radiocarbon age calibration curves 0-50000 years cal BP*. *Radiocarbon* 55 (4), 1869–1887.
- Roberts, N., 1990. Human-induced landscape change in south and southeast Turkey during the later Holocene. In: Bottema, S., Entjes-Nieborg, G., van Zeist, W. (Eds.), *Man's Role in the Shaping of the Eastern Mediterranean Landscape*. A.A. Balkema, Rotterdam, pp. 53–67.
- Rochon, A., de Vernal, A., Turon, J.-L., Matthiessen, J., Head, M.J., 1999. Distribution of recent dinoflagellate cysts in surface sediments from the north Atlantic Ocean and adjacent seas in relation to sea-surface parameters. *AASP Contrib. Ser.* 35, 7–59.
- Sancay, R.H., 2014. The occurrence of *Mediaverrucites* in the upper Miocene of the black sea, Turkey. *Palynology* 38, 28–37.
- Schlütz, F., Shumilovskikh, L.S., 2013. On the relation of *Potamomyces armatisporus* to the fossil form-type *Mediaverrucites* and its taxonomical and ecological implications. *Fungal Ecol.* 6, 309–315.
- Schneider, S., Matthaei, A., Schöffel, M., Kronwald, M., Pint, A., Schütt, B., 2015. A geoarchaeological case study in the chora of Pergamon, Western Turkey to reconstruct the late Holocene landscape development and settlement history. *Quat. Int.* 367, 62–76.
- Schwarz, O., 1936. Die Vegetationsverhältnisse Westanatoliens. *Botanische Jahrbücher für Systematik. Pflanzengesch. Pflanzengeogr.* 67, 297–436.
- Seeliger, M., Bartz, M., Erkul, E., Feuser, S., Kelterbaum, D., Klein, C., Pirson, F., Vött, A., Brückner, H., 2013. Taken from the sea, reclaimed by the sea: the fate of the closed harbour of Elaia, the maritime satellite city of Pergamum (Turkey). *Quat. Int.* 312, 70–83.
- Seeliger, M., Brill, D., Feuser, S., Bartz, M., Erkul, E., Kelterbaum, D., Vött, A., Klein, C., Pirson, F., Brückner, H., 2014. Function and age of so far undated submerged stone structures in the Bay of Elaia, NW-Turkey. *Geoarchaeology* 29, 138–155.
- Shumilovskikh, L.S., Tarasov, P., Arz, H., Fleitmann, D., Marret, F., Nowaczyk, N., Plessen, B., Schlütz, F., Behling, H., 2012. Vegetation and environmental dynamics in the southern Black Sea region since 18 kyr BP derived from the marine core 22-GC3. *Palaeogeography, Palaeoclimatology, Palaeoecology* 337–338, 177–193.
- Shumilovskikh, L.S., Schlütz, F., Achterberg, I., Bauerochse, A., Leuschner, H., 2015. Non-pollen palynomorphs from mid-Holocene peat of the raised bog Borsteler Moor (Lower Saxony, Germany). *Stud. Quat.* 32, 5–18.
- Siani, G., Paterne, M., Arnold, M., Bard, E., Metivier, B., Tisnerat, N., Bassinot, F., 2000. Radiocarbon reservoir ages in the mediterranean sea and black sea. *Radiocarbon* 42, 271–280.
- Sonjak, S., Beguiristain, T., Leyval, C., Regvar, M., 2009. Temporal temperature gradient gel electrophoresis (TTGE) analysis of arbuscular mycorrhizal fungi associated with selected plants from saline and metal polluted environments. *Plant Soil* 314, 25–34.
- Stchigel, A.M., Caldich, M., Guarro, J., Zoror, L., 2002. A new species of *Podospora* from soil in Chile. *Mycologia* 94 (3), 554–558.
- Stock, F., Knipping, M., Pint, A., Ladstätter, S., Delile, H., Heiss, A.G., Laermanns, H., Mitchell, P.D., Ployer, R., Steskal, M., Thanheiser, U., Urz, R., Wennrich, V., Brückner, H., 2016. Human impact on Holocene sediment dynamics in the eastern mediterranean – the example of Ephesus and its roman harbor. *Earth Surf. Process. Landforms* (accepted).
- Stockmarr, J., 1971. Tablets with spores used in absolute pollen analysis. *Pollen Spores* 13, 615–621.
- Strabo, 2005. *Geographica*. Translation and Comments by Albert Forbiger, 2005 Ed. Marix Verlag, Wiesbaden. (Greek to German).
- Streftaris, N., Zenetos, A., Papanthassiou, E., 2005. Globalisation in marine ecosystems: the story of non-indigenous marine species across European seas. *Oceanogr. Mar. Biol. Annu. Rev.* 43, 419–453.
- Tarasov, P., Williams, J.W., Andreev, A., Nakagawa, T., Bezrukova, E., Herzschuh, U., Igarashi, Y., Müller, S., Werner, K., Zheng, Z., 2007. Satellite- and pollen-based quantitative woody cover reconstructions for northern Asia: verification and application to late-Quaternary pollen data. *Earth Planet Sci. Lett.* 264, 284–298.
- Telesca, L., Belluscio, A., Criscoli, A., Apostolaki, E.T., Fraschetti, S., Gristina, M., Knittweis, L., Martin, C.S., Pergent, G., Alagna, A., Badalamenti, F., Garofalo, G., Gerakaris, V., Pace, M.L., Pergent-Martini, C., Salomidi, M., 2015. Seagrass meadows (*Posidonia oceanica*) distribution and trajectories of change. *Sci. Rep.* 5, 12505. <http://dx.doi.org/10.1038/srep12505>
- Tóth, B., Csosz, M., Dijksterhuis, J., Frisvad, J.C., Varga, J., 2007. *Pithomyces char-tarum* as a pathogen of wheat. *J. Plant Pathology* 89 (3), 405–408.
- Vacchi, M., Montefalcone, M., Bianchi, C.N., Morri, C., Ferrari, M., 2012. Hydrodynamic constraints to the seaward development of *Posidonia oceanica* meadows. *Estuar. Coast. Shelf Sci.* 97, 58–65.
- Van Brummelen, J., 1967. A world-monograph of the genera *ascobolus* and *Saccobolus* (ascmycetes, pezizales). *Persoonia* 1.
- Van der Wiel, A.M., 1982. A palaeoecological study of a section from the foot of the Hazendonk (Zuid-Holland, the Netherlands), based on the analysis of pollen, spores and macroscopic plant remains. *Rev. Palaeobot. Palynology* 38, 35–90.
- Van Geel, B., 1978. A palaeoecological study of Holocene peat bog sections in Germany and the Netherlands, based on the analysis of pollen, spores and macro- and

- microscopic remains of fungi, algae, cormophytes and animals. *Rev. Palaeobot. Palynology* 25, 1–120.
- Van Geel, B., 2001. Non-pollen palynomorphs. Terrestrial, Algal, and Siliceous indicators. In: Smol, J.P., Birks, H.J.B., Last, W.M. (Eds.), *Tracking Environmental Change Using Lake Sediments*, 3. Kluwer Academic Publishers, Dordrecht, pp. 1–17.
- Van Geel, B., Bohncke, S.J.P., Dee, H., 1981. A palaeoecological study of an upper late glacial and Holocene sequence from “De Borchert”, the Netherlands. *Rev. Palaeobot. Palynology* 31, 367–448.
- Van Geel, B., Hallewas, D.P., Pals, J.P., 1983. A late Holocene deposit under the west-friese zeedijknear enkhuizen (prov of noord-holland, The Netherlands): palaeoecological and archaeological aspects. *Rev. Palaeobot. Palynology* 38, 269–335.
- Van Geel, B., Klink, A.G., Pals, J.P., Wieggers, J., 1986. An upper eemian lake deposit from twente, eastern Netherlands. *Rev. Palaeobot. Palynology* 47, 31–61.
- Van Geel, B., Coope, G.R., van der Hammen, T., 1989. Palaeoecology and stratigraphy of the lateglacial type section at Usselo (the Netherlands). *Rev. Palaeobot. Palynology* 60, 25–129.
- Van Geel, B., Buurman, J., Brinkkemper, O., Schelvis, J., Aptroot, A., van Reenen, G., Hakbijl, T., 2003. Environmental reconstruction of a Roman Period settlement site in Uitgeest (The Netherlands), with special reference to coprophilous fungi. *J. Archaeol. Sci.* 30, 873–883.
- Vánky, K., 1994. *European Smut Fungi*. Gustav Fischer Verlag, Stuttgart–Jena–New York, 570.
- Van Wuijckhuise, L., Snoep, J., Cremers, G., Duvivier, A., Groeneveld, A., Ottens, W., van der Sar, S., 2006. First case of pithomyocotocosis (facial eczema) in the Netherlands. *Tijdschr. Diergeneesk.* 131 (23), 858–861.
- Vánky, K., 1998. A survey of the spore-ball-forming smut fungi. *Mycol. Res.* 102 (05), 513–526.
- Vassalo, P., Paoli, C., Rovere, A., Montefalcone, M., Morri, C., Bianchi, C.N., 2013. The value of the seagrass *Posidonia oceanica*: a natural capital assessment. *Mar. Pollut. Bull.* 75, 157–167.
- Vermoere, M., Smets, E., Waelkens, M., Vanhaverbeke, H., Librecht, I., Paulissen, E., Vanhecke, L., 2000. Late Holocene environmental change and the record of human impact and Gravgaz near Sagalassos, Southwest Turkey. *J. Archaeol. Sci.* 27, 571–595.
- Vött, A., Handl, M., Brückner, H., 2002. Rekonstruktion holozäner Umweltbedingungen in Akarnanien (Nordwestgriechenland) mittels Diskriminanzanalyse von geochemischen Daten. *Geol. Palaeontol.* 36, 123–147 (in German).
- Vött, A., Bareth, G., Brückner, H., Lang, F., Sakellariou, D., Hadler, H., Ntageretzis, K., Willershäuser, T., 2011. Olympia's harbour site Pheia (Elis, Western Peloponnese, Greece) destroyed by tsunami impact. *Die Erde* 142 (3), 259–288.
- Vujanovic, V., Goh, Yit Kheng, 2009. *Sphaerodes mycoparasitica* sp. nov., a new biotrophic mycoparasite on *Fusarium avenaceum*, *F. graminearum* and *F. oxysporum*. *Mycol. Res.* 113 (10), 1172–1180. <http://dx.doi.org/10.1016/j.mycres.2009.07.018> 
- Wall, D., Dale, B., Harada, K., 1973. Descriptions of new fossil dinoflagellates from the late quaternary of the black sea. *Micropaleontology* 19, 18–31.
- Walter, H., 1956. *Vegetationsgliederung anatoliens*. *Flora* 143, 295–326 (in German).
- Watanabe, T., 2010. *Pictorial Atlas of Soil and Seed Fungi: Morphologies of Cultured Fungi and Key to Species*, third ed. CRC Press/Taylor & Francis, Boca Raton.
- Wicklow, D.T., 1975. Fire as an environmental cue initiating ascomycete development in a tallgrass prairie. *Mycologia* 67 (4), 852–862.
- Zanchetta, G., Bini, M., Crematschi, M., Magny, M., Sadori, L., 2013. The transition from natural to anthropogenic-dominated environmental change in Italy and the surrounding regions since the Neolithic: an introduction. *Quat. Int.* 303, 1–9.
- Zenetos, A., Çınar, M.E., Pancucci-Papadopoulou, M.A., Harmelin, J.G., Furnari, G., Andaloro, F., Bellou, N., Streftaris, N., Zibrowius, H., 2005. Annotated list of marine alien species in the Mediterranean with records of world invasive species. *Mediterr. Mar. Sci.* 6, 63–118.
- Zimmermann, M., 2011. *Pergamon: Geschichte, Kultur, Archäologie*. C. H. Beck, München (in German).
- Zohary, M., 1973. *Geobotanical Foundations of the Middle East*. Gustav Fischer Verlag, Amsterdam: Swets & Zeitlinger, Stuttgart.
- Zonneveld, K., Marret, F., Versteegh, G.J.M., Bogus, K., Bonnet, S., Bouimtarhan, I., Crouch, E., de Vernal, A., Elshanawany, R., Edwards, L., Esper, O., Forke, S., Grøsfjeld, K., Henry, M., Holzwarth, U., Kiehl, J.-F., Kim, S.-Y., Ladouceur, S., Ledu, D., Chen, L., Limoges, A., Londeix, L., Lu, S.-H., Mahmoud, M.S., Marino, G., Matsuoka, K., Matthiessen, J., Mildenhall, D.C., Mudie, P., Neil, H.L., Pospelova, V., Qi, Y., Radi, T., Richerol, T., Rochon, A., Sangiorgi, F., Solignac, S., Turon, J.-L., Verleye, T., Wang, Y., Wang, Z., Young, M., 2013. Atlas of modern dinoflagellate cyst distribution based on 2405 data points. *Rev. Palaeobot. Palynology* 191, 1–197.

Chapter 7

7 Discussion

The working hypotheses outlined in part 1.2 are discussed in the following sections (7.1–7.3) considering the results of Chapters 2–6, new data, and further methodological approaches.

7.1 Coastal evolution, shoreline displacements and sea-level fluctuations in the Bay of Elaia.

- *Working hypothesis 1: In the Bay of Elaia, the peak of the postglacial marine transgression reached much further inland than today. Thereafter, alluvial and colluvial sedimentation caused a major seaward shift in the shoreline.*

7.1.1 Goal 1: Determining the spatial and temporal dimensions of coastline changes during the past millennia.

Reconstructing the coastal changes in relation to human settlement was one of the main objectives of this thesis. The results of this pioneering work are summed up here (Chapter 4, Fig. 9).

7.1.1.1 Shoreline displacements in the Bay of Elaia

Around 12000 BC: The continental shelf of the later Bay of Elaia was exposed at the final stage of the last ice age and the river mouth of the Bakırçay was in a much further westward position as compared today (Aksu et al., 1987).

6000 BC: Due to the rising sea level during the postglacial marine transgression the first transgressive facies were deposited in the first half of the 6th millennium BC at depths of 8 m b.s.l. (below sea level) in corings Ela 58 and 70.

2000/1500 BC: The rise in sea level led to a landward shift of the shoreline, reaching its greatest extension around 850 m westwards, 700 m northwards, and 200 m eastwards from its present position. The maximum northern marine transgression occurred around 2000 years BC. In the west and east, this was the case around 1500 BC, i.e., much earlier than the settlement period of Elaia. The later castle hill of Elaia protruded into the Bay of Elaia as a peninsula. Small landing sites for maritime vessels may have been situated on its north-western and south-eastern flank, but that they were used has not yet been proven by archaeological evidence. One of Elaia's graveyards was located near coring Ela 9 (Pirson, 2010). Therefore, these areas have ever been dry land. The interpretation of the thickness of the marine strata of Ela 58 in addition to coring Ela 61 leads to the conclusion that the maximum transgressive shoreline was located within the

later city area. Hence, parts of the later city were built on formerly marine sediments, which is in good agreement with other ancient cities at the Turkish Aegean coast such as Miletus, Ainos, and Ephesus (Brückner, 2005; Brückner et al., 2006, 2013, 2015).

1500–300 BC: Palynological investigations in the Bay of Elaia (Chapter 6) indicate intensified human impact beginning around 850 BC, including deforestation and farming activities. This led to enhanced erosion processes. Increased sediment load due to soil erosion from the Bozyertepe and the small unnamed episodic creek between Bozyertepe and castle hill caused a shoreline regression in the western part. No fluvial material of the nearby Bakırçay delta was found in any coring of the western and northern parts of the Bay of Elaia. A moderate shoreline regression in the eastern city district caused by denudation processes and human impact occurred. Flash floods are obvious in the corings of the eastern part of the Bay of Elaia and might have been a temporary common nuisance for the inhabitants, although nothing is found in the literature addressing this. Flash floods are the result of the higher relief energy of the nearby foothills of the steep mountain of Yuntdağ, compared to the flat hill of Bozyertepe and the castle hill in the western part. Additionally, human influence in the eastern area of the embayment has been more intense, causing soil degradation followed by erosional processes.

300–0 BC: Wide areas in the western part of the bay remained marine during the prime of Elaia, and the shoreline shift in the eastern part was minimal. The closed harbour basin was built into the open sea immediately south of the castle hill, and the open harbour zone including its ship sheds was constructed. In the meantime, the shores of the eastern city district acted as a preferable beach harbour for foreign sailors, soldiers and merchants.

0–AD 1000: Increased sediment load in the first centuries AD led to a complete siltation of the harbour sites and an ongoing seaward shift in the shoreline. The palynological results suggest that human influence ended not later than around AD 800. At that date, the shoreline was close to its present-day shape, the harbour sites were silted up, and the inhabitants had abandoned the city in favour of a more landward settlement on the so-called Püsküllü Tepeler – most probably fearing of pirate attacks (Pirson, 2009, 2010, 2014). During that period, the spit in the south-eastern part of the bay evolved and was artificially consolidated (Seeliger et al., 2015). The remaining population used the spit as a landing site for small fishing boats as the harbours of Elaia could by then no longer be reached. In addition, it is to be assumed that the saltworks in the southwestern part were in full operation since around AD 500.

7.1.1.2 Progradation of the Bakırçay delta

In contrast to the Bay of Elaia, significant shoreline displacements in mid-Holocene times of around 60 km for the Büyük Menderes Graben near ancient Miletus (Bay, 1999; Brückner et al., 2006), around 20 km for the Küçük Menderes near ancient Ephesus (Brückner, 2005; Stock, 2015), at least 26 km for the Meriç delta near ancient Ainos (Alpar, 2001), and approx. 10 km for the Troas (Kraft et al., 1980) have been reported. The reason for the relatively small shoreline displacements in the Bay of Elaia is its separation from the main Bergama Graben by the Bozyertepe (Figs. 2 & 4). Thus, it can be excluded that the Bakırçay once flowed east of this flat hill. At the time of the maximum marine transgression, the Bay of Elaia was filled by water to its maximum level and sea waves washed the slopes of the Bozyertepe, the castle hill and the bordering Yuntdağ.

Studies in the Bakırçay delta area are as yet rare. One can assume that the seaward parts of its contemporary delta had been a marine embayment once, comparable to ancient Troia, Miletus, Ainos and Ephesus. According to the foundation myth of Pergamon, the legendary Telephos landed on the shores “near to Teuthrania”, which nowadays is 15 km inland (Fig. 2, Radt, 2011). Dörpfeld (1910, 1911, 1912, 1928) and Philippson (1911) discussed the topic of a former marine flooding of the inner Bergama Graben and the region of Teuthrania but failed to reach a consensus. Van Gerkan (1956) published a vivid summary of this dispute. In an attempt to test the veracity of the above mentioned myth, a 19 m b.s.l. deep coring AD 39 was drilled just west of Teuthrania (27°02'33.7"E; 39°03'02.5" N; 10 m a.s.l.) in 2011. No marine strata were elucidated (Schneider et al., 2012; Schneider, 2014). Therefore, the myth of Teuthrania is not supported by stratigraphic evidence, although the vague term “near the shores” has to be interpreted with care. In my opinion, it might be 1 or 2 km away. However, 15 km as it is today, seems to be too far. Furthermore, the ruins of a Roman bridge (Conze et al., 1912/1913) were found around 4.5 km from the river mouth of the modern Bakırçay (Fig. 2). This led to the conclusion that the deltaic progradation of the Bakırçay has been <4.5 km since Roman times.

7.1.1.3 Summary

Summing up, the following can be concluded regarding the shoreline displacements during Holocene times in the Bay of Elaia and the Bergama Graben:

- (1) For the first time, detailed shoreline displacements in the Bay of Elaia have been reconstructed. This confirms the archaeological and historical evidence of Elaia's prime during the Hellenistic and early Roman periods, and the city's decline from late Roman times onwards.

- (2) The postglacial marine transgression started to affect the shores of the Bay of Elaia around 6000 BC.
- (3) The maximum marine transgression reached less than 1 km inland during its peak around 1500 BC. Compared to Miletus (60 km), Ainos (26 km), Ephesus (20 km) and Troia (10 km) this is rather late and the distances prograded are much shorter. The reason for this is a geomorphological one, namely the small area of the Bay of Elaia, the lack of a major river, and the different activity patterns of the geologic grabens involved.
- (4) The sediments which caused the siltation of the original embayment derive from the slopes of the Bozyertepe, the castle hill, and the Yuntdağ, whereas deltaic input from the Bakırçay was minimal.
- (5) The maximum marine transgression in the Bergama Graben reached less than 15 km inland. The delta of the Bakırçay has prograded less than 4.5 km since Roman times.

7.1.2 Goal 2: Establishing a regional sea-level curve based on RSL indicators for the Bay of Elaia and discussing it within a wider Aegean context.

This chapter deals with a robust regional sea-level curve (RSL-curve) for Elaia, which is established by choosing reliable sea-level indicators and comparing them to other studies of the Aegean Sea and the modelled curve by Lambeck (1996) and Lambeck & Purcell (2005).

7.1.2.1 Changing sea level: a general overview

The factors affecting sea-level fluctuations are diverse (isostatic-, glacial-eustatic-, steric- and geotectonic factors, sediment type and supply, as well as coastal dynamics) and have been widely discussed by the scientific community (Pirazzoli, 2005; Lambeck, 1996; Peltier, 2002; Lambeck & Purcell, 2005; Brückner et al., 2010). Knowing this, the quest to establish a worldwide or even Aegean-wide sea-level curve for the late Quaternary cannot be solved (Stanley, 1995; Vacchi et al., 2014; Khan et al., 2015). Therefore, it is only realistic to establish relative regional sea-level curves.

As mentioned above, many coastal areas of the Aegean Sea have been investigated to detect Holocene sea-level changes. Two different types of RSL-curves have been produced for the Aegean.

So-called “Type 1” curves (Brückner et al., 2010) show a peak in sea level, which reached the contemporary or even topped the modern one during mid-Holocene times between 6000 and

3500 BP⁷. These curves have been published for example by Kelletat (2005; Peloponnese), Müllenhoff (2005; ancient Miletus) and Kayan (1988; for the Datça Peninsula and the Troas). Some of them use beach rock as sea-level indicators, which is a quite poor one due to its – so far unknown – position of formation in relation to MSL (mean sea level) and evolution (Kelletat, 2005, 2006; Voudoukas et al., 2007; Knight, 2007). Others are poorly dated or include some speculations concerning the mid-Holocene peak (Kayan, 1988). In consequence, “Type 1” curves are nowadays obsolete and out-of-date when dealing with the Aegean Sea (Vacchi et al., 2014).

In contrast, “Type 2” curves present a uniform increase in sea level since 6000 BP with a modern-day maximum. For the Aegean Sea, these have been presented, for example, by Pavlopoulos et al. (2013; Lemnos Island), Vouvalidis et al. (2005) and Ghilardi et al. (2008) for the Thessaloniki coastal plain, Kolaiti & Mourtzas (in press; Western Saronic Gulf) and Poulos et al. (2009; Attico-Cycladic region).

RSL-curves for continental sites on the Turkish Aegean coast are rare. Müllenhoff (2005) published a “Type 1” curve for the Büyük Menderes Graben near ancient Miletus as well as Kraft et al. (2000) for Ephesus. Additionally, Kayan (1988) established a “Type 1” curve for the area of ancient Knidos. The same was done for ancient Troia (Kayan 1988). For the first time, Stock (2015) presents a “Type 2” sea-level curve for the region of ancient Ephesus. This is based on poor sea-level indicators characterised by unclear relationship to the palaeo-sea level. With an envelope of around 2 m, it is too imprecise to be taken into account in the following discussions.

Additionally, the general glacio-hydro-isostatic model of Lambeck (1996) and Lambeck & Purcell (2005) for the Aegean is often used as a reference. It is also a “Type 2” curve and suggests former sea levels of -130 to -110 during the LGM (Last Glacial Maximum), -60 to -44 m at 10000 BP, -8 to -2 m at 6000 BP and -1.7 to -1 m at the turn of the eras. The envelope can be minimised by choosing a specific geographical site. This was done in this study (for the region of the nearby island of Lesvos) to compare it as a reference curve with the one derived from Elaia (Lambeck, 1996).

⁷ This chapter deals with geologic terms. Therefore, the ages are stated in BP (before present; before 1950, since the chronologies are based on ¹⁴C-ages). Chronological estimations in BC (before Christ) and AD (anno Domini) are used again in the coming parts, showing an archaeological context.

7.1.2.2 Sea-level indicators: a general overview

A reliable sea-level indicator has to fulfil at least two conditions:

- (1) Its position in relation to the palaeo-sea level integrating the tidal range variations at the time of its formation should be clearly known (in sum: precision);
- (2) it must be reliably dated using radiometric techniques (^{14}C , OSL, U/Th etc.) or archaeological/architectural-historical means (in sum: reliable dating).

Selected sea-level indicators are grouped in four:

- (1) Sedimentological Geological features: tidal notches (Pirazzoli et al., 1997; Pirazzoli, 2005; Evelpidou et al., 2012a; Evelpidou & Pirazzoli, 2014; Marriner et al., 2014), marine terraces and shore platforms (Bloom & Yonekura, 1985; Marshall & Stephenson, 2011; Stephenson et al., 2012), isolations basins (Murray-Wallace & Woodroffe, 2014), raised beach ridges (Otvos, 2000) and – by unclear evidence – beachrock (Kelletat, 2006; Knight, 2007; Vousdoukas et al., 2007).
- (2) Sedimentological features: the topset/ foreset contact in Gilbert-type deltas (Dumas et al. 1988, Brückner et al., 2010) and peat from paralic swamps (Müllenhoff, 2005; Brückner et al., 2010).
- (3) Biological features: bioerosive notches (Kelletat, 2013), corals and coral reefs (e.g., *Acropora palmata*; Toscano et al., 2011), microatolls (*Porites lutea*; Scoffin & Stoddart, 1978; Kelletat, 2013; Murray-Wallace & Woodroffe, 2014), marine molluscs (Murray-Wallace et al., 2000) and living caves of sea urchins (Kelletat, 2013).
- (4) Archaeological remains: fish ponds (Evelpidou et al., 2012b; Morhange et al., 2013; Morhange & Marriner, 2015), harbour infrastructure like jetties, breakwaters and quays (Auriemma & Solinas, 2009) and private-/public buildings like pavements, graveyards or bath complexes such as the one in Bademli Ilica mentioned in Chapter 1.4 (Antonioli et al., 2007; Kelletat, 2013).

7.1.2.3 Sea-level indicators used in Elaia

Unfortunately, nearly none of the aforementioned sea-level indicators were found in the Elaia region. Therefore, the microfossil composition in connection with the transgressive contact have been used as a new sea-level indicator. In addition, the well-preserved closed harbour's western breakwater acts as an archaeological sea-level indicator.

Microfossil assemblage in connection to the transgressive contact

Several corings in the Bay of Elaia hit the bedrock at different heights above sea level. The microfossil composition in the transition zone between the bedrock and the overlying littoral zone bears information about the former sea level (Fig. 6). The first occurrence of microfossils in the sequences indicates the beginning of the transgression; however, just a few robust, larger sized foraminifers are preserved in this first high-energy stage of sea-level rise. Typical species are *Ammonia compacta* and *Elphidium crispum*. Due to the wave activity, they are transported to the lowermost part of the supratidal zone, directly above the mean sea level. Ostracods are normally absent during this stage. Rising sea level leads to permanent water coverage of the spot. This is represented by a fully established shallow marine association of foraminifers and ostracods, and acts as a valuable and reliable sea-level indicator; it is just to be added by the upward error bar of the tidal range. The first frequent occurrence of littoral foraminifers and ostracods states a shallow water depths of the site.

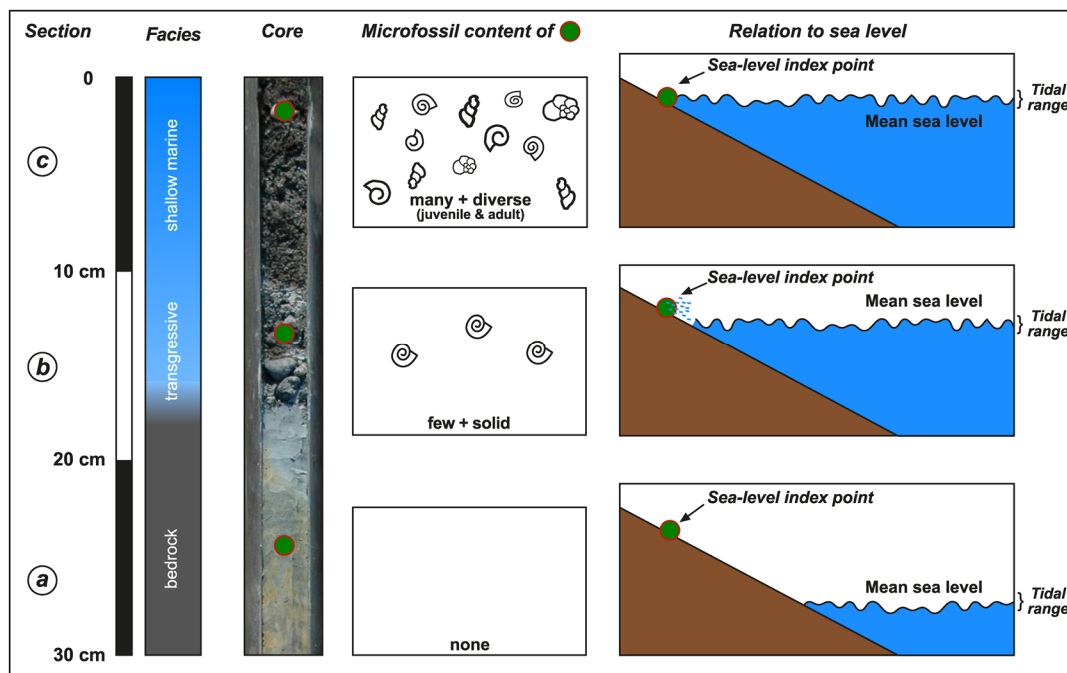


Fig. 6 Microfossil content in context of the transgressive contact within coring Ela 63 as an example. (a) Before the onset of the transgression; (b) the transgressive facies; (c) beginning of the shallow marine facies. The lowermost sample showing characteristics of (c) is to be radiocarbon dated to gain a sea-level index point.

Typical species of foraminifers are *Ammonia parkinsoniana*, *Elphidium aculeata* and *Lobatula lobatula* as well as the ostracods *Aurila convexa*, *Leptocythere bacesoni* and *Loxoconcha rhomboidea*. Plant remains and charcoal of these samples were ^{14}C -dated to prepare the RSL-curve

(Tab. 1). The sampling spot is close to the bedrock. Therefore, sediment compaction for this type of sea-level indicator is relatively minor here.

In sum, this type of indicator is of a high precision and well dateable by radiocarbon

The western breakwater of the closed harbour basin

The western breakwater of the closed harbour of Elaia consists of a basement made of stone debris, broken bricks and ceramics (Chapter 2, see also Fig. 7). The basement has a width of nearly 8 m and a vertical thickness of more than 2 m. Its asymmetric shape buffered wave energy on the seaward side and the plunging cliff-like profile on the harbour side created opportunities to anchor ships. It is topped by a massive wall of sandstone ashlars joined together by wooden dove-tail cramps (Chapter 2, Fig. 3d). This, as well as the lack of *opus caementitium* (Roman concrete) as a building material, dates the breakwater to pre-Roman times (Ganzert et al., 1984; Waelkens, 1987; Brandon et al., 2014). Additionally, the shift from open marine sediments to lagoonal sedimentation inside the closed harbour basin (Chapters 2 & 7.2.1) and written sources dealing with the early influence of the Pergamian Kings around 250 BC (Chapter 1.5) led to the conclusion that the breakwater was most probably built in the early 3rd century BC. The upper limit of the breakwaters basement can be used as reliable sea-level marker (Fig. 7).

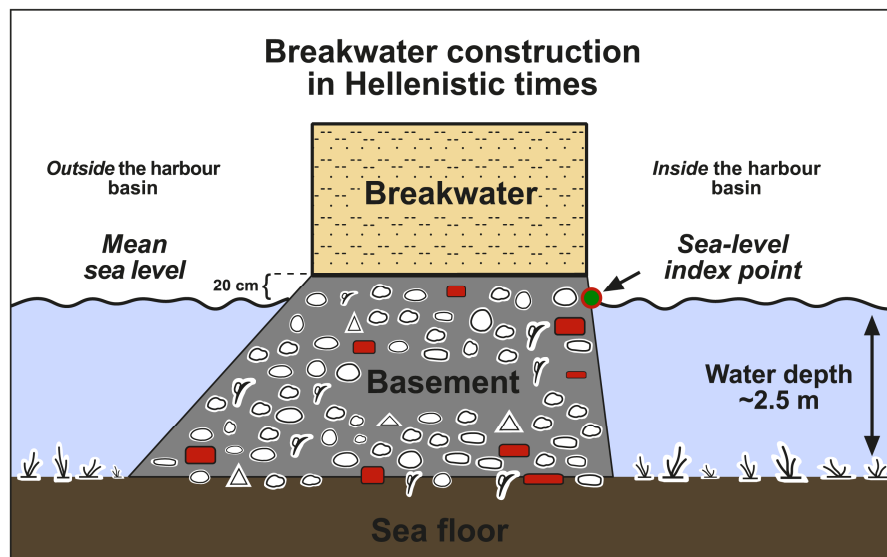


Fig. 7 Breakwater construction in Hellenistic times (cf. Chapter 2). The contact between the breakwater boulders and the basement acts as a good sea-level marker.

Thus, the functional height i.e. the upper side of the basement, was about 20 cm above the early Hellenistic sea level (Antonioli et al., 2007; Auriemma & Solinas, 2009). The sandstone ashlars of the wall on top must have been situated above the former sea level because this kind of stone

is too soft to resist constant salt-water contact. Moreover, the wave energy would have shifted the ashlars quickly, if they had been underwater and exposed to wave action for a longer time. Written sources from Roman Imperial times, such as Pliny the Younger⁸, provide insights into the construction style of breakwaters and show that the bases in those days were erected just above sea level. Afterwards a wall of ashlars was placed on top of them (Pliny; *Epistulae* 6, 31, 17). In addition, a similar construction of breakwaters is found in the submerged harbours of Capo Malfatano and Nora (Sardinia/Italy; Antonioli et al., 2007).

As a result of coring Ela 18, the upper level of the western breakwater's basement is at present 1.67 m b.s.l. (Chapter 2). However, during its construction in early Hellenistic times it was about 0.20 m above mean sea level. Thus, in the 3rd century BC sea level was **1.90 ± 0.10 m** (the error margin is the tidal range) lower than today.

With regard to Chapter 2, three different components of the breakwater might have been compacted since the time of construction:

- (1) The bedrock: As stated above, compaction of the underlying sandstone bedrock is insignificant.
- (2) The underlying marine sand: Based on coring Ela 70, the bedrock occurs at a depth of 8 m b.s. (below the surface; Chapter 2). Based on this assumption, an at least 4–5 m thick sand package between the bottom side of the breakwater's basement and the bedrock can be estimated. Many different factors influence the compactibility of sediments (e.g. mean grain size, grain-size distribution, content in pebbles and type of organic matter, the process of consolidation, the overlying mass etc.; Brain et al., 2012; Salvatore et al., 2015). In addition to ambiguities regarding the thickness of the sediment, most of these parameters are unknown in our case.
- (3) The base of the breakwater: As evidenced by the geoelectric cross-section (Chapter 2), it is assumed to have a minimum thickness of 2–3 m. Due to its heterogeneity, a detailed compaction rate of the basement is impossible to determine, but it is important to bear this in mind when interpreting the data.

Overall, compaction has to be assumed. This would result in an overestimation of the sea-level marker in relation to the time of its construction. However, many influencing factors are indeterminable. Therefore, a correction of the compaction was not done here. Nevertheless, this correction might influence just the youngest point of the modelled sea-level curve. Its other five

⁸ Pliny the Younger (Gaius Plinius Caecilius Secundus); Roman senator and advocate, AD 62-113/115.

points were reconstructed using the microfossil content in connection with the transgressive contact, which is unaffected by compaction.

In sum, this indicator is of high precision and excellently dated by archaeological, historical and sedimentological means.

7.1.2.4 A RSL-curve for the Bay of Elaia

According to the presented sea-level indicators, a “Type 2” RSL-curve based on six points is modelled (Fig. 8).

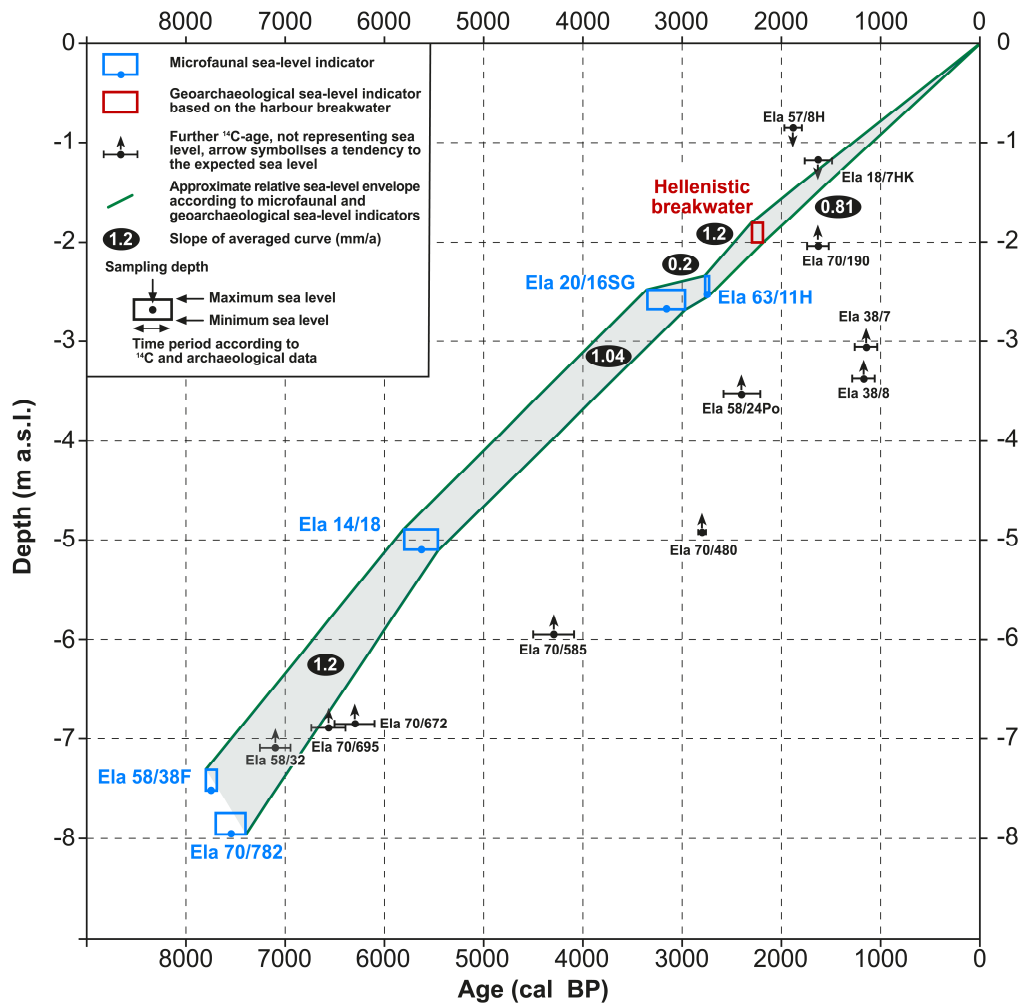


Fig. 8 Modelled RSL-curve for the Bay of Elaia based on the established sea-level indicators at the breakwater of the closed harbour (red) and the microfossil data in the context of the transgressive contact (blue).

The curve starts at a depth of 8 m b.s.l. and 7500 years BP (Ela 70/782; 7370–7639 cal BP; Tab. 1) and 7.46 m b.s.l.; around 7700 years BP (Ela 58/38F; 7825–7680 cal BP) showing an envelope of approximately 80 cm. The slope is quite steep in this part (1.2 mm/a). The envelope shrinks to just 50 cm at 5.10 m b.s.l.; around 5600 years BP (Ela 14/18; 5465–5826 cal BP) and continues at that width up to 2.66 m a.s.l.; around 3600 years BP (Ela 20/16SG; 3485–3684 cal BP) while

the slope decreases to 1.04 mm/a. The very slim 2σ -confidence interval of sample Ela 63/11 leads to a thinning of the envelope to approx. 30 cm at a depth of 2.57 m a.s.l. and 2750 years BP (Ela 63/11; 2741–2783 cal BP), which results in a slope of 0.2 mm/a. Due to the favourable error bar of the harbour's western breakwater, the curve maintains a slim envelope and steepens by 1.2 mm/a to 1.90 ± 0.10 m b.s.l. and 2300 years BP, until it goes on to the present day with a gentle slope of 0.81 mm/a.

Chapter 5 deals with the late Antique saltworks in the Bay of Elaia laying approximately 1 m b.s.l. The established RSL-curve shows a sea-level rise since 1500 BP of 1.20–1.30 m, which fully supports the temporal classification of the buildings. Although these data fit the RSL-curve, it is probably due to the vague relationship of the walls to the palaeo-sea level which are not integrated into the RSL-curve of Elaia (Fig. 8).

7.1.2.5 RSL-curve Elaia vs. Aegean-wide curves

The obtained RSL-curve for Elaia is in good agreement with the one modelled by Lambeck (1996) and Lambeck & Purcell (2005) for the area of Lesvos, Greece (Fig. 9). Between 7500 and 6000 BP Lambeck's curve is steeper in comparison to the one for Elaia. Both curves cross each other at a depth of 6.30 m b.s.l. (6600 years BP). After 6000 BP they show similar shape and steepness with a vertical difference of approx. 0.5–0.7 m whereby the estimated sea level at Elaia is below the modelled one proposed by Lambeck (1996) and Lambeck & Purcell (2005).

The RSL-curve published by Pavlopoulos et al. (2007) for the island of Skyros (Greece), a region showing uplift, is based on ^{14}C -ages on peat and organic matter and supplemented by several ages from beachrock samples. In this study both sea-level indicators correlate well for the past 3750 years. The resulting curve is of similar shape as the curve described by Poulos et al. (2009) and the one for Elaia, showing a vertical difference of approx. -0.5 m in relation to the Elaia curve.

The presented RSL-curve of Poulos et al. (2009) for the Attico-Cycladic region shows a constant rate of sea-level rise (0.9 mm/a) for the past 5500 years and is similar to the one of Elaia, with an offset of -0.4 m. This RSL-curve is based on data from several studies in the area, which use indicators such as ancient buildings, burial grounds and sedimentary proxies. As the region is said to be aseismic and tectonically stable, this led to the conclusion that the ongoing melting of glaciers mostly triggered the sea-level rise (eustatic factor) observed here, in combination with steric effects (Poulos et al., 2009).

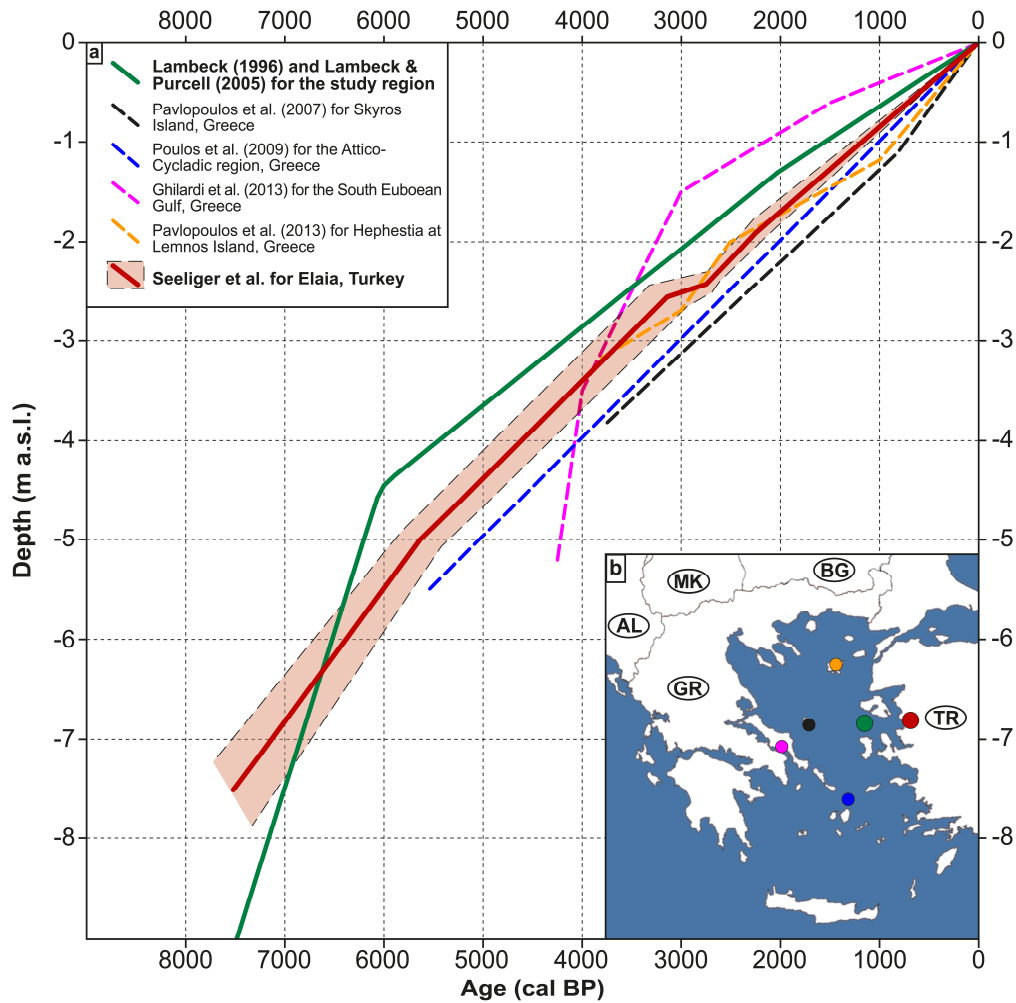


Fig. 9 Modelled RSL-curve for the Bay of Elaia compared to other curves for the Aegean region. (a) selected RSL-curves for sites in the Aegean Sea in addition to the modelled curve by Lambeck (1996) and Lambeck & Purcell (2005) for the area of Lesvos, Greece. (b) Location of the study sites in the Aegean region.

Ghilardi et al. (2013) published the most uncommon RSL-curve presented here for the area of the southern Euboean Gulf, which is characterised by a slight subsidence tendency. It is based on radiocarbon ages obtained from plant and bone fragments, showing the steepest slope of all the curves, beginning between 4200 and 3000 years BP and later even exceeding the Lambeck and Elaia curves. This is not surprising because the data derives from a thick deltaic sequence which is prone to subsidence.

Pavlopoulos et al. (2013) present a RSL-curve for the region of the ancient city of Hephestia at Lemnos (Greece), which is tectonically very active and often affected by earthquakes. Nevertheless, no geologic sea-level indicators, such as notches, are present above the contemporary sea level. This suggests an absence of uplift. The curve – based on radiocarbon ages of shells (*Cerastoderma* sp.) and organic matter – extends back to 3900 years BP. It shows a similar shape to

the one for Elaia. According to the authors, the reason for this offset between the Hephestia and the Lambeck curve is sediment compaction.

7.1.2.6 Summary

In sum, the following statements can be made for the RSL-curve of Elaia:

- (1) For the first time, a reliable “Type 2” RSL-curve is presented for a site on the Turkish Aegean coast.
- (2) The curve is in good agreement with other studies from the adjacent Aegean region. All of the curves are of the “Type 2” style, i.e., they do not show any mid-Holocene peak. Furthermore, they present similar slopes. In addition, most curves are below Lambeck’s curve; for Elaia an overall offset of around -0.7 m can be stated. The discrepancies may be due to differential tectonics.
- (3) The main reason for the negative offset compared to Lambeck’s curve is in the subsidence of the Bergama- and Zeytindağ Grabens wherefrom the Bay of Elaia is a part. The subsidence rate of the graben system is estimated to be about 1 m/ 1000 years (Aksu et al., 1987), but should be even lower (Chapters 2, 3 & 4).
- (4) Compaction can be excluded for almost all sea-level index points from Elaia, except for the one at the western breakwater. Due to the breakwater’s artificial origin, the compaction is undetectable.
- (5) The usability of the microfossil composition in connection to the transgressive contact acts as a useful new sea-level indicator and should be further tested at other sites e.g. in ancient Ainos and Kane. Its greatest strengths are the exclusion of compaction and only corings which include the transgressive contact are needed.
- (6) Sea-level rise was very constant in the Bay of Elaia with just one exception around 3000 years BP. This short period of decelerated sea-level rise is derived from the two neighbouring radiocarbon ages Ela 20/16SG and Ela 63/11H (Tab. 1); its significance should not be overestimated.
- (7) Calculated sea-level rates often suggest a constant rise at a certain rate. However, in a graben setting it is evident that an earthquake (Chapter 1.4), which triggers a sudden subsidence, causes a sudden sea-level rise. These steps in the RSL-curve are hard to detect and get lost when the known values are arithmetically averaged.

7.2 Elaia's different harbour sites during the period of prosperity

- *Working hypothesis 2: During its period of prosperity, the city of Elaia successfully operated several harbours, which can be elucidated using geoarchaeological evidence*

7.2.1 Goal 1: Describing the lifecycle of the closed harbour basin of Elaia.

For the first time, the closed harbour basin of Elaia was investigated using geoarchaeological means. Its lifecycle, from its construction to its abandonment, is discussed here.

7.2.1.1 The closed harbour basin of Elaia – a brief overview

Because it is incorporated into the main city wall and guarded by two massive breakwaters, the closed harbour basin is of special interest (Fig. 10). In early Hellenistic times, the closed harbour basin was constructed in an open shallow marine environment. After the construction of the breakwaters, the closed harbour basin was only connected to the open Mediterranean Sea by the 45 m wide entrance, resulting in a quiescent lagoon-like depositional environment (Fig. 10). This transition has been elucidated by a variety of methods. The harbour was in use during Hellenistic and early Roman times. Chapter 2 already illustrated the silting-up history of the closed harbour basin.

7.2.1.2 Construction age of the closed harbour basin

The construction age of the breakwaters can be determined by several criteria:

Architectural-historical criteria

Three features describe the construction age of the breakwaters.

Firstly, the breakwaters were erected without using Roman concrete (*opus caementicium*) which was not introduced to this region before ca. 50 BC (Ganzert et al., 1984; Waelkens, 1987; Brandon et al., 2014). Therefore, the construction of the breakwaters must have happened before this date (minimum age).

Secondly, according to coring Ela 18 the basement of the breakwater partly consists of ceramics of Hellenistic and Roman age, but does not include Classical or older ones. Thus, the breakwaters must have been erected in Hellenistic times or later (maximum age, cf. Chapter 2).

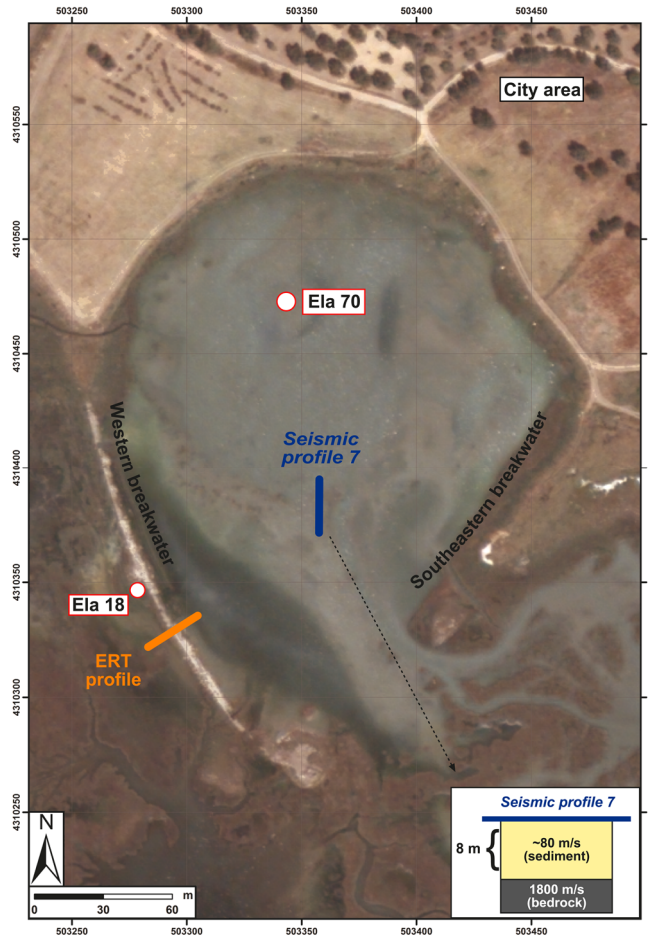


Fig. 10 The closed harbour basin of Elaia with locations mentioned in the text and a schematic view of seismic profile 7. Source: Quickbird 2 satellite image (acquired 02 April 2006; RGB composite based on bands 3, 2, 1).

Thirdly, the sandstone ashlars of the breakwater were joined together by wooden dove-tail cramps for stability. In general, this construction style can be attributed to Classical and early Hellenistic times. From the 4th century onwards it was mostly replaced by further advanced techniques, either using iron dove-tail cramps or U-cramps (Müller-Wiener, 1988; Faisst, 2013). This limits the time window of construction to the Classical or early Hellenistic period. Nonetheless, this technique may have been used even later, although it became increasingly outdated.

Historical sources

The city of Elaia came under Pergamon's rule between 246/241 BC (Allen, 1983; Pirson et al., 2015). It is probable that the Pergamenians immediately started to build the closed harbour basin. Therefore, a construction date for the breakwaters of about 245 BC seems to be realistic. During the First Macedonian War (215–205 BC) the Pergamenians already operated a fleet of at least 35 *pentere* ships, mostly stationed in Elaia. By that time, at the latest, the harbour basin must already have been erected (Livius; *Ab urbe condita* 28, 5, 1).

Coring evidence from Ela 70

The sediments of core Ela 70 form the basis for several methodological approaches to detect the marine-lagoonal transition (Chapter 6, Figs. 3 & 4).

Mean grain size

By constructing the breakwaters, the wave climate inside the closed harbour basin turned to that of a low-energy environment. This is clearly visible in the significant transition from high-energy hydrodynamic conditions (sand; mean grain size: $\sim 300 \mu\text{m}$) to low-energy ones (clayey silt; mean grain size: $< 30 \mu\text{m}$) at a depth of 4.38 m b.s. (Chapter 2, Fig. 5⁹). Therefore, the mean grain size acts as a valid indicator for this environmental change. Based on the age-depth plot of Ela 70 (Chapter 6, Fig. 3), this transition occurred in the time span 378-157 cal BC (2σ -confidence interval).

Microfossil content¹⁰

As microfossil analyses are a useful tool to reconstruct palaeoenvironmental conditions (Chapters 3 & 4), these studies are currently being carried out on samples from the sediment column of Ela 70. Because other methods have highlighted an environmental change at a depth of ca. 4 m b.s., a special focus was put on the section between 3 and 5 m b.s. Mainly foraminifers occur in the sediments of Ela 70. To a depth of 4.42 m b.s., the microfossil association is still dominated by coastal marine foraminifers like *Rosalina* sp., *Ammonia beccarii* and *Ammonia parkinsoniana*. At a depth of 4.32 m b.s. the first dominance of *Ammonia* sp. indicates more protected lagoonal conditions, typical of harbour basins (Goiran et al., 2010; Vittori et al., in press). Regarding the age-depth plot of Ela 70 (Chapter 6, Fig. 3), this transition dates to 379-91 cal BC (2σ -confidence interval).

Autotrophic and heterotrophic dinoflagellates¹¹

Dinoflagellates are unicellular organisms showing two distinctive flagella and a typical nucleus (Fensome et al., 1993). Together with diatoms and coccolithophorids, dinoflagellates represent the majority of the marine eukaryotic phytoplankton. During their lifecycle, many of them produce resistant cysts with lasting walls. Organic-walled dinoflagellate cysts (dinocysts) act as

⁹ The mean grain size is a standard parameter to study paleoenvironmental conditions. Since this tool is used in chapters 2–6, a detailed description is not given here.

¹⁰ As microfossils are used to detect palaeoenvironments in Chapters 3, 4 & 6, no detailed introduction in the methodology is given here

¹¹ As dinoflagellates are not introduced in Chapter 6 in detail, a brief summary about their biology and usability is given here.

suitable environmental proxies, because the cyst associations reflect even small changes in upper water conditions (e.g. nutrient availability, sea-surface temperature, salinity; de Vernal et al., 1997; Marret et al., 2001; Sangiorgi et al., 2002, 2005).

In addition to the examination of pollen, dinocysts were investigated as well (Chapter 6, Fig. 7). In this context, the differentiation in autotrophic and heterotrophic dinocysts is useful to detect the shift from shallow marine conditions to the harbour environment as a result of the construction of the breakwaters. As autotrophic dinocysts require light to photosynthesise, these species mostly occur in a light-flooded shallow marine environment. By contrast, heterotrophic species are unable to photosynthesise and consume organic material to survive (Fuchs et al., 2007; Campbell & Reece, 2009). The surplus of nutrients and the seclusion of the harbour water body provide a suitable habitat for heterotrophic species. The shift from dominating autotrophic dinocysts to heterotrophic ones occurs at 4.25 m b.s. in coring Ela 70. Based on the age-depth plot (Chapter 6, Fig. 3), this is dated to 274–62 cal BC (2σ -confidence interval).

Geophysics¹²

Additionally, the transition between the underlying marine sand to the harbour facies was detected by geophysical means. High damping effects caused by the high salt-water level led to the failure of depth resolving prospection methods like GPR (ground-penetrating radar) or ERT (electrical resistivity tomography). To image the bedrock depths and the marine-lagoonal transition to a depth of a few meters, shear wave refraction seismic methods were most appropriate (Dines & Lytle, 1979; Aldridge & Oldenburg, 1992). Unfortunately, the area of the closed harbour basin is covered by very shallow water and comprises muddy, poorly accessible parts. That hampers the use of refraction seismics which are in need of long geophone spreads. Therefore, only short profiles in the accessible parts of the closed harbour basin were performed by seismic Rayleigh-wave spectral analysis, which is increasingly used for engineering applications. 1D shear-wave velocity-depth distribution can be derived by fitting dispersed phase-velocities of Rayleigh-waves that result from different amplitude-depth distributions at different frequencies. In Elaia, 24 m long profiles with a spread of 24 vertical geophones were used in the MASW (multi-channel analysis of surface-waves) variant of Wilken & Rabbel (2012). Rayleigh-waves were excited at both ends of the profiles, using a steel plate and a sledge-hammer (Park et al., 1999; Xia et al., 1999).

¹² The results of the geoseismics are unpublished so far and not included in Chapters 2–6. Therefore, this section is more detailed as compared to the ones dealing with the mean grain size and the microfossil results.

Fig. 11 shows the results of profile P7. The red line indicates the shear-wave velocity depth model that provided the best data fit. It shows three major layers. The uppermost two layers (I and II) can be divided by their velocity gradient; a relatively steep gradient corresponds to the lagoonal layer showing an increase in velocity from 40 m/s to 80 m/s down to 3.5 m depth. The average velocity corresponds well with the observed low shear-wave velocities for lagoonal sediments (Rabbel et al., 2004). This is followed by a layer of a weaker velocity gradient (II), ranging from 90 m/s to 120 m/s down to approximately 7.8 m depth. Here, an abrupt increase in velocity from 120 m/s to 1800 m/s occurs, which represents the transition from the shallow marine facies to the sandstone bedrock (III).

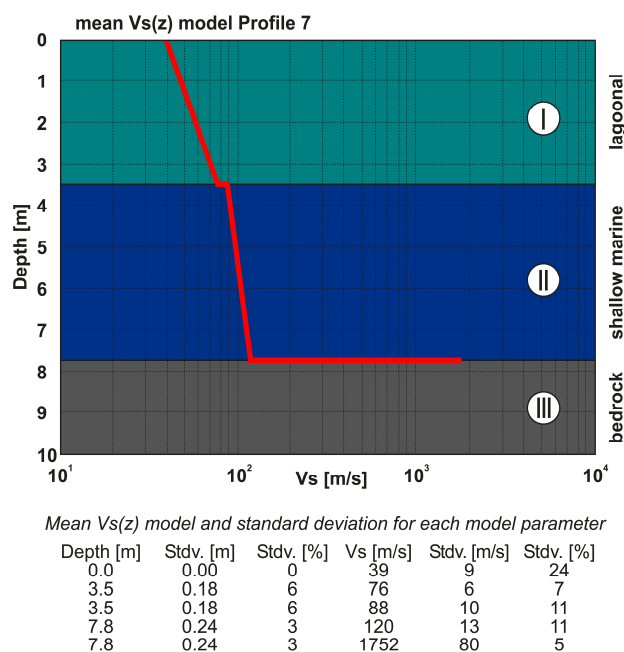


Fig. 11 Results of the geoseismic profile 7. For location cf. Fig. 10.

The uncertainty of the interface layer depths is estimated by statistical analysis (Wilken & Rabbel, 2012) to 0.18 m standard deviation for the lagoonal to marine interface and 0.24 m from the marine sediment to bedrock, which is 6 % and 3 % of the layer depth values. Nevertheless, the method presents a fairly accurate means to detect the local stratigraphy by means of shear-wave velocity. It is a point-wise estimation, integrating the data of short (24 m) seismic profiles to a 1D shear-wave velocity depth model. In sum, the transition between the shallow marine sediments and the lagoonal harbour facies was ascertained using seismics to be at a depth of 3.50 ± 0.18 m. Based on the age-depth plot of Ela 70, this corresponds to 18 cal BC–cal AD 271 (2σ -confidence interval) and so roughly to Roman times.

The temporal discrepancy with almost all the other results (Fig. 12) is caused by the different locations of the seismic profile P7 and coring Ela 70, on which the age-depth plot is based. It has to be mentioned that although seismic profile P7 is at a greater distance from the castle hill compared to coring Ela 70, the bedrock was hit at a similar depth. Therefore, without any further data, a plateau-like shape around 8 m b.s.l. for the bedrock in the area of the closed harbour basin can be assumed.

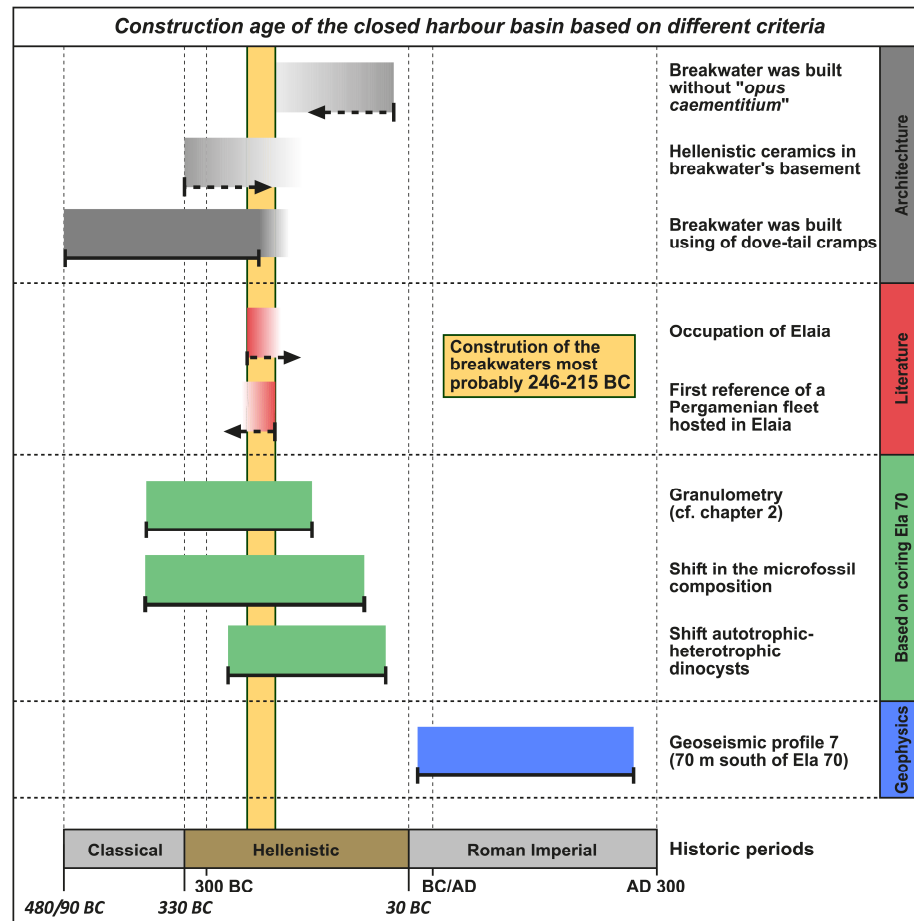


Fig. 12 Synoptic chronology of different approaches to detect the shift from shallow-marine conditions to lagoonal ones in the closed harbour basin as a result of the construction of its breakwaters. Full colour shading was used for ages based on the age-depth model of coring Ela 70 whereas shaded colours were used for limiting ages based on literary or architectural evidence. The dark yellow zone illustrates the most probable timespan for the construction of the breakwaters.

7.2.1.3 Silting up of the closed harbour basin

Elaia's closed harbour basin was in use during Hellenistic and Roman times. Its siltation is in detail described in Chapter 2. According to these results, the onset of substantial siltation occurred between the second half of the 3rd century and the end of the 4th century AD.

7.2.1.4 Tsunami impact in the Bay of Elaia?

Since the Aegean is an active tectonic region (Cocard et al., 1999; Doutsos et al., 2001; Papadopoulos, 2015) the risk of an earthquake and a subsequent tsunami should be taken into account (Schielein et al., 2007; Hadler, 2013). In recent years numerous studies have demonstrated that harbour basins act as suitable sites to preserve former tsunami. Reinhardt et al. (2006), Morhange & Marriner (2010), Bony et al. (2012), Morhange et al. (2015) and have described harbour sites which were affected by tsunami impacts.

The identification of tsunami deposits was not a focus of the studies in Elaia; however, "master core" Ela 70 (Chapter 6, Fig. 4) was chosen for an intensive search for the footprint of this natural hazard. Usually tsunami deposits show some typical characteristics, like an erosional contact to the underlying substrate, rip-up clasts, mud caps, fining-upwards sequences, allochthonous plant remains and microfauna etc. (e.g. Ruiz et al., 2010; Brill, 2012; Chagué-Goff et al., 2012; Engel, 2012) for which Ela 70 was investigated using high-resolution geochemical, granulometric and palynological methods. As a result, coring Ela 70 lacks evidence for tsunami impacts. This may be for two main reasons. Firstly, the Bay of Elaia is in a very sheltered position, at the end of the elongated Gulf of Elaia and partly secured by the island of Lesbos and the northern part of the Çeşme peninsula; this geomorphology would have weakened incoming tsunami waves. Secondly, before ca. 250 BC, the area of the later closed harbour basin was an open marine embayment, wherefore former tsunami deposits might have been reworked due to wave action or bioturbation. Later on, the sheltered closed harbour basin showed conducive conditions for the preservation of tsunamigenic sediments. Thus, tsunami, like the AD 365 event, which is reported for Phalasarna (Crete), or the AD 1856 event, which affected the island of Chios, might have hit Elaia as well (cf. Pirazzoli et al., 1992; Pirazzoli, 2005; Papadopoulos, 2015). There is, however, no positive evidence for it. In addition, no archaeological or written sources dealing with tsunami or big wave events are historically attested for the city of Elaia (pers. comm. by Prof. Felix Pirson, DAI Istanbul).

7.2.1.5 Summary

In summary, the following can be stated for the history of the closed harbour basin of Elaia:

- (1) Regarding Fig. 12 the construction date of the closed harbour basin in early Hellenistic times about 246-215 BC seems to be realistic. It is largely supported by almost all of the applied approaches. Only the geoseismic profile 7 dates the shift from open marine to lagoonal conditions to Roman times, but this is due to the different positions of the geoseismic profile and the age-depth model of coring Ela 70. One can state that the approach using literary sources (Livius; *Ab urbe condita* 28, 5, 1) is the most precise one. This is definitely true in the given case. The wide error bar of the approach using coring Ela 70 is caused by the age-depth model based on radiocarbon ages, which are displayed at the 2σ -confidence interval. Additionally, the “Hallstatt plateau” of the radiocarbon calibration curve widens the dating range of Classical and early Hellenistic ages (van der Plicht, 2004).
- (2) All presented methods show the clear environmental change from shallow marine conditions to lagoonal ones, caused by the construction of the breakwaters. Despite of the wide dating range of the geoscientific methods, they may act as valuable tools when the information from archaeological and historical sources is absent or very vague.
- (3) The silting-up process of the harbour basin accelerated during Roman times and led to the abandonment of the harbour no later than AD 500.
- (4) The sedimentary facies sequence of ELA 70 fits well to the “Ancient Harbour Parasequence” (AHP) postulated by Marriner and Morhange (2006b) derived from a summary of different harbour locations, most of them situated in the southern Mediterranean, especially in Tyre’s northern harbour.
- (5) Although the occurrence of tsunami events in the Aegean has been elucidated by other studies, no tsunamigenic sediments were detected in the closed harbour basin of Elaia.

7.2.2 Goal 2: Determining the water depths of Elaia's harbours and their accessibility by different ship classes during Hellenistic and Roman times.

The functionality of Elaia's harbours mainly depended on the water depths, which must have been sufficient for the most common ship classes of Hellenistic and Roman times.

7.2.2.1 The draughts of common war and merchant ships during Hellenistic and Roman times

Since ancient warships of the same class were built in a uniform style and equipped in the same way (oarsmen, weapons etc.), their draught can be reconstructed quite precisely. Morrison & Coates (1986, 1996) and Coates (1987) convincingly reconstructed the size and draught of Classical and Hellenistic oared warships. The most common warship classes of those days had draughts of approx. 1.10 m for the so-called threes (*trireme*; with three banks of oars) and up to approx. 1.50 m for the fifts (*pentere*; with five banks of oars; Morrison & Coates, 1986, 1996). Although warships with six or seven banks of oars are known for these periods showing draughts exceeding 1.50 m, such ships were not used by the Pergamenian fleet (Polybios: *Historíai* 16, 3–7; Murray 2012).

Compared to warships, the draughts of common merchant ships of those days greatly depended on their loading, which complicates draught reconstructions. Boetto (2010) and Auriemma & Solinas (2009) have investigated many shipwrecks and literary sources of the Mediterranean area and came to the conclusion that draughts of not more than 2.0 m seem to be realistic for most of the common merchant ships of the Hellenistic and early Roman period.

By setting the RSL-curve for Elaia (Chapter 7.1.2) and the age-depth model of Ela 58 resp. Ela 70 against each other, the former water depths of the closed harbour basin area (Fig. 13) and the open harbour area (Fig. 14) for the last millennia were identified. This results in three possible water depths plots for each of the harbour areas: a maximum, a medium and a minimum one. When dealing with age-depth models, sediment compaction should be kept in mind. Due to a lack of detailed information concerning the underlying substratum of each dated sample and in accordance with the sea-level index points (Chapter 7.1.2.3) a correction of the sediment compaction was not done while establishing the age-depth models for Ela 58 and 70.

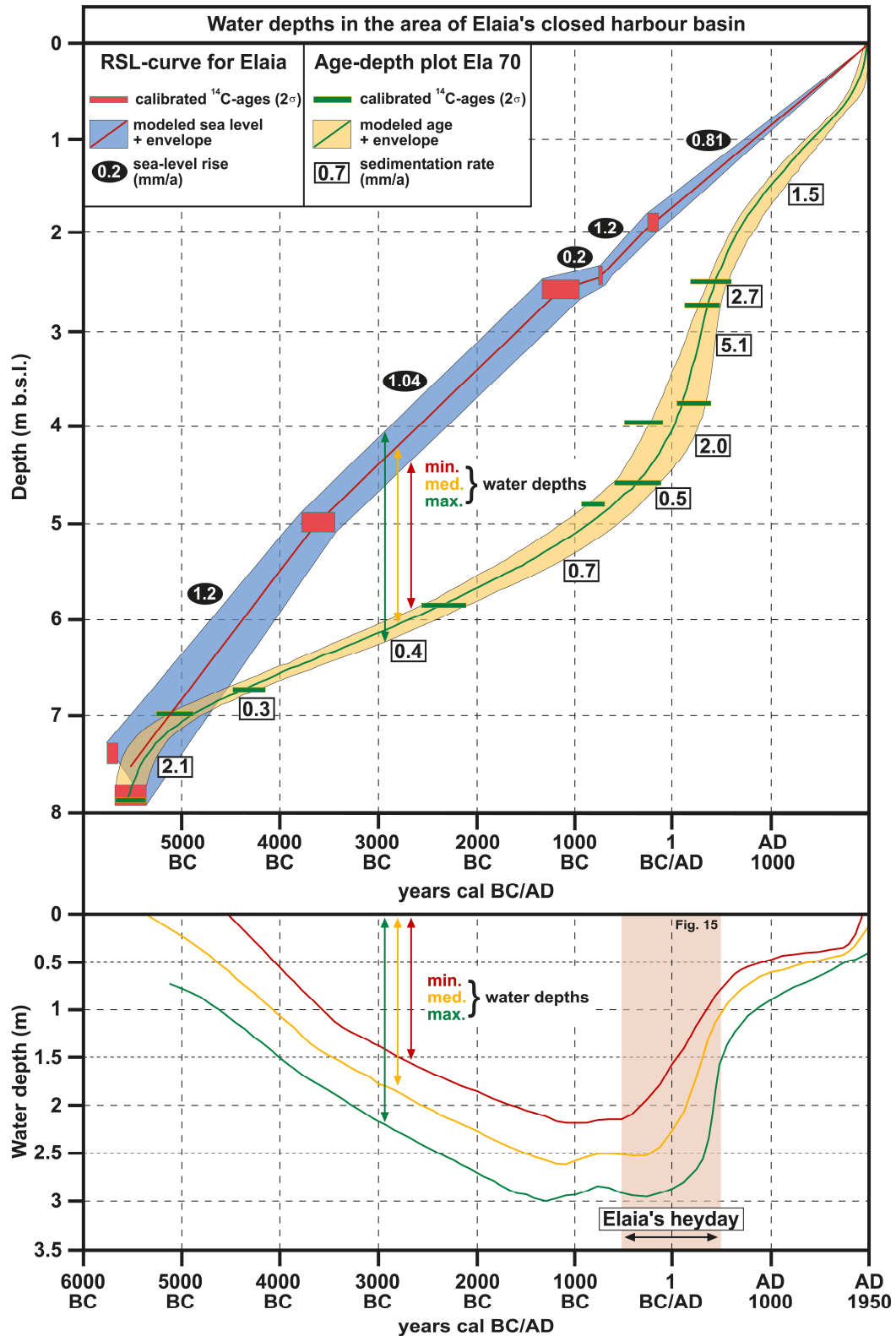


Fig. 13 Modelled water depths in the closed harbour basin of Elaia for the past 8000 years. In the upper part of the figure, the age-depth model of coring Ela 70 (yellow) is plotted against the RSL-curve (blue) for Elaia (Chapter 7.1.2). The interval in-between both graphs corresponds to the water depth. In the lower part of the figure the water depths are pictured. The most important period for the settlement of Elaia, between 490 BC and AD 500, is presented in Fig. 15.

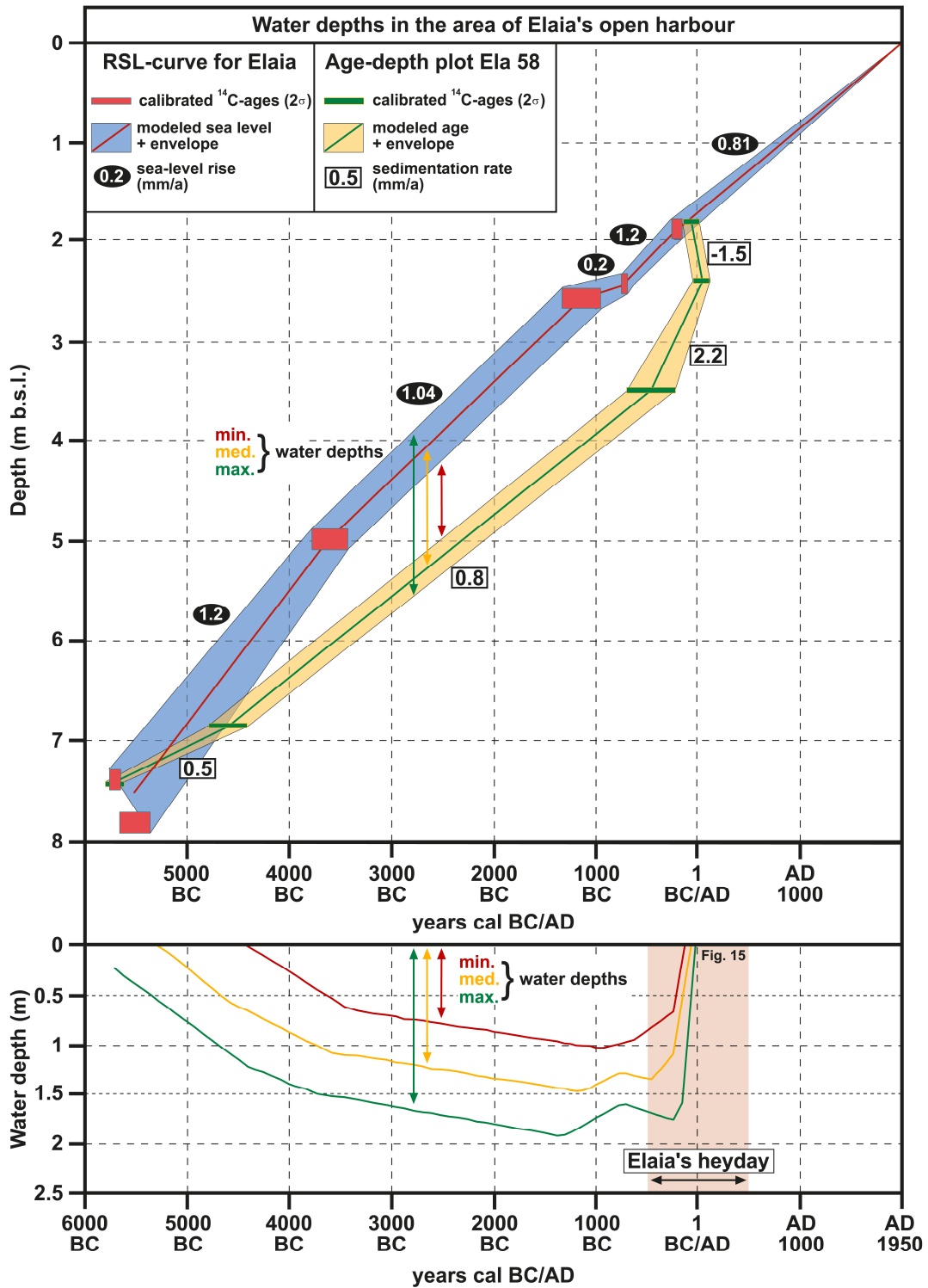


Fig. 14 Modelled water depths in the open harbour area of Elaia for the past 8000 years. In the upper part of the figure, the age-depth model of coring Ela 58 (yellow) is plotted against the RSL-curve (blue) for Elaia (Chapter 7.1.2). The interval in-between both graphs corresponds to the water depth. In the lower part of the figure the water depths are pictured. The most important period for the settlement of Elaia between 490 BC and AD 500 is presented in Fig. 15.

7.2.2.2 Reconstructed water depths of the closed and open harbours of Elaia

Fig. 15a shows the reconstructed water depths for the closed harbour basin from Classical times to late Antiquity, which includes the most flourishing period of Elaia. The draughts are for the common merchant ships and the *pentere* and *trireme* warship classes mentioned above.

According to the medium modelled water depths it was possible for all presented ship classes to enter the closed harbour basin during Hellenistic times and until around AD 150. During Roman Imperial times siltation increased, which led to a decrease in water depths. After AD 150, it was impossible for merchant ships to reach the harbour and only smaller *trireme* ships could use the basin during the entire Roman period. These results confirm and extend the results of Chapters 2 & 4.

Boetto (2010) stated that some merchant ship classes can have draughts of up to 4.5 m. In this context, it is interesting to note that the closed harbour basin of Elaia could never have accommodate such ships because its maximum water depths at the beginning of the Hellenistic period was around 3 m. As Elaia was the main harbour of the Pergamenian Empire this is a very interesting finding. Additionally, neither historical sources nor results of the corings provide an indication of dredging processes inside the closed harbour basin¹³.

Fig. 15b presents the results of water depths for the open harbour area. In this area, the water depths reached a maximum of just 1.90 m around 1400 BC. According to the medium modelled water depths it was only possible for the *trireme* class ships to reach this point, i.e. the coring site Ela 58 (Fig. 4), without running aground during the very beginning of the Hellenistic period. Later on all ships must have been beached there and hauled into the ship sheds. From Roman Imperial times onwards, the area was dry, artificially consolidated land which is in good accordance with the results outlined in Chapters 3 & 4.

¹³ Dredging activities to prevent siltation would have led to temporarily increased water depths. However, the geochemical record, the pollen analysis and the stratigraphically correct ¹⁴C-ages do not hint to any erosional unconformity within the sediment column.

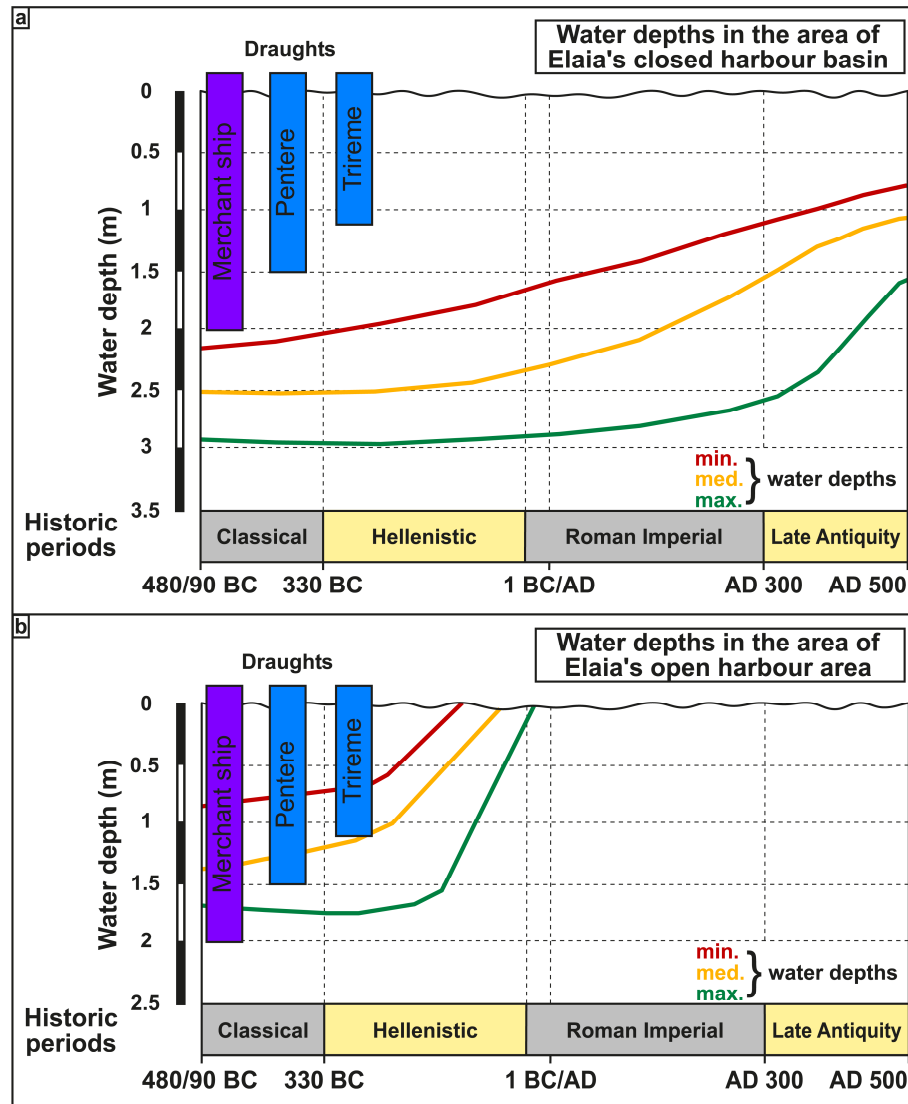


Fig. 15 Detailed view on the water depths of the closed harbour basin (a), and the open harbour area (b) from Classical times to Late Antiquity added by a simplified representation of draughts of different ship classes of those days.

7.2.2.3 Summary

To sum up, the following can be stated for the accessibility of the harbours during Elaia's prime:

- (1) The most common war and merchant ships were able to use the closed harbour basin until around AD 150. Later on, siltation prevented larger ships from entering the harbour. In late Antiquity, the closed harbour basin was also inaccessible for the shallow *trireme* ships. Following Chapter 2, the closed harbour basin has shown its contemporary configuration since around AD 500, which fits well with the modelled water depths in this chapter.

- (2) In contrast to Ephesus (Kraft et al., 2007; Stock et al., 2013; Delile et al., 2015), Marseille (Morhange et al., 2003) and Tyre (Marriner & Morhange, 2006a), no evidence of dredging is known for Elaia; also the radiocarbon dating results do not show any age inversion (Chapter 6, Fig. 4). Additionally, there is no erosional unconformity in the sediment columns of the cores, which might be due to dredging.
- (3) The open harbour area shows very shallow water depths of not more than 1 m for the Hellenistic period. Nevertheless, the area was a favorable landing site for vessels, which were stored in the adjacent ship sheds. By the transition to Roman times, the area was artificially consolidated. These results are in good agreement with the results presented in Chapters 3 & 4.
- (4) The water depths of the beach harbour (Fig. 4) area were not investigated, because the chronology of the corings of this region is insufficient to establish a suitable age-depth model. Here the assumptions made in Chapter 4 are fair to be considered. Separated by the *diateichisma* which prevented a direct contact with the inhabitants of Elaia, this area probably served as a landing site for foreign merchants and soldiers.

7.3 Human impact in the Bay of Elaia over the past millennia

- Working hypothesis 3: The temporal changes and the intensity of human impact on the environment can be elucidated by geoarchaeological research.

7.3.1 Main goal: To identify and quantify human impact on the Bay of Elaia over the past millennia.

Human impact on the environment in the Bay of Elaia is clearly documented in different archives. Broadly speaking, five temporal stages of human impact can be described.

7.3.1.1 Human impact and human-induced landscape changes over time

1) Before 850 BC

The mythical foundation of Elaia during the struggles of the Trojan War (13th/12st century BC) and a few pottery finds on the castle hill of Elaia do not bear detailed witness of those periods (Radt, 2011). Since not much is known about the pre-Classical period in Elaia, the pollen data (Chapter 6) allows human influence on the landscape to be probed during this period. Up to around 1000 BC the natural vegetation of deciduous oak forests with ash, linden and hazel was present in the environs of Elaia. Moderate pastoral activities are attested, documenting human impacts. This is represented by an increase in coprophilous fungi, which are associated with the dung of herbivores, since 1500 BC. Nonetheless, this finding should not be overinterpreted.

2) 850–250 BC

The presence of human activities become clearly obvious in the shift from natural oak forests to cultivated plants like olive, pistachio, walnut, grape and cereals around 850 BC. From this time onwards, olive was grown in Elaia. By lumbering, the former forests were degraded to macchia, which is additionally backed by the increase of *Glomus*-type spores¹⁴ which hints at intensified soil erosion.

3) 250 BC–AD 180

During Elaia's prime, human impact is strongest between ca. 170 BC and AD 180 (Chapter 6). Firstly, it is remarkable that the Elaitans managed to construct such massive breakwaters in the open-marine environment. Chapter 2 described how the area south of the castle hill was consolidated to make it urban land. The same holds true for the open harbour area and the adjacent ship sheds (Chapter 3). Like ancient Miletus, Ephesus and Ainos, wide parts of the city of Elaia

¹⁴ *Glomus* are arbuscular mycorrhizal fungi which live in symbiotic relationship to plant roots. Their occurrence in the sediment is a sign that plant roots had been exposed due to soil erosion.

were built on former marine ground (Brückner, 2005; Brückner et al., 2006, 2013, 2015). Additionally, parts of the city wall of Elaia were constructed even thicker than the city walls of Pergamon (Pirson, 2014). Therefore, the Elaïtans made every effort to build up their city, fortified it against enemies and turned the formerly minor city into a centre of commerce.

Secondly, at that time, the landscape around Elaia is a cultural one, dominated by the plantation of olive, grapes, pistachio and cereal fields. There is also evidence for pastoralism (goat and sheep).

Thirdly, during the prime of Elaia an increase in population is obvious. This led to an increase in parasites such as *Ascaris*, *Trichuris* and *Capillaria* which mostly infect humans and pigs (Reinhard et al., 2013). Stock et al. (in press) also reported parasites in the Roman harbour of Ephesus and linked these findings with the presence of a canalisation in the city or at least wastewater washed from the city area into the harbour basin. This might be a plausible scenario for Elaia as well, even though no developed canalisation system is reported for Elaia. In addition, the surplus of nutrient input into the harbour basin led to a nitrification which is clearly visible in the shift from autotrophic dinocysts to heterotrophic ones.

Fifthly, for the first time, the introduction and colonisation of the Black Sea dinocyst species *Peridinium ponticum* to the Mediterranean Sea is reported in the closed harbour basin of Elaia around 80 BC. *Peridinium ponticum* is restricted to the Black Sea and Marmara Sea (Fig. 16). It inhabits brackish water environments with mesotrophic to eutrophic upper waters conditions. The detection of this species acts as an evidence of trade and traffic relations with the Black Sea and Marmara Sea. These connections are confirmed by finds of historic seals clearly documenting trade to Rhodes, Chios, Knidos and Pamphylia (Pirson, 2008, 2010, 2012). The organisms were most probably transported as part of the bilge water of ships. Furthermore, during that time the closed harbour basin of Elaia obviously showed similar ecological conditions as the Black Sea.

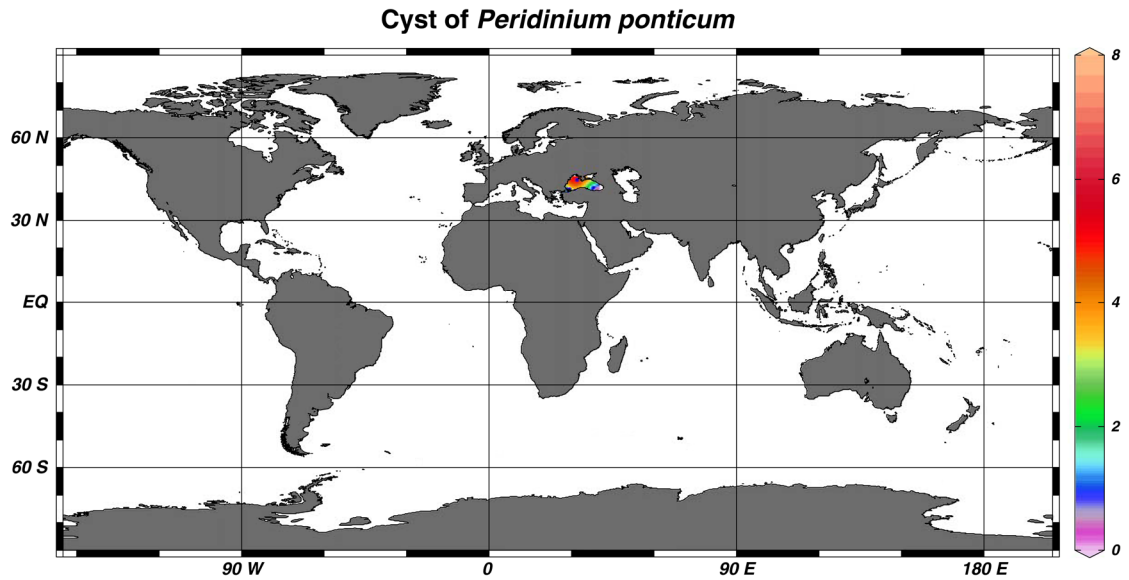


Fig. 16 Geographic distribution of *Peridinium ponticum* (Zonneveld et al., 2013).

Sixthly, pieces of carved cattle bones are present in coring Ela 58 (Fig. 17), which suggests diversified craftsmanship in the city of Elaia. It is very likely that these art objects were marketed and traded within the economic framework of Elaia.

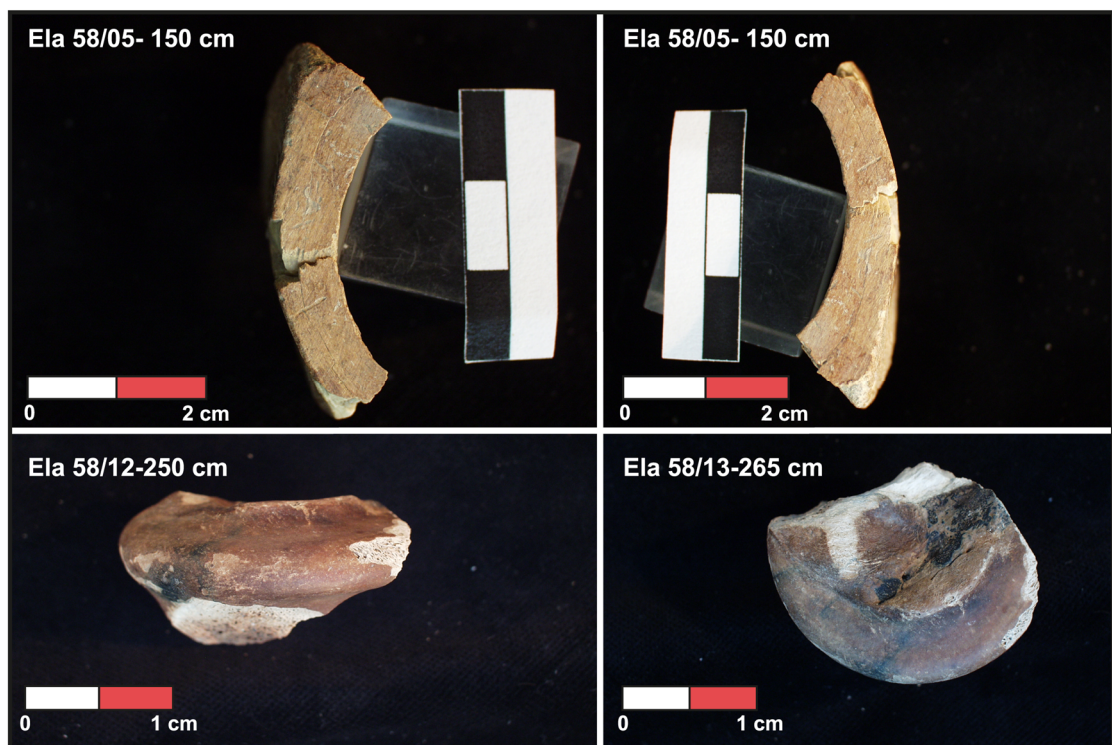


Fig. 17 Selection of carved bones out of coring Ela 58. Source: DAI Istanbul, 2011.

4) AD 180–800

Shrinking population in late Roman times led to a decrease of most of the human influence mentioned above. Reduced pollen amounts of almost all anthropogenic plants like olive in addition to rising percentages of *Glomus*-type spores (enhanced erosion) and coprophilous fungal spores (enhanced pastoralism) evoke a landscape dominated by intensive grazing activities, most probably by sheeps and goats. In addition, about 2 km south of the city in the shallow bay, saltworks were constructed, mostly built by spolia. Salt was of great economic value, not only in those times; it could easily be harvested by just a few men, thus being predestined as an economic source for the declining city (Chapter 5; Pirson, 2014).

5) After AD 800

From AD 800 onwards, human impact is insignificant. The natural vegetation of deciduous oaks did not recover in the following centuries. Instead semi-natural forest dominated by pine is characteristic of the landscape up until present day. Pine forest forms the vegetation in the Yuntdağ and Kozak regions. This fits well with the archaeological data which shows little indication of human activities after AD 800¹⁵.

7.3.1.2 Summary

To sum up, the following can be stated concerning the human impact in Elaia:

- (1) Five stages of human impact are evident by studying the environs of Elaia. Firstly, natural vegetation of deciduous oak forests occurs before ca. 850 BC; human impact is evidenced by moderate pastoralism. Secondly, a degradation period caused by lumbering and increased settlement activities is evident until around 250 BC. Thirdly, a phase of intense human impact, documented by a remarkable vegetation change, the occurrence of human parasites, higher heavy-metal concentrations, human artwork (carved bones, pottery, etc.) economic relations and intense construction activity (building of the harbours) is obvious during the prime of the settlement around 250–180 BC. Fourthly, a declining period of the city with decreasing human impact up to ca. AD 800 can be stated. Fifthly, the absence of human impact led to a new natural vegetation of pines. The natural climax vegetation (stage 1) was, however, not re-established.
- (2) Thanks to the pollen data, it is possible to detect the natural vegetation before the so far known human occupation started in the first millennium BC. Human impact during

¹⁵ Human impact on the area has become clearly visible during the last years due to the building of a new highway and the massive mining in connection with the building of the new container port in the outer Bakırçay delta.

the prime of Elaia became evident by a wide range of indicators, which are quite common and found in other studies of ancient settlements as well (cf. Brückner et al., 2006; Stock et al., in press). A special feature of Elaia is the abandonment of the city in the late 1st millennium AD and the reoccurrence of pine trees. It is surprising that the natural climax vegetation of deciduous oak forests did not repopulate the area.

- (3) Human impact in Elaia became obvious not only in the sediment archives but also in the intense building activities which changed a formerly small and unimportant Classical polis to the harbour city of the Pergamenian Empire – “Pergamon’s maritime satellite”, a term coined by Pirson (2004, 2014). After the decline, the remaining population invested great effort in order to construct the saltworks by reusing the building material of the city as spolia.

Chapter 8

8 Conclusions

For the first time, geoarchaeological research was conducted in the Bay of Elaia, which hosted the harbour city of Pergamon. As part of a wider project, under the auspices of the DAI Istanbul, this geoarchaeological study resolves questions dealing with the location and usability of the harbour sites, the coastal evolution and landscape changes caused by human impact over the past eight millennia. A view of the "bigger picture" was achieved by correlating and comparing the results of Elaia with results from selected Aegean islands and continental sites in Asia Minor.

The postglacial marine transgression drowned the shores of the later Bay of Elaia 5500 years BC, reaching its maximum around 1500 years BC about 1 km inland. Since 850 BC increasing settlement activities in the area became obvious in the palynological results, which led to accelerated erosion/sedimentation and a seaward shift in the shoreline. Former marine areas became dry land and parts of the city were built out onto former marine sediment. With the occupation of the city by the Pergamenians around 250 BC, intense building activities and an increase in population occurred. The construction of the closed harbour basin was determined using a series of interdisciplinary methods. As a result, the construction age, given by ancient literature seems to be the most reliable one dating to 246–215 BC. Nevertheless the other methods are useful to adopt at other silted-up harbour sites, where ancient literature is lacking. In the following centuries human impact was highest. The closed harbour basin, showing no indication of dredging activities, acted as a favourable sink for human waste, as evidenced by eggs of parasites, enhanced heavy-metal concentration and craftsmanship. Additionally, the first occurrence of the Black Sea dinocyst species *Peridinium ponticum* in the Mediterranean Sea documents naval traffic relations with the Black Sea region. This is supported by archaeological finds of coins, seals and ceramics originating from abroad.

During its most flourishing period, Elaia operated three different harbour sites: the closed harbour, the open harbour and a beach harbour. For the first time, estimations of the water depths led to the conclusion that the closed harbour basin could be exploited by common ship classes until AD 150. Shortly afterwards, increased siltation of the closed harbour basin led to its abandonment. The water depth in the open harbour area in front of the ship sheds was insufficient to anchor larger vessels. Instead of anchoring here, the ships were slipped to the ship sheds for maintenance work. The same also applies to the beach harbour in the eastern city district of

Elaia. As harbour infrastructure is lacking, this area acted as an area where foreign soldiers and merchants beached their ships and put up their camps.

With the loss of importance during Roman times accompanied by the gradual silting up of the closed harbour basin, the population of the city shrank and the remaining people used building material from the city to construct saltworks as an economic source of income.

For the first time, a RSL-curve for a continental site on the Turkish Aegean coast has been established with a new methodology to define reliable sea-level index points. This curve is in good agreement with the models by Lambeck (1996) and Lambeck & Purcell (2005). Additionally, it correlates well with actual RSL-curves of the adjacent Aegean region. Furthermore, ongoing research in ancient Ainos and Kane will hopefully add new data for the Aegean region.

Since Elaia is separated from the main Bergama Graben by the flat Bozyer Tepe, the marine transgression did not reach as far inland as in similar constellations in the region, such as Miletus, Ainos, Troia or Ephesus (Alpar, 2001; Brückner, 2005; Kraft et al., 1980, 2007; Stock, 2015). Geoarchaeological investigations in the inner part of the Bergama Graben have been undertaken by Schneider et al. (2013, 2014, 2015). As their focus was on colluvial and alluvial processes, they did not solve the question of the marine extension in the Bergama Graben. This research gap needs to be filled, particularly because several prehistoric settlements like the Yeni Yeldeğirmeni Tepe and the Çiftlik are located here and their relationship to the sea should be investigated (Chapter 6, Fig. 1, Horejs, 2014, 2015b).

Furthermore, a unique feature of Elaia is the relatively short period of human occupation. Therefore, the waxing and waning of human impact in contrast to natural conditions before and after the occupation phase is clearly visible. Therefore, Chapter 6 acts as one of only a few publications of this region dealing with the recovery of the “natural” environment after a prolonged period of human impact.

To sum up, the research in Elaia and this PhD thesis acts as a valuable example of interdisciplinary work looking to resolve upcoming questions which deal with shoreline displacements, sea-level studies, coastal evolution, hazards and ancient harbour research in an archaeological context. As in the foreseeable future no excavation in Elaia will be permitted by the Turkish authorities, this thesis acts as a compendium for paleogeographical and geoarchaeological reconstructions of the Bay of Elaia in a broader sense.

References

Historical sources:

- Herodot: *Historíai*. Translation by Marg, W., Artemis, Zürich 1964 (Greek to German).
- Livius: *Ab urbe condita*. Liber XXVIII. Translation by Blank-Sangmeister, U., Reclam, Ditzingen 2012 (Latin to German).
- Pausanias: *Graeciae descriptio*. Edited by Schubart, J.H.C., Kessinger Publishing, Whitefish 2009(Latin).
- Pliny: *Epistulae*. Translation and comments by Philips, H., Reclam, Stuttgart 1998 (Latin to German).
- Polybios: *Historíai*. Translation by Waterfield, R., Oxford University Press, Oxford/New York 2010 (Greek to English).
- Strabo: *Geographika*. Translation and comments by Forbiger, A., Marix, Wiesbaden 2005 (Greek to German).

References:

- Aksu, A.E., Piper, D.J.W., Konuk, T., 1987. Late Quaternary tectonic and sedimentary history of outer İzmir and Çandarlı Bays, Western Turkey. *Marine Geology* 76, 89–104.
- Aldridge, D.F., Oldenburg, D.W., 1992. Refractor imaging using an automated wavefront reconstruction method. *Geophysics* 57 (3), 378–385.
- Allen, R.E., 1983. *The Attalid Kingdom. A Constitutional History*. Oxford University Press, Oxford.
- Alpar, B., 2001. Plio-Quaternary history of the Turkish coastal zone of the Enez-Evros Delta: NE Aegean Sea. *Mediterranean Marine Science* 2 (2), 95–118.
- Altunkaynak, Ş., Yilmaz, Y., 1998. The Mount Kozak magmatic complex, Western Anatolia. *Journal of Volcanology and Geothermal Research* 85, 211–231.
- Antonioli, F., Anzidei, M., Lambeck, K., Auriemma, R., Gaddi, D., Furlani, S., Orrù, P., Solinas, E., Gaspari, A., Karinja, S., Kovačić, V., Surace, L., 2007. Sea level change during Holocene from Sardinia and northeastern Adriatic (central Mediterranean Sea) from archaeological and geomorphological data. *Quaternary Science Reviews* 26, 2463–2486.
- Auriemma, R., Solinas, E., 2009. Archaeological remains as sea level change markers: a review. *Quaternary International* 206, 134–146.
- Başaran, S., 2010. *Ainos (Enez)*. University İstanbul Press, İstanbul.
- Bay, B., 1999. *Geoarchäologie, anthropogene Bodenerosion und Deltavorbau im Büyük Menderes Delta (SW-Türkei)*. GCA, Bochum.

- Bloom, A. L., Yonekura, N., 1985. Coastal terraces generated by sea-level change and tectonic uplift. In: Woldenberg, M.J. (Ed.), *Models in geomorphology*. Allen and Unwin Inc., Winchester, United States, 139–153.
- Boetto, G., 2010. Le port vu de la mer: l'apport de l'archéologie navale à l'étude des ports antiques. *Proceedings of the International Congress of Classical Archaeology*, September 22–26, 2008, Rome, 112–128.
- Bony, G., Marriner, N., Morhange, C., Kaniewski, D., Dogan, P., 2012. A high-energy deposit in the Byzantine harbour of Yenikapi, Istanbul (Turkey). *Quaternary International* 266, 117–130.
- Brain, M.J., Long, A.J., Woodroffe, S.A., Petley, D.N., Milledge, D.G., Parnell, A.C., 2012. Modelling the effects of sediment compaction on salt marsh reconstructions of recent sea-level rise. *Earth and Planetary Science Letters* 345–348, 180–193.
- Brandon, C.J., Hohlfelder, R.L., Jackson, M.D., Oleson, J.P., 2014. *Building for Eternity: The History and Technology of Roman Concrete Engineering in the Sea*. Oxbow Books, Oxford.
- Brill, D., 2012. The tsunami history of southwest Thailand - Recurrence, magnitude and impact of palaeotsunamis inferred from onshore deposits. Ph.D. Thesis, University of Cologne, Germany.
- Brückner, H., 2005. Holocene shoreline displacements and their consequences for human societies: the example of Ephesus in western Turkey. *Zeitschrift für Geomorphologie N.F.* 137 (Suppl), 11–22.
- Brückner, H., Gerlach, R., 2011. Geoarchäologie. In: Gebhardt, H., Glaser, R., Radtke, U., Reuber, P. (Hrsg.), *Geographie*. Spektrum, Heidelberg, 1179–1186.
- Brückner, H., Müllenhoff, M., Gehrels, R., Herda, A., Knipping, M., Vött, A., 2006. From archipelago to floodplain – geographical and ecological changes in Miletus and its environs during the past six millennia (Western Anatolia, Turkey). *Zeitschrift für Geomorphologie N.F.* 142 (Suppl), 63–83.
- Brückner, H., Kelterbaum, D., Marunchak, O., Porotov, A., Vött, A., 2010. The Holocene sea level story since 7500 BP - Lessons from the Eastern Mediterranean, the Black and the Azov Seas. *Quaternary International* 225, 160–179.
- Brückner, H., Urz, R., Seeliger, M., 2013. Geomorphological and geoarchaeological evidence for considerable landscape changes at the coasts of western Turkey during the Holocene. *Geopedology and Landscape Development Research Series* 1, 81–104.
- Brückner, H., Schmidts, T., Bücherl, H., Pint, A., Seeliger, M., 2015. Die Häfen und ufernahen Befestigungen von Ainos – eine Zwischenbilanz. In: Schmidts, T., Vučetić, M.M. (Hrsg.), *Häfen im ersten Millennium AD. Bauliche Konzepte, herrschaftliche und religiöse Einflüsse*. Selbstverlag des Römisch-Germanisches Zentralmuseums, Mainz, Germany, 53–76.
- Campbell, N.A., Reece, J.B., 2009. *Biology*. Pearson Studium, London.
- Cartledge, P., 2004. *Alexander the Great. The Hunt for a New Past*. Overlook Press, New York.

- Chagué-Goff, C., Andrew, A., Szczuciński, W., Goff, J., Nishimura, Y., 2012. Geochemical signatures up to the maximum inundation of the 2011 Tohokuoki tsunami – implications for the 869 AD Jogan and other palaeotsunamis. *Sedimentary Geology* 282, 65–77.
- Coates, J.F., 1987. Reconstructing the ancient Greek trireme warship. *Endeavour* 11 (2), 94–99.
- Cocard, M., Kahle, H.-G., Peter, Y., Geiger, A., Veis, G., Felekis, S., Paradissis, D., Billiris, H., 1999. New constraints on the rapid crustal motion of the Aegean region: recent results inferred from GPS measurements (1993-1998) across the West Hellenic Arc, Greece. *Earth and Planetary Science Letters* 172, 39–47.
- Conze, A., Berlet, O., Philippson, A., Schuchhardt, C., Gräber, F., 1912/1913. *Stadt und Landschaft. Altertümer von Pergamon 1*. Walter de Gruyter, Berlin.
- Delile, H., Blichert-Toft, J., Goiran, J.-P., Keay, S., Albarède, F., 2014. Lead in ancient Rome's city waters. *Proceedings of the National Academy of Sciences of the United States of America* 111 (18), 6594–6599.
- Delile, H., Blichert-Toft, J., Goiran, J.-P., Stock, F., Arnaud-Godet, F., Bravard, J.-P., Brückner, H., Albarède, F., 2015. Demise of a harbour: A geochemical chronicle from Ephesus. *Journal of Archaeological Science* 53, 202–213.
- Demirci, A., Özden, S., Bekler, T., Pinar, A., 2015. An active extensional deformation example: 19 May 2011 Simav earthquake (Mw = 5.8), Western Anatolia, Turkey. *Journal of Geophysics and Engineering* 12 (4), 552–565.
- Dines, K.A., Lytle, R.J., 1979. Computerized geophysical tomography. *Proceedings of the IEEE* 67 (7), 1065–1073.
- Dörpfeld, W., 1910. Die Arbeiten zu Pergamon 1908–1909. *Athenische Mitteilungen* 35, 345–399.
- Dörpfeld, W., 1911. Zum Elaitischen Golf. *Hermes* 46, 444–457.
- Dörpfeld, W., 1912. Die Arbeiten zu Pergamon 1910–1911. *Athenische Mitteilungen* 37, 233–276.
- Dörpfeld, W., 1928. Strabon und die Küste von Pergamon. *Athenische Mitteilungen* 53, 117–159.
- Doutsos, T., Kokkalas, S., 2001. Stress and deformation patterns in the Aegean region. *Journal of Structural Geology* 23 (2–3), 455–472.
- Dumas, B., Gueremy, P., Hearty, P.J., Lhenaff, R., Raffy, J., 1988. Morphometric analysis and amino acid geochronology of uplifted shorelines in a tectonic region near Reggio Calabria, South Italy. *Palaeogeography, Palaeoclimatology, Palaeoecology* 68, 273–289.
- Elshanawanya, R., Zonnevelda, K., Ibrahim, M.I., Kholeif, S.E.A., 2010. Distribution patterns of recent organic-walled dinoflagellate cysts in relation to environmental parameters in the Mediterranean Sea. *Palynology* 34 (2), 233–260.

- Emre, Ö., Özalp, S., Dogan, A., Özaksoy, V., Yildirim, C., Göktas, F., 2005. Izmir yakın Çevresinin diri fayları ve deprem potansiyelleri (Active faults and earthquake potential in the Izmir region). Maden tetkik ve arama genel müdürlüğü Rapor No. 10754.
- Engel, M., 2012. The chronology of prehistoric high-energy wave events (tropical cyclones, tsunamis) in the southern Caribbean and their impact on coastal geo-ecosystems – a case study from Bonaire (Leeward Antilles). Ph.D Thesis (unpublished), University of Cologne, Germany.
- Evelpidou, N., Kampolis, I., Pirazzoli, P.A., Vassilopoulos, A., 2012a. Global sea-level rise and the disappearance of tidal notches. *Global and Planetary Change* 92–93, 248–256.
- Evelpidou, N., Pirazzoli, P., Vassilopoulos, A., Spada, G., Ruggieri, G., Tomasin, A., 2012b. Late Holocene sea level reconstructions based on observations of Roman fish tanks, Tyrrhenian Coast of Italy. *Geoarchaeology* 27, 259–277.
- Evelpidou, N., Pirazzoli P.A., 2014. Holocene relative sea-level changes from submerged tidal notches: A methodological approach. *Quaternaire* 25 (4), 383–390.
- Faisst, G.W., 2013. Apollon: sein neu erforschetes Heiligtum bei Vonitsa in Akarnanien. Books on Demand, Norderstedt.
- Fensome, R.A., Taylor, F.J.R., Norris, G., Sarjeant, W.A.S., Wharton, D.I., Williams, G.L., 1993. A classification of living and fossil dinoflagellates. *Micropaleontology Special Publication 7*, Sheridan Press, Hanover/Pennsylvania.
- Fuchs, G., Eitinger, T., Schlegel, H.G., 2007. *Allgemeine Mikrobiologie*. Thieme, Stuttgart.
- Ganzert, J., Grünewald, M., Herz, P., 1984. Das Kenotaph für Gaius Caesar in Limyra: Architektur und Bauornamentik. E. Wasmuth, Tübingen.
- Garbrecht, G., 2003. Erdbeben in der Wasserversorgungsgeschichte Pergamons. *Schriften der Wasserhistorischen Gesellschaft* 2, 119–133.
- Gehrke, H.-J., 2015. A Brief History of Pergamum. In: F. Pirson, Scholl, A. (Eds.), *Pergamon. A Hellenistic Capital in Anatolia*. Phoibos, İstanbul, Turkey, 122–143.
- Gerkan, A. van, 1956. Die ursprüngliche Mündung des Kaikos. *Nachrichten der Akademie der Wissenschaften in Göttingen* 8, 283–299.
- Ghilardi, M., Fouache, E., Queyrel, F., Syrides, G.-E., Vouvalidis, K., Kunesch, S., Styllas, M., Stiros, S., 2008. Human occupation and geomorphological evolution of the Thessaloniki Plain (Greece) since mid-Holocene. *Journal of Archaeological Science* 35 (1), 111–125.
- Goiran, J.-P., Tronchère, H., Salomon, F., Carbonel, P., Djerbi, H., Ognard, C., 2010. Palaeoenvironmental reconstruction of the ancient harbors of Rome: Claudius and Trajan's marine harbors on the Tiber delta. *Quaternary International* 216, 3–13.
- Hadler, H., 2014. Ancient Greek harbours used as geoarchives for palaeotsunami research. Case studies from Krane (Cefalonia), Lechaion (Gulf of Corinth) and Kyllini (Peloponnese). Ph.D. Thesis (unpublished), Johannes Gutenberg University of Mainz.
- Hansen, E., 1971. *The Attalids of Pergamon*. Cornell University Press, Ithaca.

- Horejs, B., 2014. Der prähistorische Umlandsurvey. In: Pirson, F. (Hrsg.), Pergamon. Bericht über die Arbeiten in der Kampagne 2013. *Archäologischer Anzeiger* 2014 (2), Hirmer, München, Germany, 141–146.
- Horejs, B., 2015. Pergamon and the Kaikos Valley in Prehistoric Times. In: F. Pirson, Scholl, A. (Eds.), Pergamon. *A Hellenistic Capital in Anatolia*. Phoibos, İstanbul, Turkey, 106–119.
- Horejs, B., 2012. Çukuriçi Höyük. A Neolithic and Bronze Age Settlement in the Region of Ephesos. In: Özdoğan, M., Başgelen, N., Kuniholm, P. (Eds.), *The Neolithic in Turkey. New Excavations & New Research*. Archaeology and Art Publications, İstanbul, Turkey, 117–131.
- Horejs, B., Milić, B., Ostmann, F., Thanheiser, B., Weninger, B., Galik, K., 2015. The Aegean in the Early 7th Millennium BC: Maritime Networks and Colonization. *Journal of World Prehistory* 28 (4), 289–330.
- Kayan, I., 1988. Late Holocene sea-level changes on the western Anatolian coast. *Palaeogeography, Palaeoclimatology, Palaeoecology* 68 (2–4), 205–218.
- Kelletat, D., 2005. A Holocene sea level curve for the eastern Mediterranean from multiple indicators. *Zeitschrift für Geomorphologie N.F.* 137 (Supplement), 1–9.
- Kelletat, D., 2006. Beachrock as Sea-Level Indicator? Remarks from a Geomorphological Point of View. *Journal of Coastal Research* 22 (6), 1558–1564.
- Kelletat, D., 2013. *Physische Geographie der Meere und Küsten*. Bornträger, Stuttgart.
- Khan, N.S., Ashe, E., Shaw, T.A., Vacchi, M., Walker, J., Peltier, W.R., Kopp, R., Horton, B.P., 2015. Holocene Relative Sea-Level Changes from Near-, Intermediate-, and Far-Field Locations. *Current Climate Change Reports* 1 (4), 247–262.
- Knight, J., 2007: Beachrock Reconsidered. Discussion of: Kelletat, D., 2006. Beachrock as Sea Level Indicator? Remarks from a Geomorphological Point of View. *Journal of Coastal Research* 22 (6), 1558-1564. *Journal of Coastal Research* 23 (4), 1074–1078.
- Knoblauch, P., 1981. Die Rolle der Strandverschiebungen bei der Rekonstruktion antiker Hafenanlagen. In: Schäfer, J., Simon, W. (Hrsg.), *Strandverschiebungen in ihrer Bedeutung für Geowissenschaften und Archäologie*. Esprint, Heidelberg, Germany, 91–114.
- Kolaiti, E., Mourtzas, N.D., in press. Upper Holocene sea level changes in the West Saronic Gulf, Greece, *Quaternary International* (2015). DOI: 10.1016/j.quaint.2015.06.024.
- Kraft, J.C., Aschenbrenner, S.E., Rapp, G., Jr., 1977. Paleogeographic reconstructions of coastal Aegean archeological sites. *Science* 195, 941–947.
- Kraft, J.C., Kayan, I., Erol, O., 1980. Geomorphic reconstructions in the environs of ancient Troy. *Science* 209, 776–782.
- Kraft, J.C., Rapp, G., Szemler, G.J., Tziavos, C., Kase E.W., 1987. The pass at Thermopylae, Greece. *Journal of Field Archaeology* 14, 181–198.

- Kraft, J.C., Kayan, I., Brückner, H., Rapp, G., Jr., 2000. A geologic Analysis of ancient landscapes and the harbours of Ephesus and the Artemisions in Anatolia. *Jahreshefte des Österreichischen Archäologischen Institutes in Wien* 69, 175–232.
- Kraft, J.C., Rapp, G.R., Kayan, I., Luce, J.V., 2003. Harbor areas at ancient Troy: Sedimentology and geomorphology complement Homer's Iliad. *Geology* 31 (2), 163–166.
- Kraft, J.C., Brückner, H., Kayan, I., Engelmann, H., 2007. The geographies of ancient Ephesus and the Artemision in Anatolia. *Geoarchaeology* 22, 121–149.
- Ladstätter, S., Pirson, F., Schmidts, T., 2015. Harbors and Harbor Cities in the Eastern Mediterranean from Antiquity to the Byzantine Period: Recent Discoveries and Current Approaches. *Byzas* 19. Phoibos, Istanbul, Turkey.
- Lambeck, K., 1996. Sea-level changes and shoreline evolution in Aegean Greece since Upper Paleolithic time. *Antiquity* 70, 588–611.
- Lambeck, K., Purcell, A., 2005. Sea-level change in the Mediterranean Sea since the LGM: model predictions for tectonically stable areas. *Quaternary Science Reviews* 24, 1969–1988.
- Lambeck, K., Purcell, A., 2007. Palaeogeographic reconstructions of the Aegean for the past 20.000 years: Was Atlantis on Athens doorstep? In: Papamarinopoulos, S.P. (Ed.), *The Atlantis Hypothesis: Searching for a Lost Land*. Heliotos Publications, Santorini, Greece, 241–257.
- Marret, F., De Vernal, A., Benderra, F., Harland, R., 2001. Late Quaternary sea-surface conditions at DSDP Hole 594 in the southwest Pacific Ocean based on dinoflagellate cyst assemblages. *Journal of Quaternary Science* 16 (7), 739–751.
- Marriner, N., Morhange, C., 2006a. Geoarchaeological evidence for dredging in Tyre's ancient harbour, Levant. *Quaternary Research* 65, 164–171.
- Marriner, N., Morhange, C., 2006b. The 'Ancient Harbour Parasequence': anthropogenic forcing of the stratigraphic highstand record. *Sedimentary Geology* 186, 13–17.
- Marriner, N., Morhange, C., 2007. Geoscience of ancient Mediterranean harbours. *Earth Science Reviews* 80, 137–194.
- Marriner, N., Morhange, C., Faivre, S., Flaux, C., Vacchi, M., Miko, S., Dumas, V., Boetto, G., Radic Rossi, I., 2014. Post-Roman sea-level changes on Pag Island (Adriatic Sea): Dating Croatia's "enigmatic" coastal notch? *Geomorphology* 221, 83–94.
- Marshall, R.J.E., Stephenson, W.J., 2011. The morphodynamics of shore platforms in a micro tidal setting: Interactions between waves and morphology. *Marine Geology* 288 (1–4), 18–31.
- McShane, R.B., 1964. *Foreign Policy of the Attalids of Pergamum*. University of Illinois Press, Champaign.
- Morhange, C., Marriner, N., 2010. Palaeo-hazards in the coastal Mediterranean: A geoarchaeological approach. In: Martini, I., Chesworth, P.W. (Eds.), *Landscapes and Societies*. Springer Netherlands, Dordrecht, Netherlands, 223–234.

- Morhange, C., Marriner, N., 2015. Archeological and biological relative sea-level indicators. In: Shennan, I., Long, A.J., Horton, B.P. (Eds.), *Handbook of Sea-Level Research*. John Wiley and Sons, Hoboken, United States, 146–156.
- Morhange, C., Blanc, F., Bourcier, M., Carbonel, P., Prone, A., Schmitt-Mercury, S., Vivent, D., Hesnard, A., 2003. Bio-sedimentology of the late Holocene deposits of the ancient harbor of Marseilles (Southern France, Mediterranean sea). *The Holocene* 13, 593–604.
- Morhange, C., Pirazzoli, P., Evelpidou, N., Marriner, N., 2012. Tectonic uplift and silting up of Lechaion, western harbour of ancient Corinth (Greece). *Geoarchaeology* 27, 278–283.
- Morhange, C., Marriner, N., Excoffon, P., Bonnet, S., Flaux, C., Zibrowius, H., Goiran J.-P., El Amouri, M., 2013. Relative sea level changes during Roman times in the Northwest Mediterranean: the 1st century AD fish tank of Forum Julii, Fréjus, France. *Geoarchaeology* 28, 363–372.
- Morhange, C., Marriner, N., Carayon, N., 2014. The geoarchaeology of ancient Mediterranean harbours. In: Arnaud-Fassetta, G., Carcaud, N. (Eds.), *French geoarchaeology in the 21st century*. CNRS Editions, Paris, France, 281–290.
- Morhange, C., Marriner, N., Baralis, A., Blot, M.L., Bony, G., Carayon, N., Carmona, P., Flaux, C., Giaime, M., Goiran, J.-P., Kouka, M., Lena, A., Oueslati, A., Pasquinucci, M., Porotov, A., 2015. Geomorphology and geoarchaeological typology of ancient harbours in lagoonal contexts. *Quaternaire* 26 (2), 117–139.
- Morrison, J.S., Coates, J.F., 1986. *The Athenian Trireme: The History and Reconstruction of an Ancient Greek Warship*. Cambridge University Press, Cambridge.
- Morrison, J.S., Coates, J.F., 1996. *Greek and Roman Oared Warships*. Oxbow Books, Oxford.
- Müllenhoff, M., 2005. *Geoarchäologische, sedimentologische und morphodynamische Untersuchungen im Mündungsgebiet des Büyük Menderes (Mäander), Westtürkei*. Ph.D. Thesis, Philipps-University Marburg. Published: Marburger Geographische Schriften 141, Marburg/Lahn.
- Müller-Wiener, W., 1988. *Griechisches Bauwesen in der Antike*. C.H.Beck, München.
- Murray, W.M., 2012. *The Age of Titans: The Rise and Fall of the Great Hellenistic Navies*. Oxford University Press, Oxford.
- Murray-Wallace, C.V., Woodroffe, C.D., 2014. *Quaternary Sea-Level Changes: A Global Perspective*. Cambridge University Press, Cambridge.
- Murray-Wallace, C.V., Beu, A.G., Kendrick, G.W., Brown, L.J., Belperio, A.P., Sherwood, J.E., 2000. Palaeoclimatic implications of the occurrence of the arcoïd bivalve *Anadara trapezia* (*Deshayes*) in the Quaternary of Australasia. *Quaternary Science Reviews* 19 (6), 559–590.
- Otvos, E.G., 2000. Beach ridges – definitions and significance. *Geomorphology* 32, 83–108.
- Özbek, O., 2010. Hamaylitarla reconsidered: A Neolithic Site and its Environmental setting in southern Thrace. *Anatolia Antiqua* 18 (1), 1–21.

- Özürlan, G., Candansayar, M.E., Sahin, M.H., 2006. Deep resistivity of the Dikili Bergama region, west Anatolia, revealed by two-dimensional inversion of vertical electric sounding data. *Geophysical Prospecting* 54, 187–197.
- Papadopoulos, G., 2015. *Tsunamis in the European-Mediterranean Region. From Historical Record to Risk Mitigation*. Elsevier, Amsterdam.
- Pavlopoulos, K., Triantaphyllou, M., Karymbalis, E., Karkanias, P., Kouli, K., Tsourou, T., 2007. Landscape evolution recorded in the embayment of Palamari (Skyros Island, Greece) from the beginning of the Bronze Age until recent times. *Géomorphologie: relief, processus, environment* 2007 (1), 37–48.
- Pavlopoulos, K., Fouache, E., Sidiropoulou, M., Triantaphyllou, M., Vouvalidis, K., Syrides, G.-E., Gonnet, A., Greco, E., 2013. Palaeoenvironmental evolution and sea-level changes in the coastal area of NE Lemnos Island (Greece) during the Holocene. *Quaternary International* 308–309, 80–88.
- Park, C.B., Miller, R.D., Xia, J., 1999. Ground roll as a tool to image near-surface anomaly. *Proceedings of the 68th SEG Meeting, September 13–18, 1998, New Orleans, United States*, 874–877.
- Peltier, W.R., 2002. On eustatic sea level history: Last Glacial Maximum to Holocene. *Quaternary Science Reviews* 21, 377–396.
- Philippon, A., 1911. Zur Geographie der Unteren Kaikosebene in Kleinasien. *Hermes* 46, 254–260.
- Pirazzoli, P.A., 1997. Sea-level changes in the Mediterranean. In: Tooley, M.J., Shennan, I., (Eds.), *Sea-level Changes. Special Publications Series, Page Bros, Norwich, Great Britain*, 152–181.
- Pirazzoli, P.A., 2005. A review of possible eustatic, isostatic and tectonic contributions in eight late-Holocene relative sea-level histories from the Mediterranean area. *Quaternary Science Reviews* 24, 1989–2001.
- Pirazzoli, P.A., Ausseil-Badie, J., Giresse, P., Hadjidaki, E., Arnold, M., 1992. Historical environmental changes at Phalasarna harbour, West Crete. *Geoarchaeology* 7 (4), 371–392.
- Plicht, J. van der, 2004. Radiocarbon, the calibration curve and Scythian chronology. In: Scott, E.M., Alekseev, A.Y., Zaitseva, G. (Eds.), *NATO Science Series 42: IV: Earth and Environmental Sciences*, Springer, Dordrecht, Netherlands, 45–61.
- Pirson, F., 2004. Elaia, der maritime Satellit Pergamons. *Istanbuler Mitteilungen* 54, 197–213.
- Pirson, F., 2008. Das Territorium der hellenistischen Residenzstadt Pergamon – Herrschaftlicher Anspruch als raumbezogene Strategie. In: Jöchner, C. (Hrsg.), *Räume der Stadt – Von der Antike bis heute*. Reimer, Berlin, Germany, 27–50.
- Pirson, F., 2010. Survey. In: Pirson, F. (Hrsg.), *Pergamon. Bericht über die Arbeiten der Kampagne 2009*. *Archäologischer Anzeiger* 2010 (2), Hirmer, München, Germany, 195–201.
- Pirson, F., 2011. Elaia. In: Pirson, F. (Hrsg.), *Pergamon. Bericht über die Arbeiten der Kampagne 2010*. *Archäologischer Anzeiger* 2011 (2). Hirmer, München, Germany, 166–174.

- Pirson, F., 2014. Elaia, der (maritime) Satellit Pergamons. *Byzas* 19 (1), 339–356.
- Pirson, F., Zimmermann, M., 2015. The Hinterland of Pergamum: Economic Resources, Rural Settlements and Political Manifestion. In: F. Pirson, Scholl, A. (Eds.), *Pergamon. A Hellenistic Capital in Anatolia*. Phoibos, İstanbul, Turkey, 144–161.
- Pirson, F., Ateş, G., Bartz, M., Brückner, H., Feuser, S., Mania, U., Meier, L., Seeliger, M., 2015. Elaia: Eine aiolische Polis im Dienste der hellenistischen Residenzstadt Pergamon? In: Matthaei, A., Zimmermann, M. (Hrsg.), *Urbane Strukturen und bürgerliche Identität im Hellenismus*. Verlag Antike, Heidelberg, Germany, 22–55.
- Poulos, S.E., Ghionis, G., Maroukian, H., 2009. Sea-level rise trends in the Attico-Cycladic region (Aegean Sea) during the last 5000 years. *Geomorphology* 107 (1–2), 10–17.
- Prokesch von Osten, A., 1837. *Denkwürdigkeiten und Erinnerungen aus dem Orient III*. Hallberger, Stuttgart.
- Rabbel, W., Stümpel, H., Woelz, S., 2004. Archeological prospecting with magnetic and shear wave surveys at the ancient city of Miletos (western Turkey). *The Leading Edge* 23 (7), 690–693+703.
- Radt, W., 2011. *Pergamon – Geschichte und Bauten einer antiken Metropole*. Primus, Darmstadt.
- Rapp, G., Hill, C., 2006. *Geoarchaeology: The Earth-Science Approach to Archaeological Interpretation*. Yale University Press, New Haven.
- Reimer, P.J., Bard, E., Bayliss, A., Beck, J.W., Blackwell, P.G., Bronk Ramsey, C., Buck, C.E., Cheng, H., Edwards, R.L., Friedrich, M., Grootes, P.M., Guilderson, T.P., Haflidason, H., Hajdas, I., Hatt, C., Heaton, T.J., Hogg, A.G., Hughen, K.A., Kaiser, K.F., Kromer, B., Manning, S.W., Niu, M., Reimer, R.W., Richards, D.A., Scott, E.M., Southon, J.R., Turney, C.S.M., van der Plicht, J., 2013. IntCal13 and MARINE13 radiocarbon age calibration curves 0–50000 years cal BP. *Radiocarbon* 55 (4), 1869–1887.
- Reinhard, K.J., Ferreira, L.F., Bouchet, F., Sianto, L., Dutra, J.M.F., Iniguez, A., Leles, D., Le Bailly, M., Fugassa, M., Pucu, E., Araújo, A., 2013. Food, parasites, and epidemiological transitions: A broad perspective. *International Journal of Paleopathology* 3, 150–157.
- Reinhardt, E.G., Raban, A., 1999. Destruction of Herod the Great's harbor at Caesarea Maritima, Israel - geoarchaeological evidence. *Geology* 27, 811–814.
- Reinhardt, E.G., Goodman, B.N., Boyce, J.I., Lopez, G., van Hengstum, P., Rink, W.J., Mart, Y., Raban, A., 2006. The tsunami of 13 December A.D. 115 and the destruction of Herodot the Great's harbour at Caesarea Maritima, Israel. *Geology* 34 (12), 1061–1064.
- Ruiz, F., Abad, M., Caceres, L.M., Vidal, J.R., Carretero, M.I., Pozo, M., Gonzalez-Delgado, M.L., 2010. Ostracods as tsunami tracers in Holocene sequences. *Quaternary Research* 73, 130–135.
- Salvatore, I., Giuseppe, M., Gabriele, C., Erminio, S., 2015. Predictive correlations for the compaction of clean sands. *Transportation Geotechnics* 4, 38–49.

- Sangiorgi, F., Capotondi, L., Brinkhuis, H., 2002. A centennial scale organic-walled dinoflagellate cyst record of the last deglaciation in the South Adriatic Sea (Central Mediterranean). *Palaeogeography Palaeoclimatology Palaeoecology* 186 (3–4), 199–216.
- Sangiorgi, F., Fabbri, D., Comandini, M., Gabbianelli, G., Tagliavini, E., 2005. The distribution of sterols and organic-walled dinoflagellate cysts in surface sediments of the North-western Adriatic Sea (Italy). *Estuarine Coastal and Shelf Science* 64 (2–3), 395–406.
- Schielein, P., Zschau, J., Woith, H., Schellmann, G., 2007. Tsunamigefährdung im Mittelmeer – Eine Analyse geomorphologischer und historischer Zeugnisse. *Bamberger Geographische Schriften* 22, 153–199.
- Schneider, S., 2014. Geoarchaeological case studies in the Bakırçay Valley – Paleogeography and Human-environmental Interactions in the Chora of Pergamon in Western Turkey. Ph.D. Thesis (unpublished), Freie Universität Berlin, Germany.
- Schneider, S., Schlöffel, M., Schütt, B., 2012. Geoarchäologische Untersuchungen im westlichen Kaikos-Tal – Bericht über die Geländearbeiten im Sommer 2011. In: Pirson, F. (Hrsg.), Pergamon. Bericht über die Arbeiten der Kampagne 2011. *Archäologischer Anzeiger* 2012 (2), Hirmer, München, Germany, 218–222.
- Schneider, S., Nykamp, M., Matthaei, A., Bebermeier, W., Schütt, B., 2013. Alluvial geoarchaeology of a small drainage basin in western Anatolia: Late Holocene landscape development and the question of the mouth of the Paleo-Bakırçay. *Quaternary International* 312, 84–95.
- Schneider, S., Matthaei, A., Bebermeier, W., Schütt, B., 2014. Late Holocene human environmental interactions in the Eastern Mediterranean: Settlement history and paleogeography of an ancient Aegean hill-top settlement. *Quaternary International* 324, 84–98.
- Schneider, S., Matthaei, A., Schlöffel, M., Kronwald, M., Pint, A., Schütt, B., 2015. A geoarchaeological case study in the chora of Pergamon, Western Turkey to reconstruct the late Holocene landscape development and settlement history. *Quaternary International* 367, 62–76.
- Scoffin, T.P., Stoddart, D.R., Rosen, B.R., 1978. The Nature and Significance of Microatolls. *Philosophical Transactions of the Royal Society* 284, 99–122.
- Seeliger, M., Bartz, M., Brückner, H., 2015. Umweltgeschichte der Bucht von Elaia. In: Matthaei, A., Zimmermann, M. (Hrsg.), *Urbane Strukturen und bürgerliche Identität im Hellenismus*. Verlag Antike, Mainz, Germany, 26–28.
- Siani, G., Paterne, M., Arnold, M., Bard, E., Metivier, B., Tisnerat, N., Bassinot, F., 2000. Radiocarbon reservoir ages in the Mediterranean Sea and Black Sea. *Radiocarbon* 42, 271–280.
- Stanley, J.D., 1995. A global sea-level curve for the late Quaternary: the impossible dream? *Marine Geology* 125, 1–6.
- Stephenson, W.J., Kirk, R.M., Kennedy, D.M., Finlayson, B.L., Chen, Z., 2012. Long term shore platform surface lowering rates: Revisiting Gill and Lang after 32 years. *Marine Geology* (299–302), 90–95.

- Stock, F., 2015. Ephesus and the Ephesia – palaeogeographical and geoarchaeological research about a famous city in Western Anatolia. Ph.D. Thesis (unpublished), University of Cologne, Germany.
- Stock, F., Pint, A., Horejs, B., Ladstätter, S., Brückner, H., 2013. In search of the harbours: New evidence of Late Roman and Byzantine harbours of Ephesus. *Quaternary International* 312, 57–69.
- Stock, F., Ehlers, L., Horejs, B., Knipping, M., Ladstätter, S., Seren, S., Brückner, H., 2015. Neolithic settlement sites in Western Turkey - palaeogeographic studies at Çukuriçi Höyük and Arvalya Höyük. *Journal of Archaeological Science: Reports* 4, 565–577.
- Stock, F., Knipping, M., Pint, A., Ladstätter, S., Delile, H., Heiss, A.G., Laermanns, H., Mitchell, P.D., Ployer, R., Steskal, M., Thanheiser, U., Urz, R., Wennrich, V., Brückner, H., in press. Human impact on Holocene sediment dynamics in the Eastern Mediterranean – the example of the Roman harbour of Ephesus. *Earth Surface Processes and Landforms* (2016). DOI: 10.1002/esp.3914.
- Toscano, M.A., Peltier, W.R., Drummond, R., 2011. ICE-5G and ICE-6G models of postglacial relative sea-level history applied to the Holocene coral reef record of northeastern St Croix, U.S.V.I.: investigating the influence of rotational feedback on GIA processes at tropical latitudes. *Quaternary Science Reviews* 30 (21–22), 3032–3042.
- Vacchi, M., Rovere, A., Chatzipetros, A., Zouros, N., Firpo, M., 2014. An updated database of Holocene relative sea level changes in NE Aegean Sea. *Quaternary International* 328–329, 301–310.
- Vernal, A. de, Rochon, A., Turon, J.L., Matthiessen, J., 1997. Organic-walled dinoflagellate cysts: Palynological tracers of sea-surface conditions in middle to high latitude marine environments. *Geobios* 30 (7), 905–920.
- Vita-Finzi, C., 1969. Late Quaternary continental deposits of central and western Turkey. *Man New Series* 4 (4), 605–619.
- Vittori, C., Mazzini, I., Salomon, F., Goiran, J.-P., Pannuzi, S., Rosa, C., Pellegrino, A., in press. Palaeoenvironmental evolution of the ancient lagoon of Ostia Antica (Tiber delta, Italy). *Journal of Archaeological Science* (2014). DOI: 10.1016/j.jas.2014.06.017.
- Vousdoukas, M.I., Velegrakis, A.F., Plomaritis, T.A., 2007. Beachrock occurrence, characteristics, formation mechanisms and impacts. *Earth-Science Reviews* 85 (1–2), 23–46.
- Vouvalidis, K.G., Syrides, G.-E., Albanis, K.S., 2005. Holocene morphology of the Thessaloniki Bay: Impact of sea level rise. *Zeitschrift für Geomorphologie N.F. Suppl.* 137, 147–158.
- Waelkens, M., 1987. The adoption of Roman building techniques in the architecture of Asia Minor. In: Macready, S., Thompson, F.H. (Eds.), *Roman Architecture in the Greek World*. Society of Antiquaries of London, Thames & Hudson Publisher, London, Great Britain, 94–105.
- Wilken, D., Rabbel, W., 2012. On the application of Particle Swarm Optimization strategies on Scholte wave inversion. *Geophysical Journal International* 190 (1), 580–594.

-
- Xia, J., Miller, R.D., Park, C.B., 1999. Estimation of near-surface shear-wave velocity by inversion of Rayleigh waves. *Geophysics* 64 (3), 691–700.
- Zimmermann, M., 2011. Pergamon: Geschichte, Kultur, Archäologie. C. H. Beck, München.
- Zimmermann, M., Matthaei, A., Ates, G., 2015. Die Chora von Pergamon: Forschungen im Kai-kostal und in der antiken Stadt Atarneus. In: Matthaei, A., Zimmermann, M. (Hrsg.), *Urbane Strukturen und bürgerliche Identität im Hellenismus*. Verlag Antike, Heidelberg, Germany, 193–236.
- Zonneveld, K.A., Marret, F., Versteegh, G.J., Bogus, K., Bonnet, S., Bouimetarhan, I., Crouch, E., de Vernal, A., Elshanawany, R., Edwards, L., Esper, O., Forke, S., Grøsfjeld, K., Henry, M., Holzwarth, U., Kieft, J.F., Kim, S.Y., Ladouceur, S., Ledu, D., Chen, L., Limoges, A., Londeix, L., Lu, S.H., Mahmoud, M. S., Marino, G., Matsouka, K., Matthiessen, J., Mildenthal, D., Mudie, P., Neil, H., Pospelova, V., Qi, Y., Radi, T., Richerol, T., Rochon, A., Sangiorgi, F., Solignac, S., Turon, J.L., Verleye, T., Wang, Y., Wang, Z., Young, M., 2013. Atlas of modern dinoflagellate cyst distribution based on 2405 data points. *Review of Palaeobotany and Palynology* 191, 1–197.

Supplementary Material

Sample code	Lab code	Material	Depth b.s.	Depth b.s.l.	$\delta^{13}\text{C}$ (‰)	Libby-age	Calibrated ^{14}C ages cal BC / cal AD (2 σ)	Calibrated ^{14}C ages cal BC / cal AD (2 σ) with relative probability	Calibrated ^{14}C ages cal BP (2 σ) with relative probability
<u><i>Ela 14/18</i></u>	UGAMS 6034	sea grass	6.46 m	-5.10 m	-14.3	5300±25	3877–3516 BC	3877–3868 BC (0.6 %) 3864–3516 BC (99.4 %)	5465–5813 BP (99.4 %) 5817–5826 BP (0.6 %)
<u><i>Ela 20/1656</i></u>	UGAMS 6027	plant remain	4.04 m	-2.66 m	-14.5	3350±25	1735–1536 BC	1735–1717 BC (3.7 %) 1693–1606 BC (88.4 %) 1583–1545 BC (7.7 %)	3485–3486 BP (0.2 %) 3494–3532 BP (7.7 %) 3555–3642 BP (88.4 %)
<u><i>Ela 58/24HK</i></u>	UGAMS 11442	charcoal	2.73 m	-1.84 m	-26.4	2080±25	175–41 BC	1537–1536 BC (0.2 %) 175–41 BC (100 %)	3485–3684 BP 2124–1990 BP (100 %)
<u><i>Ela 58/27H</i></u>	UGAMS 11443	seed	3.30 m	-2.41 m	-25.0	2020±25	91 BC–AD 52	91–69 BC (5.3 %) 60 BC–AD 52 (94.7 %)	2040–2018 BP (5.3 %) 2009–1898 BP (94.7 %)
<u><i>Ela 58/24P</i></u>	UGAMS 11444	sea grass	4.40 m	-3.51 m	-10.8	2740±25	731–299 BC	731–299 BC (100 %)	2680–2248 BP (100 %)
<u><i>Ela 58/22</i></u>	UGAMS 11445	sea grass	7.75 m	-6.86 m	-16.2	6170±30	4796–4439 BC	4796–4439 BC (100 %) 5876–5856 BC (5.4 %) 5852–5731 BC (94.6 %)	6745–6388 BP (100 %) 7825–7805 (5.4 %) 7801–7680 (94.6 %)
<u><i>Ela 58/38F</i></u>	UGAMS-11446	charcoal	8.35 m	-7.46 m	-26.1	6920±30	5876–5731 BC	5876–5856 BC (5.4 %) 5852–5731 BC (94.6 %)	7825–7805 (5.4 %) 7801–7680 (94.6 %)
<u><i>Ela 63/11</i></u>	UGAMS 11904	charcoal	4.88 m	-2.57 m	-28.0	2640±25	834–792 BC	834–792 BC (100 %)	2741–2783 BP (100 %)
<u><i>Ela 70/190</i></u>	UBA-23841	wood	1.90 m	-2.02 m	-26.1	1780±29	AD 244–385	AD 244–385 (100 %) AD 254–303 (23 %) AD 314–407 (77 %)	1565–1706 BP (100 %) 1543–1636 BP (77 %) 1647–1696 (23 %)
<u><i>Ela 70/250</i></u>	UBA-23840	wood	2.50 m	-2.62 m	-27.3	1699±29	AD 254–407	AD 254–407 (77 %)	1647–1696 (23 %)
<u><i>Ela 70/275</i></u>	UBA-23839	wood	2.75 m	-2.87 m	-28.1	1774±29	AD 139–341	AD 139–198 (10.5 %) AD 207–341 (89.5 %)	1609–1743 BP (89.5 %) 1752–1811 BP (10.5 %)
<u><i>Ela 70/377</i></u>	UGAMS-11130	charcoal	3.77 m	-3.89 m	-27.0	1960±30	39 BC–AD 120	39 BC–AD 87 (96.3 %) AD 105–120 (3.7 %)	1830–1845 BP (3.7 %) 1863–1988 BP (96.3 %)
<u><i>Ela 70/395</i></u>	ERL-18675	terr. pollen	3.95 m	-4.07 m	-26.0	2253±42	398–204 BC	398–340 BC (33.3 %) 327–204 BC (66.7 %)	2153–2276 BP (66.7 %) 2289–2347 BP (33.3 %)
<u><i>Ela 70/457</i></u>	UGAMS-11131	sea grass	4.57 m	-4.69 m	-18.2	2680±30	650–181 BC	650–181 BC (100 %)	2130–2599 BP (100 %)
<u><i>Ela 70/480</i></u>	UBA-23837	seed	4.80 m	-4.92 m	-8.2	2659±31	895–794 BC	895–867 BC (10.5 %) 858–794 BC (89.5 %)	2743–2807 BP (89.5 %) 2816–2844 BP (10.5 %)
<u><i>Ela 70/585</i></u>	UBA-23836	sea grass	5.85 m	-5.97 m	-12.7	4274±34	2597–2155 BC	2597–2155 BC (100 %)	4104–4546 BP (100 %)
<u><i>Ela 70/672</i></u>	UGAMS-11132	sea grass	6.72 m	-6.84 m	-17.7	5920±30	4529–4203 BC	4529–4203 BC (100 %)	6152–6478 BP (100 %)
<u><i>Ela 70/695</i></u>	UBA-23835	sea grass	6.95 m	-7.07 m	-12.7	6616±37	5316–4948 BC	5316–4948 BC (100 %)	6897–7265 BP (100 %)
<u><i>Ela 70/782</i></u>	UGAMS-11133	bivalve	7.82 m	-7.94 m	-0.7	7040±30	5690–5421 BC	5690–5421 BC (100 %)	7370–7639 BP (100 %)

Tab. 1 Radiocarbon data sheet. ^{14}C -AMS dating was carried out at the Centre for Applied Isotope Studies (CAIS) of the University of Georgia at Athens, USA (lab code: UGAMS), the ^{14}C Chrono Centre for Climate, the Environment, and Chronology, Queen’s University Belfast, UK (lab code: UBA), the AMS ^{14}C -Labor of the University of Erlangen-Nürnberg, Germany (lab. code: ERL). All ages were calibrated with IntCal13 or MARINE13 calibration curves using the Calib 7.1 software (Reimer et al. 2013). A marine reservoir effect of 390 ± 85 years and a ΔR of 35 ± 70 years (Siani et al. 2000) was applied. The ages are presented in calendar years BC/AD and years BP (before AD 1950) representing a 2σ -confidence interval.

Paper Contribution

Seeliger, M., Bartz, M., Erkul, E., Feuser, E., Kelterbaum, K., Klein, C., Pirson, F., Vött, A., Brückner, H., 2013. Taken from the sea, reclaimed by the sea: The fate of the closed harbour of Elaia, the maritime satellite city of Pergamum (Turkey). *Quaternary International* 312, 70–83. [Contribution: 90 %].

Durchführung der Geländearbeiten: 90 %
 Erhebung der Daten im Labor: 100 %
 Auswertung und Interpretation: 90 %
 Verfassen der Publikation: 80 %

Seeliger, M., Brill, D., Feuser, S., Bartz, M., Erkul, E., Kelterbaum, D., Vött, A., Klein, C., Pirson, F., Brückner, H., 2014. The purpose and age of underwater walls in the Bay of Elaia of Western Turkey: A multidisciplinary approach. *Geoarchaeology: An International Journal* 29, 138–155. [Contribution: 85 %].

Durchführung der Geländearbeiten: 90 %
 Erhebung der Daten im Labor: 75 %
 Auswertung und Interpretation: 75 %
 Verfassen der Publikation: 80 %

Pint, A., **Seeliger, M.**, Frenzel, P., Feuser, S., Erkul, E., Berndt, C., Klein, C., Pirson, F., Brückner, H., 2015. The environs of Elaia's ancient open harbour - A reconstruction based on microfaunal evidence. *Journal of Archaeological Science* 54, 340–355. [Contribution: 55 %].

Durchführung der Geländearbeiten: 90 %
 Erhebung der Daten im Labor: 50 %
 Auswertung und Interpretation: 40 %
 Verfassen der Publikation: 45 %

Seeliger, M., Pint, A., Feuser, S., Riedesel, S., Frenzel, P., Kelterbaum, D., Pirson, F., Bolten, A., Brückner, H. Elaia, Pergamon's maritime satellite – Rise and fall of an ancient harbour city due to shoreline migration. *Journal of Quaternary Science*. (Manuskriptnummer: JQS-16-0068).[Eingereicht 06/2016, in Begutachtung]. [Contribution: 85 %].

Durchführung der Geländearbeiten: 90 %
 Erhebung der Daten im Labor: 80 %
 Auswertung und Interpretation: 80 %
 Verfassen der Publikation: 75 %

Shumilovskikh, L.S., **Seeliger, M.**, Feuser, S., Novenko, E., Schlütz, F., Pint, A., Brückner, H., accepted. The harbour of Elaia: A palynological archive for human/environmental interactions during the last 7500 years. *Quaternary Science Reviews*. [Contribution: 30 %].

Durchführung der Geländearbeiten: 90 %
 Erhebung der Daten im Labor: 20 %
 Auswertung und Interpretation: 20 %
 Verfassen der Publikation: 25 %

Erklärung

Ich versichere, dass ich die von mir vorgelegte Dissertation selbständig angefertigt, die benutzten Quellen und Hilfsmittel vollständig angegeben und die Stellen der Arbeit – einschließlich Tabellen, Karten und Abbildungen –, die anderen Werken im Wortlaut oder dem Sinn nach entnommen sind, in jedem Einzelfall als Entlehnung kenntlich gemacht habe; dass diese Dissertation noch keiner anderen Fakultät oder Universität zur Prüfung vorgelegen hat; dass sie – abgesehen von unten angegebenen Teilpublikationen – noch nicht veröffentlicht worden ist sowie, dass ich eine solche Veröffentlichung vor Abschluss des Promotionsverfahrens nicht vornehmen werde. Die Bestimmungen dieser Promotionsordnung sind mir bekannt. Die von mir vorgelegte Dissertation ist von Univ. Prof. Dr. Helmut Brückner betreut worden.

Nachfolgend genannte Teilpublikationen liegen vor:

Seeliger, M., Bartz, M., Erkul, E., Feuser, E., Kelterbaum, K., Klein, C., Pirson, F., Vött, A., Brückner, H., 2013. Taken from the sea, reclaimed by the sea: The fate of the closed harbour of Elaia, the maritime satellite city of Pergamum (Turkey). *Quaternary International* 312, 70–83.

Seeliger, M., Brill, D., Feuser, S., Bartz, M., Erkul, E., Kelterbaum, D., Vött, A., Klein, C., Pirson, F., Brückner, H., 2014. The purpose and age of underwater walls in the Bay of Elaia of Western Turkey: A multidisciplinary approach. *Geoarchaeology: An International Journal* 29, 138–155.

Pint, A., **Seeliger, M.**, Frenzel, P., Feuser, S., Erkul, E., Berndt, C., Klein, C., Pirson, F., Brückner, H., 2015. The environs of Elaia's ancient open harbour - A reconstruction based on microfaunal evidence. *Journal of Archaeological Science* 54, 340–355.

Seeliger, M., Pint, A., Feuser, S., Riedesel, S., Frenzel, P., Kelterbaum, D., Pirson, F., Bolten, A., Brückner, H. Elaia, Pergamon's maritime satellite – Rise and fall of an ancient harbour city due to shoreline migration. *Journal of Quaternary Science* (Manuskriptnummer: JQS-16-0068). [Eingereicht 06/2016, in Begutachtung].

Shumilovskikh, L.S., **Seeliger, M.**, Feuser, S., Novenko, E., Schlütz, F., Pint, A., Brückner, H., accepted. The harbour of Elaia: A palynological archive for human/environmental interactions during the last 7500 years. *Quaternary Science Reviews*.

Köln, den 17.07.2016



(Martin Seeliger)